

**IDENTIFYING GENETIC DETERMINANTS OF COLORECTAL CANCER
SUSCEPTIBILITY IN MICE**

Lauren Ashley Van Der Kraak
Biochemistry Department
McGill University
Montreal, QC, Canada

December 2014

This thesis is submitted to the Faculty of Graduate Studies and Research in partial fulfillment of
the requirements of the degree of Doctor of Philosophy

© Lauren Van Der Kraak, 2014

i) Abstract:

Inbred mice differ with respect to colitis-associated colorectal cancer (CA-CRC) susceptibility due to inherited genetic factors. However, little is known with respect to the precise genetic variants underlying this susceptibility. We hypothesize, that similar to other complex traits, these genetic effects can be fixed by inbreeding and mapped by linkage analysis in informative mouse populations generated between CA-CRC susceptible and resistant mice. To identify novel CA-CRC susceptible and resistant strains for gene mapping, we tested 11 common inbred mouse strains for azoxymethane/dextran sulfate sodium (AOM/DSS)-induced CA-CRC, identifying a bimodal distribution pattern with respect to tumor multiplicity 12.5 weeks post-treatment initiation. This bimodal distribution pattern was not observed with respect to tumor surface area in these inbred strains suggesting that different events may regulate tumor initiation and proliferation. Re-testing of A/J and FVB/NJ CA-CRC susceptible mice at early time points in tumor development identified a unique hyper-susceptibility phenotype with FVB/NJ mice developing 5.5-fold more tumors than A/J, suggesting that CA-CRC susceptibility may be under differential genetic control in these two strains. Subsequent gene mapping identified a novel two-locus system involving mouse chromosome 9 (*colon cancer susceptibility 4, Ccs4*) and 14 that regulates tumor multiplicity in A/J. CA-CRC hyper-susceptibility is under distinct genetic control (*Ccs6*, chr 6) in FVB/NJ. These are amongst the first CA-CRC loci identified in mice and highlight an important role for genetic interactions in CA-CRC pathogenesis. Further experiments to characterize the *Ccs4* locus in recombinant congenic mice (mixed A/J and B6 background) identified the AcB60 mouse strain as hyper-susceptible with AcB60 mice developing 28-fold more tumors than either of its A/J or B6 parental strains at 7-weeks post-initiation of treatment. This was also associated with increased colitis following both acute and chronic DSS treatments. Murine models of early-onset CA-CRC are rare and therefore both AcB60 and FVB/NJ may offer unique models to the study the mechanisms associated with early-onset CA-CRC possibly leading to new genetic predictors of risk and treatment options in humans.

ii) Résumé

La pré-disposition au développement du cancer colorectal associé à la colite (CA-CRC) est différente chez les lignées des souris consanguines en raison de l'expression de certains facteurs génétiques intrinsèques. Présentement, peu de ces facteurs ont été identifiés. Nous avons donc émis l'hypothèse que, tel que défini dans plusieurs autres maladies complexes, des différences géniques pourraient être révélées par croisement de souris, et les gènes responsables pourraient donc être identifiés par une approche de cartographie génique de populations de souris soit susceptibles ou résistantes au CA-CRC. Nous avons ainsi évalué la pré-disposition au CA-CRC de 11 lignées de souris consanguines en induisant la formation de tumeurs suite à l'administration d'azoxyméthane/ dextran sodium sulfate (AOM/DSS). Le nombre de tumeurs se développant à 12.5 semaines de traitement se répartissait selon une distribution bimodale, ce qui n'était pas par contre le cas pour le volume des tumeurs, suggérant que l'initiation et la prolifération tumorales soient régulées par des événements génétiques distincts. L'évaluation de la pré-disposition des souris A/J et FVB/NJ au CA-CRC a permis d'identifier une hyper-susceptibilité unique chez les souris FVB/NJ développant 5.5-fois plus de tumeurs que les souris A/J à 8 semaines de traitement: la pré-disposition au CA-CRC est donc contrôlée différemment au niveau génétique dans ces deux lignées. L'analyse par cartographie génique a démontré que la susceptibilité des souris A/J est régulée par un système interactif de deux loci définis sur le chromosome 9 (*colon cancer susceptibility 4, Ccs4*) et le chromosome 14 respectivement. Chez la souris FVB/NJ, la pré-disposition est sous contrôle d'un nouveau locus *Ccs6* défini sur le chromosome 6. Ces deux loci représentent les premiers loci identifiés responsables du développement du CA-CRC et établissent le rôle important que des interactions génétiques jouent dans le développement du CA-CRC. Nous avons aussi défini le locus *Ccs4* dans des lignées de souris recombinantes congéniques (RCS, générées par croisement de souris A/J et B6), et identifié la souris AcB60 comme un modèle d'hyper-susceptibilité au CA-CRC. Cette souris développe 28-fois plus de tumeurs suite à 7 semaines de traitement que les souris parentales A/J ou B6. Des traitements chroniques et aigus au DSS ont permis de constater le développement d'une colite sévère chez les souris AcB60. Les lignées AcB60 et FVB/NJ représentent donc des modèles extrêmement utiles permettant de découvrir les mécanismes moléculaires responsables du développement du CA-CRC précoce. Elles pourront aussi servir à l'identification de facteurs pronostiques ou de cibles thérapeutiques pour les patients humains.

iii) Preface

The research presented within this thesis has been published as follows:

- Chapter 2:** Van Der Kraak, L, Meunier, C, Turbide, C, Jothy, S, Gaboury, L, Marcus, V, Chang, SY, Beauchemin, N, Gros, P. (2010) A two-locus system controls susceptibility to colitis-associated colon cancer in mice. *Oncotarget*. 1(6): 436-46.
- Chapter 3:** Van Der Kraak, L, Jothy, S, Beauchemin, N, and Gros, P. Characterizing the hyper-susceptibility of the AcB60 mouse strain to colitis and colitis-associated colon cancer. *In preparation*
- Chapter 4:** Van Der Kraak, L, Turbide, C, Jothy, S, Beauchemin, N, and Gros, P. Hyper-susceptibility to colitis-associated colorectal cancer in FVB/NJ mice maps to the *Ccs6* locus on mouse chromosome 6. *In preparation*
- Appendix 1:** Van Der Kraak, L., Turbide, C., Beauchemin, N., and Gros, P. Susceptibility to azoxymethane-induced colorectal cancer in inbred mice. *In preparation*

iv) Table of Contents:

i) Abstract	II
ii) Resumé	III
iii) Preface	IV
iv) Table of Contents	V
v) List of Figures	X
vi) List of Tables	XIII
vii) List of Abbreviations	XIV
viii) Acknowledgments	XVIII
Chapter 1: Introduction	1
1.1 The Colon	2
1.1.1 Gross Anatomy	2
1.1.2 Layers of the Colon Wall	2
1.1.3 Cells of the Intestinal Epithelium	3
1.2 Diseases of the Colon	4
1.2.1 Colorectal Cancer.....	4
1.2.1.1 <i>Epidemiology</i>	6
1.2.1.2 <i>Etiology</i>	7
1.2.1.3 <i>Important Cells and Pathways</i>	13
1.2.2 Inflammatory Bowel Disease.....	14
1.2.2.1 <i>Epidemiology</i>	16
1.2.2.2 <i>Etiology</i>	17
1.2.2.3 <i>Pediatric IBD</i>	19
1.2.3 Colitis-Associated Colon Cancer	21
1.2.3.1 <i>Epidemiology and Etiology</i>	21
1.2.3.2 <i>Colitis-Dysplasia-Carcinoma Sequence Progression</i>	23
1.3 Genome-Wide Association Studies	24

1.3.1 GWAS Design	25
1.3.2 Colorectal Cancer.....	26
1.3.3 Inflammatory Bowel Disease.....	29
1.3.4 Colitis-Associated Colon Cancer	31
1.3.5 The Future of GWAS	31
1.4 Mouse Models of Colon Cancer, Inflammatory Bowel Disease and Colitis-Associated Colon Cancer.....	34
1.4.1 Techniques for Gene Identification Using Mouse Models	35
1.4.2 Mouse Models of Colorectal Cancer	36
<i>1.4.2.1 Genetic Models</i>	<i>36</i>
<i>1.4.2.2 Chemical Models</i>	<i>39</i>
1.4.3 Mouse Models of Inflammatory Bowel Disease and Colitis-Associated Colon Cancer	44
<i>1.4.3.1 Genetic Models</i>	<i>45</i>
<i>1.4.3.2 Chemically-Induced Models</i>	<i>46</i>
<i>1.4.3.3 Colitis and Colitis-Associated Colon Cancer Loci: Forward Genetic Mapping Studies</i>	<i>51</i>
1.5 Thesis Objectives.....	53
Chapter 2: A Two-Locus System Controls Susceptibility to Colitis-Associated Colon Cancer in Mice	55
2.1 Connecting Text	56
2.2 Contributions of the Authors.....	56
2.3 Abstract	57
2.4 Introduction	57
2.5 Materials and Methods	59
2.6 Results.....	61
2.7 Discussion	67

2.8 Acknowledgements	72
-----------------------------------	-----------

Chapter 3: Characterizing the Hyper-Susceptibility of the AcB60 Mouse Strain to Colitis and Colitis-Associated Colorectal Cancer 74

3.1 Connecting Text	75
----------------------------------	-----------

3.2 Contributions of the Authors.....	75
--	-----------

3.3 Abstract	75
---------------------------	-----------

3.4 Introduction	76
-------------------------------	-----------

3.5 Materials and Methods	77
--	-----------

3.6 Results.....	79
-------------------------	-----------

3.7 Discussion	84
-----------------------------	-----------

3.8 Acknowledgements	90
-----------------------------------	-----------

Chapter 4: Hyper-Susceptibility to Colitis-Associated Colorectal Cancer in FVB/NJ Mice Maps to the Ccs6 Locus on Mouse Chromosome 6 94

4.1 Connecting Text	95
----------------------------------	-----------

4.2 Contributions of the Authors.....	95
--	-----------

4.3 Abstract	95
---------------------------	-----------

4.4 Introduction	96
-------------------------------	-----------

4.5 Materials and Methods	97
--	-----------

4.6 Results.....	100
-------------------------	------------

4.7 Discussion	106
-----------------------------	------------

4.8 Acknowledgements	111
-----------------------------------	------------

Chapter 5: Discussion and Future Directions 112

5.1 Discussion	113
5.1.1 The Response of Inbred Mice to CA-CRC	113
5.1.2 Genetic Control of CA-CRC in A/J and B6 Mice	114
5.1.3 Hyper-Susceptibility to CA-CRC in Inbred Mice	115
5.1.4 The Importance of Forward Genetic Mouse Studies in Dissecting Complex Trait Genetics	116
5.2 Future Directions	116
5.2.1 Defining CA-CRC Genetic Variants in Our Cohorts of Mice	118
5.2.1.1 <i>Defining the Genes Underlying Susceptibility to CA-CRC in A/J and B6 mice</i>	118
5.2.1.2 <i>Mapping the AcB60 Hyper-Susceptibility Gene</i>	120
5.2.1.3 <i>Genetic Characterization of the Ccs6 Locus</i>	120
5.2.2. Defining Mechanisms of CA-CRC Susceptibility	125
5.2.2.1 <i>Molecular Signatures of AOM/DSS Treated Tumors</i>	125
5.2.2.2. <i>Proliferation and Apoptosis Studies in AOM/DSS Treated Mice</i>	127
5.2.2.3 <i>Studying the Role of Inflammation in AOM/DSS-Induced Tumorigenesis</i>	128
5.2.3 Validation of Mouse CA-CRC Susceptibility Loci in Humans	129
5.2 Conclusions	131
Original Contributions to Knowledge	133
References	134
Appendix 1: Inbred Strain Survey to AOM-Induced CRC	163
A.1.1 Connecting Text	164
A.1.2 Contributions of the Authors	164
A.1.3 Abstract	165
A.1.4 Introduction	165
A.1.5 Materials and Methods	166

A.1.6 Results	167
A.1.7 Discussion	168
Appendix 2	173

v) List of Figures:

Chapter 1: Introduction

Figure 1.1 Anatomy of the Large Intestine	5
Figure 1.2 The inverse relationship between allele frequency and effect size for colorectal cancer genes/loci	9
Figure 1.3 Molecular alterations in sporadic and colitis-associated colorectal cancer	15
Figure 1.4 Genome-wide association study (GWAS) design	27
Figure 1.5 Important pathways in IBD identified in genome-wide association studies (GWAS)	32
Figure 1.6 Breeding of informative populations for forward genetic studies	37
Figure 1.7 Mouse inflammatory bowel disease (IBD) and colorectal cancer (CRC) susceptibility loci	40
Figure 1.8 Azoxymethane and Dextran Sulfate Sodium Structures	50

Chapter 2:

Figure 2.1 Pathology of AOM/DSS induced tumors in parental A/J and B6 mice	63
Figure 2.2 Susceptibility to CA-CRC is not controlled by the <i>Ccs3</i> locus	65
Figure 2.3 Segregation analysis of susceptibility to CA-CRC induced by the AOM/DSS protocol	68
Figure 2.4 Identification and validation of a chromosome 9 CA-CRC susceptibility locus	69
Figure 2.5 Identification of a chromosome 14 modifier of the <i>Ccs4</i> locus	70

Chapter 3:

Figure 3.1 AcB60 mice are hyper-sensitive to AOM/DSS-induced CA-CRC	81
---	----

Figure 3.2 AcB60 mice are hyper-susceptible to CA-CRC	82
Figure 3.3 Pathology of AOM/DSS, acute DSS and long-term DSS colons	86
Figure 3.4 AcB60 mice are susceptible to acute DSS-induced colitis	87
Figure 3.5 AcB60 mice are susceptible to long-term DSS-induced colitis	88
Supplemental Figure 3.1: Weight loss in acute DSS treated A/J, B6 and AcB60 mice	91
Supplemental Figure 3.2: Weight loss in long-term DSS treated A/J, B6 and AcB60 mice	92
Supplemental Figure 3.2: CA-CRC susceptibility in AcB64 recombinant congenic mice	93

Chapter 4:

Figure 4.1 Response of select inbred mouse strains to AOM/DSS-induced CA-CRC	102
Figure 4.2 Macroscopic and microscopic tumor properties in FVB/NJ and C3H/HeJ mice .	104
Figure 4.3 Segregation analysis of AOM/DSS induced CA-CRC susceptibility	107
Figure 4.4 Identification and validation of a susceptibility locus on mouse chromosome 6	108

Chapter 5:

Figure 5.1 Confirmation of the <i>Ccs3</i> and <i>Ccs5</i> loci in AOM-induced CRC	117
Figure 5.2 Breakpoints in the <i>Lmr2</i> congenic mice and phenotyping of BALB/cAnn mice for CA-CRC	121
Figure 5.3 CA-CRC susceptibility in the BcA14 recombinant congenic mouse strain	122
Figure 5.4 Generation of the <i>Ccs4</i> congenic and sub-congenic mouse lines.....	123
Figure 5.5 Allelic Composition of the <i>Ccs4</i> Congenic and Subcongenic Mouse Lines	124
Figure 5.6 Breeding scheme for the (AcB60 x 129S1)F2 mice.....	126

Appendix 1:

Figure A.1.1 Heterogeneity of response of inbred mice to AOM-induced CRC 171

Figure A.1.2 A/J and FVB/NJ colons 172

v) List of Tables:

Chapter 1:

Table 1.1 Human GWAS CRC Susceptibility Loci published prior to May 2014..... 28

Appendix 2:

Table A.2.1 Map Location and Plausible Candidate Genes for Inflammatory Bowel
Disease Loci identified using Genome-Wide Association Studies..... 174

vii) List of Abbreviations

A	Adenosine or Area
ACF	Aberrant Crypt Foci
ADH	Alcohol dehydrogenase
AFAP	Attenuated FAP
AKR1C4	Aldo-keto reductase family 1, member C4
Ala	Alanine
ALM	Adenoma Like Masses
AOM	Azoxymethane
APC	Adenomatous Polyposis Coli
ARCTIC	Assessment of Risk of Colorectal Tumors in Canada
ATG16L1	Autophagy-related protein 16-1
B6	C57Bl/6J
B10	C57Bl/10J
BBN	N-butyl-N-(4-hydroxybutyl)-nitrosamine
BMI	Body Mass Index
BMP	Bone Morphogenetic Protein
BMPR	Bone Morphogenetic Protein Receptor
<i>Bts</i>	<i>BBN-induced bladder tumor susceptibility</i>
C	Cytosine
CA-CRC	Colitis-Associated Colorectal Cancer
CAF	Cancer Associated Fibroblasts
CARD15	NOD2
Casp	Caspase
CCAT2	Colon Cancer Associated Transcript 2
CCDC	Coiled-Coil Domain Containing
<i>Ccs</i>	<i>Colon Cancer Susceptibility</i>
CD	Crohn's Disease
CD4/8	Cluster of differentiation 4/8
<i>Cdcs</i>	<i>cytokine deficiency in colitis</i>
CDH1	E-cadherin
CNV	Copy Number Variant
COLCA	Colon Cancer Associated
COX	Cyclooxygenase
CRC	Colorectal Cancer
DALM	Dysplastic Associated Masses
DCC	Deleted in Colon Cancer
DMH	Dimethylhydrazine
DNBS	2,4-dinitrobenzenesulphonic acid
DPC	Deleted in Pancreatic Cancer
DSS	Dextran Sulfate Sodium
<i>Dssc</i>	<i>dextran sulfate sodium-induced colitis</i>
EM	expectation-maximization
EMMA	Efficiency-Mixed Matrix Association
ENU	N-ethyl-N-nitrosourea

EpCAM	Epithelial cell adhesion molecule
Epith	Epithelium
eQTL	Expression QTL
FAP	Familial Adenomatous Polyposis
FCCTX	Familial Colon Cancer Type X
Fli1	Friend leukemia integration 1 transcription factor
FOBT	Fecal Occult Blood
G	Guanine
GNA	Guanine nucleotide-binding protein
GNAi	Guanine nucleotide-binding protein inhibitor
GO	Gene Ontology
<i>Gpdc</i>	<i>G protein deficiency-induced colitis</i>
GPX	Glutathione peroxidase
GREM	Gremlin
GWAS	Genome-Wide Association Study
<i>Hiccs</i>	<i>Helicobacter hepaticus-induced colitis and associated cancer susceptibility</i>
HLA	Human leukocyte Antigen
HNF	hepatocyte nuclear factor
HNPPC	Hereditary non-polyposis colon cancer
HOX	Homeodomain transcription factor
IBD	Inflammatory Bowel Disease
<i>Ibdq</i>	<i>inflammatory bowel disease quantitative trait loci</i>
IC	Indeterminate colitis
IEC	Intestinal epithelial cell
IFN	Interferon
IL	Interleukin
IL-R	Interleukin Receptor
Indels	Insertions/Deletions
iNOS	Inducible nitric oxide synthase
ip	Intra-peritoneal
IRF	Interferon regulatory factor
<i>ity</i>	<i>immunity to Typhimurium</i>
JAK	Janus Kinase
LAM	Laminin
LD	Linkage Disequilibrium
LKB1	Liver Kinase B1
<i>L. major</i>	<i>Leishmania major</i>
<i>Lmr</i>	<i>Leishmania resistance</i>
lnc	long non-coding
LOD	Logarithm of odds
LOH	Loss of heterozygosity
LP	Lamina Propria
LS	Lynch Syndrome
MAF	Minor Allele Frequency
MAM	Methylazoxymethanol
MAP	MUTYH-Associated Polyposis

Mbp	Megabase pair
M-cell	Microfold-cell
MGI	Mouse Genome Informatics
MHC	Major histocompatibility complex
Min	Multiple Intestinal Neoplasia
MLH	MutL Homolog
MM	Muscularis Mucosa
MMP	Matrix metalloproteinase
MMR	Mismatch Repair Genes
Mom	Modifier of Min
MRPL3	Mitochondrial ribosomal protein L3
MSH	MutS Homolog
MSI	Microsatellite Instability
MSS	Microsatellite Stable
MUTYH	MutY Homolog
N	Nitrogen
NCF	Neutrophil cytosol factor 4
NK	Natural Killer
NLRP	NOD-like receptor family, pyrin domain containing
NOD	Nucleotide-binding oligomerization domain-containing
NSAIDS	Non-steroidal anti-inflammatory drugs
NUDT7	Nucleoside Diphosphate Linked Moiety X-Type Motif 7
O	Oxygen
OR	Odds Ratio
OXA	Oxazolone
p53	Tumor protein 53
Par	Pulmonary Adenoma Resistance
Pas	Pulmonary Adenoma Susceptibility
PTEN	Phosphatase and tensin homolog
PTPN	Tyrosine-protein phosphatase non-receptor
PTPRJ	Receptor-type tyrosine-protein phosphatase
PMS	PMS2 postmeiotic segregation increased
PRADC1	Protease-associated domain containing 1
PSPH	Phosphoserine phosphatase
QTL	Quantitative Trait Loci
Rb1	Retinoblastoma
RCS	Recombinant Congenic Strain
RHPN2	Rhophilin
RI	Recombinant Inbred
RNA	Ribonucleic Acid
ROS	Reactive Oxygen Species
RR	Relative Risk
Sc	Subcutaneous
ScC	Susceptibility to Colon Cancer
SFXN4	Sideroflexin 4
SIR	Standardized Incidence Ratio

Skap	Src kinase associated phosphoprotein
SKT11	Serine/Threonine Kinase 11
SLC	Solute Carrier Family
Sluc	Susceptibility to lung cancer
SMAD	Mothers against decapentaplegic homolog
SNP	Single Nucleotide Polymorphism
STAT	Signal transducer and activator of transcription
T	Thymine
<i>T. crassiceps</i>	<i>Taenia crassiceps</i>
<i>Tccr</i>	<i>Taenia crassiceps resistance locus</i>
TGF	Transforming Growth Factor
Thr	Threonine
TLR	Toll-like Receptor
<i>Tm</i>	<i>Trishuris muris</i> -induced colitis
<i>Tnbs</i>	<i>trinitrobenzene sulfonic acid susceptibility</i>
TNBS	2,4,6-trinitrobenzenesulfonic acid
TNF	Tumor Necrosis Factor
T _H	T-helper
Tregs	T-regulatory cells
TWSG1	Twisted gastrulation BMP signaling modulator 1
TYK	Tyrosine Kinase
UC	Ulcerative Colitis
UTR	Untranslated Region
UACA	Uveal Autoantigen With Coiled-Coil Domains And Ankyrin Repeats
UK	United Kingdom
VEO	Very Early Onset
WNT	Wingless-type MMTV integration site family
XBP	X-box binding protein
XIAP	X-linked inhibitor of apoptosis protein
ZNF	Zinc Finger Protein

viii) Acknowledgements

First and foremost I would like to thank my supervisors, Dr. Nicole Beauchemin and Dr. Philippe Gros. The last 6 years have been such an amazing opportunity and you have both provided me with a wealth of knowledge that will aid me as I transition into the next stage of my career.

These experiments would also not have been possible without the help of my various collaborators and lab mates. I also would like to thank our lab's colon cancer team consisting of Charles Meunier and Claire Turbide for the memorable experiences.

I would like to express my appreciation to Rusty Jones and William Foulkes for all their feedback and suggestions throughout my degree. I am eternally grateful to the CIHR and the McGill Integrated Cancer Research Training Program for funding me throughout my degree.

Lastly, to all my friends and family . . . Thank you! I don't know what I would have done without you. Not only did you put up with my crazy mouse stories and bizarre hours, but you also provided the moral support necessary to get me over the hurdles and obstacles that I encountered during my degree.

Chapter 1: Introduction

(Review of the Current Literature)

1.1 The Colon

The large intestine, the second-to-last part of the digestive tract, is a long tubular organ that functions to absorb water, salts and vitamins from digested food to form fecal matter for excretion ¹. The large intestine can be divided into three sections; the cecum, the colon and the rectum and measures between 8-14 centimeters in mice and 1.5 meters in humans ^{1, 2}. The purpose of this section is a general overview of mouse and human colon anatomy focusing on the colonic mucosa, the primary site of disease in our experimental models.

1.1.1 Gross Anatomy

The mouse colon is typically divided into three sections; the proximal, mid and distal colon, with the latter situated next to the rectum (Figure 1.1A) ³. V shaped folds, which act to slow the passage of food particles through the colon, characterize the mouse proximal colon. The mid colon is flat and the distal colon has longitudinal folds ⁴. In mice, the rectum measures 1-2 mm and for all intents and purposes, the rectum will be referred to as part of the distal colon henceforth ³. The cecum and proximal colon in mice corresponds to the right colon in humans (appendix, cecum, ascending colon, and the first half of the transverse colon) and the mid and distal colon corresponds to the left colon in humans (remaining part of transverse, descending and sigmoid colons and rectum).

1.1.2 Layers of the Colon Wall

The colon wall consists of four distinct interconnected layers that act together to regulate colon function (Figure 1.1B) ¹. The adventitia and serosa, the outer most layers, surround the retroperitoneal and intraperitoneal aspects of the colon, respectively and act to stabilize and protect the colon during motion. The muscularis propria, consisting of both longitudinal and circular muscle layers produces rhythmic contractions known as peristalsis that push food through the digestive tract. The submucosa, situated between the muscularis propria and the mucosa, is composed of connective tissue and contains adipose tissue, veins, arteries and lymphatic vessels.

The mucosa, the innermost layer of the colon, is the site of disease in our models and is comprised of the muscularis mucosae, the lamina propria and the epithelium (Figure 1.1 B) ¹. The muscularis mucosae, which controls fine movements of the colon is located at the base of the lamina propria and adjacent to the submucosa. The lamina propria is a layer of connective tissue containing blood, lymphatic tissue and lymphoid cells such as eosinophils and

macrophages. It is also the source of many signalling molecules that are essential for maintaining intestinal homeostasis. The epithelium, the innermost layer, consists of a single continuous layer of intestinal epithelial cells (IECs), which form a barrier protecting the host from invasion of the microflora of the intestinal lumen ⁵. The intestinal epithelial layer is renewed every 3-5 days in most mammals and every 7 days in humans ⁶. The intestinal epithelium forms tubular glands, crypts of Lieberkühn, which extend deep into the lamina propria (Figure 1.1 C) ^{7,8}.

1.1.3 Cells of the Intestinal Epithelium

The intestinal crypt is lined with 250-300 IECs, which arose from pluripotent stem cells located at the base of the crypts ⁵. Over a period of 3 days, these new cells will differentiate into the cells that contribute to overall colonic epithelial architecture; columnar absorptive cells, goblet cells, enteroendocrine cells, m-cells, tuft cells and cup cells (Figure 1.1 C). Paneth cells are not generally present in the colon of healthy individuals, but are aberrantly expressed in disease states and hence will be discussed in this Introduction. IECs (with the exception of Paneth cells) migrate from the crypt in an upward movement towards the lumen. Differentiation begins in the lower middle portion of the crypts and culminates when the IECs reach the highest two thirds of the crypt ⁹. When cells reach the epithelium at the tip of the crypt they are shed into the lumen via anoikis, a form of programmed cell death whereby cells detach from the underlying matrix ¹⁰. In diseases such as cancer, this balance between proliferation, differentiation and apoptosis is disrupted.

Absorptive enterocytes, the most abundant IEC, are characterized by hundreds of microvilli on their apical border and function to absorb/transport nutrients ⁶. Interspersed among these enterocytes are goblet cells, which secrete mucin and trefoil proteins. These increase in abundance from the duodenum (4%) of the small intestine to the distal colon (16%). Mucins are heavily glycosylated proteins, which form a protective barrier between epithelial cells and the luminal bacteria of the colon, while also aiding in the propulsion of stool through the colon lumen. Trefoil proteins are thought to be important in stabilizing the mucous layer and healing damage regions of the epithelium. Enteroendocrine cells (1% of total epithelial cells) secrete peptide hormones that help coordinate intestinal functions. M-cells, tuft cells and cup cells are minor components of the intestinal epithelium, with little known about the function of the later

two ¹¹. M or microfold-cells overlie regions of gut-associated lymphoid tissue and serve as an interface between the luminal contents and immune cells. As mentioned, Paneth cells are not generally present in the colon of healthy individuals, but are aberrantly expressed in disease states. These metaplastic paneth cells are common in areas of high inflammation and may be a host adaptive response to a compromised epithelial barrier. Paneth cells are relatively long-lived cells that reside near the base of the crypts where they act to protect the host from luminal bacteria/pathogens through the secretion of various antimicrobial peptides ¹². Paneth cells also aid in the maintenance of intestinal stem cells.

1.2 Diseases of the Colon

The physiological, cellular and biochemical pathways controlling proliferation, differentiation and apoptosis of IECs are diverse, and involve complex interactions between many genes/proteins ⁵. IECs are continuously sampling the variable contents of the colon lumen and responding in turn. Failure to respond or disruption of the balance with respect to cell turnover can result in loss of intestinal homeostasis, leading to disease. Digestive disorders affect close to 20 million Canadians each year, with each disease associated with its own unique etiology and complications (www.cdhf.ca). Within this thesis, three diseases will be discussed; colorectal cancer, inflammatory bowel disease and colitis-associated colorectal cancer.

1.2.1 Colorectal Cancer

Colorectal cancer (CRC) is a term used for cancers arising in the colon or rectum. CRCs arise due to the accumulation of various genetic and epigenetic mutations within IECs that transform the normal colonic epithelium to invasive carcinoma and subsequent metastatic disease ¹³. Disease prognosis is largely dependent upon the stage of disease at time of diagnosis with patients having an estimated 90% 5-year survival rate when the disease is detected in the early-localized stage as opposed to a 10% survival rate upon late-stage metastatic CRC ¹⁴. This thesis uses models of non-metastatic CRC and therefore CRC metastasis will not be discussed further. Many of the clinical signs and symptoms underlying CRC development (blood in the stool, abdominal pain, weight loss and fatigue) are missed or are not present until later stages of disease and therefore routine screening of individuals is recommended to enable detection of early-stage CRC ¹⁵.

In Canada, it is recommended that individuals over the age of 50 be screened for CRC at least once every two years ¹⁶. Depending on the patient's history this may involve a fecal occult

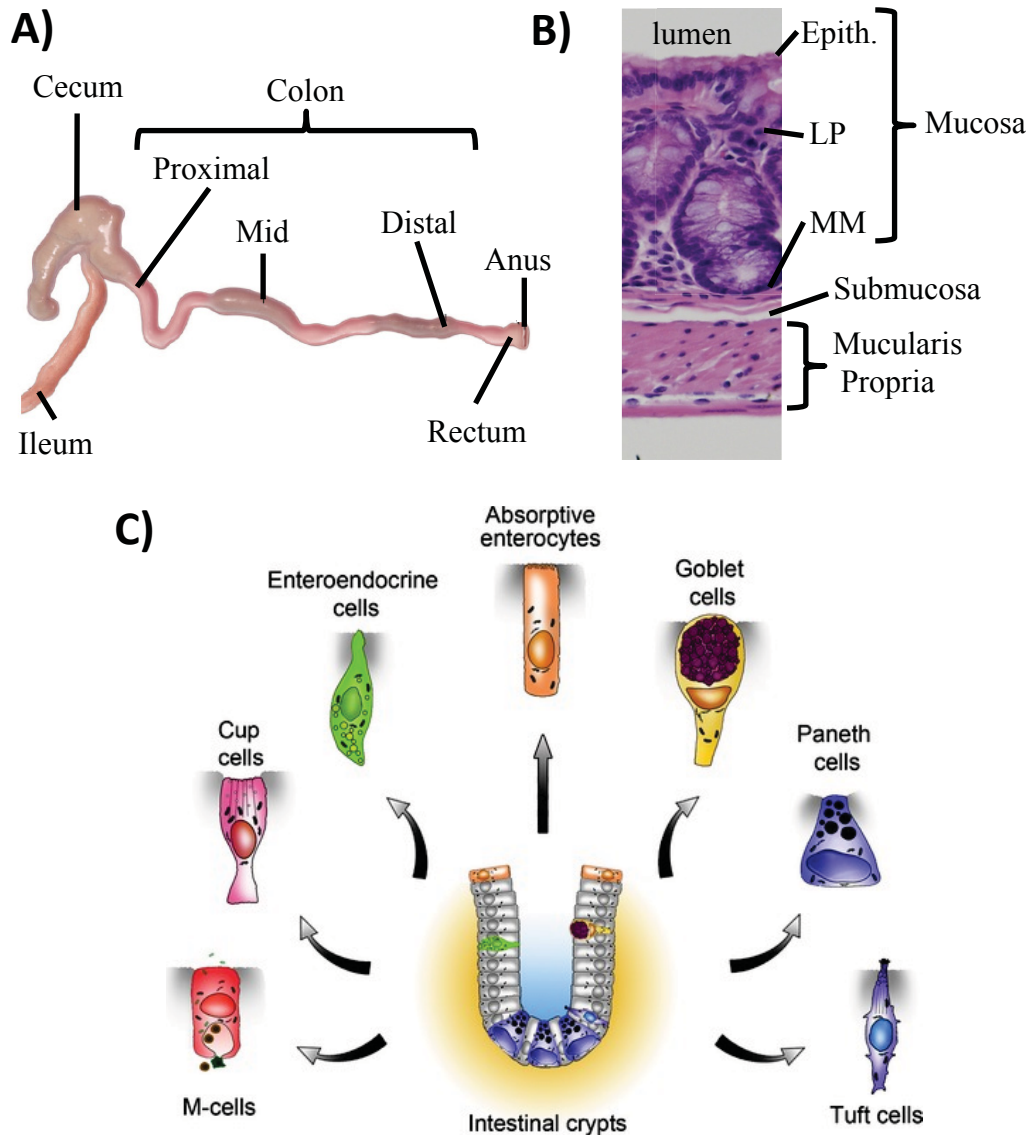


Figure 1.1: Anatomy of the Large Intestine. (A) Gross anatomy of the mouse colon. (B) Hematoxylin and Eosin stained cross section of an untreated mouse colon, showing the layers of the colon wall. The serosa/adventitia was removed during processing and therefore is not shown. Epith- epithelium, LP- lamina propria, MM- muscularis mucosa. (C) Anatomy of an intestinal crypt and representative epithelial cell types. Paneth cells are only found in the small intestine and are absent in the colon. *Adapted with permission from Treuting et al. 2012 and Gerbe et al 2012*^{3, 11}.

blood test (FOBT) or colonoscopy. These tests may be conducted earlier in individuals with strong family history of disease or symptoms consistent with CRC. Individuals with positive FOBT tests or who have suspicious lesions detected using colonoscopy are sent for additional diagnostic tests, which include computed tomography testing, ultrasound, specialized x-rays with barium enema contrast and/or blood tests. A definitive diagnosis is obtained by analyzing biopsy samples of colonic lesions collected during colonoscopy for histology and the presence of mutations or protein markers consistent with CRC. Treatment options, which vary based on cell of origin and degree of invasion, include surgery, radiofrequency ablation, cryosurgery, chemotherapy, radiation and/or targeted therapy ¹⁶.

1.2.1.1 Epidemiology

CRC is a global disease accounting for approximately 9.5% of cancer cases worldwide, with about 1 million new cases diagnosed each year ¹⁷. There is a male bias in rectal cancer, whereas colon cancer affects men and women in approximately equal proportions. Approximately, 55% of CRCs arise in developed regions within North America, Europe and Oceania ¹⁸. CRC incidence rates in developed countries have been decreasing or stabilizing over the last few years ¹⁹. However, there has been an alarming trend of increased CRC incidence in previously low risk economically transitioning countries such as Asia, parts of Africa and South America over the last few years, with rates in Eastern Europe increasing most rapidly.

Despite overall decreased or stabilizing CRC incidence in the developed world, there has been an increase in early-onset (< 50 years old) non-Mendelian associated CRCs in both North America and Europe ¹⁹⁻²². In the United States, for example, CRC incidence rates decreased by 3.4% per year between 2001 and 2010 ^{20, 22}. However, this was accompanied by a significant increase (1.3% and 1.8% per year for distal colon and rectal cancers, respectively) in individuals below 50 years of age. The etiologies of these early-onset CRCs are not well understood, but could be related to increased rates of childhood obesity and diabetes ²⁰.

The median worldwide 5-year survival for CRC is 50%, with developed countries having lower mortality rates than developing countries ¹⁷. Mortality is strongly associated with stage of disease at diagnosis and the advent of CRC screening technologies such as colonoscopy and FOBT have been attributed to earlier detection and decreased CRC mortality over the last decade ¹⁸. Since routine testing for CRC in most developed countries commences between 45 and 50

years of age, early-onset CRC patients fall into a gap in care, frequently presenting with more advanced disease at diagnosis²³. Consistent with this advanced stage of disease at diagnosis several studies have shown decreased 5-year survival rates in early-onset CRC²⁴⁻²⁶. Recent studies have challenged this notion suggesting similar survival between early and late-onset CRC²⁷⁻²⁹. In these studies, it appears that the detrimental effects of advanced disease are balanced out by better overall health conditions and faster post-operative recovery times. These early-onset CRCs are a growing concern and present their own unique risk and challenges that need to be assessed.

1.2.1.2 Etiology

CRCs arise due to the accumulation of mutations in numerous key tumor suppressors or oncogenes resulting in the transformation of the normal epithelium to adenomas and subsequent carcinomas¹³. The circumstances enabling the accumulation of these mutations are diverse involving a combination of one or more genetic, dietary, environmental and/or lifestyle risk factors, which are detailed below³⁰.

1.2.1.2.1 Genetic Risk Factors

Genetic pre-disposition is predicted to underlie approximately 35% (confidence interval: 10-48%) of CRCs, according to a Finnish, Danish and Swedish twin study, and is one of the strongest pre-disposing CRC risk factors, second only to age at diagnosis³¹. Inherited CRC syndromes are associated with earlier (<50 years) onset compared to sporadic or non-genetic associated CRC syndromes (> 60 years)³⁰. Genetically, CRCs can be further categorized on a sliding scale of pre-disposing risk, which describes the predicted effect size of a given CRC risk variant compared to the minor allele frequency (MAF, the abundance of the minor allele within a reference population) (Figure 1.2)³². At one extreme, there are the rare, but well-characterized Mendelian or Hereditary CRC syndromes, whose mutations are associated with a high penetrance of disease symptoms and are easily identified in large families with multiple affected individuals (section 1.2.1.2.1.1). The remaining CRCs are often referred to as familial CRCs and present with fewer affected individuals per family³³. These CRCs were originally hypothesized to arise due to rare, yet to be discovered, highly penetrant disease variants³⁴. However, little success has been had identifying variants in these families using whole-exome sequencing or familial mapping approaches. Therefore, it has been speculated that many of these familial CRCs may in fact arise due to polygenic mechanism of inheritance. In this model common

variants (single nucleotide polymorphisms each conferring a small amount of total disease risk) in low penetrance tumor susceptibility genes act in conjunction to modulate differential CRC susceptibility within a population and be identified using genome-wide association studies (section 1.3.2) ³³.

1.2.1.2.1.1 Hereditary Colorectal Cancer Syndromes

Hereditary CRCs arise due to highly penetrant germline mutations and these account for approximately 5% of overall disease burden. There are several forms of hereditary CRC that each present with their own unique clinical and genetic challenges. These hereditary CRCs can be subdivided into polyposis and non-polyposis syndromes.

The most well characterized polyposis CRC syndrome is Familial Adenomatous polyposis (FAP), accounting for ~1% of all CRC cases ³⁵. The clinical presentation, genetic characteristics and treatment of FAP have been extensively detailed in Galiatsatos et al ³⁶. FAP is characterized by early-onset (early 20's) of hundreds to thousands of polyps throughout the large intestine. Without prophylactic surgical treatment these benign polyps will progress to CRC by the third and fourth decades of life. FAP is an autosomal dominant condition arising due to mutations in the tumor suppressor *Adenomatous polyposis coli* (*APC*) gene on human chromosome 5q21, with more than 700 different *APC* mutations identified to date ³⁷. The remaining wild-type copy of *APC* is also lost or mutated in tumors. FAP is a heterogeneous disease with patients presenting with differences with respect to age of onset, location/number of tumors and various extra-colonic features. Extra-colonic features include dental abnormalities, congenital hypertrophy of the retinal pigment epithelium, desmoids and additional tumors (gastric, thyroid and brain) ^{35, 36}. The location of the various *APC* mutations within the gene are expected to contribute in part to some of the variation in FAP symptoms, with attenuated forms of disease being associated with mutations in the 3' or 5' untranslated regions ³⁸. However, there is still significant variation between individuals with similar mutations and mouse models have recently identified several genetic modifiers of FAP (section 1.4).

Several other hereditary polyposis CRC syndromes have been identified and together explain less than 1% of CRC risk ³⁵. Attenuated FAP (AFAP) is associated with fewer tumors (25 > and < 100) affecting more proximal regions of the colon and delayed CRC-onset compared to classical FAP ³⁹. Like FAP, AFAP is associated with dominant *APC* mutations. These

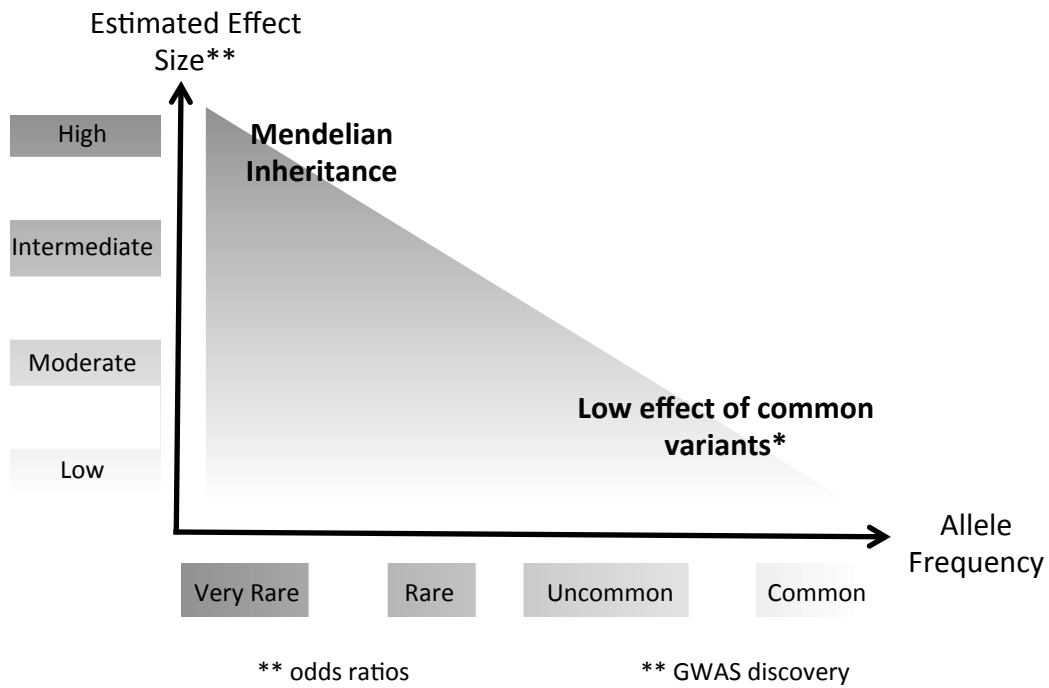


Figure 1.2: The inverse relationship between allele frequency and effect size for colorectal cancer genes/loci. Approximately 30% of CRCs arise in genetically pre-disposed individuals. The current view suggests that in CRC, as well as many other complex traits, there is an inverse relationship between allele frequency in the population and effect size (penetrance). Mendelian diseases, associated with high penetrance, but low allele frequencies represent one extreme. The other extreme are common variants or single nucleotide polymorphisms that are low penetrance. Genome wide association studies are designed to identify these uncommon or common variants with low to modest effect sizes. *Adapted with permission from Chung et al. 2010*³².

mutations are less penetrant than FAP mutations and typically cluster in the 3' or 5' untranslated regions (UTR) or exon 9. Autosomal recessive MUTYH-associated polyposis (MAP) can mimic either FAP or AFAP, with respect to early clinical presentation with patients developing between 10 and 1000 early-onset colorectal polyps⁴⁰. MAP patients also frequently develop subsequent later-onset ovarian, bladder, skin, breast and/or endometrial tumors. MAP is associated with mutations in the base excision repair gene, *MUTYH*. *MUTYH* functions to correct oxidative DNA damage to guanine residues, usually found within GAA consensus sequences, and when mutated leads to the accumulation of G:C to T:A transversions within the genome. Sequencing of colorectal tumors from MAP patients show high numbers of transversions in the *APC* gene, which explains the high prevalence of CRC in these patients. The *APC* gene has a high number (n=216) of GAA trimers in comparison to other known cancer related genes, which may explain the early-onset colorectal tumor formation in MAP patients compared to other cancer syndromes in MAP patients. Peutz-Jeghers syndrome is an early onset dominant cancer syndrome with tumors developing throughout the gastrointestinal tract⁴¹. It is characterized by mutations in the serine/threonine kinase *LKB1/STK11* and is often distinguished due to melatonin pigmentation of the lips and mouth. Juvenile polyposis (associated with mutations in the TGF- β signaling pathways genes: *BMPRIA* and *SMAD4*), hyperplastic polyposis (unknown genetic origin) and Cowden's Syndrome (mutations in *PTEN*) are examples of rare hamartomatous polyposis syndromes with pre-disposing genetic risk⁴².

Hereditary non-polyposis (HNPCC) CRC accounts for approximately 3% of all CRCs. These generally fall into three classes; Lynch Syndrome (LS), Lynch-like and Familial Colon Cancer Type X (FCCTX)⁴³. Each of these syndromes is associated with differences with respect to onset and progression of tumors and therefore proper diagnosis is essential with respect to managing and treating disease. Most HNPCC fulfill a set of diagnostic criteria referred to as the Amsterdam Criteria (described in⁴⁴). Approximately half of HNPCCs are LS. LS is described genetically, rather than clinically (Amsterdam Criteria), and is associated with autosomal dominant mutations in the mismatch repair (MMR) genes, which are essential for repairing single base mismatches and insertion/deletion loops in the DNA⁴⁵. Mutations within *MLH1* and *MSH2* account for approximately 90% of all LS cases. Other genes implicated in LS include *MSH6*, *MLH3*, *PMS2* and *EpCAM*. The aforementioned mutations lead to microsatellite instability (MSI), a tumor characteristic associated with better overall prognosis compared to

cancers lacking MSI⁴⁶. Clinically, these tumors are poorly differentiated and contain large numbers of tumor-infiltrating lymphocytes. Individuals diagnosed with LS are also at increased risk of developing endometrial, gastric, ovarian, small bowel, pancreatic, hepatobiliary and brain cancers⁴⁷. Lynch-like, also known as Tumor-Lynch Syndrome is similar to LS, but the specific genetic etiologies underlying susceptibility are not well characterized. These patients meet the Amsterdam Criteria (either I or II), have tumors showing evidence of MSI, but do not have germline mutations in the known LS genes. Most non-LS HPNCC cases are FCCTX. These tumors are defined clinically as families meeting the Amsterdam I criteria (sometimes Amsterdam II), but are microsatellite stable (MSS) and do not have MMR germline mutations^{48, 49}. The specific genetic etiology underlying these tumors is unknown, but several putative genes and pathways are discussed in detail in⁴⁸. FCCTX differs from LS with respect to later-onset, a more distal location within the colon, a higher rate of multiple adenomas and is associated with less rapid transformation. Extra-intestinal manifestations are less common in FCCTX than LS.

Hereditary CRCs have contributed significant knowledge with respect to essential genes and pathways in tumor initiation and progression. These hereditary CRCs, however also have significant genetic heterogeneity and therefore are most likely influenced by additional genetic and environmental modifiers. The study of other types of CRCs, such as those arising due to rare familial CRC genes or low penetrance tumor susceptibility genes, may contribute to increased understanding of hereditary CRCs.

1.2.1.2.1.2 Familial Colorectal Cancer Susceptibility Genes

Familial CRCs account for 25-30% of all CRC cases and are thought to arise due to either rare highly penetrant yet to be identified mutations, or multiple interacting low penetrance tumor susceptibility genes. The search for highly penetrant CRC loci in families with small numbers of affected individuals has not been highly successful^{34, 50, 51}. The largest study to date, screened 86 Finnish families using whole exon sequencing and identified 14 truncating mutations in 11 genes (*UACA*, *SFXN4*, *TWSG1*, *PSPH*, *NUDT7*, *ZNF490*, *PRSS37*, *CCDC18*, *PRADCI*, *MRPL3*, and *AKRIC4*) that were rare or absent in unaffected Finnish controls³⁴. The mechanism through which these variants act still needs to be elucidated, but these genes may help to explain some of the risk associated with CRC development. To date, more than 30 different low penetrance tumor susceptibility loci have been identified and will be presented in section 1.3.2. It is

interesting to note though that there is no overlap between the loci/gene identified in familial based mapping and genome-wide association studies, suggesting that both approaches may be essential to uncover all of the genetic variation associated with CRC risk.

1.2.1.2.2 Non-Genetic CRC Risk Factors

Regardless of underlying etiology, non-genetic factors (diet, microbial, lifestyle and environment) are known to influence CRC risk/prognosis. Support for the role of non-genetic risk factors in CRC comes from studies of first and second-generation immigrants to American and Australia^{52, 53}. These studies demonstrated a shift in CRC incidence from that of the country of ethnic origin to that of the immigrant country over two generations. This was largely attributed to significant changes with respect to diet. While numerous studies evaluating possible risk factors have been conducted, these often produced conflicting results. This could be the result of underlying differences with respect to risk in various study populations, unforeseen confounding risk factors and/or inadequate sample sizes to detect associations. Some of the discrepancies have been resolved in large-scale meta-analysis and mechanistic studies are now being undertaken.

One of the most well characterized risk factor for CRC is age. More than 60% of CRCs are diagnosed in individuals 65 or older, with 12% of these arising in individuals older than 85⁵⁴. These age related CRCs are generally referred to as sporadic cancers, due to the lack of clear genetic association or familial trends. In comparison less than 5.5% of CRCs are diagnosed in individuals under 45. This age-related increase in CRC risk is most likely due to increased time of exposure to various environmental and dietary risk factors as well as individuals having less efficient cellular repair mechanisms⁵⁵.

While studies have produced conflicting results with respect to dietary and lifestyle influence on CRC risk, it is generally accepted that CRC is associated with diets high in red meats and alcohol and low in fruits, vegetables and fiber⁵⁶⁻⁵⁸. Poor diets often contribute to obesity and individuals with a body mass index (BMI) greater than 30 are also at high risk of developing CRC⁵⁹. This risk is increased further when additional complications of obesity, such as type II diabetes are present⁶⁰. A parallel increase in CRC risk associated with a high fat diet and obesity has been confirmed in rodent models of CRC⁶¹. Smoking is an additional well-characterized CRC risk factor^{62, 63}.

The role of the microbiome in human CRC is complex, contradictory and controversial. Numerous studies have identified significant alterations with respect to microbial composition between CRC patients and healthy controls ^{61, 64, 65}. However, unique patterns are identified in different studies and can be hard to replicate. In addition it is not clear if these microbial alterations are drivers of CRC or the result of CRC development. In addition diet has been linked to alterations in microbial composition with increased anti-neoplastic metabolites and decreased CRC biomarkers in the colon following transition from a “Westernized” (low fiber, high meat/fat content) diet to “African” (high fiber, low meat/fat content) diet ⁶⁶. It is speculated that the protective effect of these high fiber diets may be regulated in part by levels of butyrate, a bacterial byproduct of fiber fermentation, in the colon, but this has yet to be validated ⁶⁷. These dietary, environmental and lifestyle risk factors have been highlighted, as they are important possibly confounding variables to consider when designing genetic studies to map tumor susceptibility genes.

1.2.1.3 Important Cells and Pathways

Regardless of the underlying CRC molecular etiology, the ability of a normal cell to progress to a tumor cell with metastatic potential requires the cell to accumulate a series of genetic mutations ⁶⁸. The progression and accumulation of these mutations fall into two categories that are mimicked in either FAP or HNPCC, suggesting the importance of hereditary cancers in understanding overall CRC progression and pathology ^{13, 68}. In CRC, the balance between cell proliferation, differentiation and apoptosis becomes progressively disrupted through the accumulation of mutations in several signalling pathways; namely the *WNT*, *RAS*, *p53*, *DCC* and *TGF- β* ⁶⁹. The earliest manifestation of colorectal neoplasia is the appearance of aberrant crypt foci (ACF), where a few crypts show either non-dysplastic or dysplastic cells, both of which are associated with mutations in the *APC* gene ⁶⁸. The ACFs will progress to form either hyperplastic or adenomatous polyps that represent benign tumors protruding into the lumen of the intestinal epithelium and are associated with mutations in the *RAS* genes. While hyperplastic polyps conserve their normal architecture and cellular morphology, adenomas exhibit abnormal cellular organization with multi-layering, enlarged nuclei and disruption of basement membrane adhesiveness ^{68, 69}. Adenomas under certain conditions may progress into carcinomas that show major structural disorganization and invasiveness. Genetic changes also accompany the

progression to the carcinoma stage following either the chromosome instability (CIN) route (85% of CRC) associated with alterations in *SMAD2*, *SMAD4*, *DCC*, *p53* or the microsatellite instability (MSI) route associated with alterations in the mismatch repair genes. Figure 1.3 A and B shows the structural and genetic changes associated with progression from the normal colon to invasive carcinoma.

1.2.2 Inflammatory Bowel Disease

Inflammatory Bowel Disease (IBD) is an umbrella term used to describe chronic-relapsing inflammatory conditions of the intestinal tract⁷⁰. While there are several subtypes of IBD, the two most common are Crohn's Disease (CD) and Ulcerative Colitis (UC). Henceforth, IBD will be used as a term to describe both CD and UC. CD and UC differ with respect to location, extent of inflammation, symptoms, as well as treatment^{70, 71}. CD is characterized by inflammation throughout the entire gastro-intestinal tract with lesions most commonly found in the small intestine and proximal colon^{42, 72}. In CD, the inflammation is transmural, traversing multiple layers of the intestine, and typically occurs in patches. In UC, inflammation arises in the rectum and spreads proximally in a continuous manner, rarely extending into the small intestine and is confined to the mucosal layer. More detailed descriptions of CD vs UC can be found in^{70, 71}. About 10-15% of clinical cases of IBD present with mixed CD and UC features and are referred to as indeterminate colitis (IC)^{73, 74}. IC is common in IBD patients under the age of 10⁷⁵. Extra-intestinal manifestations are present in 40% of IBD patients and affect the eyes, muscles, skin, kidney and liver (reviewed in⁷⁶).

IBD typically present between the ages of 15 and 30 and is associated with abdominal pain, cramping, diarrhea, weight loss and/or fatigue^{70, 77, 78}. Diagnosis is initially made using a combination of family history and clinical evaluation and is subsequently confirmed by serological and histological findings (reviewed in^{77, 78}). IBD pathology is highly dependent on the stage of the disease at presentation. Active disease is associated with decreased crypt density, crypt distortion (shortening and branching) and inflammatory cell infiltrates⁷⁹. Crypt abscesses and thinning of the protective mucin layer in the lumen of the colon are associated with active UC, whereas thickening of the bowel wall and presence of granulomas (collections of monocytes/macrophages) are more common in CD.

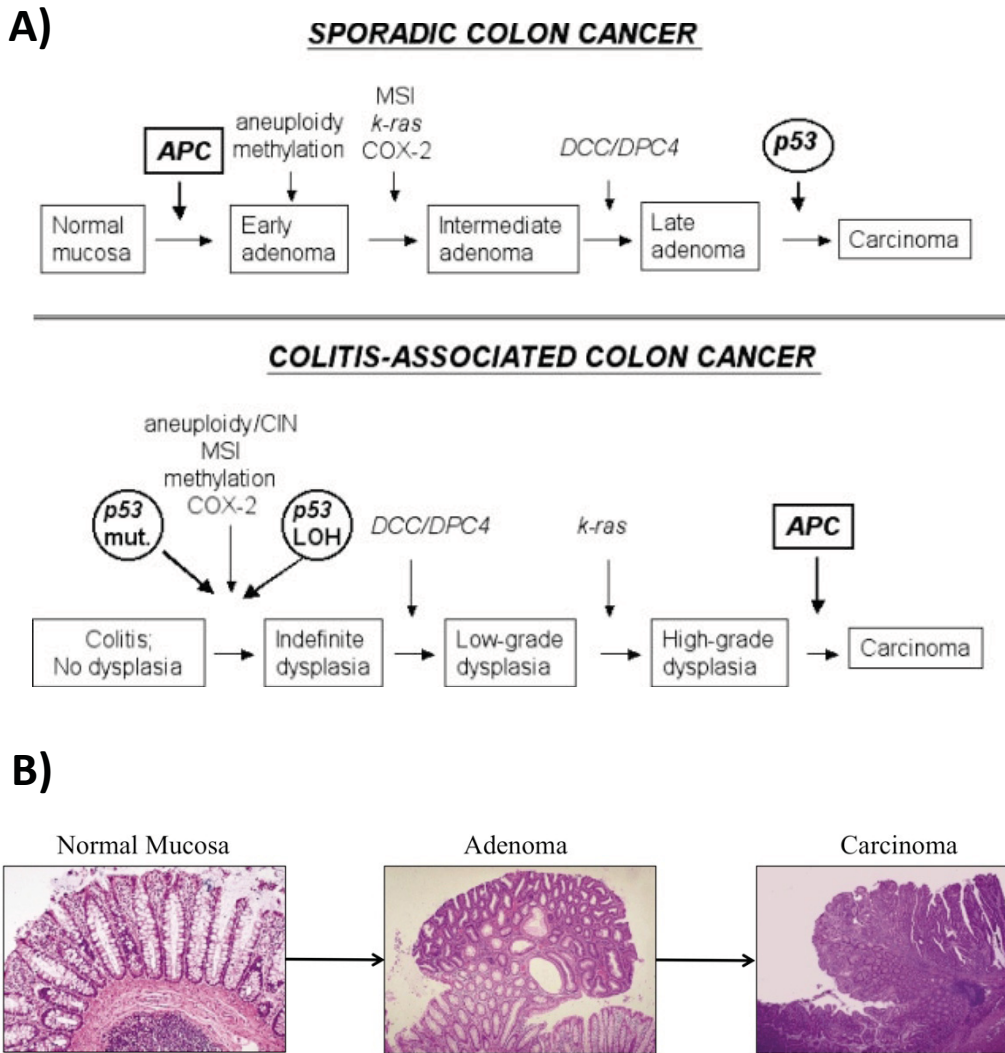


Figure 1.3: Molecular alterations in sporadic and colitis-associated colorectal cancer. (A) Molecular pathogenesis of sporadic/familial colon cancer (*top*) and colitis-associated colon cancer (*bottom*). *COX-2*, *Cyclooxygenase-2*; CIN, chromosomal instability; MSI, microsatellite instability; mut, mutation; LOH, loss of heterozygosity; *DCC*, *Deleted in Colorectal Cancer*; *DPC*, *Deleted in Pancreatic Cancer*; *APC*, *Adenomatous Polyposis Coli*. (B) Structural changes associated with sporadic CRC progression. Adapted with permission from: Itzkowitz and Yio. 2004 and Fodde et al. 2001^{68,250}.

There is no cure for patients with IBD and therefore treatment focuses on management of disease symptoms during periods of relapse and achieving longer disease-free periods. In some instances dietary changes, such as removing certain food groups, can obtain favourable results^{80, 81}. Most cases are managed medically and involve treatment with anti-inflammatory drugs, immunosuppressants, biologic agents and/or antibiotics⁷¹. Over the course of their life, 75% of CD patients will require surgery removed severely damaged tissue or to correct disease complications such as fistulas, abscesses and/or obstructions⁸². Removal of infected tissue is not a cure for CD with 80% of patients relapsing within 20 years⁸³. Colectomy, removal of infected parts or all of the colon, offers a “cure” for UC patients, but presents considerable challenges and disease risks of its own⁷⁰.

1.2.2.1 Epidemiology

The incidence rates of IBD worldwide are difficult to ascertain due to a lack of available information and variability in diagnosing IBD. It is estimated however that incidence varies from <1-24.3/100,000 people for UC and <1-20.2/100,000 people for CD in Asia, Europe, North America and the Middle East⁸⁴. There is agreement among studies that IBD rates are highest in Western and Northern Europe, Australia and North America and lowest in Africa (excluding South Africa), Asia and South America⁸⁴⁻⁸⁶. For example, Canada has one of the highest rates of IBD with ~ 0.7% of the population affected and 10,200 new cases diagnosed each year⁷⁰. UC in most countries is more common than CD, although this does not hold true in Canada and some parts of Europe where CD is more common, although this trend has been variable over the last 20 years⁸⁴.

Male to female ratios of UC and CD vary based on geographic location and age of patients⁸⁴. In Canada, there is a higher incidence of CD in females than males and no gender difference in adult UC⁷⁰. IBD is more common in the Ashkenazi Jewish population and is rare in Native North Americans^{87, 88}. North American studies suggest that Caucasians are at high risk of developing IBD and that rates are increasing in African Americans. IBD rates are lower in Latino and Asian Americans^{70, 89, 90}.

The rates of IBD have been changing dramatically over the last half of a century. A large-scale meta-analysis of 107 IBD studies (57 CD and 50 UC) showed that CD incidence increased in 75% of CD studies and 60% of UC studies over a period of at least 10 years⁸⁴.

When limited to studies conducted before 1980, 56% of CD and 29% of UC studies showed increased incidence rates and less than 6% of studies showed a decrease in incidence of UC over time. No studies reported a decrease in CD. Therefore, it was concluded that IBD incidence is increasing or stabilizing in the areas studied. IBD patients exhibit a low mortality rate and therefore the global prevalence of IBD is expected to increase.

1.2.2.2 Etiology

Despite significant advances in the diagnosis and treatment of IBD, the underlying etiologies of the disease are still not entirely understood. It is generally thought that the tissue damage underlying IBD pathology is the result of strong immune responses elicited against the commensal bacteria in the lumen of the intestine⁷². Evidence for the strong role of luminal bacteria was noted in several studies whereby mice raised in germ-free environments failed to develop signs of IBD^{91, 92}. It is less clear though as to what specifically promotes an intestinal environment favouring disease. Possible pre-disposing environmental (diet, lifestyle), microbial, immune and genetic risk factors are discussed below.

1.2.2.2.1 Genetic Risk Factors

Genetic risk has been determined as one of the most important contributors to IBD susceptibility. Twin studies in Europe estimate the concordance rate for monozygotic twins to be between 17-64% and 6-19% for CD and UC, respectively⁹³⁻⁹⁷. Between 5 and 44% of patients present with a family history of IBD at diagnosis (first degree affected relative), with more familial associations in early-onset cases^{75, 97}. Primarily, IBD has been associated with numerous common low penetrance variants (single nucleotide polymorphisms) within the genome that act together with each other and environmental/dietary factors to contribute to disease risk. These variants identified using genome-wide association studies have identified an important role for genes associated with epithelial permeability, innate immunity, regulation of cytokine secretion, pattern recognition receptors and stress responses to microbial byproducts and are discussed further in section 1.3.3⁹⁸. Recently, very early-onset IBD, arising in patients less than 5, has been associated with highly penetrant germline mutations suggesting a role for Mendelian genetics in IBD^{89, 96, 99-101}.

1.2.2.2.2 Environmental Factors

The most well established non-genetic risk factor associated with IBD is a tobacco use¹⁰². This is also the most puzzling, as smoking is protective in UC and detrimental in CD. The mechanisms through which smoking influences IBD risk are not certain, but may involve modulation of host microbiome, interactions with the immune system and/or interactions with genetic polymorphisms in metabolic enzymes. These are reviewed in^{102, 103}. Other environmental and lifestyle risk factors are more controversial and include stress, use of oral contraceptives, infections (*Helicobacter pylori*), antibiotics and childhood hygiene. These are discussed in detail in^{104, 105}.

According to a questionnaire of IBD patients, approximately 65% had self-diagnosed food intolerances compared to only 14% of non-IBD patients¹⁰⁶. While these food intolerances were not deemed to be causative of disease, they pose interesting questions with respect to the role of diet in the modulation of IBD¹⁰⁷. In fact, some patients see improvement in their disease symptoms through dietary modulation¹⁰⁸. Specific studies to assess the involvement of various food groups in IBD pathology have been variable. However, similar to CRC, IBD risk is consistently linked to diets high in red meats and low in fruits, vegetables and fiber^{107, 109}. These dietary factors are thought to modulate IBD risk through their degradation products that are produced via fermentation by the microbiome.

1.2.2.2.3 Microbial Factors

The human microbiome consists of over 100 trillion bacteria comprising more than 1000 species, with the majority inhabiting parts of the digestive tract¹¹⁰. Within the digestive tract these microbes aid in the breakdown of lipid, carbohydrate and fat products to generate essential vitamins and nutrients for the host cells. Some of these metabolites, such as acetate, propionate and butyrate are also important immune modulators^{67, 111}. Dietary choices have been shown to modify the bacterial composition within the intestinal lumen with “Westernized” diets associated with a luminal composition deemed the *Bacteroides* enterotype and carbohydrate-rich diets associated with the *Prevotella* enterotype¹¹².

The healthy intestinal microbiome consists primarily of two bacterial phyla; *Firmicutes* and *Bacteroidetes*¹⁰². In IBD there is a distinct shift in microbial composition. This intestinal dysbiosis is associated with decreased microbial diversity and decreased *Firmicutes*. There have been conflicting results with respect to *Bacteroides* levels (elevated or decreased) in IBD,

although these discrepancies may in part be related to differences in sampling locations within the intestinal tract ¹¹³. More information on the microbial changes associated with IBD pathogenesis can be found in ^{102, 113}. IBD is also associated with increased abundance of *Proteobacteria* species such as *Escherichia coli*, *Campylobacter concisus* and *Helicobacter* suggesting an important pathogenic role for these bacterial species. The role of pathogenic bacteria in IBD has been recently reviewed in ¹¹⁴. It is not clear at this time if this microbial dysbiosis drives IBD pathogenesis or is a result of IBD pathogenesis. Overall these studies highlight an important role for the microbiome in IBD and recently several therapies (probiotics, antibiotics and fecal transplants) have been proposed to target this.

1.2.2.2.4 The Immune System

IBD has been categorized as an immune disorder, involving a dysregulated immune response against the commensal bacteria of intestinal lumen. Disease etiology is complex involving numerous receptors and signalling molecules in addition to epithelial, innate and adoptive immune cells ⁹⁸. The first lines of defense against the luminal microbial contents are intestinal epithelial cells ¹¹⁵. These not only form a physical barrier, but these cells also secrete numerous proteins, including mucin and anti-microbial peptides, that strengthen their defense. Through a mechanism that is not well defined, the epithelial cell barrier is compromised in IBD patients, leading to activation of innate immune responses and the recruitment of macrophages, dendritic cells and neutrophils. These in turn secrete various cytokines and chemokines leading to the recruitment of adoptive immune cells. One of these cells types is the CD4⁺ T-cell. Upon exposure to specific antigens, these naïve cells can then differentiate into one of 4 cells types, T_H1, T_H2, T_H17 or Regulatory T cells (Treg) cells, which each secrete their own cytokines and transcription factors and are described further in ^{115, 116}. T_H1 responses are more commonly associated with CD, cell-mediated immunity and the secretion *IFN-γ*, *TNF-α* and *IL-2*. T_H2 responses are associated with UC, humoral immunity and the secretion of *IL-4*, *IL-5*, *IL-13* and *IL-10* ¹¹⁶. T_H17-immune responses are characteristic of both UC and CD and secrete *IL-17*, *IL-21* and *IL-22*. Reduced levels of Tregs have been associated with IBD pathogenesis ¹¹⁷.

1.2.2.3 Pediatric IBD

It is estimated that 20-30% of IBD cases occur in individuals below the age of 18 and that rates of pediatric IBD are increasing over time ¹¹⁸. In Canada, IBD incidence rates in the Ontario

pediatric population increased from 42.1 per 100,000 children in 1994 to 56.3 per 100,000 children in 2005 with the largest increase in children 0-4 years old (5.0%/year) and 5-9 years old (7.6%/year) ¹¹⁹. These early-onset (<10 years of age) IBDs have unique characteristics compared to adult onset IBD and are important risk factors associated with colitis-associated CRC development.

In children, IBD diagnosis varies by age. Children under the age of 2 are equally affected with UC, CD, and IC ⁷⁵. Conversely, UC is more prevalent in children diagnosed between the ages of 3 and 5 year old, whereas CD predominates in children diagnosed between 6 and 12 years of age. There is a slight male bias in early-onset IBD ¹²⁰. In addition, disease isolated strictly to the colon, is more prominent in children diagnosed with IBD prior to the age of 2 ⁷⁵.

Approximately 30% of pediatric IBD patients have a first-degree relative affected with IBD ⁷⁵. This increases to 44% in children under the age of 3, suggesting a strong genetic link to disease. Several successful studies have been undertaken to identify genetic variants associated with IBD in pediatric cohorts. In these studies, pediatric IBD is defined as individuals less than 19 years of age. In 2007, the IBD associated polymorphisms 3020insC in *CARD15* and the rs3792876 SNP in *SLC22A4/5* were determined to be more prevalent in early-onset IBD compared to adult-onset IBD ¹²¹. Seven novel IBD SNPs were also identified in pediatric genome-wide association studies (Chr 2q37, 10q22, 16q11, 19q13.11, 20q13, 21q22 and 22q13), but have since been validated in adult IBD cohorts suggesting that these are general IBD risk variants rather than specific early-onset associated risk variants ^{98, 122, 123}.

There is considerable variation with respect to phenotype and familial risk associated with IBD based on age of diagnosis. Not surprising, very-early onset (VEO; children < 5 years old) IBD forms a distinct subgroup with most showing evidence of Mendelian inheritance. To date, case studies of select VEO patients have identified mutations in *IL-10RA/B*, *IL-10*, *XIAP*, *ADAMI7*, *NCF2/RAC2* and *NCF4* ^{89, 96, 99-101}. The importance of the IL-10 pathway was recently confirmed in a large-scale screen of VEO patients (UC, CD and IC), with mutations in *IL-10RA/B* or *IL-10* being identified in 24% of the cohort ¹²⁴. The study of these VEO IBDs are important to researchers as these arise in the presence of minimal environmental and dietary risk factors and therefore may enable identification of novel IBD genetic associations that may also be important in adult onset IBD, but whose identification is masked by external complicating factors.

1.2.3 Colitis-Associated Colon Cancer

IBD-associated inflammation is the third most common CRC risk factor, after the hereditary CRC syndromes FAP and HNPCC, accounting for approximately 1-2% of total CRCs¹²⁵. These inflammation-associated CRCs are more commonly referred to as colitis-associated (CA)-CRC. Like CRC, CA-CRC is associated with the accumulation of various mutations and progresses through a well-characterized inflammation-dysplasia-carcinoma sequence⁶⁸. Dysplasia describes the abnormal growth and development of colon cells and is synonymous with the more commonly used term intraepithelial neoplasia¹²⁶.

According to the American Cancer Society, individuals at increased risk for CA-CRC should undergo routine colonoscopy at 1-2 year intervals starting 8-12 years post-disease diagnosis (www.cdfa.com). It is also recommended that at least four random colonic biopsies be taken for every 10 cm of colon examined during these routine colonoscopies, as approximately 20-50% of colon dysplasia cannot be detected by visual inspection alone^{127, 128}. Intraepithelial neoplasms are highly variable with respect to appearance and may present as raised (pendunculated or sessile) or flat (plaque or bump) lesions¹²⁹. Flat lesions are a unique feature to CA-CRC, rarely being detected in familial or sporadic CRC, and are generally associated with high risk of transformation into CA-CRC¹³⁰. These lesions are difficult to detect, although this is improving with newer screening technologies (reviewed in¹³¹). Raised polypoid lesions are further distinguished into two categories; dysplasia-associated lesions or masses (DALMs) or adenoma-like masses (ALMs) based on the presence or absence of dysplasia in the surrounding tissue¹²⁶. In older patients, ALM can resemble sporadic non-inflammatory CRC. The identification of CA-CRC can also be further complicated by large benign inflammatory pseudopolyps, which form during mucosal regeneration and ulcer healing.

1.2.3.1 Epidemiology and Etiology

The epidemiology and etiology of CA-CRC is tightly correlated with one another and therefore will be presented together. CA-CRC is the cause of death in 10-15% of IBD patients¹²⁵. CA-CRC mortality, like CRC, is approximately 50% (CD-46%, UC-50%) suggesting that between 20-30% of IBD patients will develop CA-CRC within their lifetime¹³². CA-CRC is estimated to be equally as common in both UC and CD with colonic involvement. This data comes from a large UK study that showed a relative risk (RR) of 18 for CD and 19 for UC in patients with extensive disease¹³³. Both UC and CD-CRC present with increased incidence of

multiple synchronous carcinomas (CD-CRC 11%, UC-CRC 12%) showing a high proportion of mucinous and signet ring features (CD-CRC 29%, UC-CRC 21%)¹³². These findings have subsequently been confirmed in several studies including¹³⁴⁻¹³⁶. Both UC- and CD-CRC are early-onset conditions presenting with a median age of onset between 40 and 55^{132, 137-139}. UC-CRC is primarily identified in the rectum and sigmoid colon, whereas CD-CRC is more evenly distributed between the right-colon (ascending), sigmoid colon and rectum^{132, 136}. The differences with respect to tumor location may reflect differences in location of active IBD as 76% of CD-CRCs and 100% of UC-CRCs arise in areas of macroscopic IBD. There is no increased risk of CRC in patients with CD isolated to the small intestine highlighting the importance of inflammation in CA-CRC¹³².

Quantitative estimates of overall CA-CRC risks are highly variable ranging from 2% to 40% depending on IBD severity, duration and location¹²⁵. There has been significantly more research on UC-CRC than CD-CRC, which most likely reflects the higher colonic involvement in UC (100%) than CD (60%)¹⁴⁰. CD patients are also more likely to undergo partial colectomy to manage disease symptoms and therefore identifying study populations can be difficult¹³³. Duration of IBD is hypothesized as the most significant risk factor associated with CA-CRC development¹⁴¹. Studies of CRC risk in UC reference a 2001 study by Edgan et al., which concluded that the probability of CRC was 2% after 10 years of disease, 8% after 20 years and 18% after 30 years¹³⁷. Studies of UC-CRC have also noted a high concordance between CA-CRC risk with location/extent of disease and age of disease onset. For example, Ekobom et al. identified a standardized incidence ratio (SIR) of 1.7 for proctitis (rectal only), 2.8 left-sided colitis and 14.8 pancolitis (defined as extensive colitis, or colitis involving the entire colon)¹⁴². In the high-risk pancolitis group the absolute risk of CRC 35 years post-diagnosis was 40% in early-onset (age 15 or less) UC patients compared to 30% in late-onset UC patients, respectively. The Eaden study did not confirm increased risk of CRC associated with age of UC diagnosis¹³⁷. However, the importance of age at diagnosis of UC with respect to CA-CRC risk was subsequently confirmed in another large scale meta-analysis whereby patients with UC diagnosed prior to 25 years of age were 13 and 70 times more likely to develop CA-CRC compared to older UC patients and the general population, respectively¹⁴³.

Studies of CD-CRC are complicated by the vast heterogeneity with respect to CD anatomical site, but like UC, confirm CA-CRC risk associations with duration/severity of disease

and age of onset of CD. In a study of 12 CD-CRC cases, the SIR for CRC risk in patients with CD affecting the colon was calculated to be 2.2 in patients diagnosed with CD after the age of 30 and this risk was further increased to 20.9 in younger-onset cases ¹⁴¹. The RR of CD-CRC based on duration of disease was calculated to be 2.9, 5.6 and 8.3 after 10, 20 and 30 years of disease, respectively ¹⁴⁴. In 2007, meta-analysis for CRC by disease site estimated a RR of 0.85, 4.3 and 13.4 for small bowel only, ileocolic and colon CD, respectively ¹⁴⁵. CD-CRC RR is increased to 18.2 in patients with extensive disease. Risk was also proportional to age with an increased risk of 21.5 vs 1.6 in patients younger and older than 25, respectively.

Further evidence to support a role for inflammation in CA-CRC comes from studies, which demonstrate maximal 50% reduced risk of CA-CRC with regular use of non-steroidal anti-inflammatory drugs (NSAIDs) and was reviewed in ¹⁴⁶. Other well-characterized CA-CRC risk factors include IBD with co-existence with primary sclerosing cholangitis (PSC) and a positive family history of CRC, which is associated with a 2-fold increase in CA-CRC risk ¹⁴⁷.

The specific mechanisms through which inflammation regulates CA-CRC are not well understood. It has been suggested that reactive oxygen species (ROS) produced by immune cells during colitis may play a crucial role in promoting DNA damage. Epigenetics, cytokines and the microflora are also thought to be important, mediating the cross talk between increased inflammation and CA-CRC. This is reviewed in ¹⁴⁸. It has been documented that earlier-onset IBD is associated with increased risk of CA-CRC ¹⁴³. It is also known that patients with similar IBD disease status can have variability with respect to CA-CRC onset. Therefore, it has been speculated that additional, yet to be identified, factors may be important in CA-CRC initiation and progression. One possible explanation is that patients are genetically pre-disposed. The role of genetics in both IBD and familial CRC has been well established. No loci have been mapped in humans though that regulate susceptibility to CA-CRC and a recent study demonstrated no association between UC-risk loci and UC-CRC ¹⁴⁹.

1.2.3.2 Colitis-Dysplasia-Carcinoma Sequence Progression

Most CRCs progress through the well-known adenoma-to-carcinoma sequence progression characterized by the accumulation of several mutations within various oncogenes and tumor suppressors (Figure 1.3 A). CA-CRCs however, progress through the colitis-dysplasia-carcinoma sequence associated with the development of infinite, low-grade, high-

grade dysplasia and eventually carcinoma (Figure 1.3 A) ⁶⁸. The same molecular alterations underlie all CRC development, but the timing and frequency of these molecular events are different. Mutations/deletions of *p53* are early events in CA-CRC with 50% of UC patients having *p53* mutations compared to ~10% of non-CA-CRC adenomas ^{148, 150}. *APC* mutations are rare events in CA-CRC (27.5% of high grade dysplasia) compared to 50% in non-CA-CRC adenomas ^{148, 151}. While little is known about genetic involvement underlying CA-CRC predisposition, the differences with respect to progression and mutation accumulation have led to speculations that different genes may be responsible for familial/hereditary CRC and CA-CRC.

1.3 Genome-Wide Association Studies

The completion of the Human Genome Project, the International HapMap Project and the increase in technological power has led to the advent of genome-wide association studies (GWAS) ¹⁵². GWAS assess the relationship between common genetic variants and disease predisposition. These variants are commonly referred to as single nucleotide polymorphisms (SNPs) and differ from mutations with respect to frequency (>1%) within the population. In addition to SNPs, common copy number variants (CNV) and small insertions and deletions (Indels) also underlie disease risk, although these have not been studied as frequently ¹⁵³.

Projects designed to characterize genetic variation (SNP Consortium, 1000 Genome Project) have identified more than 60 million SNPs and indels within the human genome ^{154, 155}. These variants are often inherited together leading to non-random segregation of these linked regions or haplotypes from generation to generation, a phenomenon known as linkage disequilibrium (LD) ³². This is exploited in GWAS whereby a single SNP can be used to infer alleles for other SNPs within the same haplotype block. This enables most genetic variation (> 80%) within the human genome to be captured by a relatively small number of SNPs (n= 500,000-1 million) ^{156, 157}.

GWAS are driven by the “common disease, common variant” hypothesis, which stipulates that common complex diseases, such as cancer, diabetes and IBD, are the results of common genetic variants (SNPs) within the genome ¹⁵⁸. A comprehensive listing of all published GWAS is maintained online at the National Human Genome Institute (<http://genome.gov/gwastudies>) ^{159, 160}.

1.3.1 GWAS Design

GWAS compare the prevalence of thousands of SNPs within healthy (control) and disease (case) cohorts looking for allelic imbalance indicative of disease association ¹⁵². Figure 1.4 summarizes the design of a typical GWAS consisting of an initial discovery phase (Phase 1) followed by replication phases (Phases 2-3) in additional unrelated cohorts ¹⁵⁷.

In the discovery phase, hundreds to thousands of individuals (cases and controls) are genotyped for 500,000-1 million SNPs using commercially available oligonucleotide microarray chips ¹⁵⁷. Cases and controls should be matched with respect to age, ethnicity/ancestry and gender. Additional matching criteria should be considered when external risk factors such as smoking are present that are known to have a large effect on disease-associated risk ¹⁶¹. Matching with respect to ancestry is also important to limit false positive associations due to population stratification. Population stratification refers to the presence of differences in allele frequency and genetic architecture (LD) that have arisen between different subpopulations due to genetic drift. Following the discovery phase, the top 5%-10% of SNPs are brought forward to the replication phase ¹⁵⁷. In the discovery phase very few associations reach the stringent criteria necessary for genome-wide significance.

The statistical power of GWAS is a function of sample size, effect size (measured by odds ratio, OR) and the allele frequency of the causal variant ¹⁶². The replication phase (Phase 2) is designed to confirm associations identified within the discovery phase and increase the statistical power of association through genotyping of additional samples ^{157, 161}. Several phases of replication studies may be necessary in a single GWAS to identify SNPs associated with disease risk. SNPs that fail to be confirmed are removed in subsequent rounds of analysis and therefore at each stage of replication, fewer SNPs are analyzed. Single SNPs can contribute differently to disease risk in different populations and therefore it is ideal to have similar ancestry in both the replication cohorts and discovery phase. Phase 3 studies are optional in GWAS ¹⁵⁷. This involves testing the association in populations with different ethnicity and therefore different patterns of LD, which can help to fine map the causal variant at a locus.

Positive associations or hits confirmed in the replication phase of GWAS are referred to as susceptibility loci. These generally have moderate to low effect size ($OR < 2$) and are biased towards the detection of SNPs with large minor allele frequencies ($MAF > 0.2$) ^{161, 163}. To aid in the identification of risk variants several international consortiums have been established. These

Consortiums combined data sets from several existing GWAS and use a statistical method referred to as meta-analysis to increase the power to detect disease-associated loci.

GWAS have identified thousands of susceptibility loci, however, the causal variant and/or the functional consequences of said risk alleles for most loci are still unknown¹⁶⁴. A recent review of cancer GWAS estimates that more than 70% of SNPs identified in GWAS map to intronic and intergenic regions and thus it is unclear how they function to modify disease risk¹⁶⁴. It is hypothesized that many of these intergenic/intronic SNPs are not causal, but instead map in strong LD with the causal variant (CNV, indel, SNP). Researchers are now using expression quantitative trait loci (eQTL) association, which correlates transcript expression with allelic expression of GWAS SNPs to identify possible functional consequences of GWAS variants^{165, 166}. Other techniques for fine mapping and validating GWAS loci are discussed further in Freedman et al. and highlight the importance for animal models of human disease¹⁶⁴.

1.3.2 Colorectal Cancer

The first CRC GWAS were published in 2007, with 32 loci having been identified as of May 1, 2014 (Table 1)¹⁶⁷⁻¹⁸². The first CRC GWAS identified a genomic region on 8q24 associated with colorectal adenoma risk in Northern Europeans and has since been replicated in several studies^{155, 174}. This locus was subsequently linked to CRC risk in Asians and African/European Americans as well^{183, 184}. Susceptibility to several other solid cancers also map to the 8q24 region (breast, prostate, bladder, lung, ovarian, pancreatic and brain)¹⁸⁵. Large-scale meta-analysis of these solid cancer GWAS supports the presence of a common cancer susceptibility locus mapping to this region¹⁸⁵. It has been proposed that a novel lncRNA (*colon cancer-associated transcript 2*, *CCAT2*) may underlie CRC risk at the 8q24 locus through enhanced WNT signalling and subsequent MYC regulation¹⁸⁶.

The 11q23 locus (rs3802842) identified in 2008 is associated with CRC risk in diverse populations, is prevalent in early-onset CRC (< 50 years old), and acts as a genetic modifier of Lynch Syndrome^{179, 187, 188}. The transcript and protein expression of two previously uncharacterized genes *Colon Cancer Associated 1* (*COLCA1*) and *COLCA2* are tightly correlated with genotype at rs3802842¹⁸⁹. *COLCA1* is a primate-specific gene that is expressed primarily on immune cells, whereas *COLCA2* is expressed in normal/tumor epithelial cells and immune cells. While additional studies are still required to fully characterize these genes in CRC, initial

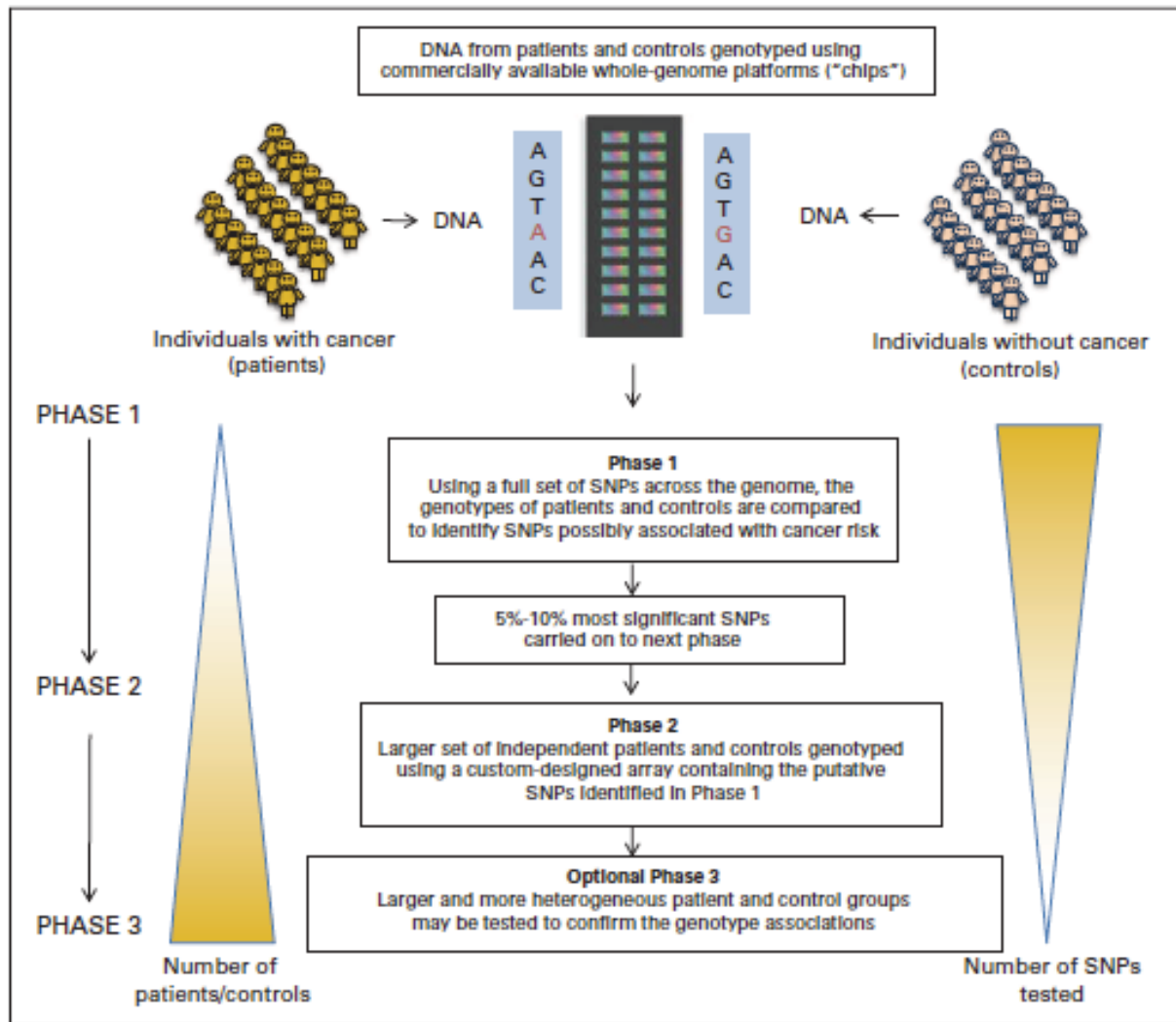


Figure 1.4: Genome-wide association study (GWAS) design. GWAS commence with the identification of two groups: affected individuals (cases) and matched (age, gender, ethnicity, lifestyle) healthy individuals (controls). Case and control DNA samples are then genotyped for polymorphisms (SNPs) evenly spaced throughout the genome. In phase I, statistical methods are used to assess for associations between SNPs and disease risk. In phase II, the top 5-10% of SNPs found to be significantly associated with disease risk in Phase I are tested in a larger set of independent cases and controls. Several different independent cohorts maybe assessed in these Phase II studies. Phase III studies are optional, but when conducted, larger and more heterogeneous populations are assessed. Positive associations identified in GWAS a referred to as susceptibility loci. *Adapted with permission from Stadler et al. 2010*¹⁵⁷.

Table 1.1: Human GWAS CRC Susceptibility Loci published prior to May 2014.

Genomic Location	Candidate Genes	SNP	Publication
1p33	<i>SLC5A9</i>	rs12080929	167
1q41	<i>DUSP10/CICP13</i> <i>DUSP10/CICP13</i>	rs6687758	168
		rs6691170	
1q25.3	<i>LAMC1</i>	rs10911251	169
2q32.3	<i>NABP1/SDPR</i>	rs11903757	169
3q26.2	<i>MYNN</i>	rs10936599	168
5q31.1	<i>PITX1/H2AFY</i>	rs647161	170
6p21	<i>SRSF3/CDKN1A</i>	rs1321311	171
6q26-27	<i>SLC22A3/SLC22A3/LPAL2/LPA</i>	rs7758229	172
8p12	<i>DUSP4</i>	rs11987193	167
8q23.3	<i>TRPS1/EIF3H</i>	rs16892766	173
8q24	<i>SRRM1P1/POU5F1B/MYC</i>	rs6983267	174, 175
9p24	<i>TPD52L3/UHRF2/GLDC</i>	rs719725	176
10p14	<i>KRT8P16/TCEB1P3</i>	rs10795668	173
10p24.2	<i>ABCC2/MRP2</i>	rs1035209	177
11q11	<i>CNV at this locus</i>	rs1944682	178
11q13.4	<i>POLD3</i>	rs3824999	171
11q23	<i>C11orf93</i>	rs3802842	179
12q13.13	<i>DIP2B/LARP4</i>	rs11169552	168
	<i>DIP2B/ATF1</i>	rs7136702	
12p13.32	<i>CCND2</i>	rs3217810	169
12p13.32	<i>RPL18P9/CCND2</i>	rs10774214	170
12q24.21	<i>TBX3</i>	rs59336	169
14q22.2	<i>BMP4</i>	rs4444235	180
15q13	<i>SCG5/GREMI</i>	rs4779584	181
16q22.1	<i>CDH1</i>	rs9929218	180
18q21	<i>SMAD7</i>	rs4939827	182
19q13.1	<i>RHPN2</i>	rs10411210	180
20p12.3	<i>BMP2</i>	rs961253	180
20p12.3	<i>HAO1/PLCB1</i>	rs2423279	170
20q13.33	<i>LAMA5</i>	rs4925386	168
Xp22.2	<i>SHROOM2</i>	rs5934683	171

studies suggest that this locus may modulate a complex network involving both immune and tumor cells. Recently, a third gene *C11orf53*, of unknown function, was found to be in strong LD with *COLCA1/2* and represents an additional candidate gene underlying CRC risk at this locus¹⁹⁰.

Interestingly, many of the SNPs identified in CRC GWAS are located in strong LD with members of the TGF- β signalling pathway suggesting that the TGF- β pathway may be important in CRC susceptibility¹⁹¹. The TGF- β signalling pathway plays a key role in proliferation, differentiation and migration of colonic cells and over-expression of *TGF- β* is associated with CRC progression¹⁹². Mutations within genes in the *TGF- β* signalling pathway have also been linked to hereditary CRC. The genes implicated in this pathway from GWAS include; *SMAD7* (18q21), *GREM1* (15q13), *BMP2* (20p12), *BMP4* (14q22.2), *RHPN2* (19q13), *LAMA5* (20q13) and *TBX3* (12q24)¹⁹³.

It is currently estimated that known CRC SNPs account for at most 5.4% of CRC heritability, suggesting that much of the genetic risk has yet to be uncovered^{180, 194, 195}. One suggestion is that some of the missing heredity may be explained by gene x gene/diet/environment interactions or rare variants that may be impossible to identify. To date, no interactions have been detected between known GWAS CRC loci, although these are quite common in mouse models of CRC¹⁹⁶⁻¹⁹⁹. However, two interactions between known CRC susceptibility loci and novel interacting SNPs were detected in 2012; rs10795668 (10p14)/rs367615 (5q21) and rs1571218 (20p12.3)/rs10879357 (12q21.1)²⁰⁰. In 2014, strong associations were detected for known SNP rs16892766 (8q23) and vegetable consumption and a novel SNP rs4143094 near *GATA3* and processed meat consumption²⁰¹. Gene x smoking interactions are estimated to explain ~ 7% of heritable CRC risk²⁰⁰.

1.3.3 Inflammatory Bowel Disease

Since the first published IBD GWAS study in 2005, more than 163 loci have been identified, the largest number for any common complex disease⁹⁸. Most of these loci have been identified in cohorts of European ancestry and are summarized in Appendix 2 of this Thesis. In 2012, a large-scale meta-analysis compiled the results of 15 GWAS studies identifying 71 novel IBD (UC and/or CD) associations, bringing the total to 163⁹⁸. Of these IBD loci, 110 are common to both UC and CD, whereas 30 and 23 are CD and UC specific, respectively,

indicating that common mechanisms are likely associated with both CD and UC pathogenesis. These loci explain 13.6% of CD and 7.5% of UC variance. Approximately, 70% of these loci overlap with other known common complex trait susceptibility loci with a significant enrichment for loci associated with immune-related disorders (42%) including type I diabetes, ankylosing spondylitis and psoriasis. This is more than a random association suggesting common pathways and mechanisms between these immune related disorders. As of May 1, 2014, four additional loci have been identified in GWAS cohorts of Asian ancestry; 4p14 (rs6856616 and rs7329174, in two distinct studies), 10q25 (rs11195128) and 11q13 (rs11235667) and 13q14 (rs7329174)^{202, 203}. To date, very few causal variants have been identified underlying IBD susceptibility risk loci and even fewer have undergone extensive functional characterization²⁰⁴. Some of the most well characterized genetic associations are *NOD2*, *IL-23R* and *ATG16LI* involved in bacterial sensing, the IL-23 inflammatory response and autophagy, respectively²⁰⁵. Deep re-sequencing of the IBD loci has shown promise identifying more than 20 rare protein-coding variants that can now be studied to try to determine the specific mechanisms underlying IBD risk^{206, 207}. These studies suggest that protein and splice site variants account for a small percentage of IBD risk (< 35%) implying that other factors such as epigenetics, RNA molecules and CNV may contribute significantly to disease risk²⁰⁷. Little is known about gene x gene/environment interactions in IBD. A recent study by Wang et al. identified four interacting gene clusters associated with IBD risk and several SNPs strongly associated with smoking and IBD risk²⁰⁸.

A complete discussion of each individual genetic GWAS associations is beyond the scope of this thesis. IBD pathogenesis is driven by aberrant immune responses against the commensal bacteria of the lumen and therefore, it is not surprising that a large number of genes within IBD loci have been associated with epithelial barrier maintenance/permeability, cytokine signalling and pathogen recognition/clearance²⁰⁹. The epithelial cell layer maintains a physical barrier between the luminal bacteria and the immune sensing cells of the lamina propria, and increased permeability is frequently observed in IBD patients and their first-degree relatives²¹⁰. Several IBD loci support the hypothesis of diminished epithelial barrier integrity in disease predisposition and harbour candidate genes such as *ECM1*, *CDH1* (*E-cadherin*), *HNF4A*, *LAMB1*, *GNAI2* and *PTPN2*^{209, 211}. IBD pathogenesis is also associated with the up-regulation of key pro-inflammatory cytokines (*IL-6*, *TNF- α* , *IL-1* and *IL-12/23*) and down-regulation of anti-inflammatory cytokines (*IL-4*, *IL-10* and *TGF- β*), a conclusion supported by GWAS^{98, 212}.

Several different components of the IL-10 pathway (*IL-10*, *IL-10RA/RB*, *STAT3*, *TYK2*, *JAK2* and *IL-27*) have been identified in GWAS ²⁰⁹. Interestingly, rare Mendelian *IL-10* and *IL-10RA/RB* mutations have also been identified in early-onset pediatric IBD suggesting that both rare and common variants may contribute to disease risk. Autophagy, the process of self-digestion, maintains cellular homeostasis through the degradation of damaged organelles, proteins and/or bacteria (xenophagy) within cells ²¹³. GWAS have identified polymorphisms in genes associated with autophagy such *ATG16L1*, *IRGM*, *NOD2*, *RIP2*, *PTPN2* and *XBPI*. A more comprehensive review of important processes and pathways in IBD is highlighted in Figure 1.5 and reviewed in ^{115, 209, 211, 214-216}.

1.3.4 Colitis-Associated Colon Cancer

Unlike familial CRC and IBD, there have been no known GWAS performed to identify genetic loci regulating susceptibility to CA-CRC. While not explicitly stated, this is most likely due to complications in obtaining a homogeneous study population. CA-CRC arises in the presence of IBD and is influenced by numerous risk factors including age at IBD-onset, and duration/extent of IBD colonic involvement ^{125, 143}. Therefore ideal study cohorts should be matched for the above variables. In addition many IBD patients undergo prophylactic colectomy and therefore CA-CRC in these patients cannot be accurately assessed ^{133, 217}.

In 2009, the UK IBD Genetics Consortium identified and published a novel UC locus situated on chr 16 (16q22) ²¹⁸. Interestingly, this locus had previously been associated with increased CRC risk ¹⁶⁸. Therefore, it has been speculated that this locus may also play an important role in CA-CRC. However, a recent study showed no association between any known UC loci and UC-CRC risk, disproving this hypothesis ¹⁴⁹. Through the use of numerous mouse models a plethora of genes have been associated with CA-CRC onset and progression and these will be discussed in section 1.4.3.

1.3.5 The Future of GWAS

There is little doubt that GWAS have been successful in identifying numerous loci (OR < 2, minor allele frequency (MAF) > 0.1) associated with common complex diseases and defining novel pathways associated with disease risk ²¹⁹. However, GWAS also have several limitations including the identification and characterization of specific causal risk variants, the detection of loci with low minor allele frequencies and the identification of interacting loci ^{148, 151}. GWAS

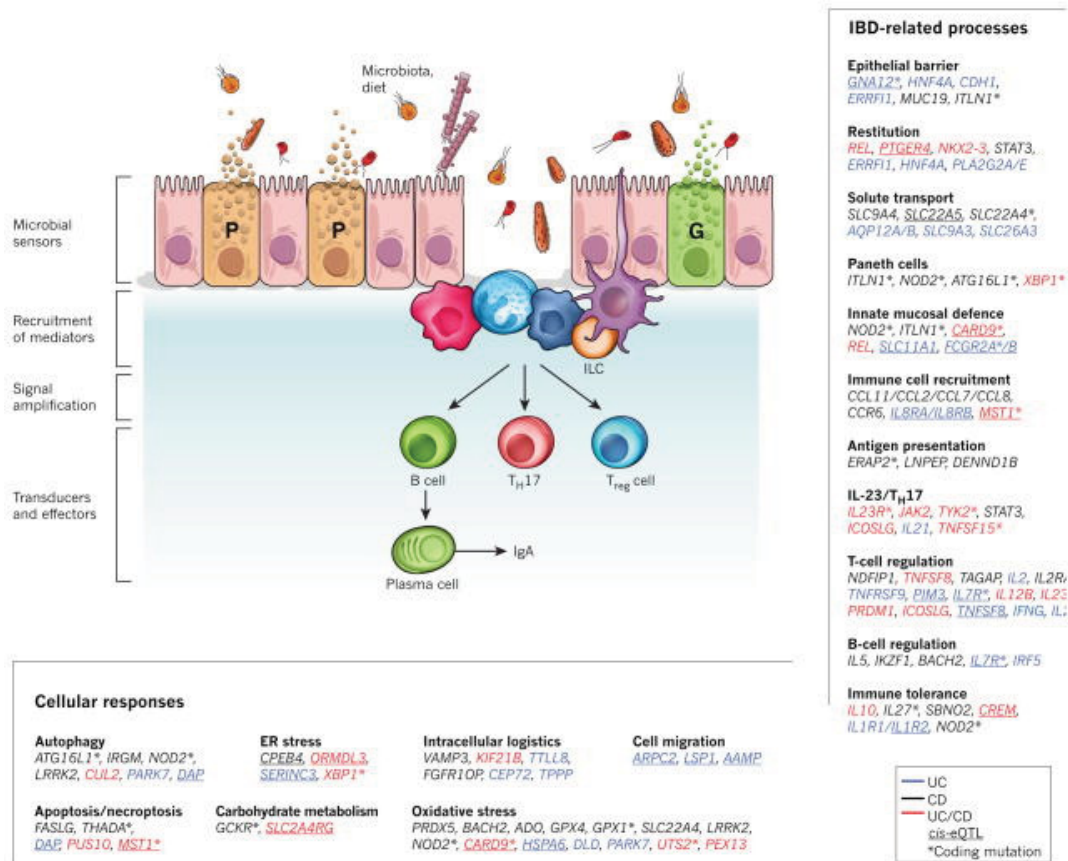


Figure 1.5: Important pathways in IBD identified in genome-wide association studies (GWAS). Maintenance of intestinal homeostasis is a coordinated effort involving intestinal epithelial, innate and adaptive immune cells. In IBD, the epithelial barrier is breached enabling strong innate immune responses to be elicited against the commensal bacteria in the intestinal lumen. This leads to the recruitment of additional cellular components including adaptive immune cells. IBD GWAS have identified numerous putative genetic variants associated with IBD initiation and progression. Some of these have been catalogued and arranged according to their function. G= Goblet Cell, P= Paneth Cell. *Adapted with permission from Khor et al. 2011*

have identified thousands of susceptibility loci, however the causal variant and/or the functional consequences of said risk alleles for most loci are still unknown¹⁶⁴. This is due to the phenomenon of LD, whereby parts of the genome are inherited together in distinct haplotype blocks. In most cases SNPs identified in GWAS are not causal, but map within the same LD block as the causal variant. Studies in diverse LD populations and eqtl association studies have provided some assistance in fine mapping the causal variants, however these tests do not provide any indication of gene function or the mechanism(s) of action of said variants^{157, 165, 166}. Mouse models of IBD and CRC provide a quick and convenient means to assess the function of select genes in disease pathology using a wide variety of knock-in, knock-down or knockout mouse lines. For example *ATG16L1* has been implicated in IBD pathology and is associated with reduced autophagy²²⁰. Using an *Atg16L1* knockout mouse and a common model of murine IBD, Paneth cells were found to be essential to *Atg16L1* driven-disease pathology, which was subsequently confirmed in human patients with the *ATG16L1* Ala300Thr SNP.

The current loci identified for CRC and IBD explain less than 5.4% and 15% of disease-associated variance, respectively^{98, 194}. In addition, researchers have speculated that it is unlikely that more SNPs with MAF > 0.1 remain to be identified in the European population. These studies suggest that much of the genetic variance underlying disease risk is still unknown and given the complex nature of these diseases the missing associations are likely the result of gene x gene/environmental interactions and/or rare variants (0.01-0.1% MAF). To date GWAS have been notoriously poor in detecting these gene x environment interactions, mainly due to the vast heterogeneity of participants and poor medical records with respect to exposure^{194, 201, 208, 221}. While gene x gene interactions have been regarded as major players in complex traits very few have been identified in IBD and CRC and none of these have been validated²⁰⁰. Interacting loci are often undetectable in the absence of their interacting partner and therefore it is not surprising that these are often not detected in GWAS as most would fail to meet the stringent genome-wide significance threshold.

To aid in mapping rare variants (MAF < 0.1) large consortiums have been formed to analyze multiple independent studies together using meta-analysis²²². While these have identified novel CRC and IBD loci these have not been very successful in identifying the target low penetrance loci with MAF < 0.1. It is now speculated that these rare variants might be more readily identified using familial-based study designs. However, these can often be difficult to

validate due to lack of additional cohorts with similar genetic architecture for follow up. Inbred mice like, humans vary with respect to susceptibility to CRC and IBD due to inherited genetic factors²²³. The genes regulating differential susceptibility between two strains can be mapped in inter-crossed mice using QTL mapping. These mouse crosses can be designed to ensure that all alleles have a MAF = 0.5 and therefore, the chance of detecting an association is based on effect size rather than MAF. These findings can then be related back to humans, identifying rare variants. An example of this is the mouse *Sccl* locus, which is associated with a variant within *PTPRJ* phosphatase with corresponding mutations, LOH and SNPs associated with human CRC being subsequently identified^{224, 225}. Mouse models are also adept at identifying interacting IBD and CRC loci^{196, 197, 199, 226-229}.

1.4 Mouse Models of Colon Cancer, Inflammatory Bowel Disease and Colitis-Associated Colon Cancer

The complex and heterogeneous genetic component of complex diseases such as IBD and CRC can be difficult to tease apart in human populations due to confounding environmental and dietary effects. However, these traits can be dissected in genetically well defined inbred and recombinant congenic mouse strains²²³. Mice are ideal models with respect to human disease as they are anatomically and genetically similar to humans, with 75% and 99% of mouse genes having human orthologs and homologs, respectively²³⁰. Also, a single mouse year is roughly equivalent to 30 human years enabling diseases that would take decades to develop in humans to be studied in a relatively short time frame (www.jax.org).

Mice are not particularly prone to the spontaneous development of either IBD or CRC and therefore induction of disease in mice can be performed using dietary modifications, infectious agents, genetic mutation or chemical reagents²³¹. These modifiable disease triggers enable researchers to alter disease parameters such that disease can be induced in a controlled and reproducible manner. Diet and housing conditions can also be controlled thus eliminating common confounding factors on disease pathogenesis²²³. Murine models of disease are associated with similar genetic events and pathways as human disease. For example, murine tumors induced using the carcinogen azoxymethane are associated with the accumulation of mutations following the same adenoma-to-carcinoma sequence progression as humans²³².

To date more than 100 different mouse models of CRC, IBD, CA-CRC have been published. For a comprehensive review of these, see^{223, 233-235}. This introduction will focus on

several widely used models of CRC, IBD and CRC, which have been used to study the effects of diet, treatment and genetics on disease risk, with a strong focus on the later.

1.4.1 Techniques for Gene Identification Using Mouse Models

Studies to identify genes modulating susceptibility to IBD or CRC in mice are conducted using one of two approaches; forward or reverse genetics. Forward genetics is a phenotype-driven approach in which mutations are identified underlying disease traits of interest through the generation of informative mouse crosses followed by linkage analysis²³⁶. This approach is commonly used, as mice, like humans vary with respect to IBD and CRC susceptibility due to inherited genetic factors^{72, 223}. Reverse genetics, the converse to forward mapping is gene-driven, and researchers characterize a range of phenotypes associated with a given mutation²³⁷. Reverse genetics is associated with the testing of knockout, knock-in, knock-down, transgenic or tissue-specific genetic modifications and is often used to confirm positive associations identified in forward genetic screens.

Reverse studies are easier to conduct and are shorter in duration than forward genetic studies, but can be hampered by inefficient knockdown or genetic background effects^{237, 238}. Reverse genetic studies also are poorly designed to detect interacting loci that fail to exhibit a phenotype in the absence of their interacting partner. As causal variants in reverse genetic approaches are often artificially generated (transgenics, knockouts, knock-ins), the relevance with respect to human disease has been questioned. Forward genetic screens are advantageous as they are conducted without bias as to the types of mutations detected, with mutations mapping to genes that are often unlikely to be tested using reverse genetic approaches and represent a spectrum of mutations more likely to be detected in human disease. Forward genetic screens are hampered by the heterogeneity within the mouse genome with many association loci having been mapped, but with very few causal variants identified²³⁶. Forward genetic screens have seen increased success with respect to the identification of causal variants with the advent of chemical mutagenesis screens such as ENU (N-ethyl-N-nitrosourea) (Described in²³⁹). The most common mouse models used in colon cancer research, $Apc^{Min/+}$, was generated in an ENU screen²⁴⁰.

Forward genetic studies typically use four distinct types of mouse populations; F2, N2, recombinant congenic mice (RCS) or recombinant inbred mice (RI)^{241, 242}. Mating susceptible and resistant mouse strains to each other and inter-crossing the resulting F1 progeny generates

informative F2 populations (Figure 1.6 A) ²⁴². Experiments with F1 mice are useful in assessing inheritance patterns of disease, whereas experiments with F2 mice are useful in detecting and mapping both single gene and multi-gene effects underlying disease development. However, with respect to terminal experiments, F2 mice can only be studied once, as each mouse is unique and once sacrificed is no longer available for additional testing. Also, defining the precise map location of gene effects detected in F2 crosses can be difficult to access in experiments including a small number of animals (< 300 mice). N2 mice are similar to F2 mice, but the F1 mice have been backcrossed to one of the two parental strains. These crosses can be advantageous as this selective breeding can increase the probability of a given phenotype. The use of inter-crossed or backcrossed mice bred to homozygosity, such as the RCS or RI strains, allows for multiple testing of genetically identical mice with well-defined crossover events enabling for precision mapping ^{241, 243}. However, these mice take several years to generate and are therefore not always a feasible option for gene mapping. RCS mice are generated through a reciprocal double backcross between a CRC susceptible and CRC resistant mouse strain followed by at least 20 generations of brother x sister matings (Figure 1.6 B). The resulting homozygous mouse strains contain approximately 12.5% of their genome from one parent (the donor strain) fixed as a set of discrete congenic segments on the other genetic background. The RI mouse strains, have 50% of their genome from each of two parental strains and were generated through 20⁺ generations of brother x sister matings from F2 mice ²⁴⁴. Gene mapping in the RCS and RI mice is possible through testing of multiple strains (each with a unique genetic composition) to identify discordant mouse strains (strains that mimic the donor parent's phenotype) ^{241, 243, 244}. These phenotypes can then be traced to the donor strain DNA. As the RCS have a smaller percentage of DNA (12.5%) from the donor strain compared to the RI mice (50%), the RCS usually produce smaller regions of genetic linkage. The RCS/RI mice are often poor at detecting interacting loci and therefore, combined RCS and F2 approaches are often used.

1.4.2 Mouse Models of Colorectal Cancer

In this section, some basic genetic models of CRC will be discussed along with a more comprehensive discussion of chemically-induced CRC.

1.4.2.1 Genetic Models

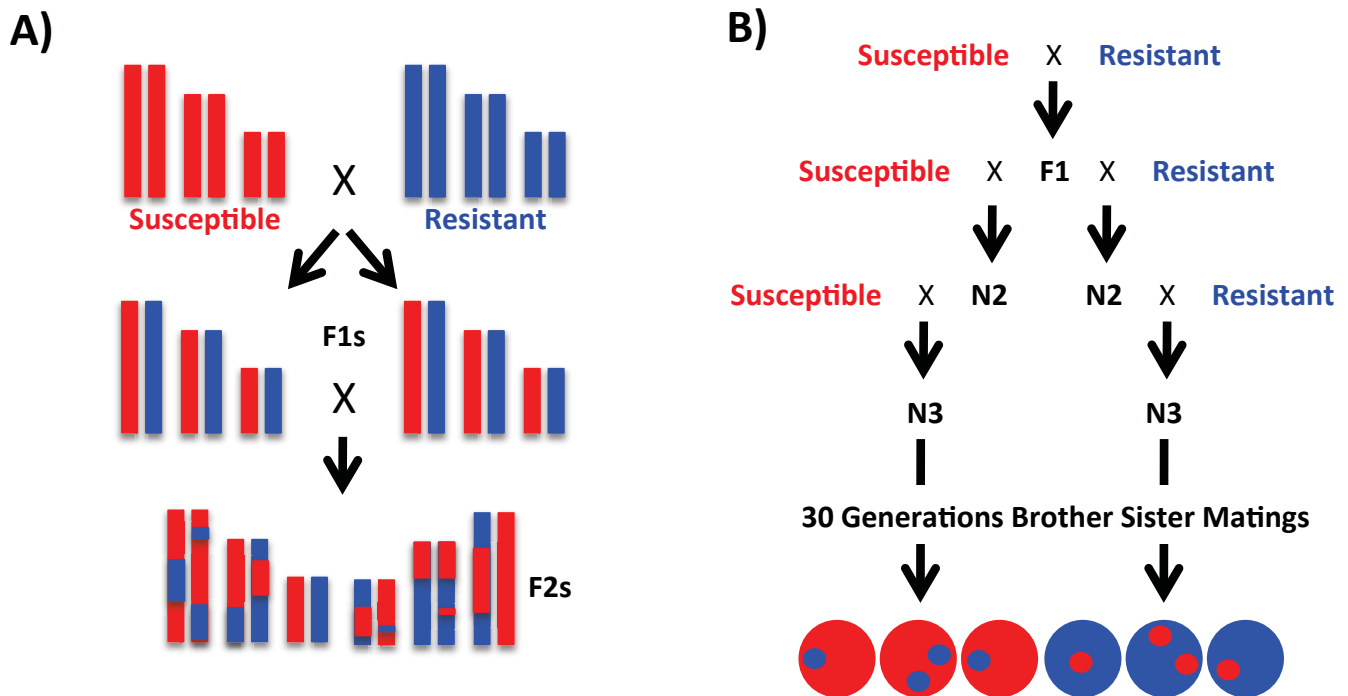


Figure 1.6: Breeding of informative populations for forward genetic studies. (A) Generating an F2 population. Susceptible and resistant mice are interbred generating the F1 mice. These mice are heterozygous at all loci. These F1s are then intercrossed generating the F2 which are a genetic mixture of susceptible and resistant alleles, with each mouse having a unique genetic combination, with 50% of their genome being contributed from the susceptible parent and 50% from the resistant parent. (B) Breeding of recombinant congenic mice via a systematic double backcross followed by 30-generations of brother-sister mating. The resulting progeny are homozygous and contain a small amount (12.5%) from one parent (susceptible or resistant) fixed as a set of discrete congenic segments on the background (87.5%) of the other parent.

Few colon-specific genetic models of CRC exist, with most models involving tumors of the small intestine with or without colonic involvement^{223, 245}. The most frequent models mimic human FAP, involving heterozygous mutations in the *Apc* gene. Over 40 different mouse models involving *Apc* mutations have been generated and characterized for susceptibility to intestinal neoplasia (Reviewed in²⁴⁶). These mouse models are valuable tools in the design and testing of novel FAP/CRC therapeutics, and in the identification of low to moderate risk tumor susceptibility genes²⁴⁷.

The most popular genetic model of CRC is the *Apc* multiple intestinal neoplasia (*Apc*^{Min+/-}) mouse, which develops between 30 and 100 tumors, depending on the genetic background, within the intestine approximately 120 days after birth²⁴⁵. This increased tumor susceptibility is attributed to a T to A transversion of nucleotide 2549, which results in the truncation of the *APC* protein after amino acid 850 and was generated using ENU treatment^{240, 248}. Tumors from *Apc* mutant mice have been shown to have similar genetic profiles to those of FAP patients despite arising predominantly in the small intestine, not the large intestine. Like in FAP patients, different mutations can induce different phenotypes with respect to both tumor multiplicity and location^{38, 246}. The *Apc*^{Δ716/+} mouse, with *Apc* truncated at amino acid 716 develops upwards of 300 tumors in the intestine, whereas the *Apc*^{Δ1638N/+} mouse develops only 10 tumors per mouse^{249, 250}. Of the *Apc* models, the *Apc*^{Δ14/+} mouse, which has exon 14 deleted, is the best model of CRC with a higher proportion of distal colon and rectal tumors compared to the other models²⁵¹.

Tumor multiplicity in *Apc*^{Min+/-} mice is highly variable depending on genetic background, diet and microbial exposure^{247, 252}. Genetically, intra-strain variation is attributed to the presence of numerous modifier loci, called *Mom* (Modifier of Min) that have been identified using forward genetic approaches. Thirteen *Mom* loci have been identified and are highlighted in Figure 1.7. *Mom1* has been mapped to a spontaneous mutation arising early in mouse genealogy in the *pancreatic secretory phospholipase A2* gene on mouse chromosome 4^{245, 253}. *Mom1* is also mutated in human CRC highlighting the relevance of mouse model to human intestinal cancer²⁵⁴. Other *Mom* loci include; *Mom2* (a spontaneous 4 bp deletion in *Atp5a1*, which has yet to be confirmed in humans); *Mom3* (chr 18, an AKR strain-dependent modifier); *Mom5* (chr 5, associated with a 50% reduction in mean tumor number); *Mom6* (chr 4, which exerts its effect exclusively in the medial small intestine); *Mom7* (chr 18, a recessive enhancer in

A/J, BTBRT<+>tf/J, and AKR mice); *Mom12* (chr 6, associated with the 129X1/SvJ background); *Mom13* (chr 6, whose effect is masked by *Mom12*); and *Mom14-18* (chr 1, 2, 10 and 18, additive loci identified in a B6 and C3H/HeJ mixed background)²⁵⁵⁻²⁵⁹. Additional studies using either ionizing radiation or sleeping beauty transposon mutagenesis have identified several other *Apc*^{Min+/-} modifiers, which are detailed in^{260, 261}. Little is known with respect to the causative mutations underlying these loci/insertion sites or their relevance to human disease.

Tumors in *Apc*^{Min+/-} mice are microsatellite stable, however approximately 15% of CRCs have microsatellite instability (MSI)³⁵. Therefore, additional mouse models have been created, primarily involving mutations in the mismatch repair (MMR) genes, to address this tumor phenotype. Unlike human Lynch Syndrome (LS) a dominantly inherited CRC syndrome, mice heterozygous for single MMR mutations are indistinguishable from wild-type mice²⁶². Homozygous MMR mutant mice develop various cancers including a high preponderance of lymphomas, a rare phenotype in human LS^{262, 263}. With respect to intestinal tumors, the MMR mutant mice, like the *Apc* models, develop tumors primarily in the small intestine. *Mlh1*^{-/-} and *Msh2*^{-/-} mice develop high numbers of intestinal tumors, whereas *Msh3*^{-/-} and *Msh6*^{-/-} mice develop relatively few. In these mice, tumor development is tightly correlated with the extent of the MMR defect, as measured by MSI. Tumor formation is enhanced in *Msh3*^{-/-}/*Msh6*^{-/-} compound mutants. The generation of compound MMR *Apc* mutants (*Apc*^{Min+/-} or *Apc*^{Δ1638N/+}) increases colon-specific phenotypes. For a more detailed overview of MMR mutant mice, please see²⁶².

1.4.2.2 Chemical Models

Genetic models of CRC best approximate hereditary CRC syndromes, with most models involving genetic inactivation of the *Apc* gene, the gatekeeper in the adenoma to carcinoma sequence of tumor progression. Most tumors though do not arise in the presence of predisposing *Apc* mutations and therefore this has promoted the development of additional mouse CRC models.

Chemically-induced models of CRC in rodents have been extensively studied over the last few decades (reviewed in²²³) with the preferred models of choice using the carcinogens azoxymethane (AOM) or 1,2-dimethylhydrazine (DMH). The tumors induced by this model resemble sporadic/familial CRC in humans (occurring in the left/descending colon) and represent

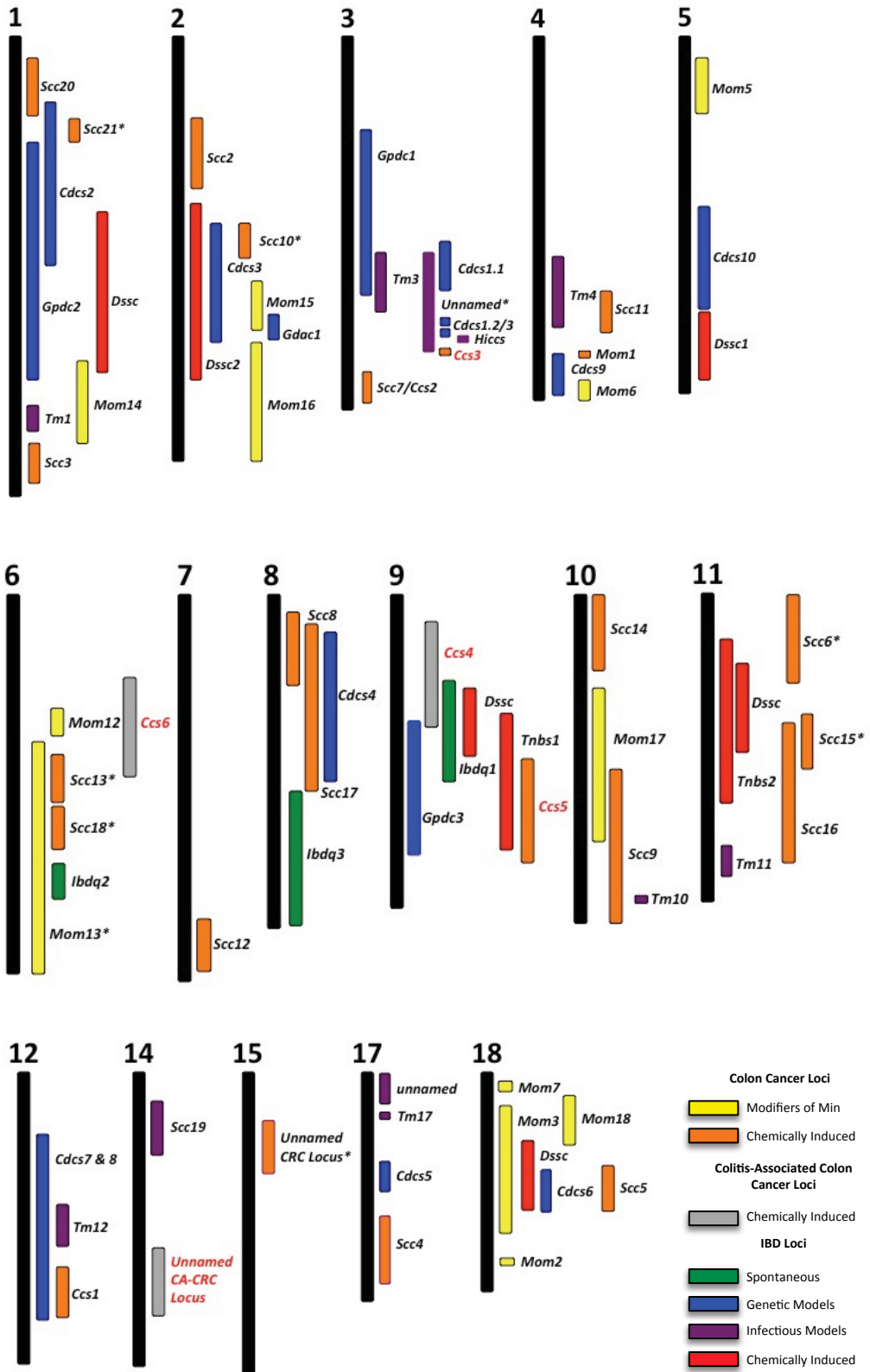


Figure 1.7: Mouse inflammatory bowel disease (IBD) and colorectal cancer (CRC) susceptibility loci. Summary of the current IBD and CRC loci mapped in inbred mice using forward genetic studies. Arranged by chromosome, each locus has been drawn to scale based on the current mapping data for each. Putative loci or loci that lack mapping data have been excluded. The three colitis-associated colon cancer loci shown have been mapped in Chapters 2 and 4 of this thesis. Loci whose precise map location is unknown (indicated with a *) have been drawn centered over the peak marker of association. Loci mapped by our lab are shown with names in red font. *Ccs*- colon cancer susceptibility, *Cdcs*- cytokine deficiency in colitis (*Il-10*^{-/-} mouse model of colitis), *Dssc*- dextran sulfate sodium-induced colitis, *Gpdc*-*G protein deficient colitis*, *Hiccs*- *Helicobacter hepaticus*-induced colitis and associated cancer susceptibility, *Ibdq*-inflammatory bowel disease quantitative trait loci (Spontaneous *SAMP1/YitFC* model of colitis), *Mom*- modifier of min (*Apc*^{Min+/-} model of CRC), *Scs*-susceptibility to colon cancer, *Tm*-*Trishuris muris*-induced colitis, and *Tnbs*- trinitrobenzene sulfonic acid susceptibility ^{196-199, 226-229, 255-259, 268-274, 311-317}.

a better model than the *Apc*^{Min/+} mouse, where tumors develop in the small intestine. The molecular and histological characteristics of these tumors have been summarized in detail in ²³².

The derivative of these carcinogens, methylazoxymethanol (MAM), was accidentally identified in a follow-up study of high levels of neurological disease in cattle from the island of Guam ²⁶⁴. The source of the neurological symptoms was attributed to high consumption of crude cycad flour, but when researchers fed rats high amounts of this flour no neurological symptoms were noted. Instead a high incidence of various cancers was noted. Follow-up studies in *Cycas circinalis*, the plant of origin of cycad flour, identified the glucoside cycasin (β -D-glucosyloxyazoxymethane) as the carcinogenic component, which is aglyconated to its activated form, MAM ^{264, 265}. AOM and DMH are pro-carcinogens that when injected intra-peritoneally (i.p.) or subcutaneously (s.c.) are converted to MAM in the liver by *Cyp2E1* ²²³. AOM is formed from the spontaneous dehydrogenation and subsequent oxidation of DMH ²⁶⁶. Further activation of AOM leads to production of a methyl cation in the colon. This in turn can react with deoxyguanosine at either the N⁷ or O⁶ position; with the latter leading to the formation of deoxymethylguanosine, resulting in mismatched base pairing and subsequent G to A transitions. Figure 1.8 A summarizes the steps in AOM and DMH activation ²²³.

It has been well established that repeated administration of AOM or DMH results in colorectal carcinogenesis in permissive mouse strains ²²³. Recently, there has been a shift towards more studies using AOM as it has longer stability, increased potency and is more colon-specific than DMH ²²³. In mice, AOM and DMH lesions are classified as either aberrant crypt foci (ACF), hyperplastic lesions or tumors ²³². Hyperplastic lesions are a form of ACF, which encompass several to hundreds of crypts ²⁶⁷. These are macroscopically visible lesions and may represent precursors to tumor development ²⁶⁸.

Inbred strains of mice differ significantly with respect to tumor development using various AOM or DMH protocols due to underlying genetic predisposition making them a good resource in the search for tumor susceptibility genes. In a large-scale study of AOM-induced CRC susceptibility of 33 inbred mouse strains, it was estimated that 68.8% and 71.3% of phenotypic variation in tumor multiplicity and surface area were attributable to strain-dependent genetic background ²⁶⁹. Prior to this study, little was known with respect to CRC susceptibility in the inbred mouse strains due to lack of a common protocol for CRC induction. It is now generally accepted that A/J, STS/A, SWR/J, ICR/Ha and FVB/N are susceptible and C57Bl/6

(B6), BALB/c, AKR and 129/Sv are resistant to AOM-induced CRC^{223, 268, 269}. While liver and lung metastasis have been observed in some AOM-induced CRC studies, metastasis is considered infrequent in this model and has only been observed after 30⁺ weeks²⁷⁰.

Several studies have been undertaken to map novel tumor susceptibility genes using either DMH or AOM, with 22 susceptibility to colon cancer (*Sc*) or colon cancer susceptibility loci (*Ccs*) identified to date. The first DMH-induced CRC locus, *Ccs1*, on mouse chromosome 12, regulates tumor progression in ICR/Ha (susceptible) and C57BL/6Ha (resistant) mice, in addition to several yet to be defined loci²⁷¹. The most comprehensive AOM/DMH-susceptibility locus studies have been mapped using a panel of informative RCS and RCS-derived F2 mice between susceptible STS/A and resistant BALB/cHeA mice¹⁹⁶⁻¹⁹⁹. *Sc*1, mapping to mouse chromosome 2, was subsequently associated with a mutation in the *Ptprj* phosphatase¹⁹⁶. *PTPRJ* phosphatase was subsequently shown to undergo loss of heterozygosity (LOH) in sporadic human CRC thereby providing additional evidence for the relevance of mouse models as a means to identify susceptibility genes in humans²²⁴. An additional 14 *Sc* loci have been mapped in these informative RCS mice mapping to mouse chromosomes 1-4, 6-8, 10, 11, 17 and 18 (Figure 1.7)¹⁹⁶⁻¹⁹⁹. These studies have identified multiple interacting loci, which include loci with no discernable effect in the absence of their interacting partner. A limitation of human studies is the ability to detect interacting loci, suggesting the importance of mouse models as a tool to map interacting tumor susceptibility loci in humans²²². Nine of these loci (*Sc*2, 3, 5, 8, 9, 11, 12, 13 and 15) have been associated with disease in crosses involving different parental inbred mouse strains suggesting that these may be common mouse CRC susceptibility loci^{269, 272}. These additional crosses have been quintessential helping to refine the *Sc*2, 3, 8 and 12 loci. Liu et al. also identified a novel, yet to be named locus, on mouse chromosome 15 using Efficient Mixed-Model Association (EMMA) mapping studies on 33-inbred mouse strains (Figure 1.7). *Sc*16-21, the most recently identified AOM-induced CRC susceptibility loci were mapped to chromosomes 1, 6, 7, 8 and 14 (Figure 1.7) in an A/J x SPRETUS/EiJ cross²⁷². An additional three *Ccs* loci have been identified (Figure 1.7). The *Ccs*2 locus, mapping to distal chr 3, was mapped between the relatively resistant CBA/J and C57Bl/6J strains²⁷³. This locus overlaps with the subsequently identified *Sc*7 locus, which has no phenotype when studied independently of its interacting partner locus, *Sc*8¹⁹⁷. It is not clear at this time if the *Ccs*2 and *Sc*7 loci represent the same locus, with differing penetrance in each genetic cross, or two

genetically distinct loci. In 2010, testing of 33 AcB/BcA RCS mouse strains by our laboratory identified the *Ccs3* locus, on mouse chr 3, as the major regulator of AOM-induced CRC susceptibility in A/J (susceptible) and B6 (resistant) mice ²⁶⁸. The *Ccs3* locus originally overlapped with the *Ccs2* and *Scs7* loci, but has subsequently been refined to a non-overlapping 2.2 Mb segment containing 12 candidate genes/transcripts ²⁷⁴. Our lab is currently investigating the role of several of these candidate genes in AOM-induced CRC. The *Ccs3* locus was subsequently validated in (A/J x B6)F2 mice ²²⁹. This screen also revealed a second locus on mouse chr 9 (*Ccs5*), which regulates tumor multiplicity in mice bearing at least one A/J-derived susceptibility allele at *Ccs3*. Similar to *Scs7*, the *Ccs5* locus does not influence tumor multiplicity independent of the *Ccs3* locus. The cellular and molecular mechanism(s) by which *Ccs5* genetically interacts and modulates penetrance and/or expressivity of *Ccs3*-determined susceptibility is unknown. Analysis of cases and controls enrolled in the Assessment of Risk of Colorectal Tumor in Canada study cohort identified a novel *Ccs3* x *Ccs5* analogous two-locus system in human CRC (unpublished data, ²²⁹). Neither loci in humans exceeded the genome-wide significant thresholds necessary to be identified independently of the mouse mapping data.

Collectively, this data serves to highlight an important role for mice in the identification of loci regulating susceptibility to CRC in mice. In particular, mouse models have been shown to be apt at identifying interacting loci, an aspect of disease pathogenesis poorly defined in humans.

1.4.3 Mouse Models of Inflammatory Bowel Disease and Colitis-Associated Colon Cancer

Over 70 different mouse models of colitis have been documented to date with most being reviewed in ^{223, 233}. Many models of colitis are also models of CA-CRC and therefore the two diseases have been grouped together to avoid redundancy. Mouse models of IBD fall into several categories based on underlying disease etiology; cell transfer, genetically engineered, congenital (spontaneous mutations), infectious and chemically induced. Rather than briefly highlight several models, that are not relevant to the methodology presented in this thesis, I will narrow the focus of this section to three relevant areas; the *Il-10* knockout genetic model of colitis/CA-CRC (due to importance of *IL-10* in early-onset IBD and CA-CRC), chemically-induced models of colitis/CA-CRC (the model used in this thesis), and the mapping of genetic loci regulating susceptibility using forward genetic approaches.

1.4.3.1 Genetic Models

With respect to modeling colitis and CA-CRC, most models are genetic, involving knockout of a specific gene or multiple genes, leading to disease pathology. These models are associated with an increase in IBD (either UC or CD) with or without subsequent CA-CRC. Some examples of genetic models associated with increased colitis with or without CA-CRC include the *Il-10*^{-/-}, *Il-2*^{-/-}, *Gpx1/2*^{-/-} and *Gnai2*^{-/-} mice (reviewed in ²³³).

The most-well characterized of the genetic models involves deletion of *Il-10* and has shed light on numerous dietary, microbial and genetic factors associated with IBD/CA-CRC initiation and progression. *Il-10* is a pleiotropic anti-inflammatory cytokine produced by monocytes and lymphocytes that acts to dampen and terminate immune responses ²⁷⁵. Polymorphisms/Mutations in *Il-10*, *Il-10RA*, *Il-10RB* and *Il-10*'s downstream target, *STAT3* have been linked to increased incidence of IBD in humans ⁹⁸. In addition, mutations resulting in loss of function of *Il-10* or its receptors have also been linked to early-onset enterocolitis in infants, characterized by severe inflammation requiring surgical removal of the affected areas of the bowel prior to the age of two ¹²⁴.

The 129/B6 *Il-10*^{-/-} knockout mouse line (*Il-10tm1Cgn*) was generated in 1993 by Kuhn et al., with mice raised in conventional or specific-pathogen free-facilities developing a high incidence of weight loss, anemia and enterocolitis 1-3 months post birth²⁷⁶. This CD4⁺ driven T_H1 associated enterocolitis is first detected in the proximal colon and then in the remaining colon, the duodenum and the proximal jejunum of the small intestine and mimics human CD, associated with discontinuous, transmural inflammation, ulceration and thickening of the bowel wall ²⁷⁶⁻²⁷⁸. However, it fails to fully recapitulate human disease due to the rare occurrence of granulomas and the absence of CD-characteristic fissures and fistulas.

Enterocolitis in *Il-10*^{-/-} mice, similar to the *Apc*^{Min+/-} model is strain-dependent, suggesting a strong role for genetic factors in disease pathogenesis. The most sensitive genetic backgrounds to are C3H/HeJBir and 129/Sv, with 100% of the mice developing severe colitis before 3 months of age ^{278, 279}. C3H/HeJBir mice, which carry a wildtype *Il-10* gene are also susceptible to spontaneous colitis ²³³. CA-CRC susceptibility has not been assessed in the C3H/HeJBir *Il-10*^{-/-} mice ²⁷⁹. On the 129/Sv background, 67% of the mice develop adenocarcinomas in the first 6 months of life ²⁷⁸. Using histopathologic means BALB/cJ *Il-10*^{-/-} mice have a higher incidence of spontaneous colitis (100%) compared to B6 *Il-10*^{-/-} (57%) at 3

months of age, but a lower incidence of colonic tumors (29%) at 6 months of age compared to 129/Sv *Il-10*^{-/-} mice. B6 *Il-10*^{-/-} mice do not develop colonic adenocarcinomas within this timeframe. NOD/LtJ *Il-10*^{-/-} mice also develop severe colitis, associated with 100% incidence of rectal prolapse, although the time frame for disease development is not highlighted²⁸⁰. These NOD/LtJ *Il-10*^{-/-} mice are not good models for CA-CRC as high incidence of rectal prolapse prevents long-term studies in these mice. Together these studies highlight an important role for genetics in colitis and CA-CRC susceptibility.

Environmental factors, specifically the intestinal microbiota, are the most significant factors regulating susceptibility to colitis and CA-CRC in *Il-10*^{-/-} mice, with mice raised in germ-free conditions failing to develop active disease²³³. In addition, disease is attenuated, limited primarily to the proximal colon, in mice raised in specific pathogen-free facilities²⁷⁶. Generally, *Helicobacter species*, *Escherichia coli* and *Campylobacter vulgatus* are associated with increased disease severity, while *Lactobacillus*, *Bifidobacterium* and certain antibiotics are considered protective in *Il-10* deficient colitis.

1.4.3.2 Chemically-Induced Models

Chemical models of colitis and CA-CRC are commonly used to study the effects of diet, treatment, microbial factors and genetics on colitis and CA-CRC susceptibility. These models are advantageous in that they are often relatively inexpensive, highly reproducible and easy to administer. An added advantage over genetic models is the ability to control the time of onset, the duration and the severity of colitis, which can be adjusted by changing the dose and/or length of the treatment protocol. In addition, unlike genetic colitis models, the inflammatory agents can be removed and thus the healing/regeneration process can be studied in detail.

1.4.3.2.1 Haptens

The use of haptens, small molecules that can elicit strong immune responses when bound to larger molecules, such as proteins, are a popular choice for the induction of colitis. These haptens include TNBS (2,4,6-trinitrobenzenesulfonic acid), DNBS (2,4-dinitrobenzenesulfonic acid) and oxazolone^{281, 282}. Intra-rectal administration of the hapten alone is not sufficient to induce colitis. Therefore, haptens are administered in diluted ethanol, which disrupts the epithelial cell barrier thus enabling the hapten to combine with native proteins and microbial by-products in the intestinal lumen to elicit an immune response resulting in colitis. Ethanol/Hapten

administration alone is not sufficient to induce CA-CRC, but a study in rats demonstrated increased tumor incidence when administered in conjunction with the known carcinogen DMH ²⁸³.

TNBS (C₆H₃N₃O₉S)-induced colitis is the most frequent model of hapten-induced colitis. When administered intra-rectally, TNBS results in a T-cell driven T_H1 immune response associated with colonic transmural inflammation and macrophage/neutrophil infiltrates, mimicking human CD in permissive mouse strains ²⁸⁴. Depending on dosing protocols, TNBS may induce acute, established or chronic colitis, although the protocols necessary for induction of these are highly variable and reviewed in ²⁸⁵. SJL mice are highly susceptible; C3H/OuJ intermediately susceptible; and strains such as B6, B10 and DBA/2J are highly resistant to TNBS colitis ²⁸⁴. BALB/c mice are susceptible to TNBS-induced colitis, but mount a more T_H2-driven immune response, suggesting a different mechanism of susceptibility in these mice. Treatment of mice with topical applications of TNBS prior to intra-rectal administration can increase sensitivity. This differential susceptibility has led to the mapping of novel susceptibility loci (see 1.4.3.3). DNBS (C₆H₄N₂O₇S)-induced colitis is phenotypically similar to TNBS colitis in the early stages, although less well studied ²⁸⁶. It is a more stable alternative to TNBS, but more selective with respect to binding partners and thus must be administered at higher concentrations than TNBS.

Oxazolone (OXA, C₃H₃NO₂) induces a T_H2 driven-response in permissive mice associated with increased *Il-4* and *Tgf-β* production, mimicking human UC ²⁸⁷. OXA induces ulceration and macrophage/neutrophil infiltrates affecting the superficial layer of the mucosa in the distal colon. SJL mice are highly susceptible to treatment with over 50% mortality. Mortality is decreased in susceptible BALB/c mice making them ideal to study treatment options of OXA-induced colitis ²⁸⁸. B6 and B10 mice are moderately susceptible, but only if pre-sensitized (OXA painted on skin) prior to treatment ²⁸⁹.

These studies of hapten-induced colitis have shed light on numerous pathogenic (*Smad7*, *Tnf-α*, *Stat3*, *Mmp9*) and protective (NK cells, *Il-10*, *Il-23*) molecules associated with IBD initiation and progression. In addition, TNBS studies have identified several possible IBD therapeutic agents (ciprofloxin, carbon monoxide, carbon monoxide), which are reviewed in more detail in ²³³.

1.4.3.2.2 Dextran Sulfate Sodium-Induced Colitis

Dextran sulfate sodium (DSS) is a long chain (5-140 kDa), negatively charged polysaccharide derived from the esterification of dextran and chlorosulfonic acid (Figure 1.8 B) (www.mpbio.com)²⁹⁰. When administered to rodents in drinking water, DSS is a highly potent inducer of colitis, mimicking human UC²⁹¹. T and B cells are not essential for DSS-induced colitis and therefore this model enables the study of both innate and adaptive immune responses in IBD^{292, 293}.

Okayasu et al. described the first use of DSS-colitis in mice in 1990 showing that either single or cyclical doses of DSS resulted in increased colitis in permissive mouse strains²⁹¹. Mice treated with DSS present with symptoms including increased weight loss, diarrhea and blood in the stool, consistent with human colitis. At sacrifice, colonic atrophy was noted arising from increased crypt atrophy. The location of colitis is highly dependent on DSS molecular weight, with low weight DSS (5 kDa) inducing lesions in the cecum and proximal colon, 40 kDa DSS inducing lesions in the mid and distal colon and high weight DSS (500 kDa) failing to induce colitis²⁹⁴. All future mention of DSS in this thesis refers to mid-weight (~36-54 kDa) DSS.

Generally, acute colitis, associated with a T_H1/T_H17-driven immune response, is induced using a single DSS treatment (2-10%, 4-8 days) and chronic colitis, associated with T_H2 driven immune response, is induced using cyclical doses of DSS (3 or more cycles, 2-10% DSS, 4-7 days per treatment) with each treatment ~ 2 weeks apart^{282, 295}. Acute colitis is associated with loss of crypts, inflammatory cell infiltrates in the mucosa and submucosa, epithelial cell erosion and ulceration²⁹⁶. Chronic colitis in mice is associated with a mixed phenotype including areas of active disease (associated with the symptoms above), area of inactivity, crypt distortion, increased cell proliferation and in some instances, dysplasia. The specific mechanism through which DSS induces colitis in permissive mouse strains is not well characterized, but is thought to be multifactorial, involving toxicity to epithelial cells, disruption of normal interactions between lymphocytes and epithelial cells, interactions with medium chain length fatty acids and the intestinal microbiome²⁹⁷⁻²⁹⁹. In addition, genetic and microbial factors have been shown to have opposing roles in acute vs chronic disease, highlighting the complex nature of IBD^{233, 300}.

Important to this thesis is the observation that inbred mice vary with respect to susceptibility to colitis due to inherited genetic factors. Most studies in inbred mice have been

conducted using the acute DSS model. In a large study of acute DSS-colitis susceptibility C3H/HeJ, C3H/HeJBir and NOD/LtJ mice were susceptible whereas B6, 129/SvPas, NON/LtJ and DBA/2J were resistant³⁰¹. Male mice are more susceptible to DSS-induced colitis in the distal colon, compared to females³⁰¹. Other studies have shown disease in CBA/J and BALB/c, but the extent of this inflammation is difficult to judge relative to the aforementioned strains due to differences with respect to choice of DSS protocol²⁹¹. This differential susceptibility in these inbred mouse strain has been exploited leading to the mapping of several DSS-induced colitis loci (see 1.4.3.3). It has also been shown that endpoint is an important parameter in DSS-induced colitis studies, with BALB/c mice recovering from acute DSS treatments, whereas B6 mice failed to resolve this colitis progressing to chronic disease³⁰². Through the generation of numerous knockout and transgenic mice, both protective and detrimental roles for various cytokines, chemokines, stress proteins, epithelial and metabolic factors have been recognized and are highlighted in²³³.

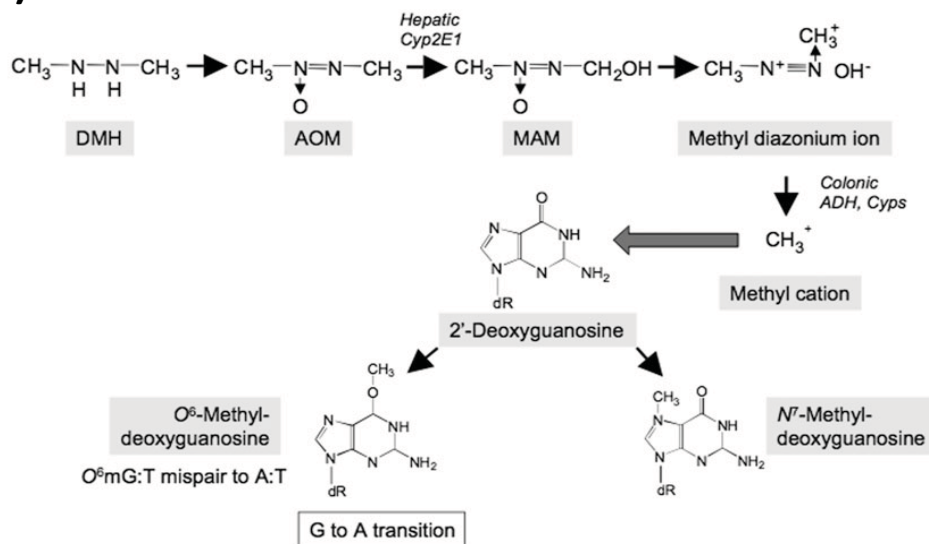
Acute DSS-induced colitis is not sufficient to induce CA-CRC in mice³⁰³. Chronic DSS-colitis can induce tumor formation in permissive mouse strains, highlighting the importance of inflammation in CA-CRC pathogenesis. However, tumor induction requires at least 4 cycles of DSS and is associated with both low incidence (< 20%) and multiplicity (< 2 tumors/colon). Combination of a carcinogen with cyclical doses with DSS can increase CA-CRC incidence (100%) in permissive mice.

1.4.3.2.3 Azoxymethane/Dimethylhydrazine Dextran Sulfate Sodium Colitis-Associated Colon Cancer

In 2003, Tanaka et al. published results showing that a single AOM injection (10 mg/kg), followed a week later by a 7-day DSS (2%) treatment, was sufficient to induce macroscopically visible tumors 20 week post-initiation in CD-1 mice³⁰⁴. Mice treated with only a single AOM or single DSS injection did not develop tumors within this 20-week period, suggesting that combined administration of both AOM and DSS is essential for tumorigenesis.

CA-CRC using 7-day cyclical DSS-treatments can be fatal in colitis-susceptible mice and therefore more often the AOM-injection is followed by 3 cyclical 4-5 day DSS (2-3%) treatments, commencing 7 days post-injection, with each treatment 16-17 days apart²²³. Similar to the DSS-model of colitis increased weight loss and rectal bleeds are noted in susceptible mice, with symptoms clustered during or shortly after each DSS treatment. As the clinical endpoint of

A)



B)

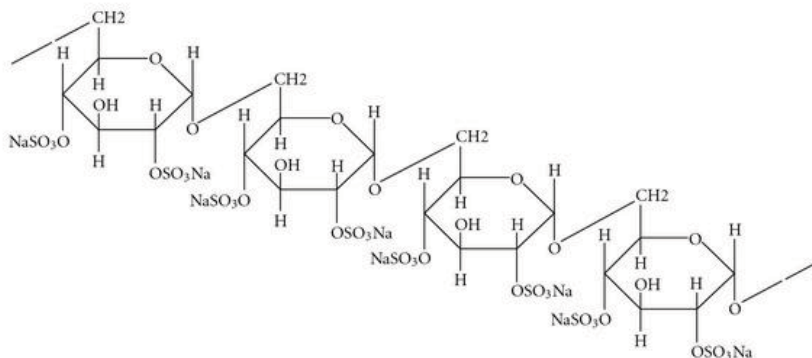


Figure 1.8: Azoxymethane and Dextran Sulfate Sodium Structures. (A) Metabolism of azoxymethane and dimethylhydrazine. AOM, azoxymethane; DMH, 1,2-dimethylhydrazine; Cyp2E1, cytochrome P450 2E1; MAM, methylazoxymethanol; ADH; alcohol dehydrogenase; Cyps, cytochrome P450 superfamily. (B) Chemical structure of dextran sulfate sodium. *Adapted with permission from Rosenberg et al. 2009 and Tanaka 2012* ^{223,290}.

the experiment approaches symptoms are more consistent with AOM-induced CRC, including the development of rectal prolapses. Similar to the AOM-only model of CRC, AOM/DSS-induced tumors develop primarily in the mid and distal colon of permissive mice. Tumors, usually tubular adenomas or adenocarcinomas, are associated with shorter latency compared to the AOM-only model of CRC and develop in areas of active inflammation. It should be noted that the AOM/DSS studies primarily use DSS in the ~36 to 54 kDa range and hence the localization of disease in the mid and distal colon. AOM/DSS-induced tumors are non-metastatic.

While it is known that the inbred strains of mice differ with respect to CA-CRC susceptibility due to genetic predisposition, studies vary markedly with respect to choice of carcinogen, dose, number of DSS treatments, and time to sacrifice, all of which can greatly influence total tumor numbers²²³. In a study of AOM/DSS-induced CRC in 4 strains of inbred mice, BALB/c mice were the most susceptible and B6 mice had an intermediate phenotype, whereas C3H/HeJ and DBA/2 mice were resistant³⁰⁵. Other studies suggest that Swiss Webber, CBA/J, CD-1 and FVB/NJ mice may be susceptible^{303, 304, 306, 307}.

Numerous studies have been published since 2003 identifying key dietary, microbial and genetic factors associated with CA-CRC initiation and progression. Liang et al. recently published results highlighting shifts in the colon microbiome following AOM/DSS-treatment highlighting an important role for certain *Lactobacillus* and *Bacteroides* species³⁰⁸. The AOM/DSS model has also been used to study the human microbiome directly through the use of fecal transplants into B6 mice³⁰⁹. AOM/DSS studies have also demonstrated key roles for *Nfkβ*, *Tgf-β*, *Tnf-α*, *Cox2*, *p53* and *iNOS* in tumorigenesis. These and other key pathways are discussed in greater detail in³¹⁰.

1.4.3.3 Colitis and Colitis-Associated Colon Cancer Loci: Forward Genetic Mapping Studies

Inbred mice vary with respect to susceptibility to both colitis and CA-CRC due to inherited genetic factors leading to the mapping of more than 30 different colitis susceptibility loci (Figure 1.7). In addition, a single locus has been identified that regulates susceptibility to colitis and CA-CRC, the *Hicss* locus, on chromosome 3³¹¹. Unlike human CA-CRC though, lesions in this model are found primarily in the proximal colon. The loci mentioned above have been mapped using spontaneous (SAMP1/YitFC), chemical (DSS, TNBS), genetic (*Il-10*^{-/-},

Gnai^{-/-}, *Gpx1/2^{-/-}*) and infectious (*Helicobacter*, *Trichuris Muris*) models of colitis and CA-CRC^{226-228, 311-316}. Despite differences with respect to strains of mice tested and models of colitis used, these studies share a common feature the identification of multiple genetic loci regulating susceptibility.

As shown in Figure 1.7, there is significant overlap between the different loci. These overlaps occur between similar models (ie. infectious colitis- *Trichuris* and *Helicobacter*, chemical colitis- DSS and TNBS), but also different models (ie. chemical- DSS and genetic *Il-10^{-/-}* mice). One example, with four overlapping loci, is mouse chromosome 9. These loci include; *Ibdq1* locus (spontaneous colitis in SAMP1/YitFc mice); an unnamed DSS susceptibility loci mapped in NOD/LtJ mice; an SJL TNBS locus, *Tnbs2*; and an *Gnai2^{-/-}* C3H associated locus, *Gpdc3*^{226, 227, 312, 313}. *Il-10ra* maps to this locus and represents an attractive candidate gene being associated with both early and adult onset IBD^{98, 124}. In chapter 2 of this thesis, we map a novel A/J-derived CA-CRC locus to this region, *Ccs4*³¹⁷. This suggests that the same locus could regulate susceptibility to both CA-CRC and colitis, although additional experiments are necessary as the involvement of the colitis loci in CA-CRC and the implication of the *Ccs4* locus in colitis have not been studied. It is also interesting to note that several of these IBD loci also overlap with known CRC loci (*Mom*, *Scs* and *Ccs*) (Figure 1.7), despite the lack of inflammation in these CRC models. Again, it poses questions about possible common mechanisms in IBD and CRC.

As mentioned earlier in this introduction, more than 163 IBD susceptibility loci have been mapped, the largest number for any common disease⁹⁸. Therefore, it is possible to question the need for these forward genetic colitis studies in mice. These mouse models offer a significant advantage over human studies; the ability to detect interacting loci. For example, *Dssc1* and *2* are interacting loci, as are *Gpdc1* and *2*^{226, 313}. *Gpdc3* was also shown to interact with an unnamed locus on chromosome 7 that has no effect on its own³¹³. There are also numerous interactions between the *Cdcs* loci, which regulate differential susceptibility to colitis in *Il-10* deficient mice on a B6 vs C3H/HeJBir background²²⁸. The ability to detect interacting loci in mice may serve as a guide to identifying these loci humans. These studies also highlight a serious gap in the literature, which this thesis aims to fill, relating to the identification of low penetrance CA-CRC genes.

1.5 Thesis Objective

CA-CRC is a complex disease arising from a combination of dietary, lifestyle, microbial and genetic factors. In addition, disease risk is tightly correlated, with severity, location and duration of colonic inflammation (IBD). CA-CRC risk is increased in early-onset IBD patients and this specific subset of IBD patients is increasing in Canada, suggesting that CA-CRC may be a growing concern for future generations¹¹⁸. Our lab is interested in understanding various genetic contributions to complex traits. In humans, low penetrance disease susceptibility genes can be identified in genome-wide association studies. These have been highly successful in mapping numerous IBD and familial CRC loci, but no CA-CRC loci have been mapped, most likely due to complication in identifying a uniform study population.

The complex and heterogeneous genetic components of complex diseases can be difficult to tease apart in human populations due to confounding environmental and dietary effects. However, these traits can be dissected in genetically well defined inbred, and recombinant congenic mouse strains, in which single gene effects fixed by inbreeding can be mapped by linkage analysis and identified by positional cloning. The mouse is the animal model of choice for these analyses because: 1) of the similarity of genetic lesions to humans; 2) chemical inducers of CRC are available, which reduces the contributions of environmental factors on pathogenesis; 3) diverse inbred strains are available, which vary with respect to disease susceptibility due to inherited genetic factors; and 4) the sequence of the mouse genome is known, including dense haplotype maps, facilitating positional cloning. Numerous mouse models of CRC, IBD and CA-CRC have been generated to study the influence of diet, genetics and microbial factors on disease risk. However, while numerous IBD and familial CRC loci have been mapped in mice, again there is little known with respect to genetic contributions to CA-CRC in mice. *Therefore, the objectives of this thesis center on filling this gap in the current literature.*

This will involve:

- 1) identifying novel susceptible and resistant strains of mice for gene mapping and*
- 2) mapping low penetrance susceptibility genes using informative F2 and recombinant congenic populations.*

To address these questions, we have used the azoxymethane/dextran sulfate sodium (AOM/DSS) models of CA-CRC. This is an ideal model as the tumors that develop mimic human CA-CRC arising primarily in the mid and distal colon and this model enables both innate

and adaptive immunity to be studied. In addition, unlike genetic models, the doses of carcinogen and DSS can be adjusted, which may help to resolve subtle phenotype differences. Numerous AOM-only and DSS-induced susceptibility loci have been mapped in inbred mice and therefore, we will use these studies as a framework to guide gene identification in our model.

Chapter 2: A Two-Locus System Controls Susceptibility to Colitis-Associated Colon Cancer in Mice

This manuscript was previously published as follows:

Van Der Kraak, L, Meunier, C, Turbide, C, Jothy, S, Gaboury, L, Marcus, V, Chang, SY, Beauchemin, N, and Gros, P. (2010) A two-locus system controls susceptibility to colitis-associated colon cancer in mice. *Oncotarget*. 1(6): 436-46.

2.1 Connecting Text

A/J and B6 mice are highly susceptible and resistant to azoxymethane (AOM)-induced colorectal cancer (CRC), which mimics familial CRC in humans. Using a panel of commercially available RCS mice, our lab mapped the differential susceptibility between these two strains to a 2.2 Mbp locus, *Ccs3*, on distal mouse chromosome 3²⁶⁸. Subsequent mapping in an (A/J x B6)F2 population identified a second locus, *Ccs5*, that regulates tumor burden in mice carrying at least one susceptibility allele at *Ccs3*²²⁹. The *Ccs5* locus was mapped after this chapter was published and therefore it will not be mentioned further.

In 2003, Tanaka et al. published a novel colitis-associated (CA)-CRC model, which involved a single injection of AOM followed by treatment with the inflammatory stimulant dextran sulfate sodium (DSS)³¹⁸. This AOM/DSS-model mimics CRC that arises in patients with the inflammatory bowel diseases (IBD), ulcerative colitis or Crohn's disease. Both familial and CA-CRC are associated with the accumulation of mutations in several different tumor suppressors/oncogenes. While similar molecular alterations underlie all CRC development, the timing and frequency of these events differ, which has led to speculations that different genes may regulate susceptibility to familial and CA-CRC^{148, 150, 151}. Therefore, our objective for this chapter was to assess if the *Ccs3* locus was involved in CA-CRC susceptibility in A/J and B6 mice and if not to map the corresponding genetic effect.

In this chapter CRCs are classified as hereditary, sporadic or inflammatory. This reflects, the current opinions of CRC genetics at the time of publication and hence the categories are different than those discussed in the Introduction. Familial CRC, associated with polymorphisms in low penetrance tumor susceptibility genes, are categorized as part of sporadic CRCs in this chapter.

2.2 Contribution of the Authors

The experiments included in this chapter were planned as part of a collaborative effort between LVDK, CM, NB and PG. CT performed the carcinogen injections. CT and CM were responsible for the experiments summarized in Figure 2.2. LVDK prepared all DSS treatments, monitored the mice, scored the colons and completed the in-house genotyping for the F2 experiment. LVDK, CM and CT sacrificed the F2 mice. DNA extractions were a collaborative effort between LVDK, CM and an undergraduate project student, Li Hsia (Alicia) Cheong. CM and LVDK prepared cassettes for histological processing, which were subsequently analyzed by

SJ, LG, VM and SYC. LVDK wrote the paper and prepared the figures with feedback from PG and NB. Susan Gauthier, mentioned in the Acknowledgements, was responsible for generating the F1 and F2 mice

2.3 Abstract

We have previously shown that the differential susceptibility of the A/J (susceptible) and C57BL/6J (B6, resistant) mouse strains to azoxymethane (AOM)-induced colorectal cancer (CRC) is controlled by the chromosome 3 locus, *Ccs3*. We report that A/J and B6 mice also show differential susceptibility to colitis-associated (CA)-CRC induced by combined administration of AOM and dextran sulfate sodium. This differential susceptibility is not controlled by *Ccs3*, but is under distinct genetic control. Linkage analyses in (A/J x B6)F2 mice detected a major CA-CRC susceptibility locus on chromosome 9 (*Ccs4*), which controls tumor multiplicity and tumor surface area. Susceptibility alleles at *Ccs4* are inherited in a recessive fashion, with A/J alleles associated with susceptibility. We also detected a second locus on chromosome 14 that acts in an additive fashion with *Ccs4*. Strikingly, F2 mice homozygous for A/J alleles at both loci (*Ccs4* and chromosome 14) are as susceptible to CA-CRC as the A/J controls, while mice homozygous for B6 alleles are as resistant as the B6 controls, thus supporting the role of two interacting loci in this CA-CRC model. This indicates that susceptibility to chemically induced CRC and susceptibility to CA-CRC are under distinct genetic control in mice, and probably involve distinct cellular pathways.

2.4 Introduction

Colorectal cancer (CRC) is the third most common cause of cancer-related deaths worldwide³¹⁹. CRC etiologies can be classified as hereditary (10%), sporadic (<90%) or inflammatory (1-2%)³²⁰. Hereditary CRCs arise due to highly penetrant germline mutations³⁵. The two most common syndromes are familial adenomatous polyposis (FAP) and hereditary non-polyposis colon cancer (HNPCC) that arise due to mutations in the *APC* (*Adenomatous polyposis coli*) gene and mismatch repair genes (*MSH2*, *MLH1*, *MSH6* and *PMS2*), respectively. Sporadic CRCs are thought to have a heterogeneous etiology, including a combination of complex environmental and genetic components³²¹. Recently, several genome-wide association studies (GWAS) have revealed as many as ten common low-penetrance genetic variants contributing to sporadic CRC risk: these genes or loci are found on human chromosomes 8, 10,

11, 14, 15, 18, 19 and 20^{173-175, 179, 181, 322}. Inflammation, in the form of the inflammatory bowel diseases (IBD), ulcerative colitis (UC) and Crohn's disease (CD), represents the third most common risk factor for CRC after FAP and HNPCC⁶⁸. These colitis-associated (CA) CRCs have many similar molecular alterations to sporadic CRCs and therefore were originally considered to be a subtype of sporadic CRCs. However, the timing and frequency of these molecular events differ, which has led to speculations that different genes may be responsible for sporadic CRC and CA-CRC^{68, 320}. Both CD and UC are influenced by a variety of environmental and genetic factors including low penetrance susceptibility genes. To date, GWAS studies point to > 30 genetic loci/genes for susceptibility to CD and UC, with several shared loci involved in the T_H17 response (*NOD2*, *IL23R*, *IL12B*, *JAK2*, *STAT3*)^{123, 323, 324}. Allelic differences in the class II human leukocyte antigens (HLA) on chromosome 6 are associated with both increased and decreased risk of CA-CRC³²⁵. Interestingly, loss of heterozygosity (LOH) on chromosome 6 has been previously reported as a unique feature of CA-CRC, distinguishing it from sporadic CRC and UC³²⁶.

In addition to human GWAS studies, significant contributions have been made towards identifying tumor susceptibility genes using carcinogen-induced mouse models. Sporadic CRC can be modeled through repeated administration of the colon-specific carcinogens 1,2-dimethylhydrazine (DMH) or its metabolite azoxymethane (AOM)³²⁷. DMH studies in recombinant congenic lines derived from BALB/c (resistant) and STS/A (sensitive) progenitors have identified the *Sccl* locus (*Ptprj* phosphatase) as a major regulator of susceptibility to intestinal tumors^{196, 197}. Subsequently, *PTPRJ* phosphatase was shown to undergo loss of heterozygosity (LOH) in sporadic human CRC²²⁴. Our lab has mapped a novel major CRC susceptibility locus *Ccs3*, on mouse chromosome 3, which controls the differential susceptibility of A/J (susceptible) and C57Bl/6J (B6, resistant) strains to AOM-induced CRC²⁶⁸.

On the other hand, CA-CRC can be modeled in mice using a single injection of either DMH or AOM followed by intermittent oral administration of inflammation-provoking dextran sulfate sodium (DSS)²⁸². This treatment causes thickening of the mucosa, leukocytic infiltration and increased vascular density with permeabilization of the epithelial cell barrier. Several candidate genes have been implicated in CA-CRC in mice. For example, *Il-2/b_{b2}* and *Il-10* appear to play a protective role in CA-CRC, with increased incidence of colonic inflammation and adenocarcinomas in mice bearing inactivating mutations at these genes^{278, 328}. Likewise, the

key activator *Nfkb* plays a critical role in inflammation and CA-CRC, and inactivation of *Ikkb* (the *Nfkb* activating kinase) or *Tnfa* (the upstream activator of *Nfkb*) result in reduced tumor burden^{329, 330}. While the aforementioned genes are crucial in CRC development no studies have been undertaken to identify low penetrance CA-CRC susceptibility loci in mice.

We have undertaken genetic studies in mice to identify genetic loci that regulate susceptibility to CA-CRC, and that may be relevant to human cancer. Here, we show that A/J (susceptible) and B6 (resistant) mice show differential susceptibility to CA-CRC. This is controlled by a novel two-loci system on chromosome 9 (*Ccs4*) and 14 with an additive effect.

2.5 Materials and Methods

2.5.1 Ethics Statement

This investigation has been conducted in accordance with the national and international guidelines set forth by the Declaration of Helsinki and the McGill University review board.

2.5.2 Animals

Inbred A/J, C57BL/6J (B6) and (A/J x B6)F1 mice were originally purchased from Jackson Laboratory (Bar Harbor, ME, USA). The AcB/BcA recombinant congenic strain set was derived from a double backcross (N3) between A/J and B6 parents at McGill University. The breeding scheme used for the derivation of these strains, and genotype data for these animals established for 625 informative markers has been previously described³³¹. The (A/J x B6)F2 mice were generated by systematic brother-sister mating from a (A/J X B6)F1 hybrid. All mice were maintained at the Animal Care Facility of McGill University according to the guidelines of the Canadian Council on Animal Care. They were fed regular chow and water ad libitum. All experiments were conducted on mice that were a minimum of 8 weeks of age with a minimum of 5 mice per experimental group. For the duration of the experiments mice were weighed/visually monitored a minimum of twice per week for clinical symptoms. Animals showing signs of discomfort were humanely sacrificed immediately.

2.5.3 Azoxymethane-Induced CRC

The protocols for induction of colorectal cancer (CRC) by azoxymethane (AOM), the collection of colons, harvesting of tumors and normal mucosa, and scoring methodology were previously described²⁶⁸. Briefly, 10 week-old mice were injected with the carcinogen AOM (Sigma, St Louis, MO, USA) once per week for 8 weeks (intra-peritoneal injections of 10 mg/kg).

Mice were sacrificed at 19 weeks and the entire colon was fixed in 10% phosphate-buffered formalin and subsequently scored for the number of tumors and hyperplastic lesions.

2.5.4 Colitis-Associated CRC

Induction of colitis-associated colorectal cancer (CA-CRC) was performed using a combination of AOM and dextran sulfate sodium (DSS Salt Reagent Grade MW 36,000-50,000, MP Biomedicals LCC, Solon, OH, USA). Mice were given a single injection of AOM (10 mg/kg i.p) on day zero, followed by three 4 day cycles of 3% DSS in drinking water. The first treatment was administered exactly a week after the AOM injection with each subsequent treatment 17 days apart. Following the final DSS treatment, mice were given normal water until the end of the experiment (week 14 or 19). The 3% DSS solution was prepared by dissolving DSS in tap water and filter-sterilized using a 0.22 μm filter (Stericup® Filter Units, Millipore). Fresh 3% DSS was replenished every second day for the duration of treatment. Mice were monitored for DSS consumption during treatment (averaged per cage), with no significant differences being detected amongst the groups. At the end of experiment the mice were sacrificed and their colons collected and tumors enumerated²⁶⁸. Tumors were measured using a clear transparency of 1 mm² graph paper and total surface area determined based on the total number of squares overlaying the tumor (measured to the nearest 0.25 mm²).

2.5.5 Histology

The mice were sacrificed and the large intestine (anus to cecum) was removed, washed in PBS and fixed in 10% phosphate-buffered formalin. Fixed tissues were dehydrated in ethanol and paraffin-embedded prior to sectioning (6 μm thickness). Samples were subsequently deparaffinized, mounted onto slides, stained with eosin and counterstained with hematoxylin, following standard histological procedures. Tumor grading and scoring of inflammation according to recommendations of Wirtz *et al.*²⁸² was performed by four pathologists (SJ, LG, VM, and SYC). Images were acquired using a Zeiss Axiovert instrument (Zeiss Canada, Toronto, ON, Canada) and processed using Adobe Photoshop (www.adobe.com)²⁶⁸.

2.5.6 Linkage and Quantitative Trait Loci (QTL) Mapping

Genomic tail DNA was extracted using a standard proteinase K treatment³³¹. The genomic DNA was genotyped for a combined total of 142 single nucleotide polymorphisms

(SNPs) and microsatellite markers with coverage at approximately 25 Mb intervals throughout the genome. SNPs and microsatellite markers polymorphic between A/J and B6 were chosen from the Mouse Genome Informatics (<http://www.informatics.jax.org/>) database. Initial genotyping was performed using a custom-designed panel of SNPs and run using Sequenom iPLEX Gold technology. Additional genotyping of microsatellite markers was done by either standard (α - ^{32}P)-dATP labeling PCR reactions with separation on 6% denaturing polyacrylamide gels or non-radioactive PCR with subsequent separation on 2%-3% agarose gels and ethidium bromide staining. All QTL linkage analyses were performed using R/qtl and the EM maximum likelihood or Hayley-Knott algorithms³³². A one-dimensional scan was performed using the scan-one function and empirical genome-wide significance was calculated by permutation testing (1000 tests). To search for possible two gene interactions, a two-dimensional scan was performed using the two-QTL model. Linkage analysis was conducted using tumor multiplicity and tumor surface area as independent phenotypic markers of differential susceptibility to CA-CRC.

2.5.7 Statistical Analysis

Data is expressed as the mean +/- the standard deviation and all analyses were performed using the Student's t-test. Results were considered significant if the $p \leq 0.05$.

2.6 Results

2.6.1 A/J mice are Susceptible to Colitis-Associated Colorectal Cancer

In the present study, we investigated whether the two test strains, A/J and B6, differ in response to colitis-associated colon cancer development (CA-CRC). A/J and B6 mice were treated with a single dose of azoxymethane (AOM) followed by 3 subsequent treatments of dextran sulphate sodium (DSS) (Figure 2.1 A). Colons were examined at 3, 10, 14 or 19 weeks post-treatment and graded for degree of inflammation, and presence of hyperplastic lesions, and tumors. Inflammation was scored as described in²⁸². At 3-weeks post-treatment (Figure 2.1 B and C) grades 1 and 3 inflammation scores were present in A/J and B6 colons, as defined by either a more scattered lymphocyte infiltration (Figure 2.1 B) or a larger extended infiltration with increased thickening of the mucosa (Figure 2.1 C). By 10 weeks post-treatment, B6 mice generally had higher inflammatory scores than A/J mice with low-grade dysplasia becoming apparent in some animals (Figures 2.1 D and E). At 10 weeks, B6 mice demonstrated larger

areas of extended inflammation, as noticed previously²⁸². By 19 weeks, flat lesions with clearly defined circular boundaries were identified and scored as hyperplastic lesions. Tubular adenomas were also detected (> 0.5 mm diameter) protruding into the lumen of the colon. The multiplicity and surface area of these tumors were used as the second and third quantitative traits in our genetic analyses. These lesions were mainly identified in the distal portion of the colon with scattered tumors being found occasionally in the proximal portion. After 14 weeks, mice showed decreased amounts of inflammation with almost complete disappearance of the inflammation by week 19. On the other hand, A/J mice developed significantly more tubular adenomas relative to their B6 counterparts 14-19 weeks post initiation. An example of such lesions is shown in Figure 2.1 F after a 19-week treatment period showing grade 3 inflammatory foci (Figure 2.1 F, arrows). These results indicate that A/J mice, although seemingly less susceptible to initial DSS-induced inflammation, nevertheless are highly susceptible to developing CA-CRC later on, compared to B6 mice.

2.6.2 CA-CRC susceptibility in A/J is Independent of Alleles at the *Ccs3* Locus

To quantify the differential susceptibility of the A/J and B6 mouse strains to CA-CRC, mice were subjected to the AOM/DSS protocol and their colons examined 19 weeks post-treatment initiation for tumor multiplicity. Results in Figure 2.2 B show that, on average, A/J mice developed a greater number of colon tumors than their B6 counterpart ($p < 0.01$). Although the absolute tumor numbers in the A/J and B6 strains showed experimental variability, we consistently observed significant differences in tumor multiplicity between these two strains in independent experiments (Figure 2.2 B and Figure 2.3 A).

Inbred A/J and B6 mouse strains are either highly susceptible or fully resistant, to carcinogen-induced CRC, respectively²⁶⁸. This is determined by the *Ccs3* locus on chromosome 3. The *Ccs3* locus was mapped as a monogenic trait using phenotype/genotype correlation in a set of AcB/BcA recombinant congenic mouse lines³³¹: these mice contain a small amount (12.5%) of DNA from one parent fixed as a set of discrete congenic segments on the background (87.5%) of the other parent. To assess a possible contribution of *Ccs3* to differential susceptibility of A/J and B6 mice to CA-CRC, we phenotyped 3 informative recombinant congenic mouse strains, namely BcA71, BcA72, and BcA87 that carry an A/J derived *Ccs3* chromosomal segment fixed on a B6 background (Figure 2.2 C). These 3 congenic lines responded to an 8-week AOM induction treatment by developing tumor numbers within the

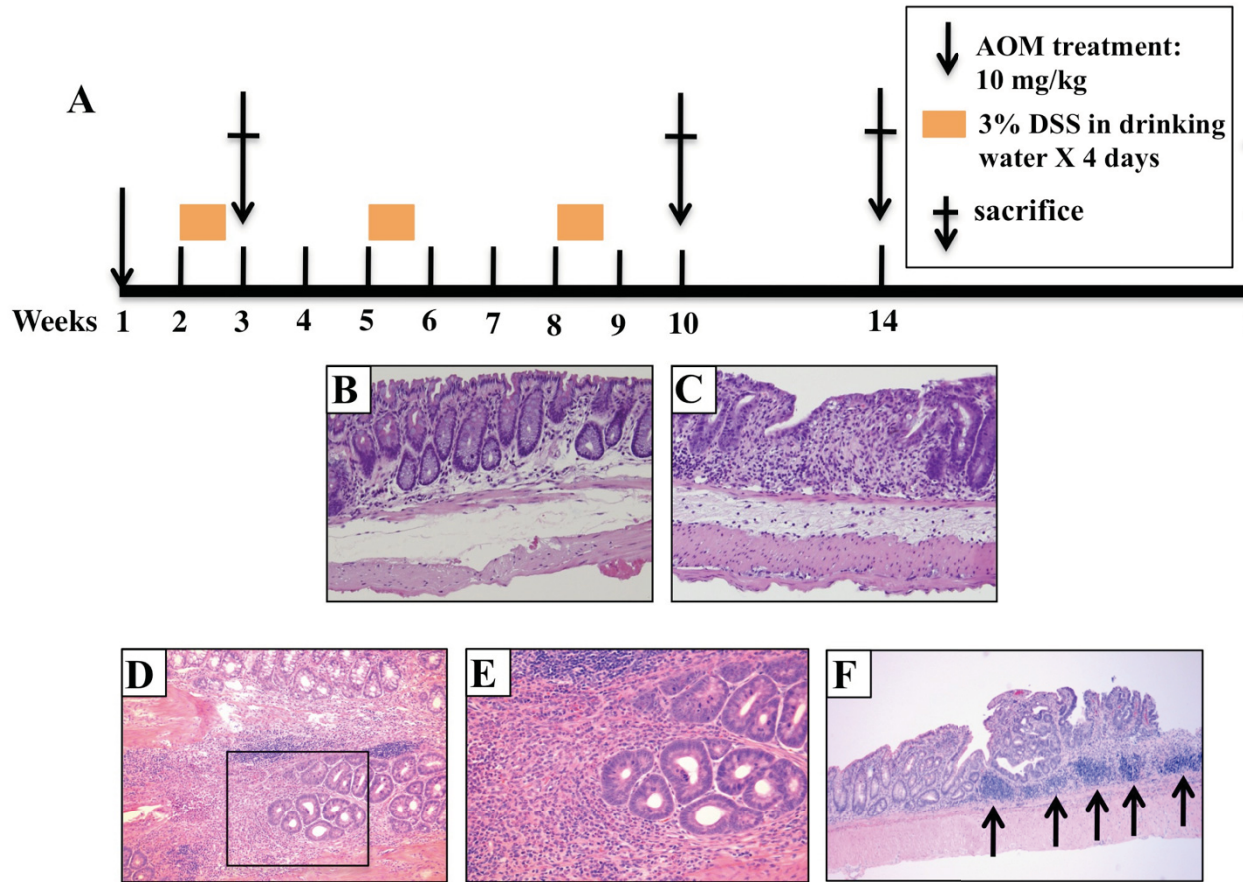


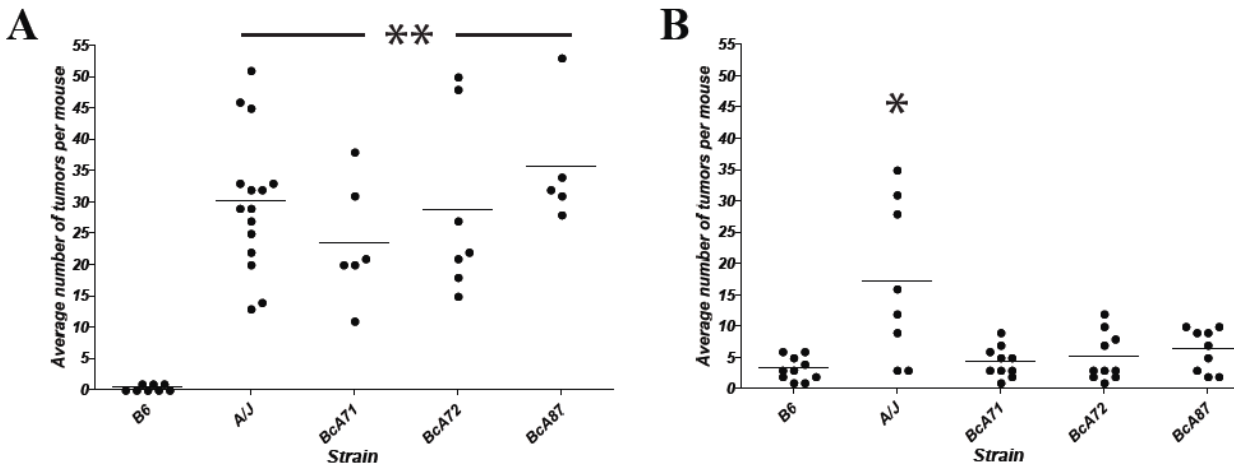
Figure 2.1: Pathology of AOM/DSS induced tumors in parental A/J and B6 mice. (A) Mice were treated with a single AOM injection and 3 consecutive periods of DSS and were sacrificed at either week 3, 10, 14, or 19 post-injection. H&E staining indicates that the animals developed grade 1 (B) or 3 inflammation (C) at 3 weeks (10 x magnification) in A/J and B6 mice, respectively. This is followed by low grade dysplasias at 10 weeks (10 x (D) and 40 x (E) magnification, respectively) and adenomas at 19 weeks (10 x magnification (F)). The arrows indicate sites of grade 3 inflammation in this panel.

range of those detected in the A/J parents, which were significantly higher than the parental B6 strain ($p < 0.005$) (Figure 2.2 A). However, in the AOM-DSS protocol, BcA71, BcA72, and BcA87 congenic lines showed low tumor numbers that were similar to those detected in parental B6 controls, and significantly different from those measured in A/J controls (Figure 2.2 B). These results suggest that the *Ccs3* locus does not impact on the differential susceptibility of A/J and B6 mice to CA-CRC, and that the inter-strain difference for this trait is controlled by other genetic loci.

2.6.3 Genetic Analysis of the CA-CRC Susceptibility Trait

The mode of inheritance (monogenic vs polygenic) of the A/J vs B6 differential response to CA-CRC was investigated by segregation analysis in informative (A/J x B6)F1 and F2 mice. (A/J x B6)F1 and F2 mice were treated with the AOM/DSS protocol, and 14 weeks later colons were scored for tumor multiplicity, tumor surface area and number of hyperplastic lesions (Figure 2.3 A, B and C, respectively). As indicated previously, the A/J parental mice displayed a significantly higher number of tumors per mouse (average = 38, $p < 0.0001$) and a larger tumor surface area (average = 128 mm², $p < 0.05$) relative to the B6 mice (average = 9 for multiplicity, and 47 mm² for surface area). The (A/J x B6)F1 mice showed tumor numbers (average = 14) and surface area (58 mm²) that were similar to that of the B6 parent, suggesting that susceptibility to AOM/DSS-induced CRC is inherited as a recessive trait in this cross. Tumor multiplicity and surface area were not normally distributed in the (A/J x B6)F2 animals with a preponderance of resistant animals, suggesting a simple genetic control for a recessive trait associated with susceptibility to CA-CRC. Gender had no significant effect on the phenotypic distribution [data not shown]. Since development of CRC is usually preceded by the appearance of hyperplastic lesions, we scored these lesions on the same 14-week treated colons. A/J mice showed approximately a two-fold greater number of hyperplastic lesions (average = 9) compared to B6 mice (average = 4), whereas (A/J x B6)F1 and (A/J x B6)F2 mice displayed a similar number of hyperplastic lesions (average = 8) relative to A/J mice, suggesting different patterns of inheritance and possibly different genetic controls for development of tumors vs hyperplastic lesions.

2.6.4 A Genome-Wide Scan Reveals a Major CA-CRC Susceptibility Locus on Chromosome 9



C

Marker	Position in Mb	RCS Strain		
		BcA 71	BcA 72	BcA 87
D3Mit164	7.52	2	2	2
D3Mit62	17.47	2	2	2
D3Mit203	26.84	2	2	2
D3Mit21	37.02	2	1	2
D3Mit224	45.77	2	1	2
D3Mit335	56.82	2	1	2
D3Mit137	78.64	2	2	2
D3Mit101	96.45	2	2	2
D3Mit266	103.69	2	2	1
D3Mit106	111.84	2	2	1
D3Mit216	123.14	2	2	2
D3Mit145	128.56	2	2	2
D3Mit110	131.57	1	1	1
D3Mit254	131.71	1	1	1
rs30453708	133.53	1	1	1
D3Mit256	136.01	1	1	1
D3Mit255	136.24	1	1	1
D3Mit16	136.74	1	1	1
D3Mit194	138.43	1	1	1
D3Mit351	139.26	1	1	1
D3Mit257	142.09	1	1	1
D3Mit258	142.91	1	1	1
D3Mit292	145.97	1	2	1
D3Mit18	147.41	1	2	1
D3Mit323	152.40	1	2	1

Ccs3 locus

Figure 2.2: Susceptibility to CA-CRC is not controlled by the *Ccs3* locus. Tumor response of parental A/J and B6 mice and RCS strains BcA71, BcA72, and BcA87 mouse strains (encompassing the *Ccs3* locus) to AOM (A) or AOM/DSS treatment (B). * $p < 0.01$ to B6; ** $p < 0.005$ to B6. (C) Haplotype of the above RCS for the *Ccs3* locus. Alleles at each locus are identified as ‘1’ in white (A/J) and ‘2’ in grey (B6). The proximal boundary of the *Ccs3* locus is defined by a resistant strain not shown in this figure.

To further investigate the genetic determinant(s) of CA-CRC susceptibility, a whole genome scan was performed in 148 (A/J x B6)F2 mice using tumor multiplicity and surface area as quantitative traits. In this analysis, genome-wide significance was assessed at a LOD score > 3.53. The results presented in Figure 2.4 A identify one significant linkage on chromosome 9 that influences both tumor multiplicity and tumor area (LOD 4.06 and LOD 4.96, respectively). These results indicate that development of CA-CRC in A/J vs B6 mouse strains is controlled by a genetic locus located on chromosome 9. We subsequently assessed the haplotype of the mice at the chromosome 9 peak markers to validate the directionality of the association with respect to tumor number (D9Mit67, 36.8 Mbp, Figure 2.4 B) and tumor area (rs13480182, 49.2 Mbp, Figure 2.4 C). This was congruent with our F1 distribution with mice inheriting two A/J alleles having significantly higher tumor numbers ($n = 19$, $p < 0.01$) and tumor surface areas ($A = 80 \text{ mm}^2$, $p < 0.01$) than mice inheriting at least one B6 allele. No differences were noted with respect to these measurements in mice inheriting either one or two B6 alleles ($n = 11$; $A = 36 \text{ mm}^2$ and $n = 11$; $A = 37 \text{ mm}^2$, respectively). We have attributed this locus the temporary designation *Ccs4*, for colon cancer susceptibility locus 4. *Ccs4* is unrelated to the *Ccs3* locus on chromosome 3 that controls susceptibility to AOM-induced colon tumorigenesis in the same strains, suggesting distinct mechanistic basis for susceptibility to CRC (*Ccs3*) and CA-CRC (*Ccs4*).

2.6.5 Identification of a Chromosome 14 *Ccs4* modifier

(A/J X B6)F2 mice homozygous for A/J alleles at *Ccs4* are on average more susceptible to CA-CRC with respect to tumor multiplicity and surface area than F2 mice heterozygous or homozygous for B6 alleles at this locus. However, CA-CRC susceptible *Ccs4*^{al/a} F2 mice displayed considerable phenotypic variance with respect to tumor numbers and surface area, suggesting the possible contribution of additional genetic loci regulating tumor multiplicity on the permissive *Ccs4*^{al/a} genetic background. This was investigated by a two-dimensional genome scan, followed by assessing the contribution of A/J and B6 haplotypes to tumor numbers for all linkage peaks showing LOD scores > 2. Both methods identified a single significant interaction of *Ccs4* with a locus on the distal part of chromosome 14 (peak marker rs13482311, 93.5 Mbp). Haplotype analysis showed an additive and very strong effect of the two loci. Two-loci linkage analysis yielded LOD scores of 9.0 and 11.3 for the combined loci, explaining 24.5% and 29.7%

of the phenotypic variation for tumor multiplicity and area, respectively. F2 mice that are homozygous for A/J alleles at both chromosome 9 and 14 loci display tumor multiplicity and surface areas comparable to the A/J controls (average = 31 vs 38 and 154 mm² vs 138 mm², respectively) while F2 mice doubly homozygous for B6 alleles at both loci show tumor numbers similar to that of the B6 parental controls (average = 9 vs 8 and 25 mm² vs 47 mm², for multiplicity and surface area, respectively) (Figure 2.5). These results identify a two-locus system regulating susceptibility to CA-CRC in mice.

2.7 Discussion

IBD, in the form of UC and CD, represent a major risk factor for CRC. The resulting CA-CRC occurs in a subset of IBD patients, which has prompted the search for low penetrance tumor susceptibility genes, thought to mediate progression of IBD to CA-CRC. Mapping of these genes in humans can be complicated by the vast genetic and environmental heterogeneity of the populations studied and hence inbred mice have been used to study CA-CRC whereby environmental factors and genetic backgrounds can be fixed. Chromosomal regions and individual loci identified by genetic analysis as regulating susceptibility to CA-CRC in mice represent valuable candidates for validation in cohorts of human clinical specimens. We have shown that A/J and B6 mice were susceptible and resistant, respectively to CA-CRC, as modeled using a single injection of AOM and repeated cycles of the inflammatory stimuli dextran sulfate DSS. Using an (A/J x B6)F2 cross we mapped a novel two-loci system on mouse chromosome 9 (*Ccs4*) and 14, whereby animals homozygous for either A/J or B6 alleles at both loci show susceptibility/resistance characteristics similar to that of the parental strain, indicating that this two-loci system explain a large portion of the phenotypic variance distinguishing the two parents.

Both sporadic and CA-CRC arise from deregulation of the organized epithelial and stromal cells of the colon and harbor similar molecular alterations underlying CRC development¹³. However, the timing and frequency of these molecular events are different with mutations or LOH at *p53* occurring early in CA-CRC while they arise late in sporadic CRC, and *APC* mutations are rare events in CA-CRC contrary to sporadic CRC⁶⁹. This has led to speculation that appearance and progression of both sporadic CRC and CA-CRC may be influenced by different sets of genes. Results from our study support this contention. Indeed, although A/J is susceptible to both CRC and CA-CRC and although B6 is resistant to both pathologies, results

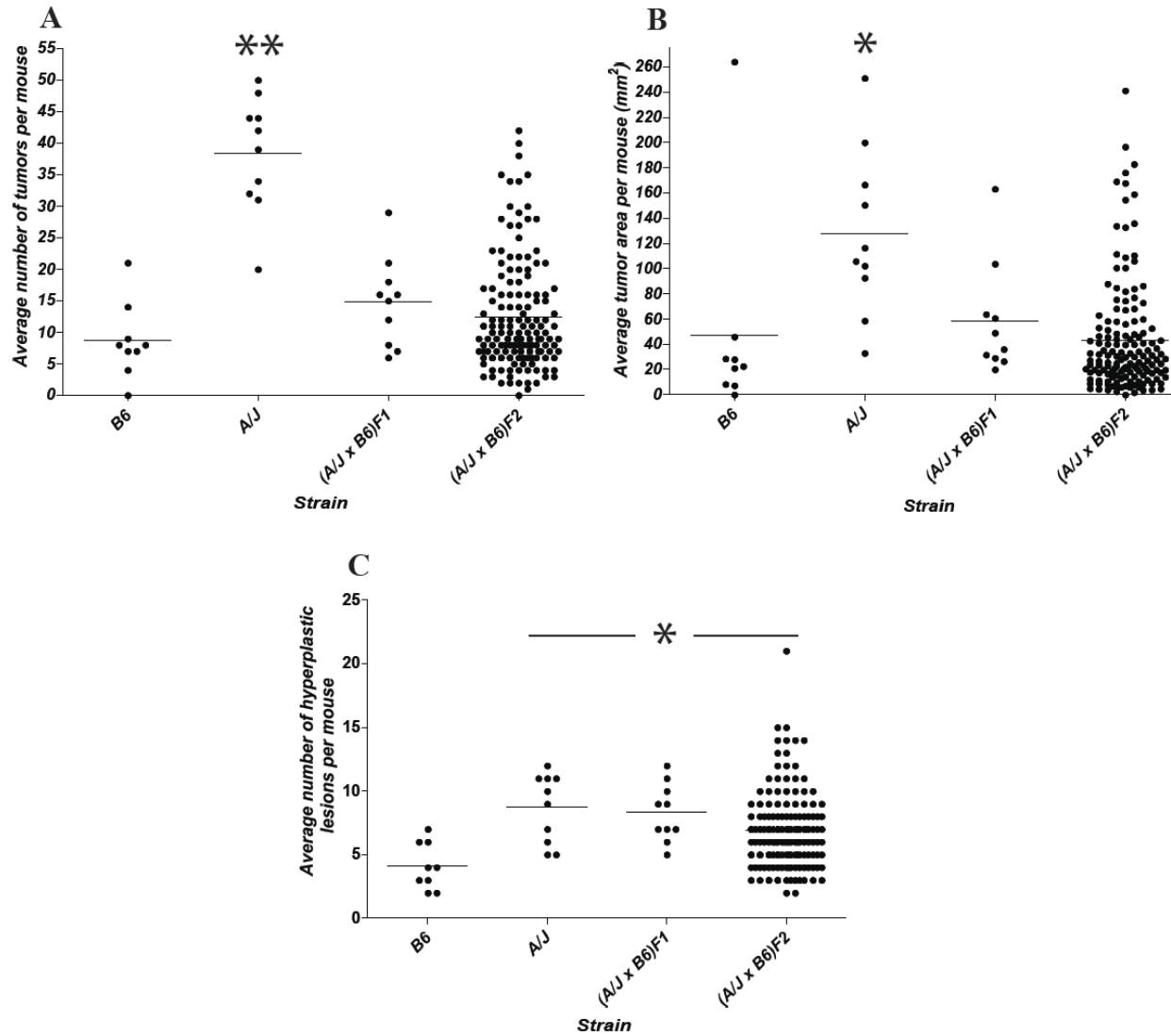


Figure 2.3: Segregation analysis of susceptibility to CA-CRC induced by the AOM/DSS protocol. Distribution of tumor multiplicity (A), tumor surface area (B) and multiplicity of hyperplastic lesions (C) in A/J, B6, (A/J x B6)F1 and 148 segregating (A/J x B6)F2 animals. * $p < 0.05$ to B6, ** $p < 0.0001$ to B6.

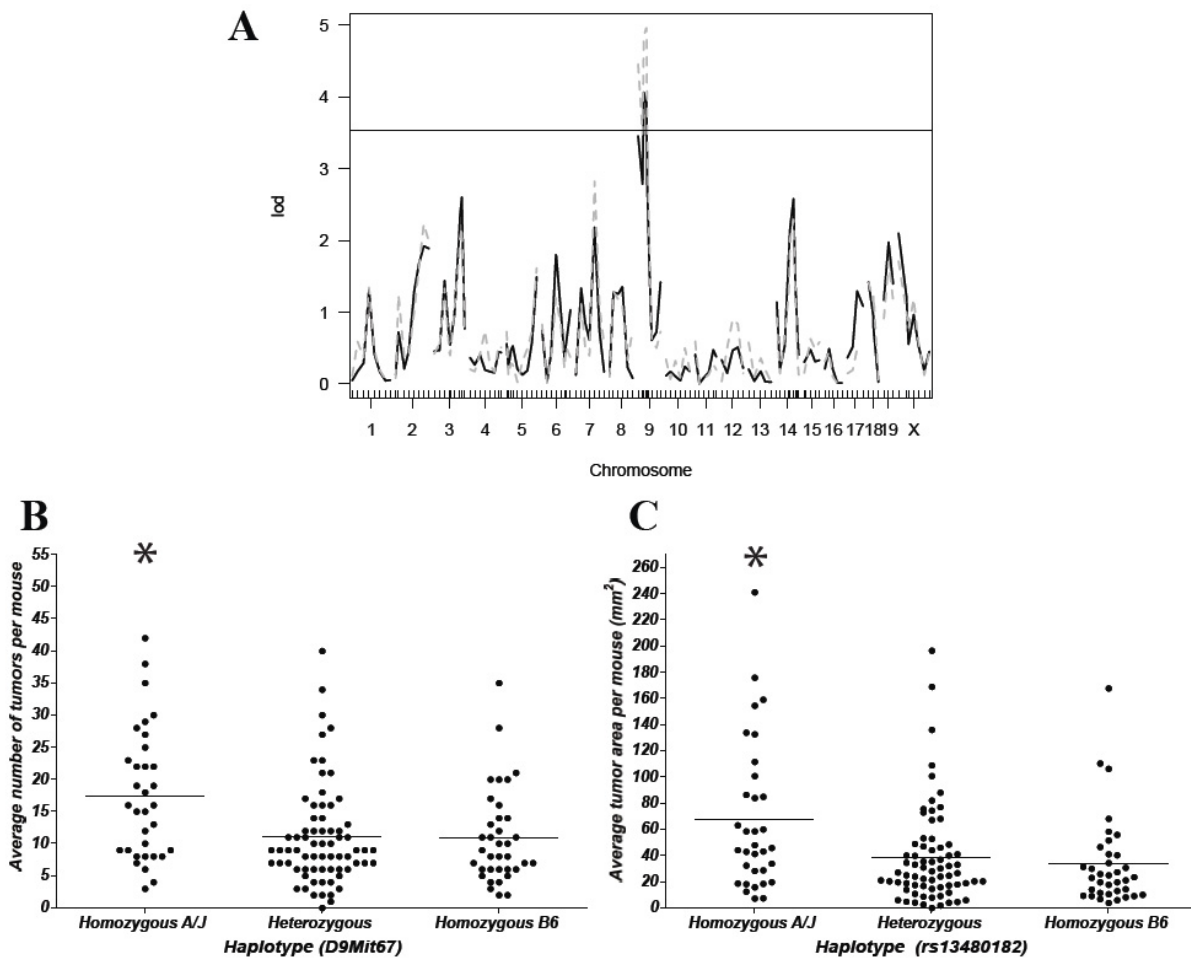


Figure 2.4: Identification and validation of a chromosome 9 CA-CRC susceptibility locus. (A) Genome-wide scan for AOM/DSS-induced tumor multiplicity (black solid line) and AOM/DSS-induced tumor surface area (grey dashed line). The genome scans identified a single significant hit (genome-wide significance threshold is 3.53) on chromosome 9 regulating tumor multiplicity (LOD 4.06) and tumor surface (LOD 4.96) following AOM/DSS treatment. Haplotype association validating the chromosome 9 association at peak markers D9Mit67 with respect to tumor number (B) and rs13480182 with respect to tumor surface (C). * $p < 0.01$ to B6.

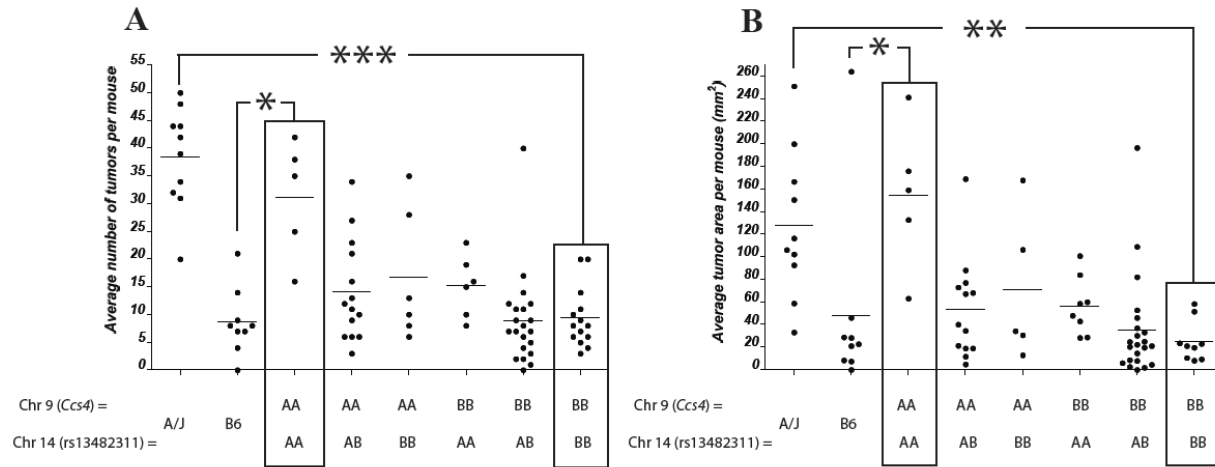


Figure 2.5: Identification of a chromosome 14 modifier of the *Ccs4* locus. Genetic influence of a chromosome 14 locus (peak marker rs13482311) on tumor number (A) or tumor surface (B) for (A/J x B6)F₂ mice homozygous for either A/J or B6 alleles at *Ccs4* (D9Mit67 with respect to tumor number and rs13480182 with respect to tumor surface). Black boxes indicate mice that are either homozygous A/J or homozygous B6 across both loci. * $p < 0.05$, ** $p < 0.001$, *** $p < 1 \times 10^{-6}$.

obtained here with subsets of recombinant congenic strains informative for the *Ccs3* locus, together with formal genetic linkage analyses in segregating (A/J X B6)F2s have identified distinct and non-overlapping genetic controls for both traits. Interestingly, the gene for the p105 NFkB subunit maps within the 5Mbp physical interval delineating *Ccs3* and *p105*^{-/-} mice develop spontaneous intestinal inflammation similar to human IBD²⁶⁸. It is tempting to speculate that the lack of association of *Ccs3* with CA-CRC in our studies indirectly suggests that it is not an NFkB-mediated differential response to inflammatory stimulus that is responsible for A/J vs B6 inter-strain differences in susceptibility to CA-CRC.

Scrutiny of published literature and the MGI database (Mouse Genome Informatics) reveal that *Ccs4* overlaps a previously mapped mouse quantitative trait locus (QTL) that regulates response to infection in the form of differential control of tissue repair following injury. A locus regulating differential susceptibility of BALB/c (susceptible) and B6 (resistant) mice to cutaneous leishmaniasis induced by infection with *Leishmania major*, and designated *Lmr2*, has been mapped to a ~10 Mbp interval on chromosome 9 that overlaps the genetic interval defined herein for the *Ccs4* locus³³³. The genetic difference at *Lmr2* is expressed as a vigorous wound healing response required for lesion resolution following cutaneous infection with *L. major*. A number of candidate genes have been proposed for *Lmr2* including *Tirap*, *Fli1*, *Il-10ra*, as well as members of the *Mmp* family, and *Aplp2*. Recently, a functional promotor polymorphism in the *Fli1* gene has been proposed as a strong candidate for *Lmr2*³³³. The possibility that the *Ccs4*-controlled differential susceptibility to CA-CRC may involve differential response to, and recovery from acute inflammation-induced tissue injury requires further investigation. Indeed, DSS treatment has been shown to cause permeabilization of the epithelial cell barrier resulting in increased cellular turnover to repair tissue damage, a response that may be under the control of *Ccs4*. It is also interesting to note that a similar two-locus system involving chromosome 9 and 14 has been shown to regulate differential brain toxicity of human amyloid precursor protein expressed in transgenic 129sv and FVB mice³³⁴. Although this two-locus system has been mapped in another strain pair, and with a low degree of resolution, it is nevertheless interesting to note that it regulates response to a toxic substance in the form of degree of tissue damage.

The *Ccs4* confidence interval is very large and stands at ~ 41Mbp delineated by rs29835542/rs3723670 with peak markers D9Mit67 (36.84 Mbp) and rs13480182 (49.23 Mbp) for tumor multiplicity and area, respectively. The chromosome 14 locus maps to an ~ 30 Mb

region with peak marker rs13482311 (93.5 Mbp). The large size of the physical intervals for the two-loci precludes a detailed discussion of positional candidates for the genetic effects on CA-CRC. Nevertheless, using Gene Ontology classification (GO ontology browser) response to stimulus, tissue repair or cancer, several potential candidates arise for the *Ccs4* locus. Interleukin 18 (*Il-18*; position 50.4Mb) has been shown to modulate response to chemically induced colitis in mice ³³⁵. Also, mice bearing a mutation in *Casp12* (53.4 Mbp), an upstream effector of *Il-18*, show increased resistance to acute inflammation, but also increased susceptibility to CA-CRC ³³⁶. *Retinoblastoma 1* (*Rb1*; 73.6Mbp), a known tumor suppressor, is known to be up-regulated in CRC samples compared to the normal mucosa ³³⁷. The formal identification of the gene responsible for *Ccs4* and associated QTLs on this portion of chromosome 14 will involve the creation and characterization of congenic and sub-congenic lines to narrow down the physical interval of *Ccs4*, as well as the formal evaluation of positional candidates, including the creation and testing of loss-of-function mutations *in vivo*.

The *Ccs4* locus is syntenic to regions found on human Chrs. 11, and 15 while the chromosome 14 locus is syntenic to regions of human chromosome 13. Although more than 30 human IBD loci have been identified with several mapping to the above chromosomes, none overlap with these loci. However, one human CRC susceptibility locus (11q23) falls within the current *Ccs4* interval ¹⁷⁹. The 11q23 locus, associated with a gender-independent increased rectal cancer risk and a moderate colon cancer risk, maps to a 60 kb region on human chromosome 11 containing 3 ORFs (*C11orf53*, *FLJ45803*, *LOC120376*) and a nearby gene involved in humoral immune response, *POU2AF1* ³³⁸. To date no non-synonymous polymorphisms have been identified within this locus and it does not appear to act in cis or trans-regulation with any other known CRC loci.

Potential two-locus systems regulating pre-disposition to colorectal cancer or to inflammatory bowel disease are extremely difficult and statistically challenging to detect in human GWAS studies. The identification of a two-locus system in mice involving chromosome 9 (a possible homolog of the 11q23 human locus) and chromosome 14 provides a novel candidate region of interest and interacting locus which can be readily tested in available GWAS datasets for relevance to related human pathologies.

2.8 Acknowledgments

We are indebted to Susan Gauthier for expert technical assistance. This work was supported by research grants to PG and NB from the Canadian Cancer Society Research Institute and the Canderel Initiative Program of the Goodman Cancer Research Centre. PG is a James McGill Professor of Biochemistry. LVDK received a studentship from the Canadian Institute of Health Research Training Program to the Goodman Cancer Research Centre. There are no potential conflicts of interest to declare.

Chapter 3:
Characterizing the Hyper-Susceptibility of the AcB60 Mouse Strain to Colitis and Colitis-Associated Colorectal Cancer

Manuscript in Preparation:

Van Der Kraak, L, Jothy, S, Beauchemin, N, and Gros, P. Characterizing the hyper-susceptibility of the AcB60 mouse strain to colitis and colitis-associated colon cancer.

3.1 Connecting Text

In Chapter 2, A/J and C57BL/6J (B6) mice were shown to be susceptible and resistant, respectively, to colitis-associated (CA) colorectal cancer (CRC). CA-CRC susceptibility in these mice is under the genetic control of a two-locus system, involving mouse chromosome 9 (*Ccs4*) and chromosome 14. This two-locus system was mapped in (A/J x B6)F2 mice and testing of the (A/J x B6)F1 mice showed that CA-CRC susceptibility behaved as a recessive trait, with A/J alleles being associated with increased susceptibility.

F2 populations are useful in mapping multi-gene interactions regulating complex traits, but generally provide only approximate genetic maps of the genes underlying a phenotype of interest. However, use of inter-crossed or backcrossed mice bred to homozygosity can aid in precision mapping of genetic effects. Therefore, we proposed to fine map the genetic effect underlying the *Ccs4* locus using of AcB/BcA recombinant congenic (RCS) mouse lines³³¹.

The AcB/BcA mice contain a small amount (12.5%) of DNA from one parent (A/J or B6) fixed as a set of discrete congenic segments on the background (87.5%) of the other parent. There are 36 AcB/BcA RCS strains each with a unique allelic contribution from the parental A/J and B6 mice. In an attempt to refine the genetic interval underlying the *Ccs4* locus, we tested a panel of 32 RCS strains for susceptibility to CA-CRC identifying a novel hyper-susceptibility strain, AcB60. *In this chapter we characterize the unique phenotype of these AcB60 mice to CA-CRC and colitis and discuss future plans for mapping this genetic effect.*

3.2 Contributions of the Authors

The experiments presented in this chapter were planned as part of a collaborative effort between LVDK, NB and PG. Claire Turbide (acknowledged for her contributions) performed the initial carcinogen injection. LVDK bred the mouse strains, administered all treatments (except the carcinogen), performed the sacrifice and analyzed the samples for tumor multiplicity and surface area. LVDK prepared samples for histology, which were embedded and sectioned at the Goodman Cancer Centre Histology Facility and subsequently analyzed by SJ. LVDK wrote the paper and prepared the figures with input from NB and PG.

3.3 Abstract

In a routine screen we identified the AcB60 recombinant congenic mouse strain (RCS) as hyper-susceptible to colitis-associated colon cancer (CA-CRC), developing 28-fold more tumors

than either of its A/J or B6 parental strains 7-weeks post-initiation of treatment. Additional testing of AcB60 mice revealed increased susceptibility to DSS-induced colitis, which was associated with increased mortality, colonic inflammation and ulceration compared to A/J and B6. It is hypothesized that hyper-susceptibility to both colitis and CA-CRC in the AcB60 mouse strain is the result of a novel mutation that arose during its generation and not a unique arrangement of A/J and B6 alleles, as this phenotype has not been seen in any of the other RCS or (A/J x B6)F2 mice tested to date. Murine models of early-onset CA-CRC are rare and therefore AcB60 may offer a unique model to the study the mechanisms associated with this disease possibly leading to new genetic predictors of risk and treatment options in humans.

3.4 Introduction

The inflammatory bowel diseases (IBD), ulcerative colitis (UC) and Crohn's disease (CD) are characterized by chronic and relapsing inflammation and ulceration within the colon or entire intestinal tract, respectively. Canada has one of the highest rates of IBD worldwide with approximately 233,000 individuals affected, an increase of 0.2% since 2000 ^{339, 340}. Rates of pediatric IBD are increasing rapidly, with an Ontario study citing a 5.0%-7.6% increase in IBD incidence per year in children ages 0-9 ¹¹⁹. The risk of serious medical complications in IBD patients increases with duration of disease making this shift towards early-onset a significant concern.

Colitis-associated colon cancer (CA-CRC), which develops in areas of active colonic inflammation, is listed as cause of death in approximately 15% of all IBD patients ^{125, 132}. Patients with IBD diagnosed prior to 25 years of age were 13 and 70 times more likely to develop CRC compared to older IBD patients and the general population, respectively ¹⁴³. Extent and duration of inflammation are important CA-CRC risk factors, with risk of UC-CRC increasing from 2% to 18% after 10 and 30 years of active disease, respectively, with risk increasing with increasing surface area of colonic involvement ^{235, 341}. Some studies have also shown that CA-CRC risk is reduced with regular use of non-steroidal anti-inflammatory drugs, further supporting a role for inflammation in CA-CRC ¹⁴⁶.

However, extent and duration of active inflammation cannot explain all of the variability associated with CA-CRC and therefore it has been hypothesized that genetic factors may be important with respect to disease initiation and progression ¹⁴⁸. Risk of both CRC and IBD have

been linked to common single nucleotide polymorphisms in low penetrance disease susceptibility genes^{98, 222}. However, no CA-CRC loci have been mapped in humans to date. In addition, no associations have been shown between known UC-risk loci and UC-CRC¹⁴⁹.

Inbred mice, like humans, vary with respect to CA-CRC due to predisposing genetic factors, which can be fixed by inbreeding and mapped by linkage analysis²²³. We have previously identified a novel two-locus system involving mouse chromosomes 9 (*Ccs4*) and 14 regulating susceptibility to azoxymethane/dextran sulfate sodium (AOM/DSS)-induced CA-CRC in A/J (susceptible) and B6 (resistant) mice. The AcB/BcA recombinant congenic mouse strains contain a small amount (12.5%) of DNA from one parent (A/J or B6) fixed as a set of discrete congenic segments on the background (87.5%) of the other parent and can be used to fine map genetic loci regulating susceptibility to complex traits in A/J and B6 mice³³¹. While testing a panel of RCS mice to fine map the *Ccs4* genetic interval, AcB60 mice were identified as hyper-susceptible to CA-CRC developing early-onset tumors associated with increased colonic inflammation, a phenotype not seen in either the parental A/J or B6 mice. Herein, we further characterize this unique phenotype in AcB60 mice, with the intent of subsequent mapping, which may shed light on important phenotypes and genetic factors regulating colitis and CA-CRC susceptibility in humans and pave the way for novel early detection screening programs.

3.5 Materials and Methods

3.5.1 Ethics Statement

All experiments were conducted in accordance with the national and international guidelines set forth by the Declaration of Helsinki, the McGill Institutional Review Board and the Canadian Council on Animal Care.

3.5.2 Mice

The AcB/BcA recombinant congenic mice (RCS) were generated through a reciprocal double backcross between A/J and B6 parental mice at McGill University followed by 30 generations of brother x sister matings. The genotype of these mice and a detailed breeding scheme is described in more detail in³³¹. A/J and C57Bl/6J (B6) mice were bred in house from breeding stocks originally purchased from Jackson Laboratory (Bar Harbour, ME, USA). For all experiments, mice were housed on a 12-hour light/dark cycle within the McGill Comparative Animal Resource Centre on beta-chip or wood shaving bedding. Mice were fed regular chow

(Charles River 5075) and water ad libitum. All experiments were conducted on 9 week or older mice according to McGill Protocol AUP 5183. Mice were weighed and visually monitored a minimum of twice per week for clinical symptoms of colitis and CA-CRC. Mice showing signs of discomfort were humanely sacrificed immediately.

3.5.3 Induction of Colitis-Associated Colon Cancer

Colitis-associated (CA-CRC) was induced according to the methods described in Van Der Kraak et al ³¹⁷. Briefly, mice were given a single injection of azoxymethane (AOM, Sigma, St Louis, MO, USA; 6 or 10 mg/kg) intraperitoneally on day zero. This was followed one week later with 2% or 3% dextran sulfate sodium (DSS, Salt Reagent Grade, MW 36,000-50,000, MP Biomedicals LCC, Solon, OH, USA) in drinking water for 4 days. Two or three DSS cycles were administered, with each treatment 17 days apart. Following the final DSS treatment, mice were given normal water until the end of the experiment (between 7 and 9 weeks). The specific doses for each experiment are described in detail in the results section.

At sacrifice, the large intestine (anus to cecum) was removed, washed in PBS and fixed in 10% phosphate-buffered formalin overnight for subsequent scoring and histological analysis. Colons were scored under a 10x microscope objective for the phenotypes of tumor multiplicity and surface area. Only lesions larger than 0.5 mm² were included in the analysis. Surface area was calculated by overlaying tumors with 1 mm² graph paper transparencies and determining the number of squares occupied by each tumor to the nearest 0.25 mm².

3.5.4 Induction of Acute Colitis

To induce acute colitis, A/J, B6 and AcB60 mice were treated with 4% DSS in drinking water for 5 days followed by 3 days without treatment. Mice were monitored daily for symptoms of colitis including rectal bleeding, weight loss, ruffling and hunching. Animals that developed persistent rectal bleeds associated with additional symptoms of weight loss, ruffling and hunching or who became moribund were sacrificed immediately. Mice were sacrificed on day 8 and serum, colon and spleen samples were collected. Colon length was assessed as the distance from the ileal-cecal junction to the rectum and compared to untreated control mice. The distal left 2 cm of the colon was removed and flash frozen in liquid nitrogen and the remaining colon was fixed in 10% phosphate-buffered formalin overnight for subsequent histological analysis.

3.5.5 Induction of Long Term Colitis

To assess the effects of long term DSS treatment on colitis and CA-CRC, A/J, B6 and AcB60 mice were treated with two four-day cycles of 2% DSS each 17 days apart. Mice were sacrificed 3 days after the final DSS treatment on day 28. Similar to the acute DSS experiments mice were monitored for symptoms of colitis (rectal bleeding, weight loss, ruffling and hunching) and moribund mice were humanely sacrificed immediately. On day 28, mice were sacrificed and organs were harvested and analyzed as described for the acute DSS experiments. The same untreated mice were used as controls for colon length in both the acute and long-term DSS experiments.

3.5.6 Histology

Phosphate-buffered formalin fixed AOM/DSS, acute DSS and long term DSS treated tissues were dehydrated in ethanol, paraffin-embedded and sectioned (5 μ m) at the Goodman Cancer Centre Histology Facility (Montreal, QC, Canada). As inflammation can vary between the proximal and distal colon, the right distal 2 cm of DSS-treated colons were sent for analysis. Samples were mounted onto slides, de-paraffinized and stained with hematoxylin and eosin (H & E) following standard histological procedures. Grading of both tumors and inflamed regions was assessed in a blinded fashion by Dr. Serge Jothy (SJ) according to the recommendations of Wirtz et al.²⁸². Histology images were obtained from slides scanned using a ScanScope XT digital scanner (Aperio Technologies, Vista, CA, USA).

3.5.7 Statistical Analyses

All statistical analyses were performed using GraphPad Prism software (GraphPad Software, Inc. La Jolla, CA, USA). Results were considered significant if $p \leq 0.05$ using one way-ANOVA and the Bonferroni post-test.

3.6 Results

3.6.1 AcB60 Mice are Hypersensitive to Colitis-Associated Colorectal Cancer

We tested A/J, B6 and 32 RCS mouse strains for AOM/DSS-induced (10 mg/kg AOM, 3 treatments of 3% DSS; Figure 3.1 A) CA-CRC susceptibility, with most strains behaving as expected, with phenotypes within the range of the A/J and B6 parental controls when sacrificed 13 to 15 weeks post-injection [data not shown]. AcB60 mice however, developed signs of colitis

(rectal bleeds, weight loss, ruffling and hunching) becoming moribund following the second DSS treatment. By 9 weeks post-injection, all AcB60 mice had succumbed to treatment, compared to less than 20% of the A/J or B6 mice (Figure 3.1 B).

To determine if AcB60's increased sensitivity to AOM/DSS was due to increased tumor burden A/J, B6 and AcB60 colons were analyzed for the phenotypes of tumor multiplicity and surface area. Five AcB60 colons collected from mice sacrificed between days 38 and 62 were compared to three colons from B6 (days 45 and 62) and A/J (day 62). Consistent with previous experiments, A/J mice were susceptible ($n = 50 \pm 21$) developing significantly more tumors than resistant B6 mice ($n = 8 \pm 3$, $p \leq 0.01$) (Figure 3.1 C). AcB60 mice had similar tumor numbers ($n = 62 \pm 10$) to A/J mice and statistically more tumors than B6. Interestingly, AcB60 tumor surface area was larger ($A = 246 \pm 50$) than either A/J ($A = 127 \pm 69$, $p \leq 0.05$) or B6 ($A = 19 \pm 8$, $p \leq 0.001$), despite some AcB60 mice having been sacrificed 24 days earlier than the A/J mice (Figure 3.1 D). This data suggested that AcB60 tumors may demonstrate earlier onset and be more rapidly proliferating than tumors from either of its parental strains.

3.6.2 AcB60 Mice are Hyper-susceptible to Colitis-Associated Colorectal Cancer

To confirm the AcB60 phenotype, A/J, B6 and AcB60 mice were re-tested using a modified AOM/DSS protocol (6 mg/kg AOM, 2% DSS, 2 cycles; Figure 3.2 A). This protocol was chosen with the intent of reducing AOM/DSS fatalities in the AcB60 mice. At 7-weeks post-initiation, mice were sacrificed and their colons collected and enumerated for the phenotypes of tumor multiplicity and surface area (Figure 3.2 B). Under this new protocol, the AcB60 mice averaged 35.5 tumors per mouse whereas A/J and B6 mice had less than 2 tumors on average (Figure 3.2 C). A similar trend was observed with respect to surface area whereby AcB60 mice had larger tumors (average A per tumor = 3.5 mm^2) and greater tumor burden ($A = 125.8 \text{ mm}^2$) compared to A/J and B6 (Average A per tumor < 1.7 mm^2 , $A < 3 \text{ mm}^2$) (Figure 3.2 D). No differences with respect to tumor multiplicity or surface area were noted between A/J and B6 at this early time point.

Pathology of AOM/DSS-treated samples confirmed the hyper-susceptibility of the AcB60 mice with numerous adenomas detected (Figure 3.3). H & E-stained B6 colonic sections showed similar pathology to untreated samples, while A/J colons had a few adenomas with low-grade dysplasia (lgd) and minimal colonic inflammation (Figure 3.3 A-D). AcB60 mice however, had multiple adenomas with both lgd (96%) and high-grade dysplasia (hgd, 4%) and

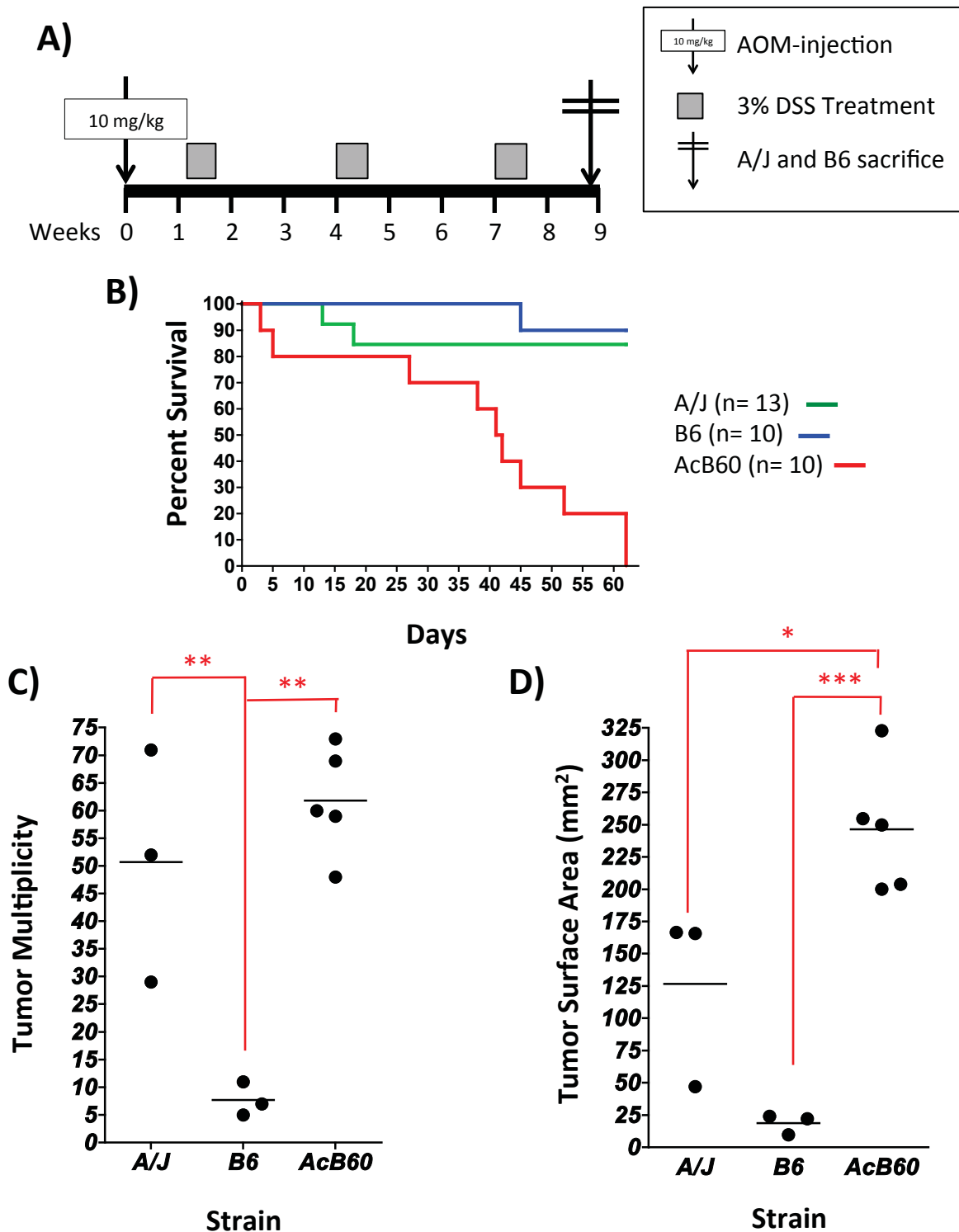


Figure 3.1: AcB60 mice are hyper-sensitive to AOM/DSS-induced CA-CRC. A/J, B6 and AcB60 mice were subjected to the AOM/DSS protocol (10 mg/kg AOM, 3 cycles 3% DSS) with all AcB60 mice succumbing to treatment 62 days post-initiation (A and B). Colons from AcB60 (sacrificed day 38-62), B6 (day 45 and 62) and A/J (day 62) mice were collected, fixed in formalin and scored for the phenotypes of tumor multiplicity (C) and surface area (D). * $p \leq 0.05$ ** $p \leq 0.01$, *** $p \leq 0.001$ using one-way ANOVA.

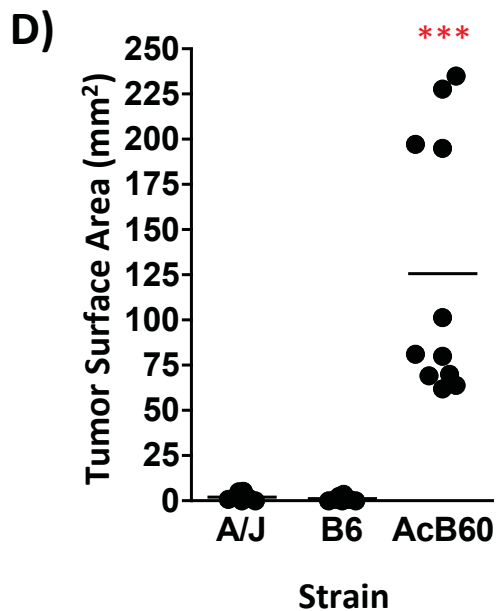
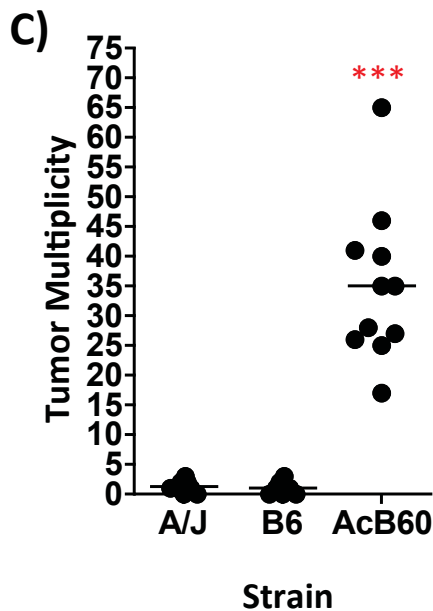
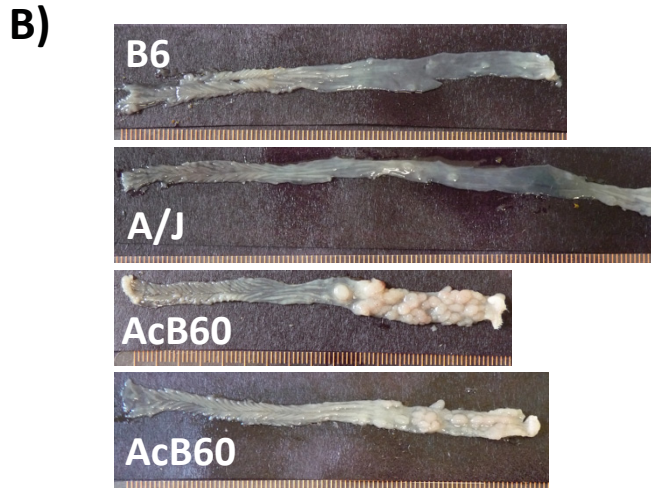
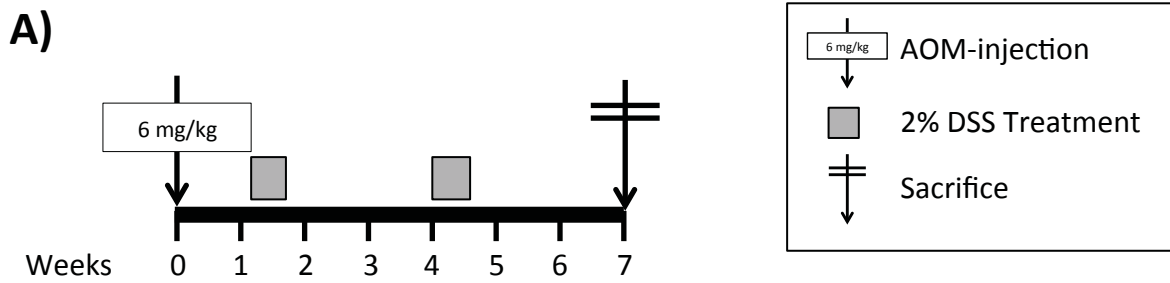


Figure 3.2: AcB60 mice are hyper-susceptible to CA-CRC. (A) A/J, B6 and AcB60 mice were subjected to a modified AOM/DSS protocol (6 mg/kg AOM, 2 cycles of 2% DSS and 7 weeks post-initiation were sacrificed and their colons collected). (B) Representative images of A/J, B6 and AcB60 colons. Colons were subsequently scored for the phenotypes of tumor multiplicity (C) and surface area (D). *** $p \leq 0.001$ to all other strains using one-way ANOVA.

higher levels of colonic inflammation associated with multiple inflammatory foci, increased vascular density and wall thickening (Figure 3.3 E and F). Overall, these results support that AcB60 mice are hyper-susceptible to CA-CRC and this is a unique phenotype not detected within their parental A/J or B6 mice.

3.6.3 AcB60 mice are Susceptible to DSS-Induced Colitis

AcB60 AOM/DSS-treated colons showed significant inflammation compared to A/J and B6 colons seven weeks post-initiation. To assess maximal inflammatory response to DSS-induced inflammation, A/J, B6 and AcB60 mice were treated with 4% DSS for 5 days, followed by 3 days without treatment (Figure 3.4 A). Mice were monitored daily for symptoms of colitis (rectal bleeds, soft stool, weight loss) with AcB60s male mice presenting with bloody stool as early as 3 days post-initiation. The health of the AcB60 male mice rapidly declined with 85% of the mice succumbing to treatment 6 days post-initiation compared to none of the A/J or B6 male controls (Figure 3.4 B). This was associated with increased weight loss in AcB60 male mice relative to A/J and B6 commencing 5 and 6 days post-initiation, respectively (Supplemental Figure 3.1 A). These phenotypes were less pronounced in females, with only a single AcB60 succumbing to treatment on day 6 (Figure 3.4 B). Female AcB60 mice also had a trend towards increased weight loss, but this was not statistically significant. (Supplemental Figure 3.1 B).

Consistent with published literature, DSS-treated mice had significantly shorter colons than untreated control mice, with no significant differences between genders. Pooled analysis of B6 colons showed a 13.9% reduction in average colon length on day 8 of treatment, compared to 25.5% in A/J mice (day 8) and 23.9% and 28.6% on day 6 and 8, respectively in AcB60 mice (Figure 3.4 C). The similarity between A/J and AcB60 colons suggests that colon atrophy is not the primary driver of DSS-associated death in these high dose DSS experiments.

Pathology of DSS-treated colons revealed the presence of small flat adenomas associated with Igd in all three-mouse strains on day 6 or 8 of treatment. Both A/J (Day 8) and AcB60 (Day 6 and 8) colons had higher levels of colonic inflammation (average inflammatory score = 2) compared to B6 (inflammatory score = 1), associated with moderate inflammation and multiple foci. The most striking phenotype visible on H & E-treated slides was extent of ulceration. B6 mice developed a few small ulcers and had evidence of a few infiltrating lymphocytes, whereas A/J mice developed both small and large ulcers affecting on average less than 40% of the mucosal surface (Figure 3.3 G and H). AcB60 mice however, developed high levels of

ulceration affecting between 50-90% of the mucosa (Figure 3.3 I). A single inflammatory pseudopolyp was also detected. Together, these results confirm the physical findings associated with increased susceptibility to DSS-induced colitis in AcB60 mice.

3.6.4 Response of AcB60 Mice to Long Term DSS-Induced Colitis

Acute DSS experiments reflect maximal inflammation in treated mice, but requires higher DSS concentrations than used in the AOM/DSS protocol. To better assess the effects of DSS treatments within our CA-CRC experiments A/J, B6 and AcB60 mice were treated with two 4-day cycles of DSS each 17 days apart and sacrificed 28 days post-initiation (Figure 3.5 A). As expected, this lower dose of DSS was less toxic with 66.7% of AcB60 male and 87.5% (7 of 8 mice) of female AcB60 mice surviving to 28 days (Figure 3.5 B). All A/J and B6 mice survived the duration of the experiment. For the duration of the experiment, changes with respect to initial body weight were monitored, but were not statistically different between strains (Supplemental Figure 3.2).

On day 28 post-initiation, AcB60 mice had significantly greater colon atrophy (23.0%) compared to both A/J (10.7%) and B6 (9.7%), suggesting a more severe colitis phenotype in AcB60 mice (Figure 3.5 C). This was confirmed by pathology. Scoring of H & E-stained colonic sections showed minimal infiltrating immune cells and only small ulcers in A/J and B6 colons (Figure 3.3 J-M). AcB60 colons however had multiple inflammatory foci, increased vascular density and thickening of the colonic wall (Figure 3.3 N-O). Areas of sessile adenomas were also detected in AcB60 samples although the overall presence of adenomas in these long-term DSS-treated mice was rare. This data supports increased colitis in the AcB60 mice; however, the lack of abundant adenomas suggest that DSS-treatment alone is not sufficient to induce hyper-CA-CRC susceptibility in AcB60 mice.

3.7 Discussion:

The AcB/BcA RCS mouse strains, have been used to map numerous loci underlying A/J and B6 differential susceptibility to various complex traits including CRC, malaria and salmonella infection^{268, 342, 343}. In these studies, multiple RCS strains were tested, with the intent of identifying discordant strains, which mimic the donor strain phenotype (B6 in AcB mice and A/J in BcA mice). Occasionally, outlier strains are identified, presenting with hyper-phenotypes outside of the normal parental range. While it is possible for these to be the result of unique

combinations of A/J and B6 alleles, more often these hyper-phenotypes are the result of mutations that arose during breeding and became fixed in subsequent generations. For example in 2012, Wiltshire *et al.* identified BcA68 as an outlier strain having low levels of high-density lipoprotein cholesterol³⁴⁴. This was subsequently mapped to a *de novo* loss of function mutation in the *ApoA1* gene. In 2003, our lab identified a T > A transversion in the pyruvate kinase gene, which disrupts the protein (I90N) leading to increased malaria resistance in AcB55 and AcB61 mice³⁴⁵.

In this study, we tested a panel of 32 RCS mice for susceptibility to AOM/DSS-induced CA-CRC identifying AcB60 as hyper-susceptible developing 28-fold more tumors than either of its parental strains 7-weeks post-initiation. These AcB60 tumors were also on average 2-times larger than A/J or B6 tumors, suggesting that they may be rapidly proliferating, a speculation that we are currently investigating. AcB60 mice also had higher overall levels of colonic inflammation associated with increased colon atrophy, inflammatory cell infiltration and ulceration, as well as decreased survival in male AcB60 mice. In an acute model of DSS-colitis, a single AcB60 mouse had an inflammatory pseudopolyp, which are suggested to arise due to ulceration and subsequent regeneration in areas of active disease¹²⁵. Pseudopolyps have been linked to increased CA-CRC risk and therefore may contribute to hyper-CA-CRC susceptibility in the AcB60 mouse.

We suspect that AcB60's unique phenotype is the result of a mutation that arose during its generation and not a novel rearrangement of A/J and B6 alleles as this phenotype was not seen in any of the other 31 RCS or (A/J x B6)F2 mice tested using the AOM/DSS protocol. We also speculate that this mutation may be important in other inflammation-based pathologies. Scrutiny of the published literature showed that AcB60 mimicked A/J, its parental background strain in most studies including those on AOM-induced colon cancer, malaria, *Candida albicans*, cystic fibrosis, *Legionella pneumophila* and asthma susceptibility^{268, 331, 346-348}. In a study of murine *Taenia crassiceps cysticercosis* (*T. crassiceps*), AcB60 mice were discordant mimicking the resistant B6 parents, however, this is attributed to the presence of a resistant B6 allele at the *T. crassiceps resistance locus 1* (*Tccr1*)³⁴⁹. Both the AcB64 and AcB60 RCS mouse strains are hyper-resistant to *Salmonella enterica* serovar Typhimurium infection relative to the resistant A/J parent, presenting with increased survival and decreased bacteria load in both the liver and spleen³⁴³. In the AcB64 strain, susceptibility is under complex genetic control mapping to

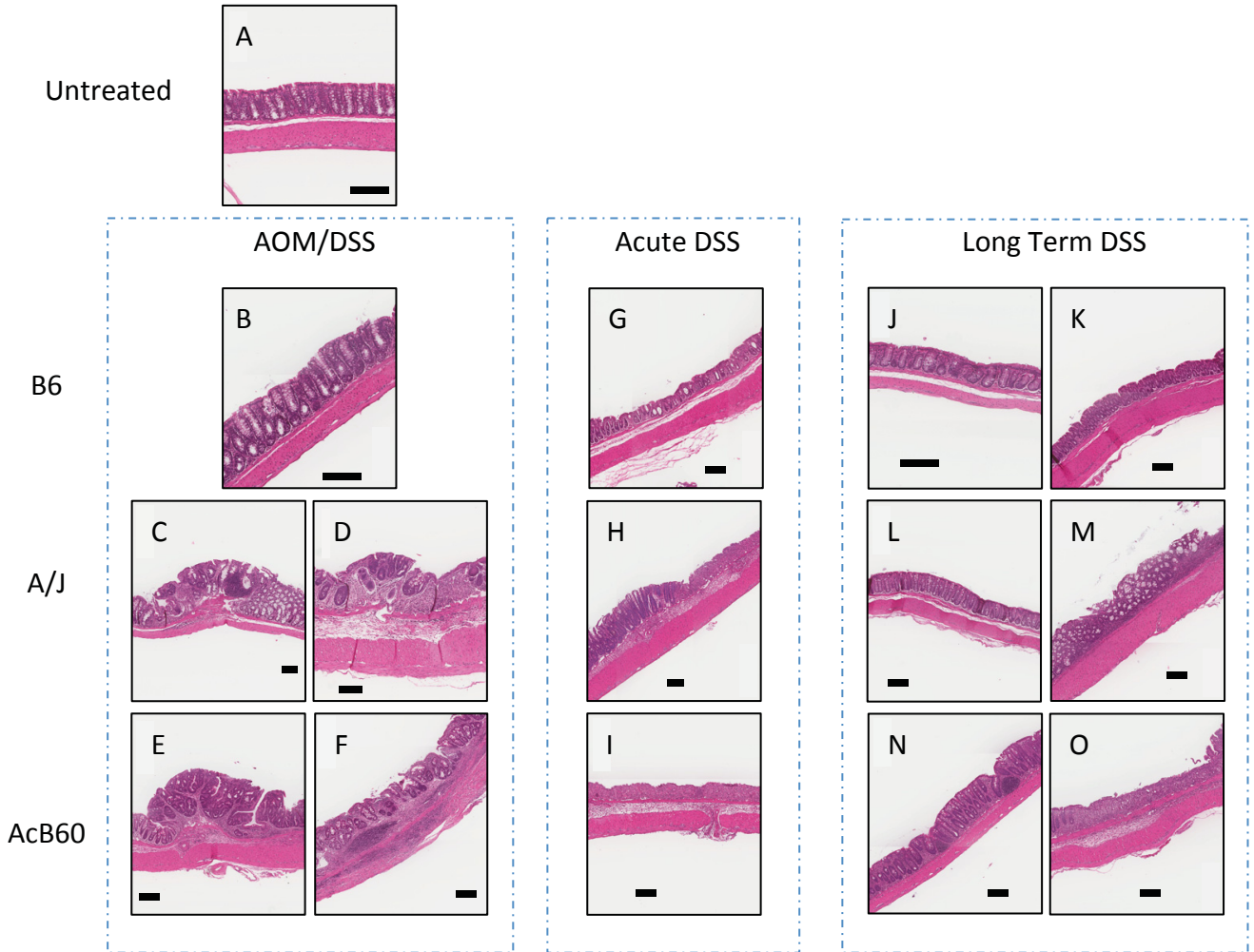


Figure 3.3: Pathology of AOM/DSS, acute DSS and long-term DSS colons. Pathology of H & E stained untreated (A) and AOM/DSS treated (6 mg/kg, 2% DSS, 2 cycles) colons 7-weeks post initiation showing minimal evidence of inflammation in B6 colons (B), adenomas associated with lgd (C) and low levels of scattered infiltrating mononuclear cells (D) in A/J and adenomas with lgd (E) and high levels of inflammation associated with multiple foci and increased wall thickening (F) in AcB60. Acute DSS treatment (5 days 4% DSS, 3 days off) was associated with minimal ulceration in B6 (G), moderated (< 40%) ulceration in A/J (H) and high levels of ulceration (between 50-90%) in AcB60 (I). Long-term DSS treatment (2 cycles 2% DSS) was associated with minimal ulceration and inflammatory changes in B6 28-days post-treatment initiation (J, K). A/J colons showed minimal inflammation and evidence of mucosal healing/regeneration (L, M). AcB60 colons showed increased evidence of ulceration, infiltrating lymphocytes and thickening of the mucosa (N, O). The black bars represent 0.2 mm on each slide. Collectively, this data supports that AcB60 mice are more sensitive to both CA-CRC development and ulceration/inflammation following AOM/DSS and DSS treatment compared to either of its parental A/J or B6 strains.

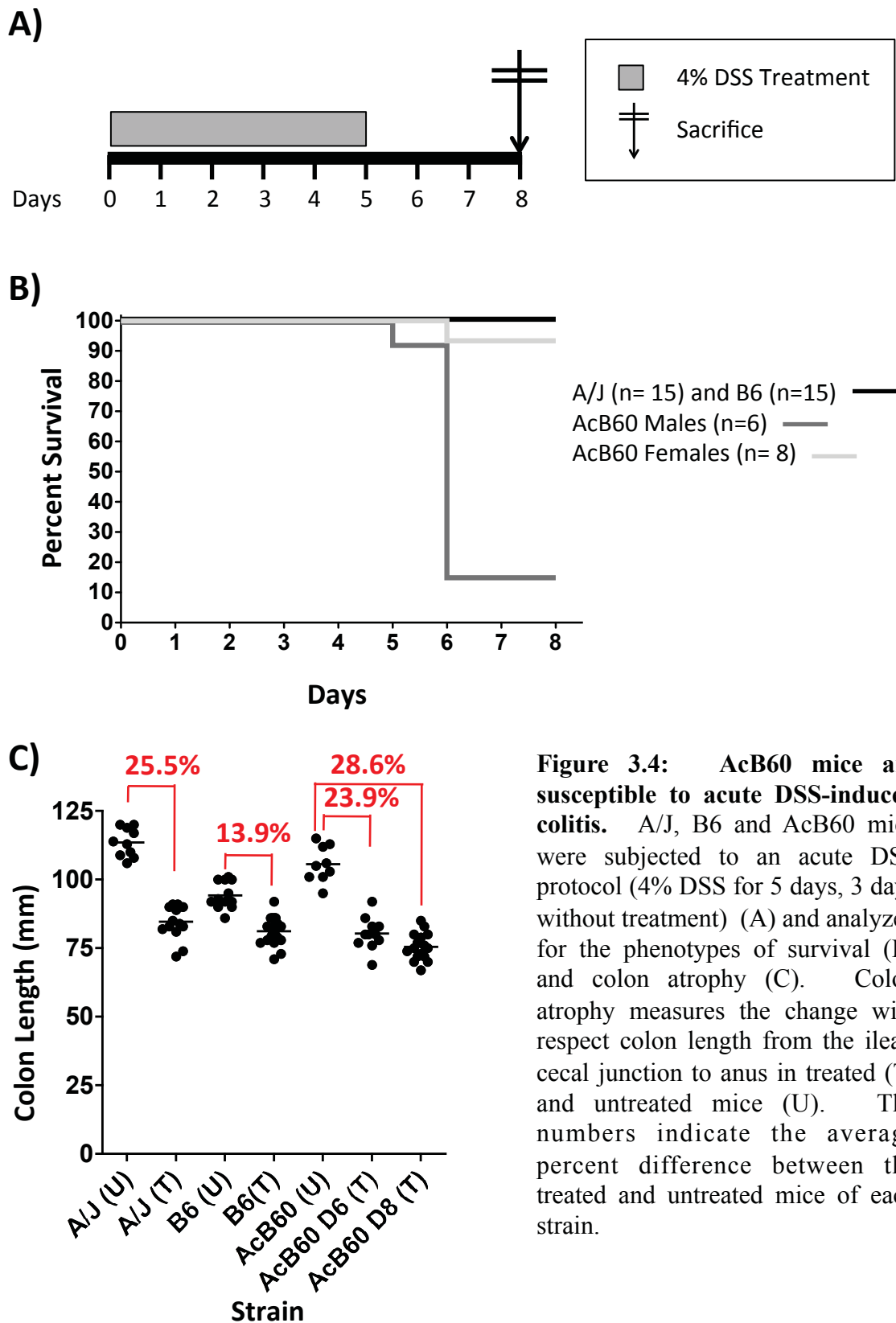


Figure 3.4: AcB60 mice are susceptible to acute DSS-induced colitis. A/J, B6 and AcB60 mice were subjected to an acute DSS protocol (4% DSS for 5 days, 3 days without treatment) (A) and analyzed for the phenotypes of survival (B) and colon atrophy (C). Colon atrophy measures the change with respect colon length from the ileal-cecal junction to anus in treated (T) and untreated mice (U). The numbers indicate the average percent difference between the treated and untreated mice of each strain.

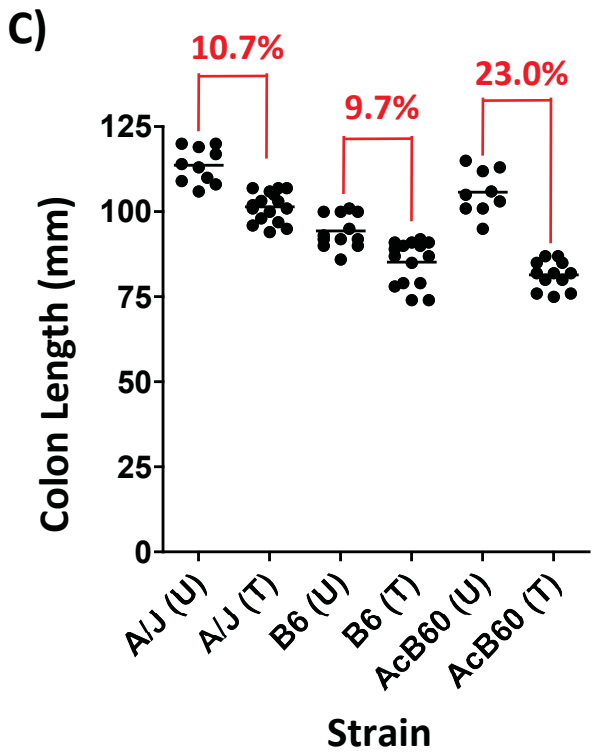
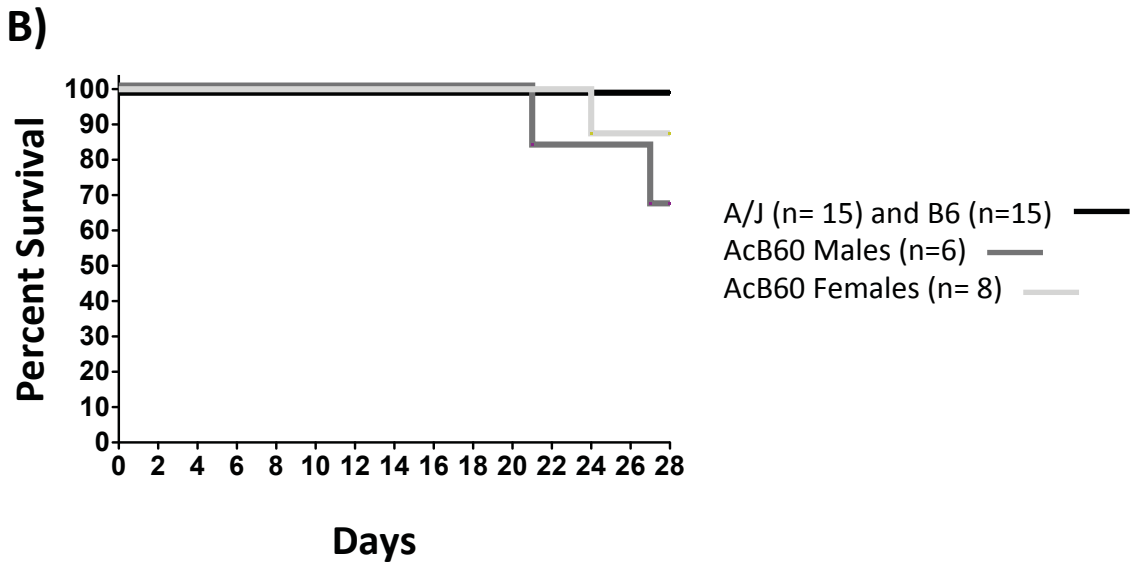
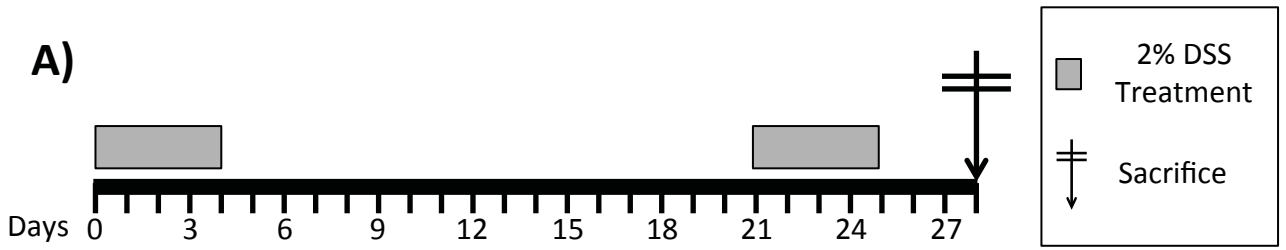


Figure 3.5: AcB60 mice are susceptible to long-term DSS-induced colitis. A/J, B6 and AcB60 mice were subjected to the long term DSS protocol (two cycles of 4-days of 2% DSS, with each cycle 17 days apart) and sacrifice on Day 28 (A) and analyzed for the phenotypes of survival (B) and colon atrophy (C). Colon atrophy measures the change in colon length from the ileal-cecal junction to anus in treated (T) and untreated mice (U). The numbers indicate the average percent difference between the treated and untreated mice of each strain.

several *immunity to Typhimurium (Ity)* loci (*Ity6*, *7* and *8*) with each locus explaining a small proportion of the phenotypic variance. The *Ity8* locus on chromosome 15 was subsequently confirmed in an (AcB60 x DBA/2J)F2 cross, although the proportion of the phenotypic variance linked to *Ity8* in this cross has not been published³⁵⁰. Both *Salmonella* and IBD susceptibility have been linked to genetic variants in *Slc11a1*, *TLR4*, *NOS* and *MHC Class II* suggesting that similar mechanisms may be important with respect to disease prognosis^{98, 351}. However, while the AcB64 mice had increased mortality (50%) and signs of colitis (increased weight loss, rectal bleeding and colon atrophy) relative to A/J and B6 in the AOM/DSS experiments, it did not have increased tumor burden relative to A/J 14-weeks post-injection (Supplemental Figure 3.3). This would suggest that AcB64 is not a hyper-susceptible strain with respect to CA-CRC and unfortunately, the AcB64 mouse line has since been culled preventing further experimentation. No causative mutations have been identified underlying *Salmonella* resistance in AcB64 and AcB60 at the *Ity8* locus and therefore, we cannot elaborate further on a plausible role for the *Ity8* locus in CA-CRC.

Our future work will involve mapping and validating the mutation(s) underlying AcB60's hyper CA-CRC susceptibility. We are not certain if the mutation underlying increased susceptibility is on the A/J or B6 background of AcB60 and therefore to map this effect, we will cross it to a third strain, the colitis and CA-CRC resistant 129S1/SvImJ (129S1) [unpublished phenotypes from our lab]. The 129S1 genome is well characterized, which will facilitate the identification of single nucleotide polymorphisms for gene mapping (<http://www.sanger.ac.uk/resources/mouse/genomes/>). Once mapped, the causative mutation underlying increased susceptibility can be identified using whole exome sequencing. AcB60 mice are homozygous susceptible at the *Ccs4*/Chromosome 14 modifier loci known to regulate differential CA-CRC susceptibility in A/J and B6 mice and therefore, we consider that increased colitis could be driving CA-CRC on this already permissive genetic background³³¹. Therefore, we propose to map this mutation first in (AcB60 x 129S1)F2 mice using the acute model of DSS-induced colitis, before conducting experiments on CA-CRC susceptibility.

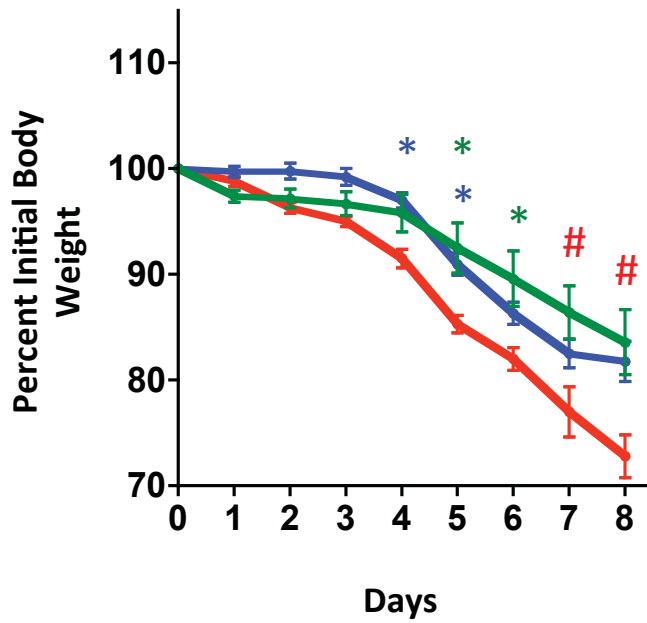
Mouse models of colitis and CA-CRC hyper-susceptibility are rare and scrutiny of the published literature revealed that AcB60 appears to be amongst the most susceptible with respect to early-onset colitis and CA-CRC. For example *Nlrp3*^{-/-}, *Pycard*^{-/-} and *Casp1*^{-/-} mice are highly susceptible to high dose DSS-induced colitis with the majority of mice succumbing to treatment

between 8 and 14 days post-initiation^{336, 352, 353}. While these mutations are associated with increased CRC susceptibility tumor burden is significantly lower, with longer latency than that seen in the AcB60 mice, although one must consider that these were independent experiments with multiple variables. Other models associated with early onset tumors formation include NOD1 deficient mice, which develop large tumors 10-weeks post initiation following treatment with an AOM/DSS protocol³⁵⁴. We hope that the identification of the gene underlying this unique AcB60 phenotype can be applied to human studies on early-onset IBD and CA-CRC, with the hopes of identifying those at risk, thus enabling earlier detection of disease and possible novel treatment options.

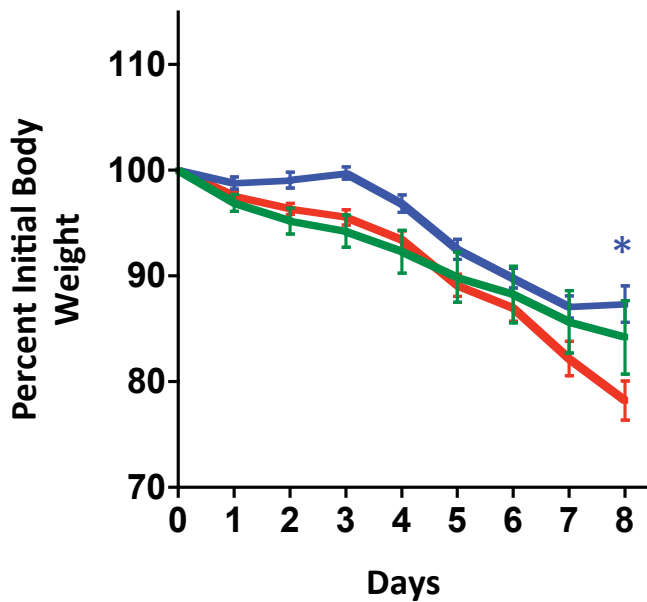
3.8 Acknowledgments

We are greatly indebted to Claire Turbide for her assistance with the azoxymethane injections. This research was supported by research grants to NB and PG from the Cancer Research Society. PG is a James McGill professor in Biochemistry. LVDK is a recipient of a McGill Integrated Cancer Research Training Program Fellowship and a Canadian Institutes of Health Research Doctoral Award- PA: Digestive Health (SHOPP).

A)

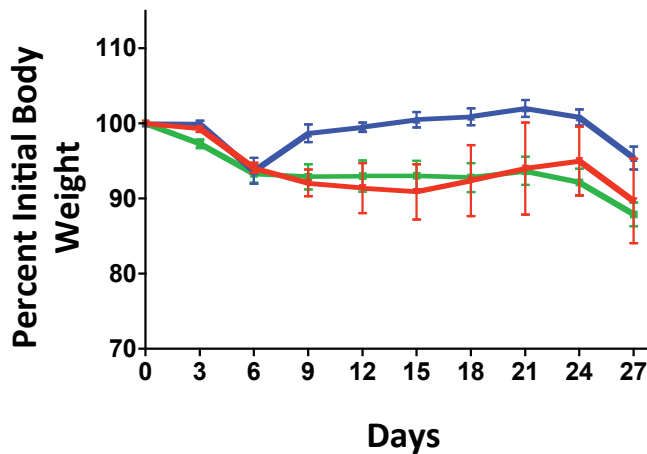


B)

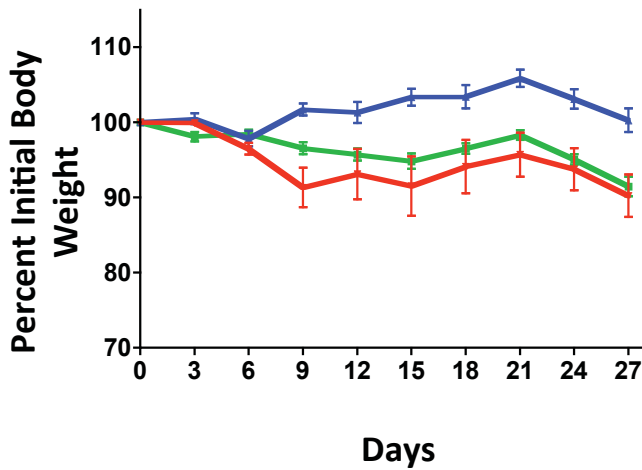


Supplemental Figure 3.1: Weight loss in acute DSS treated A/J, B6 and AcB60 mice. A/J, B6 and AcB60 mice were subjected to an acute DSS protocol (5 days 4% DSS, 3 days no treatment). Male (A) and female (B) mice were weighed every day and analyzed with respect to percent weight change relative to their initial (day 0) weight. Green line- A/J, blue line- B6 and red line- AcB60. * $p \leq 0.05$ AcB60 relative to B6, * $p \leq 0.05$ AcB60 relative to A/J using one-way ANOVA. # too few mice for ANOVA.

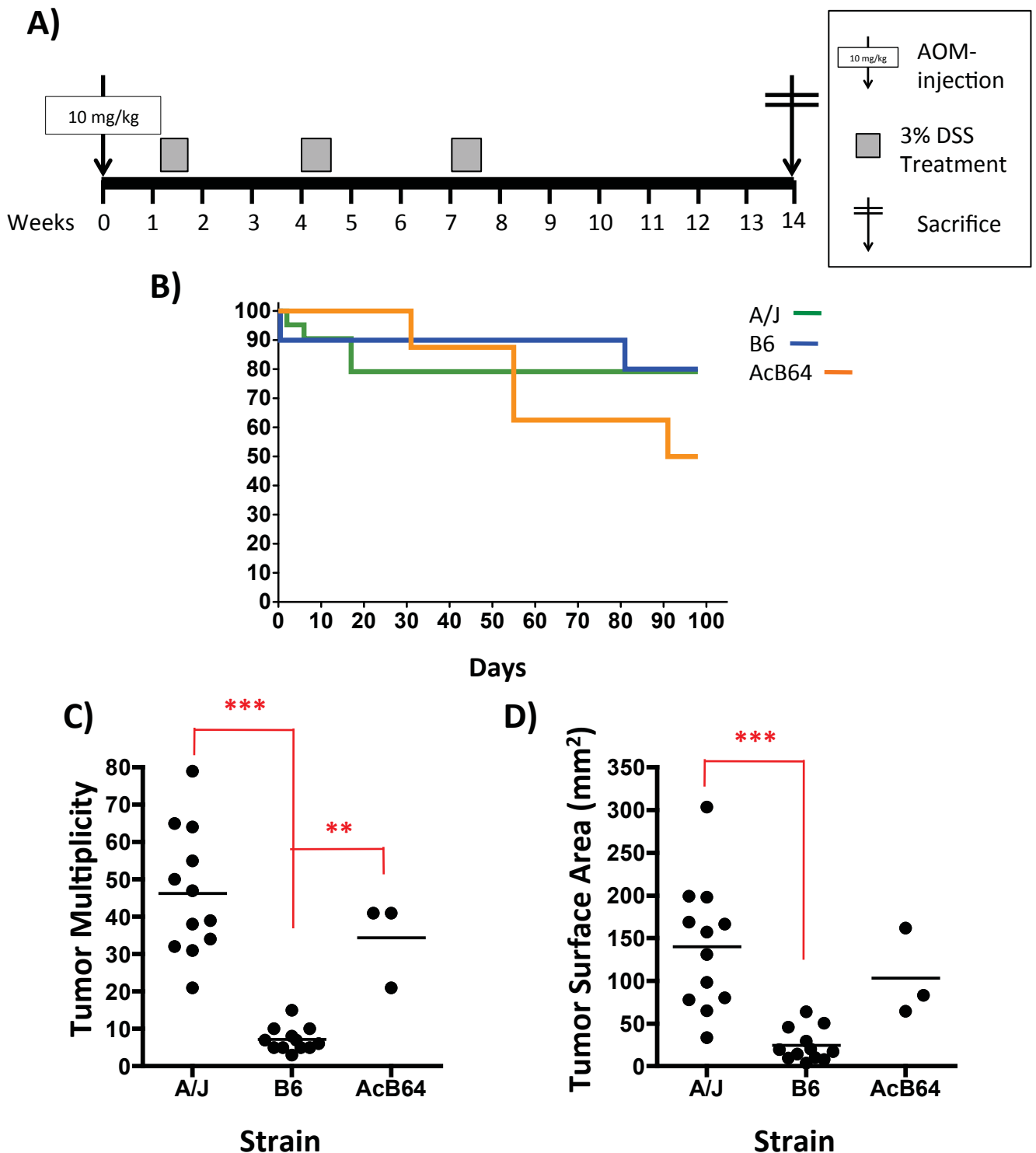
A)



B)



Supplemental Figure 3.2: Weight loss in long-term DSS treated A/J, B6 and AcB60 mice. A/J, B6 and AcB60 mice were subjected to the long term DSS protocol consisting of two cyclical DSS treatments (4 days each at 2%) with each treatment 17 days apart and sacrificed 28 days post-injection. Male (A) and Female (B) mice were weighed every 3 days. Weights are represented as the mean percent weight change relative to day 0 +/- the standard error. Green line- A/J, blue line- B6 and red line- AcB60.



Supplemental Figure 3.3: CA-CRC susceptibility in AcB64 recombinant congenic mice. A/J, B6 and AcB64 mice were subjected to the AOM/DSS protocol (10 mg/kg AOM, 3 cycles 3% DSS) (A) with 50% mortality in the AcB64 mice during the fourteen week treatment window (B). Fourteen weeks post-initiation colons from A/J, B6 and AcB64 mice were collected, fixed in formalin and scored for the phenotypes of tumor multiplicity (C) and surface area (D). ** $p \leq 0.01$, *** $p \leq 0.001$ using one-way ANOVA.

**Chapter 4: Hyper-Susceptibility to Colitis-Associated Colorectal Cancer in FVB/NJ Mice
Maps to the *Ccs6* Locus on Mouse Chromosome 6**

Manuscript in Preparation:

Van Der Kraak, L, Turbide, C, Jothy, S, Beauchemin, N, and Gros, P. Hyper-susceptibility to colitis-associated colorectal cancer in FVB/NJ mice maps to the *Ccs6* locus on mouse chromosome 6.

4.1 Connecting Text

It is known that inbred mice vary with respect to colorectal cancer (CRC) susceptibility due to inherited genetic factors ²²³. However, little is known with respect to response of the inbred mouse strains to colitis-associated (CA)-CRC relative to each other. Different studies use different doses of carcinogen, different inflammatory treatments (dose and duration) as well as different tumor latency periods, all of which are known to influence both tumor multiplicity and surface area. *Therefore, the first objective of this chapter was to characterize the response of several inbred mouse strains to azoxymethane/dextran sulfate sodium (AOM/DSS)-induced CA-CRC.* In Chapter 2, we successfully mapped a novel two locus-system involving mouse chromosomes 9 (*Ccs4*) and 14, which regulates susceptibility to AOM/DSS-induced CA-CRC in susceptible A/J and resistant B6 mice ³¹⁷. We hypothesized that additional, yet to be identified loci may regulate CA-CRC susceptibility in other inbred mice. *Therefore, the second objective of this chapter was to map novel CA-CRC susceptibility loci in these inbred mouse strains.*

4.2 Contributions of the Authors

The experiments presented in this chapter were planned as part of a collaborative effort between LVDK, NB and PG. CT performed the initial carcinogen injection. LVDK bred the mouse strains, administered all treatments (except the carcinogen), performed the sacrifice, analyzed samples for tumor multiplicity and surface area, extracted the DNA, genotyped mice for in house markers and performed the time-course colonoscopies. LVDK also prepared samples for histology, which were embedded and sectioned at the Goodman Cancer Centre Histology Facility and subsequently analyzed by SJ. LVDK wrote the paper and prepared the figures with input from NB and PG.

4.3 Abstract

Inbred strains of mice differ in susceptibility to colitis-associated colorectal cancer (CA-CRC). We tested 10 inbred strains of mice for their response to azoxymethane/dextran sulfate sodium (AOM/DSS)-induced CA-CRC and identified a bimodal distribution pattern when tumor multiplicity was used as a phenotypic marker of susceptibility. In this screen, FVB/NJ mice had a higher tumor burden than several other susceptible strains (12.5 weeks post-treatment) suggesting that FVB/NJ mice might behave as a hyper-susceptible strain. FVB/NJ hyper-susceptibility was also detected as early as 8-weeks post-treatment, with FVB/NJ mice

developing 5.5 fold more tumors than A/J or B6 mice, which are standard susceptible and resistant controls, respectively. Linkage analysis in informative (FVB/NJxC3H/HeJ)F2 mice identified a novel susceptibility locus, designated *colon cancer susceptibility 6* (*Ccs6*) on proximal mouse chromosome 6. Mice homozygous for FVB/NJ alleles at this locus had increased tumor multiplicity compared to homozygous C3H/HeJ mice. This locus overlaps with several other cancer susceptibility loci, suggesting that a general tumor susceptibility locus may map to this region of chromosome 6.

4.4 Introduction

Colorectal cancer (CRC), cancer of the colon and rectum, is a complex disease with more than 1 million new cases diagnosed each year³⁵⁵. Inflammation, in the form of inflammatory bowel disease (IBD), which includes ulcerative colitis (UC) and Crohn's disease (CD), represents the third most important risk factor for CRC after familial adenomatous polyposis (FAP) and hereditary non-polyposis colon cancer (HNPCC), which themselves are caused by highly penetrant germline mutations⁶⁸. Duration of IBD is tightly correlated with inflammation or colitis-associated (CA)-CRC development. Studies of CRC risk in UC reference a 2001 study by Eaden et al., which concluded that the probability of CRC was 2% after 10 years of disease, 8% after 20 years and 18% after 30 years¹³⁷. Studies of UC-CRC have also noted a high concordance between CA-CRC risk with location/extent of disease and age of disease onset. For example, Ekobom et al. identified a standardized incidence ratio (SIR) of 1.7 for proctitis (rectal only), 2.8 left-sided colitis and 14.8 pancolitis (defined as extensive colitis, or colitis involving the entire colon)¹⁴². Similar observations have been observed for CD^{144, 145}.

In humans, patients with similar disease patterns (UC extent and duration), but that significantly differ with respect to CA-CRC development have been identified¹⁴⁹. Therefore, it has been hypothesized that additional risk factors, in the form of low penetrance tumor susceptibility genes may contribute to CA-CRC development. Low penetrance susceptibility genes have previously been demonstrated to be important in the development of both IBD and CRC^{98, 159}. However, no association has been formally demonstrated between CA-CRC and any of the 163 known IBD loci or CRC predisposing loci, suggesting that CA-CRCs may have a unique set of pre-disposing genetic risk factors^{98, 149, 159}.

Inbred mice, like humans, vary with respect to both dextran sulfate sodium (DSS)-induced colitis and azoxymethane (AOM)/DSS-induced CA-CRC and have been used as a tool

to study the influence of dietary, lifestyle and genetic factors in disease ²²³. Similar to humans, the role of inflammation in CA-CRC in inbred mice appears to vary in a strain dependent manner. For example, C57Bl/6 (B6) and BALB/c, are resistant and susceptible, respectively to both DSS-induced colitis and AOM/DSS-induced CRC, while C3H/HeJ are susceptible to DSS-colitis, but resistant to CA-CRC ^{301, 305}. The differential susceptibility of inbred mice can be exploited to identify and characterize pre-disposing CA-CRC genetic risk factors using forward genetic approaches. In 2010, we identified a novel two-locus system involving mouse chromosome 9 (*Ccs4*) and chromosome 14, which regulates AOM/DSS CA-CRC susceptibility in A/J (susceptible) and B6 (resistant) mice ³¹⁷. We hypothesize that different genetic factors, separate from the *Ccs4* and chromosome 14 loci, may exist and moderate CA-CRC susceptibility in other inbred mice, which can be mapped by linkage analysis and identified by positional cloning.

We studied the response of 10 common inbred mouse strains to CA-CRC and detected a bimodal distribution pattern in the response of these inbred strains when tumor multiplicity was used as a quantitative measure. FVB/NJ were identified as a hyper-susceptible strain, with tumors developing as early as 4 weeks post-treatment initiation. Susceptibility to CA-CRC in these FVB/NJ mice is under the genetic control of a novel *colon cancer susceptibility 6* (*Ccs6*) locus positioned on mouse chromosome 6.

4.5 Materials and Methods

4.5.1 Ethics

All animal experiments were conducted in compliance with the rules and regulations set out by the Canadian Council on Animal Care (CCAC) and the McGill Comparative Animal Resource Centre (Protocol AUP 5183).

4.5.2 Mice

Male and female 129S1/SvImJ, A/J, AKR/J, BALB/cByJ, C3H/HeJ, C57Bl/6J (B6), CBA/J, DBA/2J, FVB/NJ and NOD/ShiLtJ mice were purchased from Jackson Laboratory (Bar Harbor, ME, USA). The (FVB/NJxC3H/HeJ)F1 mice were generated by mating a FVB/NJ female with a C3H/HeJ male in house and the resulting F1 progeny mice were inter-crossed thus generating the (FVB/NJ x C3H/HeJ)F2 mice. All mice were housed on a 12-hour light/dark cycle in the McGill Comparative Animal Resource Centre and fed regular chow (Rodent Chow 5075, Charles River) and water ad libitum. Experiments were conducted on mice 8 weeks of age

or older. Mice were weighed and visually monitored a minimum of twice a week for clinical symptoms of colitis and CA-CRC. Animals showing signs of discomfort were humanely sacrificed.

4.5.3 Induction of Colitis-Associated Colon Cancer

CA-CRC was induced using combined administration the colon-specific carcinogen azoxymethane (AOM, Sigma, St Louis, MO, USA) and dextran sulfate sodium (DSS, Salt Reagent Grade MW 36,000-50,000, MP Biomedicals LCC, Solon, OH, USA). These methods are described in detail in Van Der Kraak *et al.*³¹⁷. Briefly, mice were given a single injection of AOM (6 or 7.5 mg/kg i.p) on day zero, followed by two or three 4-day cycles of either 2% or 3% DSS in drinking water. The specific doses for each experiment are described in the results section. The first DSS treatment was administered exactly one week after the AOM injection with each subsequent treatment 17 days apart. Following the final DSS treatment, mice were given normal water until the end of the experiment (between weeks 8 and 12.5). At sacrifice, the large intestine (anus to cecum) was removed, washed in phosphate-buffered saline (PBS) and fixed in 10% phosphate-buffered formalin for subsequent scoring and histological analysis.

4.5.4 Tumor Counts

At the end of the experiment, the animals were sacrificed, their colons removed, flushed with PBS and fixed for a minimum of 24 hours in 10% phosphate buffered formalin. Using a 10x microscope objective, colons were evaluated for the phenotypes of tumor multiplicity and tumor surface area. Tumor surface area was estimated using a clear transparency of 1 mm² graph paper. The number of squares overlaying each lesion was measured to the nearest 0.25 mm².

4.5.5 Linkage Analysis and QTL Mapping

Tail DNA samples were extracted using a standard proteinase K extraction protocol³³¹. A total of 82 (FVB/NJ x C3H/HeJ)F2 samples (36 most susceptible and 46 most resistant mice) along with 1 FVB/NJ and 1 C3H/HeJ mouse were genotyped for 1449 single nucleotide polymorphisms (SNPs) on the Illumina Medium Density Linkage Analysis panel at The Centre for Applied Genomics (TCAG) at the Hospital for Sick Children (Toronto, ON, Canada). Of the SNPs tested on the panel, 596 markers were polymorphic between C3H/HeJ and FVB/NJ.

QTL linkage analysis, using susceptibility as a binary trait, was conducted using R/qtl software and the EM maximum likelihood algorithm. Both one and two-dimensional scans were

performed and genome-wide significance was calculated using permutation tests (1000 tests). Additional genotyping of microsatellite markers near peak markers of association (D6Mit223, D17Mit33) for all (FVB/NJ x C3H/HeJ)F2 mice was performed using standard PCR with subsequent separation on 3% agarose gels with ethidium bromide staining. Primer sequences can be found online at the Mouse Genome Informatics webpage (<http://www.informatics.jax.org/>).

4.5.6 Histological Analysis

Phosphate-buffered formalin fixed AOM/DSS-treated tissues were dehydrated in ethanol, paraffin-embedded and sectioned (5 μ m) at the Goodman Cancer Centre Histology Facility (Montreal, QC, Canada). Samples were mounted onto slides, de-paraffinized and stained with hematoxylin and eosin (H & E) following standard histological procedures. Grading of both tumors and inflammation was assessed in a blinded fashion by a pathologist (SJ) according to recommendations of Wirtz et al.²⁸². Histological changes were recorded with a Leica DM4000 B microscope equipped with a Leica DFC320 digital camera, using the LAS V3.8 software (Leica Microsystems, Richmond Hill, ON) or scanned using a ScanScope XT digital scanner (Aperio Technologies, Vista, CA, USA).

4.5.7 Colonoscopy

Tumor development in AOM/DSS-treated mice was monitored by colonoscopy using a Karl Storz Hopkins Rigid Telescope connected to an Olympus HD camera head (OTV-SProH-HD-L08E). Mice were scoped prior to treatment initiation and at 4 and 8 weeks post-initiation to monitor tumor development in real time. To avoid changes in diet, mice were not fasted prior to scoping. Mice were anesthetised during the procedure with 1.5-2% isoflurane according to McGill standard operating procedures. The procedures were recorded using the Olympus Video System Centre (CV-180) and still-frame photographs extracted using Div X Player software (<http://www.divx.com/>).

4.5.8 Statistical Analyses

All statistical analyses were calculated using GraphPad Prism software (GraphPad Software, Inc. La Jolla, CA, USA) using one way-ANOVA and the Bonferroni post-test. Results were significant if $p \leq 0.05$. Select measurements in the results sections are listed as the value \pm the standard deviation.

4.6 Results:

4.6.1 Inbred Mice Have a Bimodal Distribution Pattern of Susceptibility to CA-CRC

To identify genetic factors regulating susceptibility to CA-CRC, we tested 10 inbred mouse strains for susceptibility to CA-CRC. These strains were chosen from the 36-genetically well-characterized Mouse Phenome Project Priority Strains at Jackson Laboratory to reflect common background strains used in both cancer and IBD related research. Briefly, male and female mice were given a single injection of AOM (7.5 mg/kg) followed by 3 subsequent treatments with 3% DSS and monitored over a period of 12.5 weeks (Figure 4.1 A). For all strains, with the exception of A/J, equal numbers of male and female mice were tested (B6: n= 5, all other strains: n= 4 per gender). In this experiment, 75% of the NOD/ShiLtJ females developed severe colitis symptoms prompting sacrifice within the first 5 weeks of the experiment. No macroscopically visible tumors were detected in these mice at sacrifice [data not shown]. Two FVB/NJ mice were sacrificed in week 7 and 9 respectively, following the development of rectal prolapses, the endpoint in our experimental protocol. These mice had high tumor multiplicity (n= 18 and 26) and surface area (A= 55 mm² and 126 mm²) when sacrificed, suggestive of early-onset of tumors in these mice.

At 12.5 weeks post-treatment initiation, mice were sacrificed and their colons collected and fixed in 10% phosphate-buffered formalin and subsequently examined for the phenotypes of tumor multiplicity and tumor surface area. Tumor incidence was 100% in the mice tested. As expected, A/J mice were highly susceptible averaging 36 ± 5 tumors/mouse, while B6 mice were resistant averaging 11 ± 2 tumors/mouse (Figure 4.1 B, ³¹⁷). Interestingly, the remaining inbred strains demonstrated a bimodal distribution pattern whereby mice were either A/J-like or B6-like with respect to tumor multiplicity. AKR/J (n= 6 ± 7), C3H/HeJ (n= 8 ± 4) and 129S1/SvImJ (n= 11 ± 5) were similar to B6 and resistant to CA-CRC. BALB/cByJ (n= 37 ± 5), CBA/J (n= 26 ± 6), FVB/NJ (n= 37 ± 6) and NOD/ShiLJ (n= 43 ± 12) were susceptible to CA-CRC. With respect to tumor multiplicity, only the DBA/2J mice had an obvious gender effect with DBA/2J females behaving as resistant (n= 12.0 ± 5.0) and DBA/2J males behaving as susceptible (n= 31 ± 17). The bimodal distribution pattern was not observed with respect to CA-CRC tumor surface area in these inbred strains (Figure 4.1 C) suggesting that different events may regulate tumor initiation and proliferation in the various mouse strains. AKR/J and C3H/HeJ had the lowest tumor burden of the tested mice (A < 25 mm²), while FVB/NJ mice had the highest tumor

burden ($A = 262 \pm 169$).

4.6.2 FVB/NJ Mice are Hyper-Susceptible to CA-CRC

In our initial inbred strain survey for CA-CRC susceptibility, FVB/NJ mice were highly susceptible with respect to both tumor multiplicity and surface area (Figure 4.1 B and C). Interestingly, FVB/NJ mice had significantly higher tumor burden ($p < 0.01$), than several other susceptible mouse strains, namely A/J, BALB/cByJ and CBA/J ($A = 85-138 \text{ mm}^2$). In addition 25% FVB/NJ mice in our first experiment had to be sacrificed early due to complication associated with large tumor burden. Therefore, we hypothesized that FVB/NJ may have a unique phenotype possibly reflecting early-onset of tumor development, which may be associated with unique genetic determinant in this strain

To test this hypothesis, A/J, B6 and FVB/NJ male and female mice were treated with AOM/DSS (7.5 mg/kg AOM, 2 or 3 cycles of 3% DSS) and sacrificed at 8 weeks post-initiation of treatment and their colons subsequently analyzed for the phenotypes of tumor multiplicity and surface area (Figure 4.1 D and E). The response of mice receiving 2 or 3 DSS treatments [data not shown] was very similar and therefore the two experimental groups were combined. FVB/NJ mice had significantly greater tumor multiplicity ($n = 20 \pm 9$, $p \leq 0.05$) and greater tumor burden ($A = 72 \pm 41$, $p \leq 0.05$) than either A/J ($n = 4 \pm 5$, $A = 7 \pm 10$) or B6 ($n = 5 \pm 5$, $A = 15 \pm 17$) mice at this earlier time point, suggesting that different genetic events regulate susceptibility in A/J and FVB/NJ mice.

4.6.3 FVB/NJ Tumor Characteristics

To better characterize FVB/NJ's hyper-susceptibility, we studied tumor development in real time in AOM/DSS treated (6 mg/kg AOM, two cycle 2% DSS) mice using colonoscopy. Mice were scoped at pre-determined intervals (0 weeks, 4 weeks and 8 weeks) and monitored for the presence of tumors. In treated FVB/NJ mice, tumors were detected as early as 4 weeks post-injection and rapidly increased in size between 4 and 8 weeks (Figure 4.2 A). No tumors were detected in untreated control mice scoped at the same time intervals. Hence CA-CRC hyper-susceptibility in FVB/NJ mice is associated with early-onset tumor formation.

To further characterize the micro and macroscopic properties of FVB/NJ tumors relative to C3H/HeJ, the resistant strain used in our subsequent mapping studies, AOM/DSS treated (6 mg/kg AOM, 2% DSS two treatments) FVB/NJ and C3H/HeJ mice, were sacrificed 9 weeks

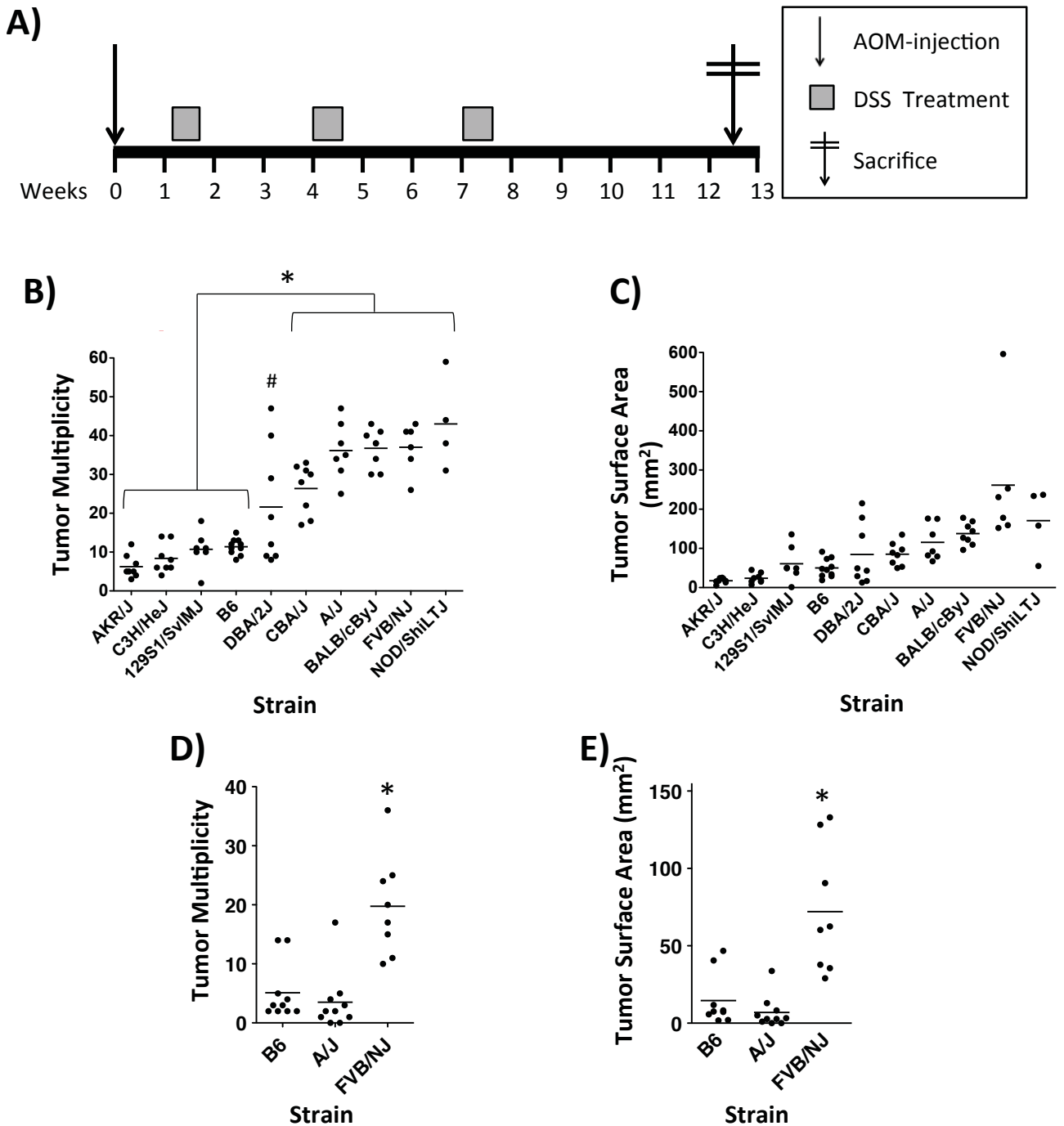


Figure 4.1: Response of select inbred mouse strains to AOM/DSS-induced CA-CRC. (A) Male and female inbred mice were subjected to the AOM/DSS protocol (7.5 mg/kg AOM, 3 cycles 3% DSS) and sacrificed 12.5 weeks post-injection. Mice were subsequently analyzed for the phenotypes of tumor multiplicity (B) and surface area (C). * $p \leq 0.05$ using one-way ANOVA. # $p \leq 0.05$ to B6, 129S1/SvImJ and CBA/J. FVB/NJ mice had significantly greater tumor multiplicity (D) and surface area (E) relative to A/J and B6 8-weeks post AOM/DSS-treatment initiation (7.5 mg/kg AOM, 2 or 3 cycle of 3% DSS), suggesting that different genetic factors regulate susceptibility to CA-CRC in A/J and FVB/NJ mice.

post-injection and their colons collected, paraffin-embedded, sectioned and stained with haematoxylin and eosin (Figure 4.2 B). Stained slides were then scored for the presence of various lesions and inflammation relative to untreated mice (Figure 4.2 D). At sacrifice, all of the C3H/HeJ had cleared the inflammation induced by DSS treatment. FVB/NJ mice with high tumor burden demonstrated evidence of increased inflammation in the vicinity of the tumors (Wirtz et al score of 1-2), but the average inflammatory score was similar between FVB/NJ and C3H/HeJ mice²⁸². The most common lesions detected in all mice were adenomas. C3H/HeJ adenomas were generally benign with most having no evidence of dysplasia (71%) and the remaining showing evidence of low-grade dysplasia (lgd) (Figure 4.2 C and E). FVB/NJ had more adenomas than C3H/HeJ. Most adenomas in the FVB/N mice were lgd (83%) with a minority of lesions showing high-grade dysplasia (hgd) (16%) (Figure 4.2 C, F-H). A single FVB/NJ mouse developed an invasive adenocarcinoma located near the anus (Figure 4.2 I).

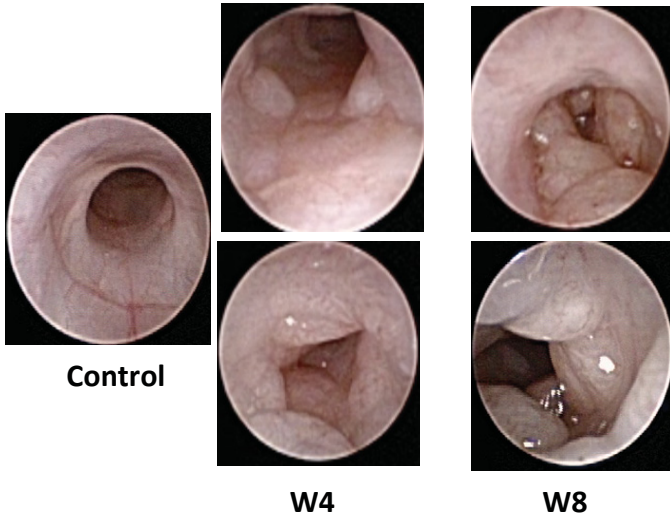
4.6.4 Analysis of CA-CRC Susceptibility in (FVB/NJ x C3H/HeJ)F1 and F2 mice

To define genetic determinant regulating hyper-susceptibility to CA-CRC in FVB/NJ mice, informative (FVB/NJ x C3H/HeJ)F1 and F2 mice were bred and subjected to the AOM/DSS protocol (6 mg/kg injection, two cycles of 2% DSS) (Figure 4.3 A). At 9 weeks post-initiation, the mice were sacrificed and the colons collected and enumerated for the phenotypes of tumor multiplicity and surface area. FVB/NJ primarily develop large tumors and therefore only lesions $\geq 2 \text{ mm}^2$ were included in this experimental analysis. Consistent with our previous experiment, FVB/NJ mice had significantly higher tumor multiplicity ($n= 14$, $p \leq 0.01$) and larger surface area ($A= 65 \text{ mm}^2$, $p \leq 0.01$) than the resistant C3H/HeJ mice ($n= 3$, $A= 10 \text{ mm}^2$) (Figure 4.3 B and C). The (FVB/NJ x C3H/HeJ)F1 female mice were resistant ($n= 2$, $A= 9 \text{ mm}^2$), similar to the C3H/HeJ parents, suggesting that tumor susceptibility in females is recessive. Male (FVB/NJ x C3H/HeJ)F1 mice had a bimodal distribution with respect to susceptibility overlapping with both the C3H/HeJ and FVB/NJ parental phenotypes. The (FVB/NJ x C3H/HeJ)F2 mice exhibited a range of phenotypes, clustering towards resistance. A similar gender effect to the F1 mice was noted in these F2 mice. A similar overall trend was noted with respect to surface area in the (FVB/NJ x C3H/HeJ)F1 and F2 mice.

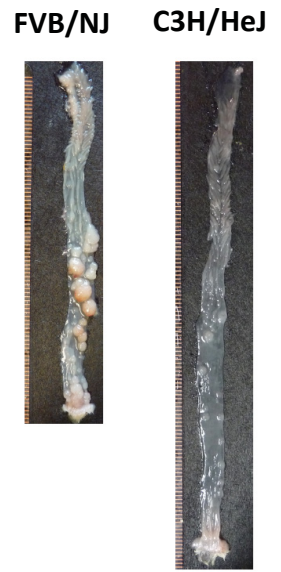
4.6.5 Identification of the *Ccs6* Locus on Mouse Chromosome 6

To map genetic factors regulating susceptibility to CA-CRC in FVB/NJ mice, 82

A)



B)



C)

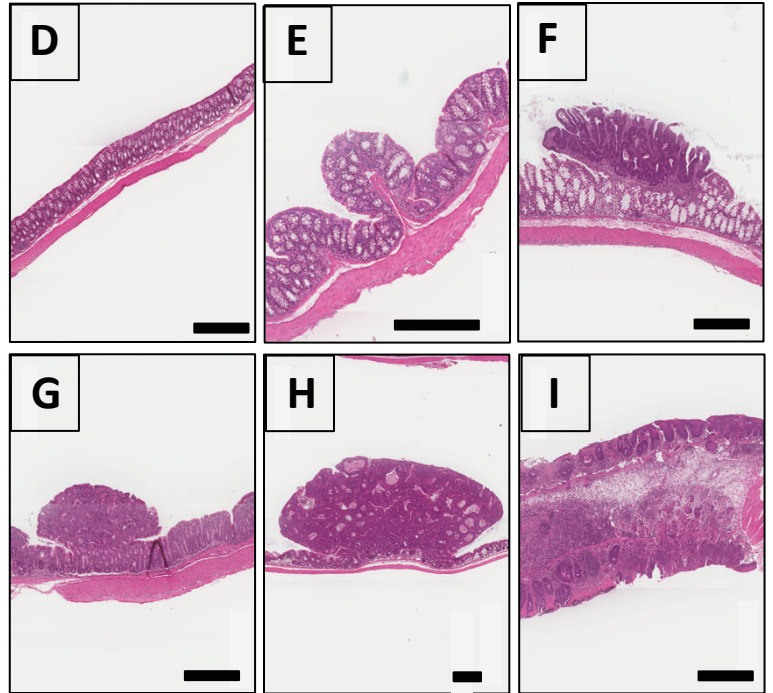
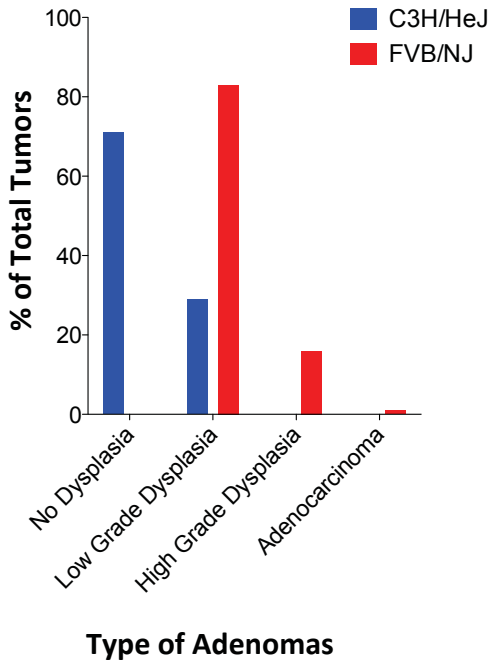


Figure 4. 2: Macroscopic and microscopic tumor properties in FVB/NJ and C3H/HeJ mice. FVB/NJ and C3H/HeJ mice were treated with a single AOM injection and 2 consecutive periods of DSS (2%) and sacrificed 9 weeks post-injection. (A) To track tumor development in real time, FVB/NJ AOM/DSS-treated mice were monitored using colonoscopy at pre-determined time intervals (0, 4 and 8 weeks). (B) Representative images of FVB and C3H/HeJ colons. 9-week FVB/NJ and C3H/HeJ colons were subsequently hematoxylin and eosin stained. (C) Degree of dysplasia in the adenomas identified in the colon sections. Following injection, the normal untreated colon (D) is transformed with C3H/HeJ mice developing adenomas associated with low-grade dysplasia (lgd) (E). In FVB/NJ mice, numerous adenomas with lgd (F) and high-grade dysplasia (hgd) (G) were detected. This included both small (G) and large (H) adenomas. A single invasive adenosquamous carcinoma was detected near the anus in an FVB/NJ mouse (I). The black bar in each figure denotes 0.5 mm.

(FVB/NJ x C3H/HeJ)F2 mice were genotyped for 596 polymorphic markers evenly spaced throughout the genome. These 82 mice were chosen to represent the most susceptible (n= 36) and resistant (n= 46) (FVB/NJ x C3H/HeJ)F2 mice with respect to tumor multiplicity. A whole genome scan was performed using susceptibility as a binary trait, identifying a single significant association (LOD 3.99, 40.8 Mbp) above genome-wide significance (LOD = 3.86) (Figure 4.4 A). This was increased to 5.4 (peak marker rs13478727, 43.5 Mbp) when gender was used as a covariate. Figure 4.4 B denotes the haplotype of the 82 (FVB/NJ x C3H/HeJ) mice at the peak marker of association. The initial genome scan detected a secondary peak on mouse chromosome 17 (LOD=3.35, peak marker 29.9 Mbp). Subsequently, all 167 (FVB/NJ x C3H/HeJ)F2 mice were genotyped for chromosome 6 (D6Mit223, 45.3 Mbp) and chromosome 17 (D17Mit33, 34.7 Mbp) near the peak markers of association. This confirmed the chromosome 6 association, but the analysis failed to validate a contribution of chromosome 17 (Figure 4.4 C).

Haplotype association studies indicated that consistent with our observations in (FVB/NJ x C3H/HeJ)F1s, this chromosome 6 locus had a significant gender effect. Female mice inheriting two FVB/NJ alleles had significantly higher tumor numbers (n= 8, $P \leq 0.05$) than heterozygous females (n= 2) (Fig. 4 C). Female mice inheriting two C3H/HeJ alleles at D6Mit223 had tumor numbers similar to heterozygous mice (n= 3), but were not statistically different than mice inheriting two FVB/NJ alleles. Closer inspection revealed a single outlier mouse (n= 30 vs n= 0-4 remaining mice), preventing statistical significance from being achieved. The haplotype of this mouse on chromosome 6 was assessed revealing a crossover from CC to FF between 45.4 Mbp and 63.8 Mbp. Consistent with the female results, male mice inheriting two copies of FVB/NJ alleles developed significantly more tumors (n= 12) than mice inheriting a C3H/HeJ allele (n= 3 two alleles, n= 6 one allele) (Fig. 4 C). Similar to the (FVB/NJ x C3H/HeJ)F1 males, heterozygous F2 male mice at D6Mit223 had a large distribution of phenotypes (n= 0-30 tumors). This chromosome 6 locus has been given the designation *Ccs6* for *colon cancer susceptibility 6*. Together these results support that the *Ccs6* locus regulates CA-CRC susceptibility in a recessive manner, with FVB/NJ alleles being associated with susceptibility.

4.7 Discussion:

In this study we characterized the response of 10 common inbred mouse strains to

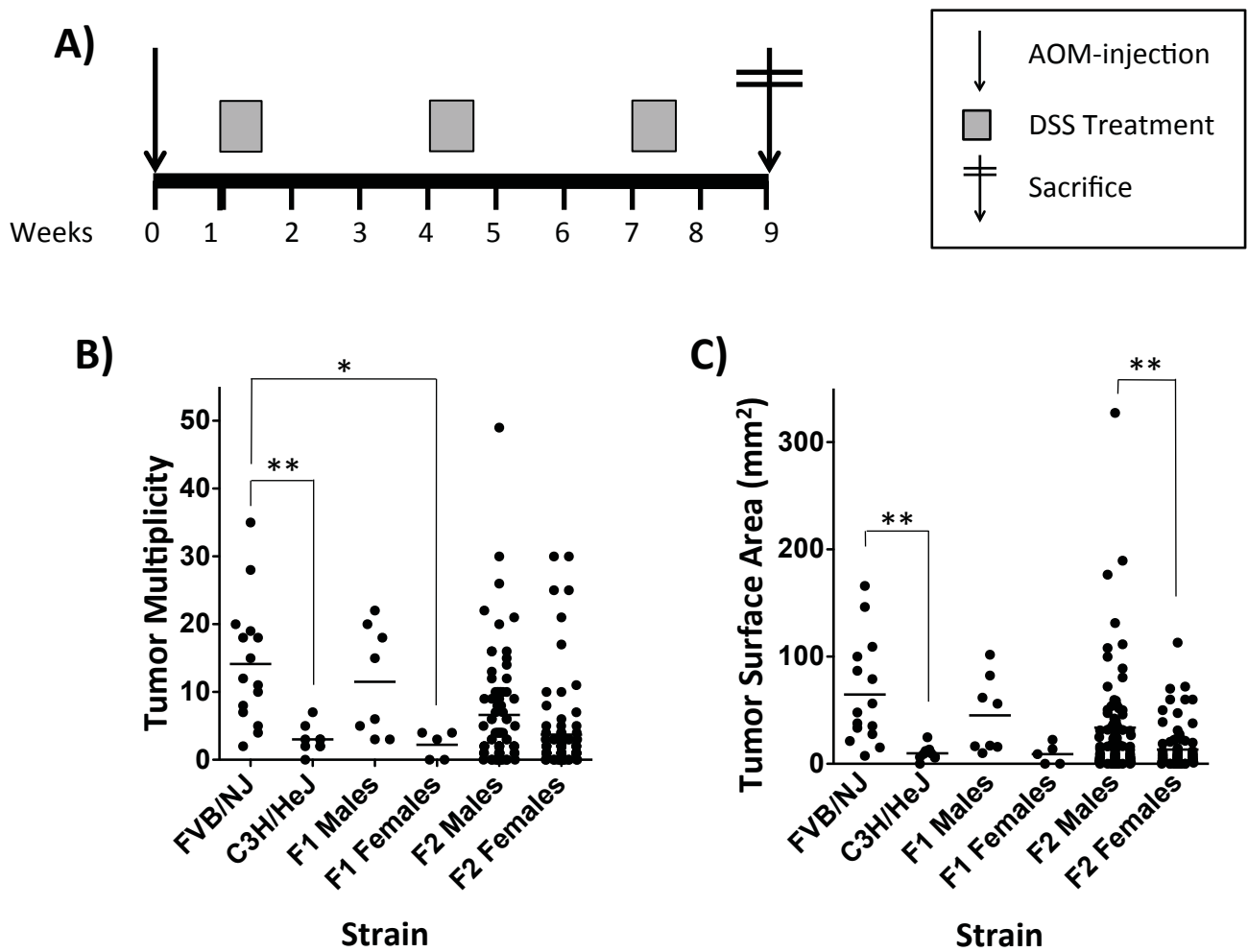


Figure 4.3: Segregation analysis of AOM/DSS-induced CA-CRC susceptibility. (A) To map novel FVB/NJ associated CRC-susceptibility loci FVB/NJ, C3H/HeJ, 13 (FVB/NJ x C3H/HeJ)F1 and 167 (FVB/NJ x C3H/HeJ)F2 mice were subjected to the AOM/DSS protocol (6 mg/kg AOM; 2 cycles 2% DSS) and scored for the phenotypes of tumor multiplicity (B) and tumor surface area (C) 9 weeks post-initiation. Only tumors with surface area > 2mm² were included in the analysis. * $p \leq 0.05$, ** $p \leq 0.01$, *** $p \leq 0.001$ using one-way ANOVA.

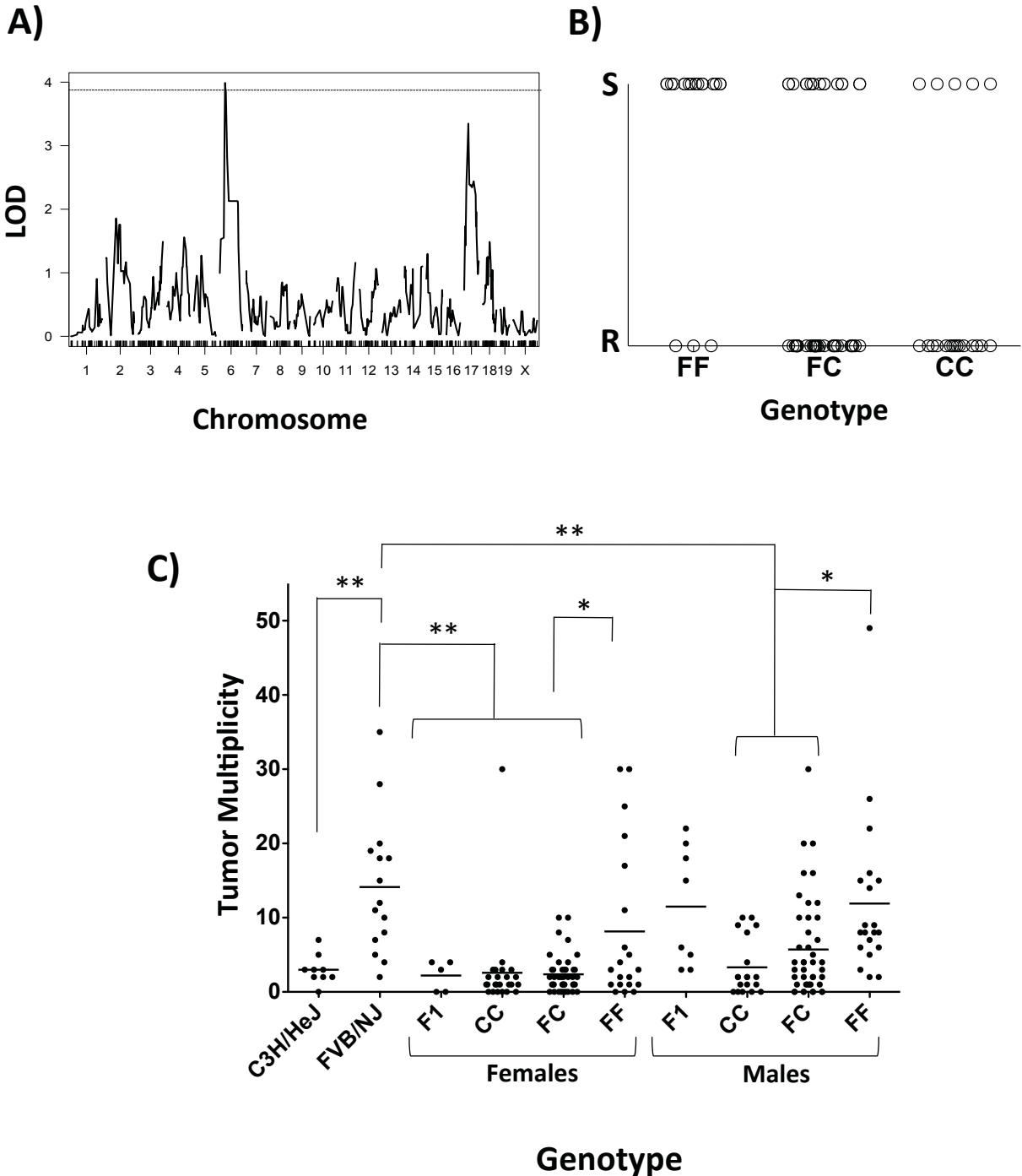


Figure 4.4: Identification and validation of a susceptibility locus on mouse chromosome 6. (A) A genome-wide scan in 82 (FVB/NJ x C3H/HeJ)F2 mice for AOM/DSS-induced CRC susceptibility as a binary trait identified a single significant hit (significance threshold is 3.86, dotted line) on mouse chromosome 6 (LOD= 3.99). (B) Haplotype association with respect to susceptibility at the chromosome 6 peak marker of association from the genome scan (gnf06.037.785, 40.75 Mb). FF- homozygous FVB/NJ, FC= heterozygous, CC= homozygous C3H/HeJ, S- susceptible, R- resistant. (C) Haplotype association in the 167 (FVB/NJ x C3H/HeJ)F2 mice at marker D6Mit223 (45.3 Mb) to validate the chromosome 6 association from the genome scan. * $p \leq 0.05$, ** $p \leq 0.01$ one-way ANOVA.

AOM/DSS-induced CA-CRC, identifying a bimodal distribution with respect to tumor multiplicity. Our conclusions support the general trends previously reported in the literature, demonstrating susceptibility in A/J, BALB/c, CBA/J and FVB/NJ mice and resistance in C3H/HeJ and B6 mice^{303, 305, 307, 317}. This is the first study to assess 129S1/SvImJ, AKR/J and NOD/ShiLtJ. DBA/2 males were previously reported as highly resistant to AOM/DSS-induced CRC, but are susceptible in our model³⁰⁵. This discrepancy may reflect differences with respect to dose of carcinogen and DSS concentration used in the two studies, genetic heterogeneity (and drift) in the mouse strains and/or different environmental conditions such as housing, bedding and food. NOD/ShiLtJ females were highly sensitive to DSS-induced inflammation in our model, consistent with published literature^{284, 298}. Interestingly, inbred mice did not reveal a bimodal distribution pattern with respect to CA-CRC-induced tumor surface area suggesting that different events may regulate tumor multiplicity and tumor proliferation in different inbred mouse strains. FVB/NJ mice had the highest tumor surface area and hence this strain was selected for additional gene mapping studies.

We have shown that FVB/NJ mice are hyper-susceptible to CA-CRC, with tumors visible as early as 4 weeks post-initiation, which progress to adenomas (with lgd or hgd) and the occasional invasive adenocarcinoma, 9 weeks post-initiation. Using an (FVB/NJ x C3H/HeJ)F2 cross, we mapped a novel CA-CRC locus on mouse chromosome 6 (*Ccs6*). Susceptibility in females is recessive, with the FVB/NJ allele conferring susceptibility, whereas males show a bimodal distribution overlapping with both the FVB/NJ and C3H/HeJ parental strains. Regardless of gender, mice homozygous for either C3H/HeJ or FVB/NJ alleles at the *Ccs6* locus show susceptibility/resistance characteristics similar to those of the parental strain.

The *Ccs6* locus is ~ 39 Mbp, delineated by rs13478697 (31.8 Mbp) and a C3H/HeJ chromosomal inversion (D6Mit124, 71.8 Mb) and encompasses 559 genes with peak markers mapping to 40.8 Mbp (gnf06.037.785) and 43.9 Mbp (rs13478697, gender as a covariate). The large physical interval of the *Ccs6* locus precludes elucidation of specific candidate genes at this time. However, the *Ccs6* maximal interval overlaps with several previously published cancer and IBD loci in humans and mice, which are of interest to our studies.

In mice, the *Ccs6* interval overlaps with the *susceptibility to colon cancer 13* locus, which is one of several loci that regulate the differential susceptibility of BALB/cHeA (resistant) and STS/A (susceptible) mice to AOM-induced CRC¹⁹⁹. While this locus has not been formally

validated, a suggestive linkage near *Sccl3* was also identified in an (A/J xSPRET/EiJ)N2 AOM-induced CRC screen, although again formal evaluation of this association is necessary²⁷². We have previously shown that AOM and AOM/DSS-induced CRC are under differential genetic control in A/J and B6 mice, and therefore it is tempting, but premature to suggest that the *Ccs6* and *Sccl3* loci are unlinked³¹⁷. The *Ccs6* locus also overlaps with two chemically induced lung cancer loci (*Sluc7*; peak marker 26.3 Mb and *Par4*; peak marker, 17.3 Mb) mapped in O20 and SWR/J mice, respectively^{356, 357}. A recent study has suggested that most mouse CRC loci (*Sccl/Ccs*) and lung cancer loci (*Sluc/Pas*) are found together in pairs, suggesting that common genetic events may influence susceptibility to both cancers^{358 359}. The *Ccs6* locus also overlaps with a NON/ShiLtJ N-butyl-N-(4-hydroxybutyl)nitrosamine (BNN)-induced bladder tumor susceptibility locus 2 (*Bts2*, peak marker 59.1 Mbp)³⁶⁰. Interestingly, FVB/NJ mice are susceptible to both lung and bladder suggesting that a common cancer locus may map to this region of chromosome 6. The genetic variants underlying susceptibility at the above loci have not been identified.

Scrutiny of published murine literature for AOM/DSS and chromosome 6 has identified several plausible candidate genes. *Nucleotide-binding oligomerization domain containing 1* (*NOD1*, 54.9 Mbp), involved in bacterial pathogen detection, plays a protective role in AOM/DSS-induced CA-CRC with *NOD1*^{-/-} mice developing increased tumor burden and colonic inflammation 10 weeks post initiation³⁵⁴. *Caspase2* (*Casp2*) is a highly conserved member of the caspase family of genes thought to be involved in regulating apoptotic response³⁶¹. While the role of *Caspase 2* has not been characterized with respect to CA-CRC, studies of another inhibitory caspase, *Caspase 1*, show increased tumor burden following AOM/DSS treated in *Casp1*^{-/-} mice compared to wild-type mice³⁶².

The *Ccs6* locus is syntenic to regions found on human chromosomes 1, 2, 4 and 7, overlapping with several published human IBD loci (rs11209026, rs10486483, rs4722672 and rs4728142) and one lung cancer locus (rs7671167)^{98, 363}. While the specific genetic variants underlying susceptibility for these loci are not known, possible candidate genes include *IRF5*, *IL23r*, *IL12rb* and the *HOX* family of genes. The strong overlap with known IBD genes might be indicative of inflammation as a driving factor in FVB/NJ CA-CRC susceptibility and therefore, as part of ongoing work we are characterizing the role of the *Ccs6* locus in acute DSS-induced inflammation. Interestingly, the IBD genes mentioned above have also been associated

with the development of various cancers³⁶⁴⁻³⁶⁷. The *HOX* genes and *IRF5* are particularly intriguing candidates as they have been associated with increased invasion. Mouse models of invasive carcinoma are rare, and while only a single invasive adenosquamous carcinoma was identified in our FVB/NJ mice, it should not be overlooked. It is possible that at later time points than those used in our model that the frequency of these invasive lesions might increase. Other interesting candidate genes include *Braf*, a known proto-oncogene, *Skap* (*Src kinase associated phosphoprotein 2*), a member of the src family kinases, and numerous genes associated with V(D)J recombination of immunoglobulins and T-cell receptors (www.informatics.jax.org).

The vast number of genes, including plausible candidates within the *Ccs6* locus makes identification of the causative mutation difficult. Therefore, in order to reduce the number of candidate genes to be sequenced we first wish to reduce the *Ccs6* locus. The generation and characterization of congenic and sub-congenic mice enables fine mapping of genetic loci. Given the significant overlap between *Ccs6* and other cancer loci, we will first characterize the response of additional mouse strains to CA-CRC at this early 9-week time point, including SWR/J, BALB/c and NON/ShiLtJ. The identification of additional hyper-susceptible CA-CRC strains may enable the use of pre-existing congenic, recombinant congenic and/or collaborative cross mice to fine map the *Ccs6* locus. In addition, the FVB/NJ genome has been recently sequenced identifying both unique and evolutionary conserved polymorphisms, which may enable identification of common haplotypes in susceptible and resistant mouse strains³⁶⁸. CA-CRC susceptibility loci are difficult to identify in human populations and therefore, the *Ccs6* locus may provide a platform to facilitate the identification of these predisposing genes in humans.

4.8 Acknowledgements

This research was supported by research grants to NB and PG from the Cancer Research Society. PG is a James McGill professor in Biochemistry. LVDK is a recipient of a McGill Integrated Cancer Research Training Program Fellowship and a Canadian Institutes of Health Research Doctoral Award- PA: Digestive Health (SHOPP).

**Chapter 5:
Discussion and Future Directions**

5.1 Discussion

Colitis-associated (CA) colorectal cancer (CRC) represents a CRC subtype arising in patients with the inflammatory bowel diseases (IBD) ulcerative colitis (UC) and Crohn's Disease (CD) ¹²⁵. Genetically, CA-CRCs are linked to common genetic variants in a class of genes referred to as tumor susceptibility genes. The association of CA-CRC with these susceptibility genes is similar to other complex traits such as familial CRC and IBD. While numerous familial CRC (> 30) and IBD (> 163) loci have been mapped in human genome-wide association studies (GWAS), the intersection between the two has yet to be defined (Table 1.1 and Appendix 2). In addition the known CRC and IBD loci only explain a small proportion of total disease genetic risk, suggesting that additional factors, most likely in the form of gene x gene interactions and/or rare variants have yet to be identified. These genetic interactions and rare variants are also suspected to be important in CA-CRC.

Studies of susceptibility to IBD, familial and CA-CRC using knockout, knock-in and transgenic mice have provided additional information concerning important pathways/genes associated with disease initiation and progression ³¹⁰. These reverse genetic studies however, are poor at detecting interacting loci. Forward genetic studies, which exploit differential disease susceptibility in inbred mice, enables mapping of interacting loci through the generation of informative F₂, N₂ or recombinant congenic crosses. Again numerous loci (including interacting loci) have been mapped for both familial CRC and IBD in inbred mice (Figure 1.7). However, only a single CA-CRC locus has been detected, which regulates *Helicobacter hepaticus*-induced CRC susceptibility ³¹¹. This *Helicobacter* model however, is a poor recapitulation of human disease, with mice developing lesions exclusively in the proximal colon. We therefore hypothesized that pre-disposing CA-CRC loci could be mapped using forward genetics and the azoxymethane/dextran sulfate sodium (AOM/DSS) model of CA-CRC, which better approximates human CA-CRC, with tumors developing primarily in the mid and distal colon.

5.1.1 The Response of Inbred Mice to Colitis-Associated Colon Cancer

In *Chapter 4*, we assessed AOM/DSS-induced CA-CRC in 10 inbred strains of mice identifying a bimodal distribution pattern when using tumor multiplicity as a measure of susceptibility. A/J, BALB/cByJ, CBA/J, FVB/NJ and NOD/ShiLtJ were susceptible and 129S1/SvImJ, AKR/J, B6 and C3H/HeJ were resistant supporting the current literature ^{303, 305, 307},

³¹⁷. Only the DBA/2J mice had an obvious gender effect with DBA/2J females behaving as resistant and DBA/2J males behaving as susceptible. DBA/2N male mice were shown by Suzuki et al. to be relatively resistant to AOM/DSS-induced CA-CRC ³⁰⁵. This discrepancy may be attributable to genetic drift between the N and J DBA/2 sub-lines housed in different facilities and/or variations in diet and housing conditions. Genetic drift has been seen before in the B6 sub-strains ³⁶⁹. This study also showed variability with respect to tumor surface area between susceptible and resistant mouse strains, suggesting that different events may regulate initiation and progression of CA-CRC in these mice.

Efficiency mixed model association (EMMA) mapping, a statistical program designed to correct for genetic relatedness and population structure in inbred mice, has recently been applied to map several novel disease susceptibility loci following large scale inbred strain surveys ^{269, 370-372}. We are currently investigating possible CA-CRC loci using this approach, and while we have fewer strains than most other studies, the clear divide between resistance and susceptibility in these mice, may work to our advantage.

5.1.2 Genetic Control of Colitis-Associated CRC in A/J and B6 mice

Both familial and CA-CRC tumors acquire a series of mutations in several key oncogenes and tumor suppressors enabling their transformation from benign adenomas to invasive carcinomas ⁶⁸. However, the timing and frequency of mutations in these CRCs differ (Figure 1.3), which has led to speculation that CA-CRC and familial CRC arise due to different pre-disposing genetic variants.

In *Appendix 1*, we investigate AOM-induced CRC susceptibility (mimics familial CRC) in 16-inbred mouse strains. BALB/cByJ and DBA/2J male mice are resistant to AOM-induced CRC, yet susceptible to AOM/DSS-induced CA-CRC, which support the notion that familial and CA-CRC have different pre-disposing risk factors in some mice. However, strains such as A/J and B6 mice were susceptible and resistant, respectively, to both AOM and AOM/DSS-induced CRC, with AOM-induced CRC susceptibility primarily under the control of a 2.2 Mbp locus (*Ccs3*) on mouse chromosome 3 ²⁶⁸. In *Chapter 2*, testing of BcA71, 72 and 87 RCS mice, who have 87.5% of their genome from B6, but are highly susceptible to AOM-induced CRC due to the presence A/J *Ccs3* susceptibility alleles, demonstrated no involvement of the *Ccs3* locus in AOM/DSS-induced CA-CRC, with all three strains testing as resistant. These results support the hypothesis that familial and CA-CRC have different pre-disposing genetic factors in A/J and B6

mice. Linkage analyses in 148(A/J x B6)F2 mice detected a major CA-CRC susceptibility locus on chromosome 9 (*Ccs4*), which controls tumor multiplicity and tumor surface area in a recessive manner with A/J alleles being associated with susceptibility. We also detected a second locus on chromosome 14 that acts in an additive fashion with *Ccs4*. Strikingly, F2 mice homozygous for A/J alleles at both loci (*Ccs4* and chromosome 14) were as susceptible to CA-CRC as the A/J controls, while mice homozygous for B6 alleles were as resistant to CA-CRC as the B6 controls. At this time, the *Ccs4* locus will be the focus of future studies as its phenotypic effects appears more significant than that of the chromosome 14 locus. Following the identification of the causative *Ccs4* gene, the chromosome 14 locus will be revisited. These are the amongst the first CA-CRC loci identified in mice, and the first loci to regulate susceptibility to tumors in the mid and distal colon. This also highlights a role for genetic interactions in CA-CRC genetic pre-disposition.

5.1.3 Hyper-Susceptibility to CA-CRC in Inbred Mice

Early-onset IBD is associated with a higher risk of CA-CRC ¹⁴³. With IBD rates increasing in the pediatric population, it can be hypothesized that early-onset CA-CRC may be a concern in the near future ¹¹⁹. Characterizing the genes associated with early-onset CA-CRC may aid in identifying individuals at risk of CA-CRC, who may benefit from surgical procedures such as colectomy. In addition, early-onset CA-CRCs arise in the presence of fewer environmental and lifestyle risk factors than late-onset CA-CRC and therefore may involve different genes and pathways compared to late-onset disease.

In this thesis, we identified two different hyper-susceptible CA-CRC strains; AcB60 and FVB/NJ. In *Chapter 3*, AOM/DSS treatment in AcB60 mice (A/J and B6 mixed background) is associated with 100% mortality in these mice 9-weeks post initiation compared to less than 20% of the A/J and B6 parental mice. At earlier times points, 7-weeks post treatment initiation, AcB60 mice developed 35.5 fold more tumors than either A/J or B6. Despite testing numerous other A/J and B6 mixed background strains, this phenotype appears unique to AcB60, suggesting that this phenotype is likely the result of a de novo mutation and not a rearrangement of A/J and B6 alleles. Further characterization showed high levels of colonic inflammation and ulceration in AcB60 mice following both high dose acute and low dose chronic DSS treatments suggesting that inflammation may be a crucial driver of CA-CRC susceptibility in these mice. When conducting our inbred mouse strain survey to AOM/DSS in *Chapter 4*, FVB/NJ mice were

susceptible to CA-CRC, but had higher average tumor burden (assessed using surface area) than several other susceptible strains. Sacrificing of FVB/NJ mice at early time-points in tumor development (8 weeks vs 12.5 weeks) clearly demonstrated FVB/NJ's hyper-susceptibility, with FVB/NJ mice developing 5.5 fold more tumors than the prototypic A/J susceptible mouse mice. This hyper-susceptibility was mapped to a novel locus, *Ccs6*, on mouse chromosome 6 in (FVB/NJ x C3H/HeJ)F2 mice.

5.1.4 The Importance of Forward Genetic Mouse Studies in Dissecting Complex Trait Genetics

As mentioned earlier, interacting loci are hypothesized to play an important role with respect to CRC susceptibility, but are difficult to detect in human GWAS²⁰⁰. This is because these interacting loci have low/to no penetrance in the absence of their interacting partner or are not at high enough frequency in the population to be detected. Forward genetic studies in mice offer an advantage, whereby alleles can be fixed by inbreeding to have minor allele frequencies of 0.5 thus leaving equal opportunity for detection of all alleles and increasing the likelihood of identifying genetic interactions.

Our laboratory has previously mapped a two-locus system regulating susceptibility to AOM-induced CRC involving mouse chromosomes 3 (*Ccs3*) and 9 (*Ccs5*) in A/J and B6 mice²²⁹. To assess the penetrance of these loci in isolation and in combination, we generated *Ccs3* x *Ccs5* congenic mice (homozygous A/J at both the *Ccs3* and *Ccs5* loci on a B6 background, Figure 5.1 A) and tested these mice for AOM-induced (8 weekly injections, 6 mg/kg) CRC along side B6, *Ccs3* (homozygous A/J) and *Ccs5* (homozygous A/J) mice. At 19-weeks post-initiation, the *Ccs3* x *Ccs5* mice had a greater tumor burden than the sum of the burden in mice inheriting *Ccs3* or *Ccs5* homozygous A/J alleles independently, thus showing an interactive effect of the two loci (Figure 5.1 B and C). As expected, the *Ccs5* locus shows no effect on tumor burden in isolation with *Ccs5* homozygous A/J mice behaving identically to the parental B6 mouse strain. This is the first confirmation of this two-locus system in an independent cross. It is unlikely that the gene underlying the *Ccs5* locus phenotype would be detected in classical reverse genetic studies, thus validating the need for more forward genetic mapping studies.

5.2 Future Directions

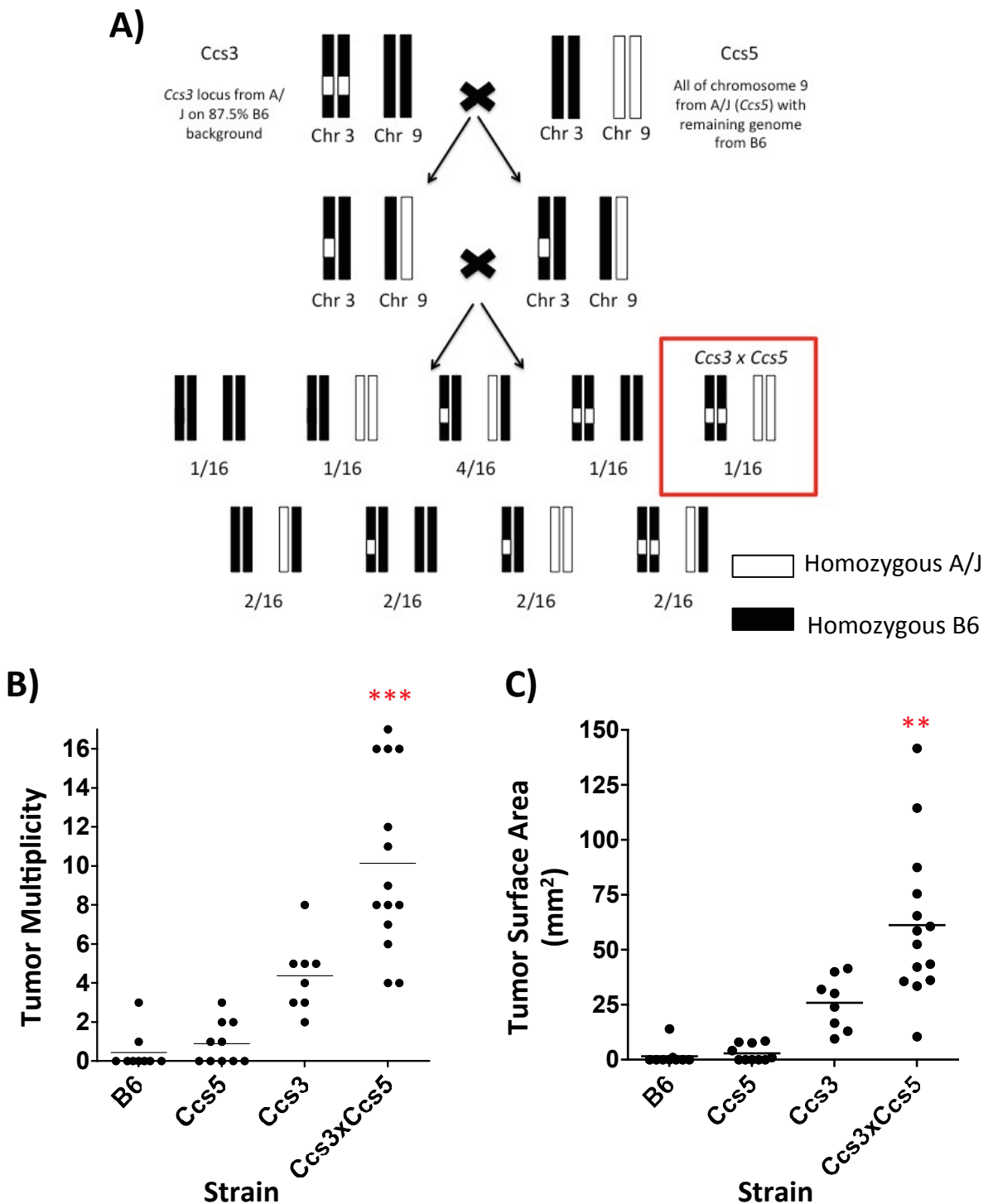


Figure 5.1: Confirmation of the *Ccs3* and *Ccs5* loci in AOM-induced CRC. (A) Breeding scheme for the *Ccs3* x *Ccs5* congenic mice. Briefly, B6, *Ccs3*, *Ccs5* and *Ccs3* x *Ccs5* mice were given 8 weekly injections of 6 mg/kg AOM and sacrificed 19-weeks post-initiation. Mice were subsequently analyzed for the phenotypes of tumor multiplicity (B) and surface area (C). ** $p \leq 0.01$ and *** $p \leq 0.001$ to all other strains tested.

The future directions of this thesis involve defining the specific gene effects underlying increased susceptibility in to CA-CRC in inbred mice, understanding the mechanisms involved in this differential susceptibility, and translating this knowledge into human studies.

5.2.1 Defining CRC Genetic Variants in Our Cohorts of Mice

The long-term goal of this project is to identify the specific polymorphisms or mutations underlying differential CA-CRC susceptibility in each of our three susceptible mouse strains (A/J, AcB60 and FVB/NJ). Progress on these goals will best be made using a sequential approach. First, the genetic interval will be reduced (or identified in the case of AcB60) using commercially available mice and if necessary, novel mouse genetic crosses bred in-house. After reduction of the *Ccs4* and *Ccs6* loci to a manageable number of candidate genes < 30, candidate genes will be sequenced using tail DNA from A/J/B6 (*Ccs4*) and FVB/NJ/C3H/HeJ (*Ccs6*) and other informative mice for polymorphisms or mutations underlying increased susceptibility to CA-CRC. Should multiple variants be identified within our locus of peak linkage, we will prioritize the analysis of genomic variants with respect to a) unique variants not seen in the other RCS mouse strains (for the AcB60 mice); b) obvious loss-of-function mutations (base deletion/missense variant causing premature termination of the polypeptide), c) intronic mutations in donor or acceptor splice sites likely to affect RNA processing/splicing and d) missense mutations affecting residues with cross-species conservation. As AcB60 mice's hyper-susceptibility is thought to be the result of a novel mutation, this will be identified using whole exome sequencing. Finally, validation of causative polymorphisms/mutations will be tested using either knock-in, knock-down, knockout or gene transfer experiments. Each step of this sequential approach is highly dependent on the previous and hence only the reduction of the genetic interval will be discussed in more detail in the subsequent sections.

5.2.1.1 Defining the Genes Underlying Susceptibility to CA-CRC in A/J and B6 mice

The *Ccs4* confidence interval is very large (~41 Mb) and therefore, we will decrease the size of the *Ccs4* interval to reduce the number of candidate genes needing to be systematically analyzed. Our original objective was to reduce this genetic effect in the RCS mouse strains introduced in Chapter 3. However, the 32 strains that we tested did not have perfect genotype-phenotype correlation [data not shown]. While discouraging, this does not rule out the involvement of *Ccs4* locus in our model for several reasons. Firstly, discordant mouse strains

(phenotypically mimick the donor parent) were identified and this was correlated with the inheritance of *Ccs4* donor parental alleles. Secondly, the RCS are a mixed genetic background and re-assortment of the parental alleles may produce new phenotypes or eliminate other phenotypes seen in the parental strains. Additionally, as shown in Chapter 3, the RCS genome has acquired *de novo* mutations that arose during their generation^{344, 346}. Therefore, it is possible that one of these mutations may mask or alter the CA-CRC phenotype. Finally, the RCS have not been genotyped on chromosome 9 between 12.3 Mbp and 31.0 Mbp and therefore it is possible that our gene of interest maps within these uncharacterized regions or that crossover events may exist in the RCS genome that are not captured by the current markers³³¹. Part of our current research is focused on determining the RCS haplotypes of this previously uncharacterized region.

Since reduction of the *Ccs4* locus was not possible in the RCS mice, we sought to generate congenic mice, which have all of their genome from B6, with the exception of all (congenic) or part (sub-congenic) of the *Ccs4* locus, which is from A/J. These mice take several years to generate. Therefore, we first looked into possible commercially available congenic lines. The *Lmr2* locus, which regulates inflammation and wound healing, following cutaneous infection with *Leishmaniasis major* in BALB/cAn Bradley (susceptible) and B6 (resistant mice) overlaps with the *Ccs4* locus and has a series of nine congenic mouse strains available (Figure 5.2 A)³³³. Given the similarity between this phenotype and DSS-induced inflammation, we sought to determine if the *Lmr2* congenic mice were a suitable alternative to study the involvement of the *Ccs4* locus in CA-CRC. Therefore, we tested BALB/cAnn mice, the closest equivalent to BALB/cAn Bradley mice available in Canada, for susceptibility to CA-CRC. Unfortunately, the BALB/cAnn mice did not recapitulate the A/J susceptibility phenotype to CA-CRC, developing fewer tumors than A/J mice (Figure 5.2 B). Therefore, the *Lmr2* congenic mice were deemed insufficient for *Ccs4* fine mapping studies.

Therefore, over the last few years, we have designed our own congenic line of mice in house. The BcA14 RCS mouse line has an A/J *Ccs4* locus and is more susceptible to CA-CRC than its B6 parent and therefore was chosen as the A/J allele donor for the congenic lines (Figure 5.3)³³¹. The congenic mice were generated through 4-6 generations of marker-assisted backcrossing to B6, starting with the BcA14 mouse line (Figure 5.4)³⁷³. The sub-congenic lines are the result of novel crossovers within the *Ccs4* minimal interval that occurred during breeding.

The allelic composition of these mice is denoted in Figure 5.5 A, and we are currently assessing the breakpoint of the BcA14 B6 allele between 12.3 Mbp and 33.4 Mb. Figure 5.5 B demonstrates a hypothetical example of interval reduction in congenic and sub-congenic mouse lines. These lines can now be tested for CA-CRC susceptibility.

5.2.1.2 Mapping the AcB60 CA-CRC Hyper-Susceptibility Gene

In Chapter 3, AcB60 mice were shown to be hyper-susceptible to both DSS-induced colitis and AOM/DSS-induced CA-CRC, which has been attributed to a novel mutation that arose during its generation. We wish to map this effect, but it is unclear if the AcB60 mutation lies on the A/J or B6 background and therefore an informative cross to a third strain (129S1) will be generated. 129S1 has been chosen for several reasons. Firstly, 129S1 is resistant to both colitis and CA-CRC (Chapter 4 and unpublished data from Dr. Philippe Gros' laboratory). Secondly, the MHC complex, whose antigens in mice are denoted as H-2 haplotypes, are important with respect to colitis susceptibility with A/J and B6 mice having different haplotypes (*a* and *b* respectively) (www.jax.org)⁹⁸. 129S1 has the B6 H-2 haplotype, which may help to reduce confounding effects of this locus in our mapping studies. Finally, the 129S1 genome is well characterized, which will facilitate the identification of SNPs for gene mapping (<http://www.sanger.ac.uk/resources/mouse/genomes/>).

To map the AcB60 locus, we will follow a similar approach to that laid out in Chapters 2 and 4, using (AcB60 x 129S1)F1 and F2 mice (Figure 5.6). Segregation analysis in (AcB60 x 129S1)F1 and F2 mice will be used to establish the mode of inheritance (dominant, recessive) and verify the complexity (mono or polygenic) of genetic control to acute DSS-induced colitis (4% DSS, 5 days on, 3 days off). The reasoning behind studying the colitis and not the CA-CRC phenotype is two-fold; 1) the colitis phenotype is easy to induce and easy to measure and 2) the AcB60 mouse is homozygous A/J (susceptible) at both our previously mapped *Ccs4* and chromosome 14 modifier loci. It is not clear, without additional segregation studies, if these two loci are important for the penetrance of the AcB60 mutation. The major gene effect in AcB60 will be mapped using a genome-wide scan of approximately 60 informative (AcB60 x 129S1)F2 male mice using survival and percent ulceration as quantitative traits and SNPs informative for A/J, B6 and the 129S1 parental genomes.

5.2.1.3 Genetic Characterization of the *Ccs6* Locus

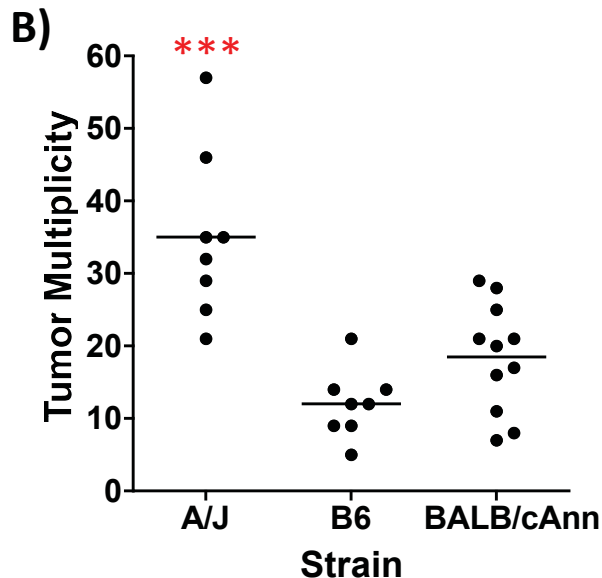
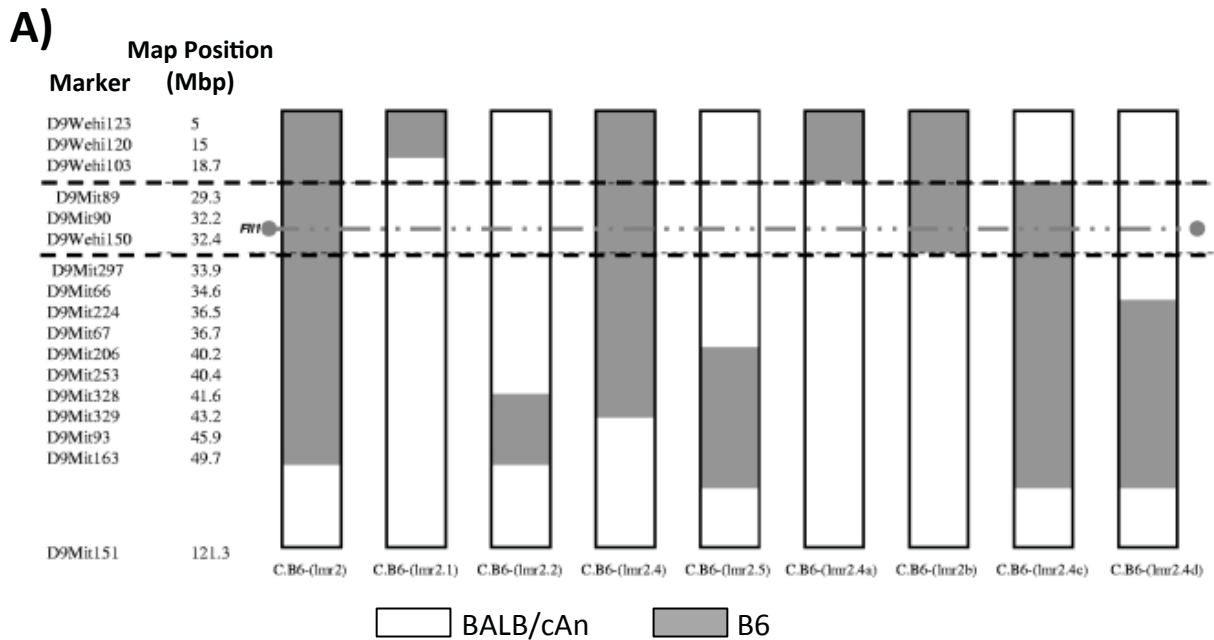


Figure 5.2: Breakpoints in the *Lmr2* congenic mice and phenotyping of BALB/cAnn mice for CA-CRC. (A) Breakpoints on chromosome 9 in the *Lmr2* congenic mice available from Dr. Simon Foote. (B) A/J, B6 and BALB/cAnn were treated using the azoxymethane/dextran sulfate sodium (AOM/DSS) CA-CRC protocol (10 mg/kg AOM followed one week later by 3 cycles 3% DSS, with each cycle 17 days apart). Mice were sacrificed 16 weeks post initiation and analyzed for the phenotype of tumor multiplicity. *** $p \leq 0.001$ to all other strains using a one-way ANOVA and Bonferroni post-correction. Panel A was adapted with permission from Sakhianandeswaren et al. 2010³³³.

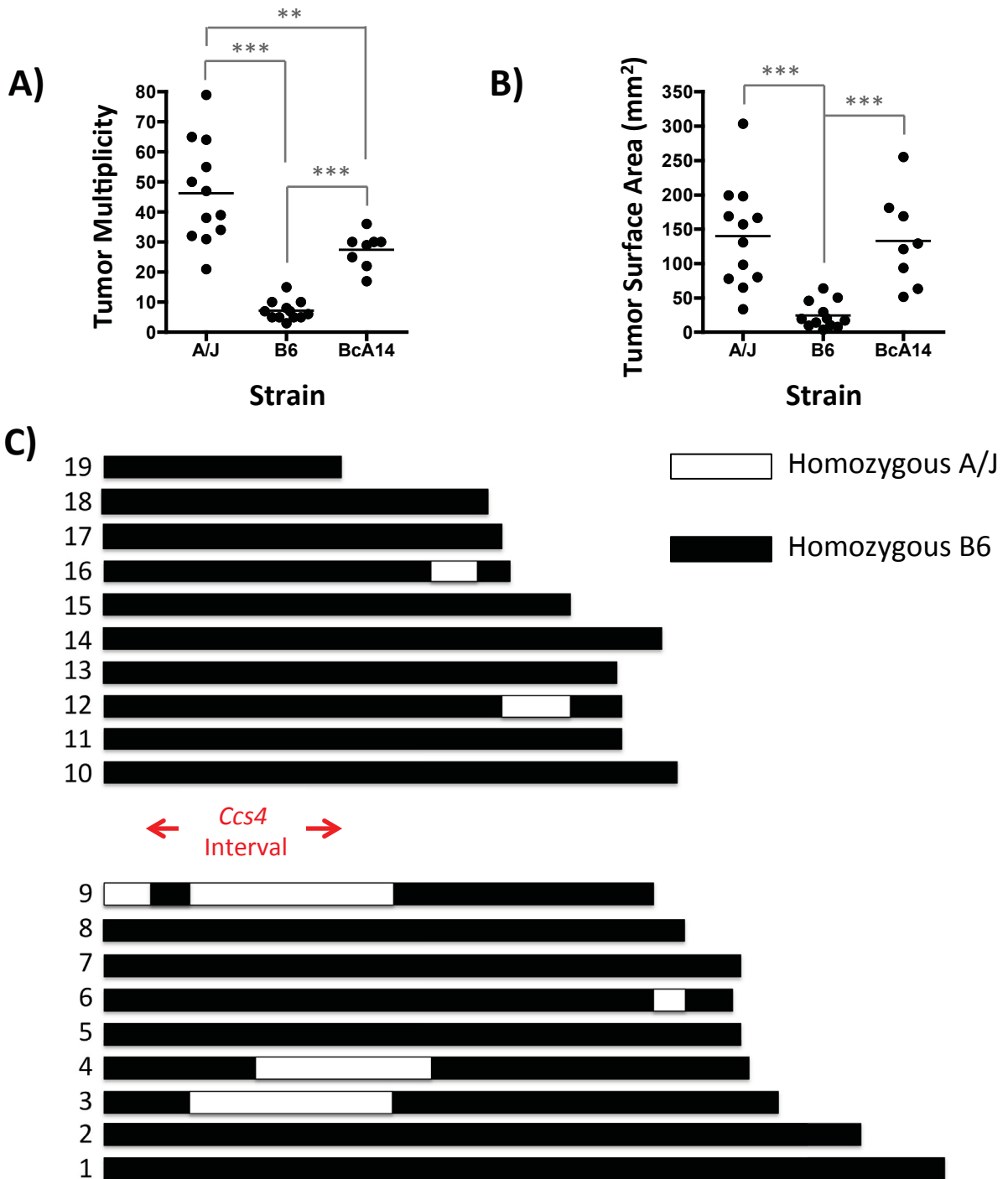


Figure 5.3: CA-CRC susceptibility in the BcA14 recombinant congenic mouse strain. A/J, B6 and BcA14 mice were subjected to the AOM/DSS protocol (7.5 mg/kg AOM; 3 cycles 3% DSS) and sacrificed 14 weeks post-initiation. At sacrifice colons were collected, fixed in formalin and scored for the phenotypes of tumor multiplicity (A) and surface area (B). (C) Haplotype of the BcA14 mouse strain, highlighting the presence of homozygous A/J allele at the *Ccs4* locus.

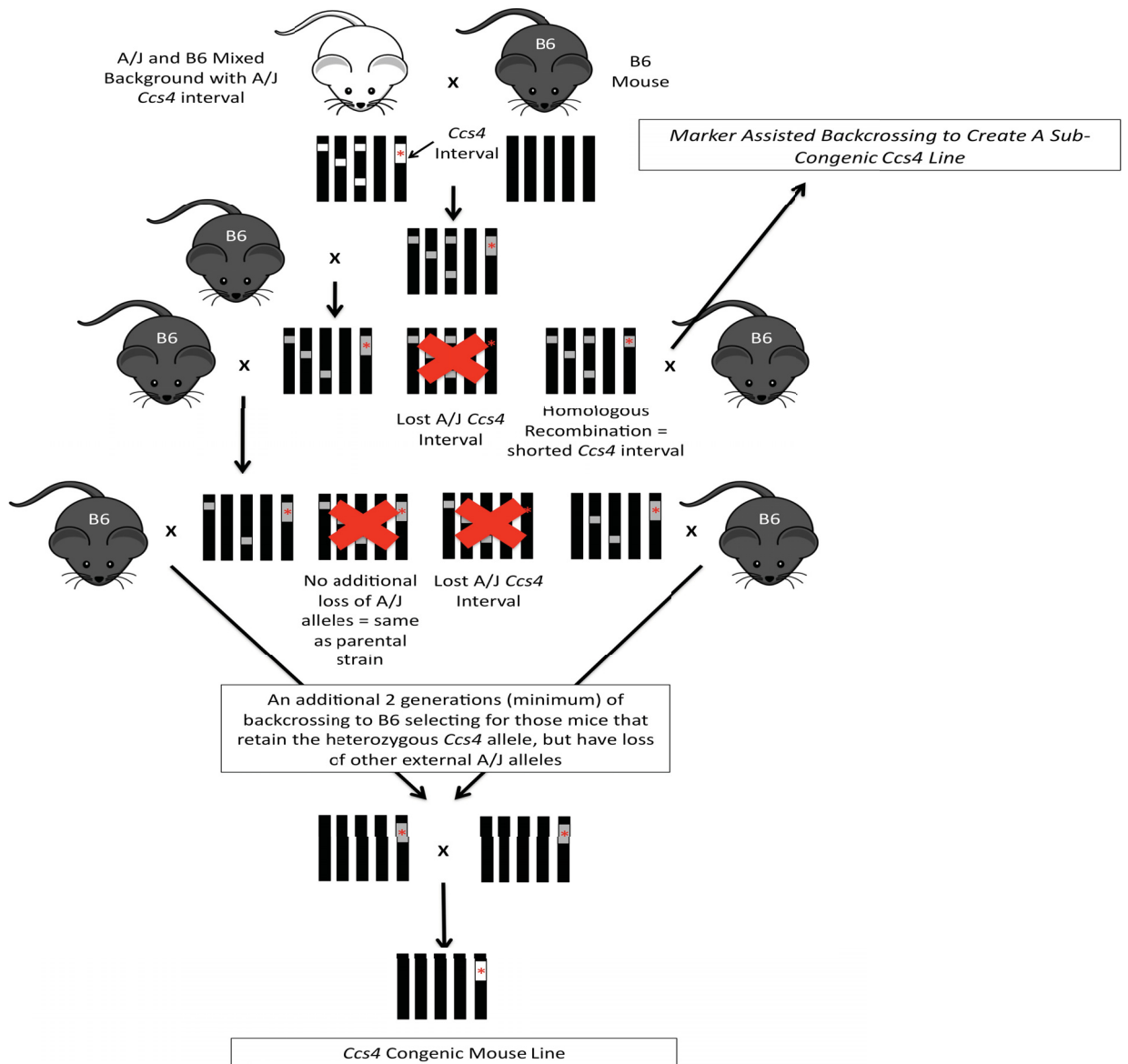


Figure 5.4: Generation of the *Ccs4* congenic and sub-congenic mouse lines. Briefly BcA14 mice were mated with B6 mice generating (BcA14 x B6)F1 mice. These mice were subsequently backcrossed to B6 mice selecting for retention of the heterozygous *Ccs4* locus and loss of non-*Ccs4* A/J alleles. Following the loss of all non-*Ccs4* A/J alleles, heterozygous *Ccs4* congenic mice were bred together to generate the pure *Ccs4* line. The sub-congenic lines were bred in the same fashion, selecting for mice that had undergone a genetic crossover resulting in a smaller *Ccs4* minimal interval.

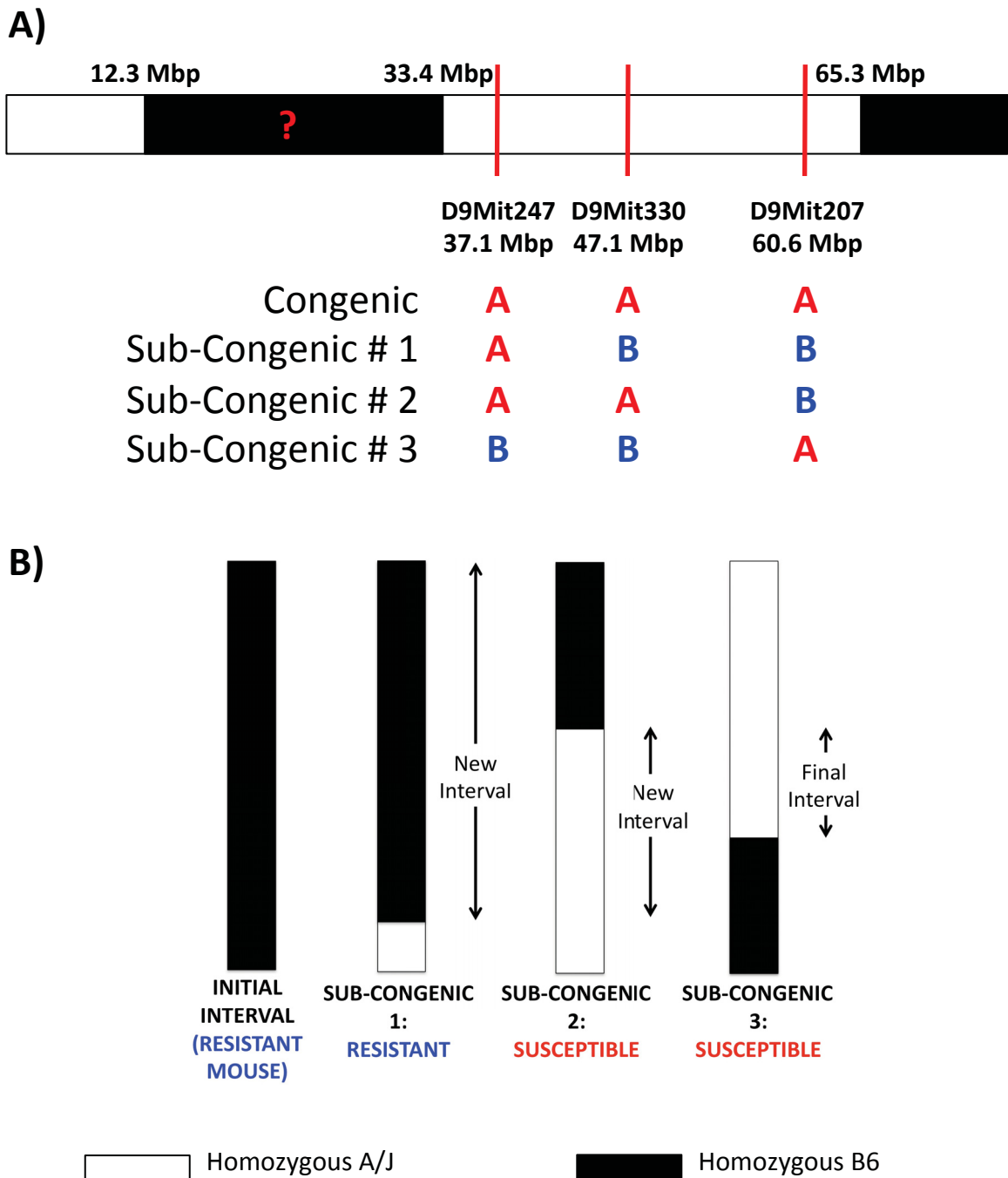


Figure 5.5: Allelic composition of the *Ccs4* congenic and sub-congenic mouse lines. (A) Genotype of the *Ccs4* congenic and subcongenic mice. We are currently refining the breakpoint between 12.3 and 33.4 Mbp in these mice. **(B)** A hypothetical experiment demonstrating the reduction of a genetic interval using congenic and sub-congenic mice.

Similar to the *Ccs4* locus, the *Ccs6* locus is large covering ~39 Mbps encompassing 559 genes making identification of the causative genetic variant difficult without further reduction of the genomic interval. Unlike A/J and B6 mice, which have the RCS, there are no known FVB/NJ congenic or RCS mice. Therefore, while it is possible to generate congenic mice using a similar approach to the *Ccs4* congenic mice using a *Ccs6* homozygous FVB/NJ (FVB/NJ x C3H/HeJ)F2 mouse as the FVB/NJ donor and random backcrossing to C3H/HeJ, this will take 3-4 years to complete. As discussed in Chapter 4, the *Ccs6* locus overlaps with several other cancer loci that have been mapped in diverse inbred strains^{224, 356, 357, 359, 360}. Thus, it is possible that some of these strains may also be hyper-susceptible to CA-CRC. Therefore, our first objective is to test these strains (SWR/J, BALB/cByJ and NON/ShiLtJ) for susceptibility to AOM/DSS-induced CRC at the early 9-week time point. Many of these strains have congenic or RCS mice commercially available, which depending on results of the inbred strain testing, could be used to fine map this locus. If no other susceptible strains are identified in our screen, we will revisit the possibility of generating congenic mice.

5.2.2 Defining Mechanism of CA-CRC Susceptibility

Defining the specific polymorphisms or mutations underlying CA-CRC susceptibility is only part of our project objectives. During our studies of AOM/DSS susceptibility, we identified numerous adenomas in our susceptible mouse strains. These lesions differed between strains with respect to extent of inflammation, degree of vascularization, tumor size, as well as time of tumor onset. Therefore, we hypothesize that these unique properties may reflect differences in mutagenic spectrums in these adenomas as well as the activation of different oncogenic pathways. Therefore, we are interested in identifying possible common and distinct molecular signatures in our various crosses. In addition, we plan to further characterize the role of inflammation in each of our crosses.

5.2.2.1 Molecular Signatures of AOM/DSS Treated Tumors

To better characterize unique molecular signatures associated with CA-CRC susceptibility and resistance, we will use genome-wide methods to establish RNA (transcriptome) and protein (proteome) signatures in AOM/DSS-treated normal and colonic adenoma samples. Briefly, total colon (normal) and tumor RNA and protein (3 pooled samples/group) from each of these crosses will be used for transcriptional profiling (either RNA-

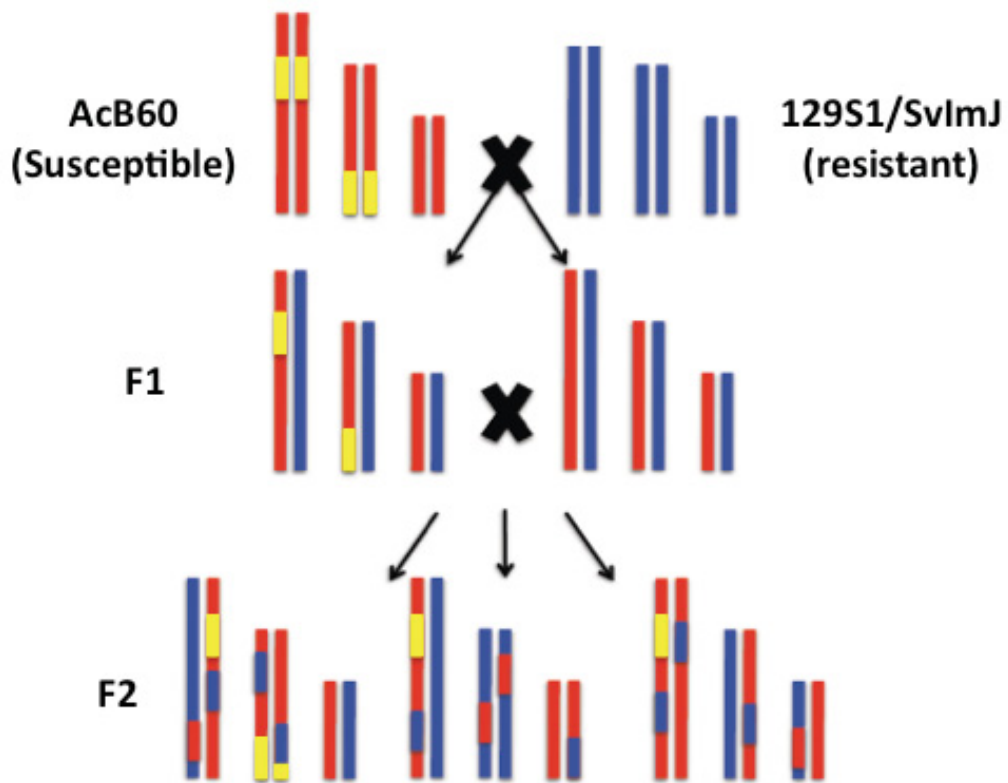


Figure 5.6: Breeding scheme for the (AcB60 x 129S1)F2 mice. AcB60 male mice will be bred to 129S1 female mice generating the F1 population. These mice will subsequently be inter-crossed generating the F2 mice for testing in our acute DSS experiments. Yellow indicates B6 alleles, red are A/J alleles and blue are 129S1 alleles.

seq or Affymetrix oligonucleotides chips) or protein profiling (Kinex KAM-1.2FN antibody microarrays), according to the manufacturer's recommendations. Validation of unique signatures will be performed using qRT-PCR and/or immunoblotting.

As mentioned previously, we are interested in identifying both common CRC susceptibility signatures, in addition to unique signatures related to each of the identified genetic loci. To better understand the *Ccs4* and chromosome 14 loci, we wish to compare both A/J and B6 mice. In addition, following successful testing of the *Ccs4* congenic mice, we wish to analyze the signatures in these mice. This will enable focus on unique *Ccs4*-associated signatures and pathways. In the AcB60 model A/J, B6 and AcB60 normal and tumor samples will be compared. Unfortunately, the 7-week tumors from A/J and B6 are hard to isolate due to their small size and therefore it may be necessary to compare tumors from the 9-week samples. In the FVB/NJ model, we wish to compare FVB/NJ and C3H/HeJ signatures at 4 weeks, 8-weeks and the clinical endpoint with respect to FVB/NJ tumors. FVB/NJ tumors are unique with respect to their early-onset enabling us to study specific genetic signatures associated with both early (4 week) and late (8-week) FVB/NJ tumors. Our histological analysis identified a single invasive adenocarcinoma and therefore we are also interested in study terminal CRC, to determine if increased invasion is a common phenotype and if so if it is associated with unique gene expression signatures. These 4 and 9-week colonic lesions will be obtained by colonic biopsy from the same mouse as the terminal tumor samples, thus reducing mouse-to-mouse specific variations in gene expression. CRC has a long latency period and rarely are tumors detected at onset in humans. Studying these lesions may allow us to determine the earliest genetic alterations associated with disease pathology and potentially aid in identifying novel targets for therapy.

5.2.2.2 Proliferation and Apoptosis Studies in AOM/DSS-Treated Mice

The balance between proliferation and apoptosis is crucial in maintaining tissue homeostasis. In cancer, this balance is disrupted leading to an increased in cell number and the formation of tumors. With respect to the AOM/DSS studies, we wish to determine if tumor formation is driven through increased proliferative ability of cells or decreased apoptosis of existing cells. There are many commercially available assays and protocols designed to address this question in both fresh and fixed tissue. We will address this question first in fixed tissue

using immunohistochemistry and the Phospho-Histone H3 (Ser10) and cleaved Caspase-3 (Asp 175) antibodies from Cell Signalling Technologies. Phospho-Histone H3 is an immunomarker for cells actively undergoing mitosis, whereas Caspase-3 is a key player in the apoptotic cascade.

5.2.2.3 Studying the Role of Inflammation in AOM/DSS-Induced Tumorigenesis

The role of inflammation in CA-CRC is controversial. Large-scale meta-analysis clearly highlights a role for inflammation, showing increased CA-CRC risk associated with more extensive colitis and with increasing duration of colitis^{137, 141, 142}. Yet, as shown by Connelly et al., there are patients with similar disease that differ with respect to CA-CRC development¹⁴⁹. In mice, NOD/ShiLtJ mice are susceptible and 129S1 mice are resistant to both colitis and CA-CRC, suggesting that inflammation could be driving factors in determining CA-CRC susceptibility in these strains^{226, 301}. However, C3H/HeJ mice are highly susceptible to DSS-colitis, yet resistant to CA-CRC. In addition, Arthurs et al. clearly demonstrated similar inflammatory profiles in *Il-10*^{-/-} mice infected with *E. faecalis* and *E. coli*, with only the later being associated with increased CA-CRC,³⁷⁴. Therefore, we are interested in determining the involvement of inflammation in our CA-CRC models.

In Chapter 2, the AOM/DSS studies (10 mg/kg AOM, a single 3% DSS treatments) indicated increased inflammation in B6 colons relative to A/J 3-weeks post-initiation. This led us to hypothesize that inflammation, while important, may not be crucial in driving CA-CRC susceptibility in A/J and B6 mice. However, when we assessed inflammation in A/J and B6 mice in Chapter 3, we saw variable amounts of inflammation between A/J and B6 depending on the DSS-dose, length of DSS treatment and time of sacrifice. This suggests that A/J and B6 mice may vary in their ability to initiate, amplify and clear inflammation at the site of injury. Therefore to obtain a more accurate picture of inflammation in these mice, we propose to treat A/J and B6 mice using the AOM/DSS protocol (10 mg/kg AOM and 3 cycles of 3% DSS) and study inflammation in real time using colonoscopy. The mice will be scoped each week to assess healing and scored according to the protocols described in³⁷⁵. In addition, the *Ccs4* congenic mice will be studied along side A/J and B6 mice using the acute DSS protocol described in Chapter 3, to assess direct involvement of the *Ccs4* locus in colonic inflammation.

AcB60 mice were shown in Chapter 3 to have significantly higher inflammation and ulceration compared to A/J and B6 mice following acute and long-term DSS and AOM/DSS treatment. As part of ongoing work from Chapter 3, we are assessing serum *Il-18* and *KC*

(*Cxcl1*) levels in these acute and long-term DSS-treated mice to obtain quantitative measures of inflammation.

In Chapter 4, we mapped the *Ccs6* locus, which regulates CA-CRC hyper-susceptibility in FVB/NJ and C3H/HeJ mice. To study the involvement of this locus in colonic inflammation, we will generate additional (FVB/NJ x C3H/HeJ)F2 mice selecting for those that carry homozygous FVB/NJ or C3H/HeJ alleles at the *Ccs6* locus (marker D6Mit223). These mice will then be assessed for acute DSS susceptibility using similar methodology to that discussed in Chapter 3.

The tumor microenvironment encompasses the blood vessels, immune cells, signalling molecules and stoma cells surrounding a tumor³⁷⁶. Tumor cells secrete signals, which lead to the recruitment of fibroblasts and inflammatory cells, which in turn secrete various chemokines and cytokines that can influence tumor growth and metastasis. Some of these changes influenced by this cross-talk are reversible whereas others are permanent resulting in the accumulation of mutations within tumor cells. These recruited cells include macrophages, mast cells, cancer-associated fibroblasts (CAF), neutrophils, t-cells and blood cells. Macrophages, for example, can elicit both pro and anti-tumor effects when recruited to the tumor microenvironment, whereas CAFs are associated with the secretion of pro-tumorigenic growth factors. A detailed review of cells in the tumor microenvironment and their influence on tumor growth and metastasis are described in³⁷⁶. Understanding which type of cells infiltrate the tumors in our various models may shed light on mechanisms of tumorigenesis in our model. We will first assess immune cells in the tumor microenvironment. Paraffin-embedded colon samples from treated and untreated mice will be sectioned and stained using commonly available antibodies for macrophages (F4/80+), neutrophils (*Gr-1*+), dendritic cells (*CD11c*) and T-cells (*CD49b*, *CD4*, *CD8*, *Foxb3*) according to the protocols described by Dupaul-Chicoine et al.³³⁶. If significant differences in cell recruitment are noted, transcript profiles of chemokine and cytokines known to attract these cells may be assessed for differences.

5.2.3 Validation of Mouse CA-CRC Susceptibility Loci in Humans

A major goal of our studies is to translate knowledge obtained from the mouse models studied in this thesis to clinical situation of human CRC. The rationale for comparing mouse loci with data from human GWAS is that certain pre-disposing gene effects in a complex trait such as CA-CRC may not meet the stringent genome-wide thresholds of significance established in

human studies (due to genetic heterogeneity, incomplete penetrance in the population sampled), but may nevertheless contribute to disease in certain populations or under certain conditions. In mice, where external variables can be better controlled and the genetic background fixed, these predisposing gene effects may map as strong monogenic or digenic traits that can then be used as guides in understanding human CA-CRC. In addition, as mentioned, previously interacting loci are rare non-validated findings in human CRC GWAS, whereas these are quite common in mouse studies.

Possible associations of the *Ccs4* locus, chromosome 14 modifier locus, *Ccs6* locus and when identified, the AcB60 mutation(s) will be investigated in humans using a) linkage/association studies in the Assessment of Risk for Colorectal Cancer Tumors in Canada (ARCTIC) cohorts of individuals in collaboration with Dr. Thomas Hudson at the Ontario Cancer Research Institute (lead author of many GWAS studies) and b) sequencing of causative genes in human primary CA-CRC tumors, available through the ARCTIC cohort or from collaborating pathologists and clinicians. Due to the strong underlying presence of colonic inflammation in the studied AcB60 model, we also wish assess this mutation in human IBD tissue samples.

The large-scale human ARCTIC project involves 3 separate populations (Ontario, Newfoundland and Seattle, WA) of CRC patients (with tumor tissue available for most samples from Ontario), along with geographical and age-matched controls. A first cohort of 2400 patients and controls has been genotyped for ~600,000 SNPs, and at least 2400 additional cases and controls are available for replication. This is the same cohort that we previously used to validate the *Ccs3/5* loci (unpublished data, ²²⁹). Neither the *Ccs3/Ccs5* loci in humans exceeded the genome-wide significant thresholds necessary to be identified independently of the mouse mapping data, which also highlights the importance of mouse studies as guides for gene identification in humans.

The *Ccs4* and chromosome 14 loci at their current sizes show synteny to human chromosomes 11, 13, 15 and 19 with small components on human chromosomes 3, 6 and 7. This includes a known CRC loci mapped in the ARCTIC cohort to human chromosome 11q23, but further studies are necessary to determine if the *Ccs4* and 11q23 have the same underlying genetic etiologies ³⁷⁷. The 11q23 locus has been linked to differential expression of three genes *colon cancer associated 1 (COLCA1)*, *COLCA2* and *C11orf53* that are in tight linkage

disequilibrium with one another^{190, 378}. *COLCA2* and *C11orf53* have mouse homologues *Gm684* and *1810046K07Rik*, respectively. While the specific gene function of *C11orf53* is unknown, *COLCA2* is broadly expressed in diverse tissues including tumor cells, immune cells and epithelial cells and is associated with increased lymphocyte density in the lamina propria, a phenotype common to CA-CRC¹⁸⁹. We are currently investigating the expression of these genes in A/J, B6, the AcB/BcA RCS and (A/J x B6)F2 mice. Should an association be detected in mice, further mouse studies may aid in refining these loci in humans as currently the three genes are in LD with each other and therefore the specific gene driving CRC susceptibility at this locus is unknown. To assess the *Ccs6* locus mapped in the FVB/NJ/C3H/HeJ cross, the ARCTIC data will be examined for associations mapping in human *Ccs6* syntenic regions on chromosomes 1, 2, 4 and 7, although we will reduce the interval before assessing this.

A second approach will be to determine if human clinical specimens of CRC carry mutations in the gene regulating susceptibility at the loci studied herein. Following the identification of the causal variants underlying susceptibility in the various mouse crosses, the corresponding human genes would be sequenced in primary CRC tumors and germline DNA from cases and controls to search for mutations. In addition to the ARCTIC samples, additional collaborations with pathologists who have access to fresh colon tumors and bio-banked material including DNA samples from colon tumors have been secured. Of particular interest are samples from patients with CA-CRC.

5.3 Conclusions

In this thesis, we utilized the AOM/DSS mouse model to map novel genetic factors regulating susceptibility to CA-CRC in mice. These are the first AOM/DSS-induced CA-CRC loci to be identified to date. In Chapter 2, we explored the role of a two-locus system in CA-CRC. These two-locus systems are rarely identified in human CRC and, due to the low penetrance of each locus in isolation, they are unlikely to be detected in classical knockout, knock-in or transgenic mouse models reiterating the need for forward genetic screens in complex trait genetic studies. In Chapters 3 and 4, we identified two novel CA-CRC hyper-susceptibility phenotypes. As genetic involvement in CA-CRC progression in humans is poorly understood, we hope that these models will lead to the identification of novel prognostic markers of disease progression that can be used for earlier detection and increased survival of patients. In addition,

these CA-CRC models are highly reproducible and easy to manipulate which may assist researchers with respect to CA-CRC therapeutic development. Finally, CA-CRC is usually detected at advanced stages in human patients. We hope to be able to study the early stages of tumor development in these hyper-susceptible mice to gain insight into mechanisms association with tumor initiation *in vivo*.

Original Contributions to Knowledge

- 1) Identification of a novel two-locus system involving mouse chromosome 9 (*Ccs4*) and 14 that regulates susceptibility to azoxymethane-dextran sulfate sodium-induced colitis-associated colon cancer (CA-CRC) in A/J and B6 mice. These are the first CA-CRC loci identified that regulate tumor susceptibility in the distal and mid colon, similar to human CA-CRC, and demonstrate a role for interacting loci in CA-CRC susceptibility.
- 2) Identification of AcB60 mice as a novel model of colitis and CA-CRC hyper-susceptibility. Murine models of early-onset CA-CRC are rare and therefore AcB60 may offer a unique model to study the mechanisms associated with this disease possibly leading to new genetic predictors of risk and treatment options in humans.
- 3) Characterization of 10 inbred mouse strains for susceptibility to AOM/DSS-induced CRC. This is the largest study of its kind and identified a bimodal distribution pattern of susceptibility when using tumor multiplicity as a measure of disease. This knowledge should help facilitate the search for novel genetic associations underlying CA-CRC susceptibility using forward genetic approaches.
- 4) Identification of a novel CA-CRC hyper-susceptibility locus, *Ccs6*, in FVB/NJ mice. This is amongst the first CA-CRC loci identified and may shed light on unique pre-disposing genetic factors in early-onset tumorigenesis.

References:

1. Standring, S., Neil R. Borley, and Henry Gray (2008) *Gray's Anatomy: The Anatomical Basis of Clinical Practice*, Churchill Livingstone/Elsevier, Edinburgh.
2. Cook, M. J. (1965) *The Anatomy of the Laboratory Mouse*, Academic Press, London.
3. Treuting, P. M., and Suzanne M. Dintzis (2012) *Comparative Anatomy and Histology A Mouse and Human Atlas*, Academic, Oxford.
4. Menard, D., Dagenais, P., and Calvert, R. (1994) Morphological changes and cellular proliferation in mouse colon during fetal and postnatal development, *Anat Rec* 238, 349-359.
5. Peterson, L. W., and Artis, D. (2014) Intestinal epithelial cells: regulators of barrier function and immune homeostasis, *Nat Rev Immunol* 14, 141-153.
6. van der Flier, L., Clevers H. (2009) Stem cells, self-renewal, and differentiation in the intestinal epithelium., *Annu Rev Physiol* 71, 241-260.
7. Rao, J.N., and Wang, J.Y. (2010) Intestinal Architecture and Development, In *Regulation of Gastrointestinal Mucosal Growth*, Morgan & Claypool Life Sciences, San Rafael (CA).
8. Barker, N. (2014) Adult intestinal stem cells: critical drivers of epithelial homeostasis and regeneration, *Nat Rev Mol Cell Biol* 15, 19-33.
9. Reya, T., Clevers H. (2005) Wnt signalling in stem cells and cancer., *Nature* 434, 843-850. .
10. Shaker, A., and Rubin, D. C. (2010) Intestinal stem cells and epithelial-mesenchymal interactions in the crypt and stem cell niche, *Translational research : the journal of laboratory and clinical medicine* 156, 180-187.
11. Gerbe, F., Legraverend, C., and Jay, P. (2012) The intestinal epithelium tuft cells: specification and function, *Cell Mol Life Sci* 69, 2907-2917.
12. Bevins, C. L., and Salzman, N. H. (2011) Paneth cells, antimicrobial peptides and maintenance of intestinal homeostasis, *Nat Rev Microbiol* 9, 356-368.
13. Fearon, E. R., Vogelstein B. (1990) A genetic model for colorectal tumorigenesis., *Cell* 61, 759-767.
14. Horner, M., Ries LAG, Krapcho M, Neyman N, Aminou R, Howlader N, Altekruse SF, Feuer EJ, Huang L, Mariotto A, Miller BA, Lewis DR, Eisner MP, Stinchcomb DG, Edwards BK (eds). SEER Cancer Statistics Review, 1975-2006, National Cancer Institute. Bethesda, MD, http://seer.cancer.gov/csr/1975_2006/, based on November 2008 SEER data submission, posted to the SEER web site, 2009.
15. Colon Cancer Canada Statistis (2014) <http://coloncancercanada.ca/>.

16. Major, D., Bryant, H., Delaney, M., Fekete, S., Gentile, L., Harrison, M., Mai, V., Nicholson, E., and Taylor, Y. (2013) Colorectal cancer screening in Canada: results from the first round of screening for five provincial programs, *Curr Oncol* 20, 252-257.
17. World Health Organization. (2008) *World Cancer Report 2008*, International Agency for Research on Cancer, Lyon.
18. World Health Organization. (2012) GLOBOCAN 2012: Estimated Cancer Incidence, Mortality and Prevalence Worldwide in 2012, International Agency for Research on Cancer. <http://globocan.iarc.fr>.
19. Umar, A., and Greenwald, P. (2009) Alarming colorectal cancer incidence trends: a case for early detection and prevention, *Cancer Epidemiol Biomarkers Prev* 18, 1672-1673.
20. Ahnen, D. J., Wade, S. W., Jones, W. F., Sifri, R., Mendoza Silveiras, J., Greenmyer, J., Guiffre, S., Axilbund, J., Spiegel, A., and You, Y. N. (2014) The increasing incidence of young-onset colorectal cancer: a call to action, *Mayo Clin Proc* 89, 216-224.
21. Davis, D. M., Marcet, J. E., Frattini, J. C., Prather, A. D., Mateka, J. J., and Nfonsam, V. N. (2011) Is it time to lower the recommended screening age for colorectal cancer?, *J Am Coll Surg* 213, 352-361.
22. Siegel, R., Desantis, C., and Jemal, A. (2014) Colorectal cancer statistics, 2014, *CA Cancer J Clin* 64, 104-117.
23. Dozois, E. J., Boardman, L. A., Suwanthanma, W., Limburg, P. J., Cima, R. R., Bakken, J. L., Vierkant, R. A., Aakre, J. A., and Larson, D. W. (2008) Young-onset colorectal cancer in patients with no known genetic predisposition: can we increase early recognition and improve outcome?, *Medicine (Baltimore)* 87, 259-263.
24. Taylor, M. C., Pounder, D., Ali-Ridha, N. H., Bodurtha, A., and MacMullin, E. C. (1988) Prognostic factors in colorectal carcinoma of young adults, *Can J Surg* 31, 150-153.
25. Marble, K., Banerjee, S., and Greenwald, L. (1992) Colorectal carcinoma in young patients, *J Surg Oncol* 51, 179-182.
26. Cusack, J. C., Giacco, G. G., Cleary, K., Davidson, B. S., Izzo, F., Skibber, J., Yen, J., and Curley, S. A. (1996) Survival factors in 186 patients younger than 40 years old with colorectal adenocarcinoma, *J Am Coll Surg* 183, 105-112.
27. Li, Q., Cai, G., Li, D., Wang, Y., Zhuo, C., and Cai, S. (2014) Better long-term survival in young patients with non-metastatic colorectal cancer after surgery, an analysis of 69,835 patients in SEER database, *PLoS One* 9, e93756.
28. Li, M., Li, J. Y., Zhao, A. L., and Gu, J. (2011) Do young patients with colorectal cancer have a poorer prognosis than old patients?, *J Surg Res* 167, 231-236.

29. Schellerer, V. S., Merkel, S., Schumann, S. C., Schlabrakowski, A., Fortsch, T., Schildberg, C., Hohenberger, W., and Croner, R. S. (2012) Despite aggressive histopathology survival is not impaired in young patients with colorectal cancer : CRC in patients under 50 years of age, *Int J Colorectal Dis* 27, 71-79.
30. Lin, O. S. (2009) Acquired risk factors for colorectal cancer, *Methods Mol Biol* 472, 361-372.
31. Lichtenstein, P., Holm, N. V., Verkasalo, P. K., Iliadou, A., Kaprio, J., Koskenvuo, M., et al. (2000) Environmental and heritable factors in the causation of cancer--analyses of cohorts of twins from Sweden, Denmark, and Finland, *N Engl J Med* 343, 78-85.
32. Chung, C. C., Magalhaes, W. C., Gonzalez-Bosquet, J., and Chanock, S. J. (2010) Genome-wide association studies in cancer--current and future directions, *Carcinogenesis* 31, 111-120.
33. Houlston, R. S., and Peto, J. (2004) The search for low-penetrance cancer susceptibility alleles, *Oncogene* 23, 6471-6476.
34. Gylfe, A. E., Katainen, R., Kondelin, J., Tanskanen, T., Cajuso, T., Hanninen, U., et al. (2013) Eleven candidate susceptibility genes for common familial colorectal cancer, *PLoS Genet* 9, e1003876.
35. de la Chapelle, A. (2004) Genetic predisposition to colorectal cancer., *Nat Rev Cancer* 4, 769-780.
36. Galiatsatos, P., and Foulkes, W. D. (2006) Familial adenomatous polyposis, *Am J Gastroenterol* 101, 385-398.
37. Beroud, C., and Soussi, T. (1996) APC gene: database of germline and somatic mutations in human tumors and cell lines, *Nucleic Acids Res* 24, 121-124.
38. Torrezan, G. T., da Silva, F. C., Santos, E. M., Krepischi, A. C., Achatz, M. I., Aguiar, S., et al. (2013) Mutational spectrum of the APC and MUTYH genes and genotype-phenotype correlations in Brazilian FAP, AFAP, and MAP patients, *Orphanet journal of rare diseases* 8, 54.
39. Knudsen, A. L., Bisgaard, M. L., and Bulow, S. (2003) Attenuated familial adenomatous polyposis (AFAP). A review of the literature, *Fam Cancer* 2, 43-55.
40. Cheadle, J. P., and Sampson, J. R. (2007) MUTYH-associated polyposis--from defect in base excision repair to clinical genetic testing, *DNA Repair (Amst)* 6, 274-279.
41. Beggs, A. D., Latchford, A. R., Vasen, H. F., Moslein, G., Alonso, A., Aretz, S., et al. (2010) Peutz-Jeghers syndrome: a systematic review and recommendations for management, *Gut* 59, 975-986.
42. Calva, D., and Howe, J. R. (2008) Hamartomatous polyposis syndromes, *Surg Clin North Am* 88, 779-817, vii.

43. Kravochuck, S. E., Kalady, M. F., Burke, C. A., Heald, B., and Church, J. M. (2014) Defining HNPCC and Lynch syndrome: what's in a name?, *Gut*.
44. Lynch, H. T., Lynch, P. M., Lanspa, S. J., Snyder, C. L., Lynch, J. F., and Boland, C. R. (2009) Review of the Lynch syndrome: history, molecular genetics, screening, differential diagnosis, and medicolegal ramifications, *Clin Genet* 76, 1-18.
45. Jasperson, K., Tuohy T.M., Neklason D.W., Burt R.W. (2010) Hereditary and familial colon cancer., *Gastroenterology* 138, 2044-2058.
46. Boland, C., Goel A. (2010) Microsatellite instability in colorectal cancer., *Gastroenterology* 38, 2073-2087.e2073.
47. Barrow, E., Robinson, L., Alduaij, W., Shenton, A., Clancy, T., Laloo, F. et al. (2009) Cumulative lifetime incidence of extracolonic cancers in Lynch syndrome: a report of 121 families with proven mutations., *Cin Genet* 75, 141-149.
48. Dominguez-Valentin, M., Therkildsen, C., Da Silva, S., and Nilbert, M. (2015) Familial colorectal cancer type X: genetic profiles and phenotypic features, *Mod Pathol.* 28, 30-36.
49. Lindor, N. M. (2009) Familial colorectal cancer type X: the other half of hereditary nonpolyposis colon cancer syndrome, *Surg Oncol Clin N Am* 18, 637-645.
50. Cleary, S. P., Zhang, W., Di Nicola, N., Aronson, M., Aube, J., Steinman, A. et al. (2003) Heterozygosity for the BLM(Ash) mutation and cancer risk, *Cancer Res* 63, 1769-1771.
51. Guda, K., Moinova, H., He, J., Jamison, O., Ravi, L., Natale, L., et al. (2009) Inactivating germ-line and somatic mutations in polypeptide N-acetylgalactosaminyltransferase 12 in human colon cancers, *Proc Natl Acad Sci U S A* 106, 12921-12925.
52. Thomas, D. B., and Karagas, M. R. (1987) Cancer in first and second generation Americans, *Cancer Res* 47, 5771-5776.
53. McMichael, A. J., McCall, M. G., Hartshorne, J. M., and Woodings, T. L. (1980) Patterns of gastro-intestinal cancer in European migrants to Australia: the role of dietary change, *Int J Cancer* 25, 431-437.
54. Howlader, N., Noone, A.M., Krapcho, M., Garshell, J., Miller, D., Altekruse, S.F. et al. SEER Cancer Statistics Review, 1975-2011, National Cancer Institute. Bethesda, MD, http://seer.cancer.gov/csr/1975_2011/.
55. Gorbunova, V., Seluanov, A., Mao, Z., and Hine, C. (2007) Changes in DNA repair during aging, *Nucleic Acids Res* 35, 7466-7474.
56. Ben, Q., Sun, Y., Chai, R., Qian, A., Xu, B., and Yuan, Y. (2014) Dietary fiber intake reduces risk for colorectal adenoma: a meta-analysis, *Gastroenterology* 146, 689-699 e686.

57. Birt, D. F., and Phillips, G. J. (2014) Diet, genes, and microbes: complexities of colon cancer prevention, *Toxicol Pathol* 42, 182-188.
58. Chan, A., Giovannucci, E.L. (2010) Primary prevention of colorectal cancer, *Gastroenterology* 138, 2029-2043.e2010.
59. Harriss, D., Atkinson, G., George, K., Cable, N.T., Reilly, T., Haboubi, N. et al. (2009) Lifestyle factors and colorectal cancer risk: systematic review and meta-analysis of associations with body mass index., *Colorectal Dis.* 11, 547-563.
60. Ogunleye, A., Ogston, S.A, Morris, A.D., Evans, J.M. (2009) A cohort study of the risk of cancer associated with type 2 diabetes, *Br J Cancer.* 101, 1199-1201.
61. Park, S. Y., Kim, J. S., Seo, Y. R., and Sung, M. K. (2012) Effects of diet-induced obesity on colitis-associated colon tumor formation in A/J mice, *International journal of obesity* 36, 273-280.
62. Botteri, E., Iodice, S., Bagnardi, V., Raimondi, S., Lowenfels, A. B., and Maisonneuve, P. (2008) Smoking and colorectal cancer: a meta-analysis, *JAMA* 300, 2765-2778.
63. Liang, P., Chen, T.Y., Giovannucci, E. (2009) Cigarette smoking and colorectal cancer incidence and mortality: systematic review and meta-analysis., *Int J Cancer.* 124, 2046-2015.
64. Akin, H., and Tozun, N. (2014) Diet, microbiota, and colorectal cancer, *Journal of clinical gastroenterology* 48 Suppl 1, S67-69.
65. Kostic, A. D., Gevers, D., Pedomallu, C. S., Michaud, M., Duke, F., Earl, A. M. et al. (2012) Genomic analysis identifies association of Fusobacterium with colorectal carcinoma, *Genome Res* 22, 292-298.
66. Vipperla, K, Ou, J, Wahl, E, Ruder, E and O'Keefe, S. (2014) A 14-day in-house dietary modification of a 'Western' diet to an 'African' diet changes the microbiota, its metabolome, and biomarkers of colon cancer risk FASEB 28:825.
67. Jobin, C. (2014) GPR109a: the missing link between microbiome and good health?, *Immunity* 40, 8-10.
68. Itzkowitz, S. H., Yio X. (2004) Inflammation and Cancer: IV. Colorectal cancer in inflammatory bowel disease: the role of inflammation., *Am J Physiol Gastrointest. Liver Physiol* 287, G7-17.
69. Kinzler, K., Vogelstein B. (1996) Lessons from hereditary colorectal cancers., *Cell* 87, 159-170.
70. Crohn's and Colitis Foundation of Canada (2012) The Impact of Inflammatory Bowel Disease in Canada: 2012 Final Report and Recommendations. <http://www.crohnsandcolitis.ca>.

71. Kozuch, P. L., and Hanauer, S. B. (2008) Treatment of inflammatory bowel disease: a review of medical therapy, *World J Gastroenterol* 14, 354-377.
72. Westbrook, A., Szakmary, A., Schiestl, R.H. (2010) Mechanisms of intestinal inflammation and development of associated cancers: Lessons learned from mouse models., *Mutat Res* 705, 40-59.
73. Guindi, M., and Riddell, R. H. (2004) Indeterminate colitis, *J Clin Pathol* 57, 1233-1244.
74. Carvalho, R. S., Abadom, V., Dilworth, H. P., Thompson, R., Oliva-Hemker, M., and Cuffari, C. (2006) Indeterminate colitis: a significant subgroup of pediatric IBD, *Inflamm Bowel Dis* 12, 258-262.
75. Heyman, M. B., Kirschner, B. S., Gold, B. D., Ferry, G., Baldassano, R., Cohen, S. A., et al. (2005) Children with early-onset inflammatory bowel disease (IBD): analysis of a pediatric IBD consortium registry, *J Pediatr* 146, 35-40.
76. Evans, P. E., and Pardi, D. S. (2007) Extraintestinal manifestations of inflammatory bowel disease: focus on the musculoskeletal, dermatologic, and ocular manifestations, *MedGenMed* 9, 55.
77. Conrad, K., Roggenbuck, D., and Laass, M. W. (2014) Diagnosis and classification of ulcerative colitis, *Autoimmun Rev* 13, 463-466.
78. Chang, H. H., and Chiang, B. L. (2014) The diagnosis and classification of autoimmune coagulopathy: An updated review, *Autoimmun Rev* 13, 587-590.
79. Geboes, K., and Dalle, I. (2002) Influence of treatment on morphological features of mucosal inflammation, *Gut* 50 Suppl 3, III37-42.
80. Sung, M. K., and Park, M. Y. (2013) Nutritional modulators of ulcerative colitis: clinical efficacies and mechanistic view, *World J Gastroenterol* 19, 994-1004.
81. Brown, A. C., Rampertab, S. D., and Mullin, G. E. (2011) Existing dietary guidelines for Crohn's disease and ulcerative colitis, *Expert Rev Gastroenterol Hepatol* 5, 411-425.
82. Lewis, R. T., and Maron, D. J. (2010) Efficacy and complications of surgery for Crohn's disease, *Gastroenterol Hepatol (N Y)* 6, 587-596.
83. Ahmed, T., Rieder, F., Fiocchi, C., and Achkar, J. P. (2011) Pathogenesis of postoperative recurrence in Crohn's disease, *Gut* 60, 553-562.
84. Molodecky, N. A., Soon, I. S., Rabi, D. M., Ghali, W. A., Ferris, M., Chernoff, G., et al. (2012) Increasing incidence and prevalence of the inflammatory bowel diseases with time, based on systematic review, *Gastroenterology* 142, 46-54.
85. Burisch, J., and Munkholm, P. (2013) Inflammatory bowel disease epidemiology, *Curr Opin Gastroenterol* 29, 357-362.

86. Cosnes, J., Gower-Rousseau, C., Seksik, P., and Cortot, A. (2011) Epidemiology and natural history of inflammatory bowel diseases, *Gastroenterology* 140, 1785-1794.
87. Congilosi, S. M., Rosendale, D. E., and Herman, D. L. (1992) Crohn's disease--a rare disorder in American Indians, *West J Med* 157, 682.
88. Lynch, H. T., Brand, R. E., and Locker, G. Y. (2004) Inflammatory bowel disease in Ashkenazi Jews: implications for familial colorectal cancer, *Fam Cancer* 3, 229-232.
89. Wang, Y. R., Loftus, E. V., Jr., Cangemi, J. R., and Picco, M. F. (2013) Racial/Ethnic and regional differences in the prevalence of inflammatory bowel disease in the United States, *Digestion* 88, 20-25.
90. Basu, D., Lopez, I., Kulkarni, A., and Sellin, J. H. (2005) Impact of race and ethnicity on inflammatory bowel disease, *Am J Gastroenterol* 100, 2254-2261.
91. Schultz, M., Tonkonogy, S.L., Sellon, R.K., Veltkamp, C., Godfrey, V.L., Kwon J., et al. (1999) IL-2-deficient mice raised under germfree conditions develop delayed mild focal intestinal inflammation., *Am J Physiol.* 276, G1461-1472.
92. Sellon, R., Tonkonogy, S., Schultz, M., Dieleman, L.A., Grenther, W., Balish, E., et al. (1998) Resident enteric bacteria are necessary for development of spontaneous colitis and immune system activation in interleukin-10-deficient mice., *Infect Immun.* 66, 5224-5231.
93. Jess, T., Riis, L., Jespersgaard, C., Hougs, L., Andersen, P. S., Orholm, M. K., et al. (2005) Disease concordance, zygosity, and NOD2/CARD15 status: follow-up of a population-based cohort of Danish twins with inflammatory bowel disease, *Am J Gastroenterol* 100, 2486-2492.
94. Orholm, M., Binder, V., Sorensen, T. I., Rasmussen, L. P., and Kyvik, K. O. (2000) Concordance of inflammatory bowel disease among Danish twins. Results of a nationwide study, *Scand J Gastroenterol* 35, 1075-1081.
95. Halfvarson, J., Bodin, L., Tysk, C., Lindberg, E., and Jarnerot, G. (2003) Inflammatory bowel disease in a Swedish twin cohort: a long-term follow-up of concordance and clinical characteristics, *Gastroenterology* 124, 1767-1773.
96. Thompson, N. P., Driscoll, R., Pounder, R. E., and Wakefield, A. J. (1996) Genetics versus environment in inflammatory bowel disease: results of a British twin study, *BMJ* 312, 95-96.
97. Halme, L., Paavola-Sakki, P., Turunen, U., Lappalainen, M., Farkkila, M., and Kontula, K. (2006) Family and twin studies in inflammatory bowel disease, *World J Gastroenterol* 12, 3668-3672.
98. Jostins, L., Ripke, S., Weersma, R. K., Duerr, R. H., McGovern, D. P., Hui, K. Y., et al. (2012) Host-microbe interactions have shaped the genetic architecture of inflammatory bowel disease, *Nature* 491, 119-124.

99. Shim, J. O., Hwang, S., Yang, H. R., Moon, J. S., Chang, J. Y., Ko, J. S., et al. (2013) Interleukin-10 receptor mutations in children with neonatal-onset Crohn's disease and intractable ulcerating enterocolitis, *Eur J Gastroenterol Hepatol* 25, 1235-1240.
100. Somasundaram, R., Deuring, J. J., van der Woude, C. J., Peppelenbosch, M. P., and Fuhler, G. M. (2012) Linking risk conferring mutations in NCF4 to functional consequences in Crohn's disease, *Gut* 61, 1097; author reply 1097-1098.
101. Zeissig, Y., Petersen, B. S., Milutinovic, S., Bosse, E., Mayr, G., Peuker, K., et al. (2014) XIAP variants in male Crohn's disease, *Gut*.
102. Morgan, X. C., Tickle, T. L., Sokol, H., Gevers, D., Devaney, K. L., Ward, D. V., et al. (2012) Dysfunction of the intestinal microbiome in inflammatory bowel disease and treatment, *Genome Biol* 13, R79.
103. Ananthakrishnan, A. N., Nguyen, D. D., Sauk, J., Yajnik, V., and Xavier, R. J. (2014) Genetic polymorphisms in metabolizing enzymes modifying the association between smoking and inflammatory bowel diseases, *Inflamm Bowel Dis* 20, 783-789.
104. Loftus Jr, Edward V. "Epidemiology of inflammatory bowel disease." *GI Epidemiology: Diseases and Clinical Methodology* (2013): 273.
105. Molodecky, N. A., and Kaplan, G. G. (2010) Environmental risk factors for inflammatory bowel disease, *Gastroenterol Hepatol (N Y)* 6, 339-346.
106. Ballegaard, M., Bjergstrom, A., Brondum, S., Hylander, E., Jensen, L., and Ladefoged, K. (1997) Self-reported food intolerance in chronic inflammatory bowel disease, *Scand J Gastroenterol* 32, 569-571.
107. Cohen, A. B., Lee, D., Long, M. D., Kappelman, M. D., Martin, C. F., Sandler, R. S., and Lewis, J. D. (2013) Dietary patterns and self-reported associations of diet with symptoms of inflammatory bowel disease, *Dig Dis Sci* 58, 1322-1328.
108. Rajendran, N., and Kumar, D. (2010) Role of diet in the management of inflammatory bowel disease, *World J Gastroenterol* 16, 1442-1448.
109. Chapman-Kiddell, C. A., Davies, P. S., Gillen, L., and Radford-Smith, G. L. (2010) Role of diet in the development of inflammatory bowel disease, *Inflamm Bowel Dis* 16, 137-151.
110. Qin, J., Li, R., Raes, J., Arumugam, M., Burgdorf, K. S., Manichanh, C., et al. (2010) A human gut microbial gene catalogue established by metagenomic sequencing, *Nature* 464, 59-65.
111. Tedelind, S., Westberg, F., Kjerrulf, M., and Vidal, A. (2007) Anti-inflammatory properties of the short-chain fatty acids acetate and propionate: a study with relevance to inflammatory bowel disease, *World J Gastroenterol* 13, 2826-2832.

112. Wu, G. D., Chen, J., Hoffmann, C., Bittinger, K., Chen, Y. Y., Keilbaugh, S. A., et al. (2011) Linking long-term dietary patterns with gut microbial enterotypes, *Science* 334, 105-108.
113. Hold, G. L., Smith, M., Grange, C., Watt, E. R., El-Omar, E. M., and Mukhopadhyaya, I. (2014) Role of the gut microbiota in inflammatory bowel disease pathogenesis: what have we learnt in the past 10 years?, *World J Gastroenterol* 20, 1192-1210.
114. Mukhopadhyaya, I., Hansen, R., El-Omar, E. M., and Hold, G. L. (2012) IBD-what role do Proteobacteria play?, *Nat Rev Gastroenterol Hepatol* 9, 219-230.
115. Geremia, A., Biancheri, P., Allan, P., Corazza, G. R., and Di Sabatino, A. (2014) Innate and adaptive immunity in inflammatory bowel disease, *Autoimmun Rev* 13, 3-10.
116. Brand, S. (2009) Crohn's disease: Th1, Th17 or both? The change of a paradigm: new immunological and genetic insights implicate Th17 cells in the pathogenesis of Crohn's disease, *Gut* 58, 1152-1167.
117. Boden, E. K., and Snapper, S. B. (2008) Regulatory T cells in inflammatory bowel disease, *Curr Opin Gastroenterol* 24, 733-741.
118. Benchimol, E. I., Fortinsky, K. J., Gozdyra, P., Van den Heuvel, M., Van Limbergen, J., and Griffiths, A. M. (2011) Epidemiology of pediatric inflammatory bowel disease: a systematic review of international trends, *Inflamm Bowel Dis* 17, 423-439.
119. Benchimol, E., Guttman, A., Griffiths, A.M., Rabeneck, L., Mack, D.R., Brill, H., et al. (2009) Increasing incidence of paediatric inflammatory bowel disease in Ontario, Canada: evidence from health administrative data., *Gut* 58, 1490-1497.
120. Ruel, J., Ruane, D., Mehandru, S., Gower-Rousseau, C., and Colombel, J. F. (2014) IBD across the age spectrum-is it the same disease?, *Nat Rev Gastroenterol Hepatol* 11, 88-98.
121. de Ridder, L., Weersma, R. K., Dijkstra, G., van der Steege, G., Benninga, M. A., Nolte, I. M., et al. (2007) Genetic susceptibility has a more important role in pediatric-onset Crohn's disease than in adult-onset Crohn's disease, *Inflamm Bowel Dis* 13, 1083-1092.
122. Kugathasan, S., Baldassano, R. N., Bradfield, J. P., Sleiman, P. M., Imielinski, M., Guthery, S. L., et al. (2008) Loci on 20q13 and 21q22 are associated with pediatric-onset inflammatory bowel disease, *Nat Genet* 40, 1211-1215.
123. Imielinski, M., Baldassano, R.N., Griffiths, A., Russell, R.K., Annese, V., Dubinsky, M., et al. (2009) Common variants at five new loci associated with early-onset inflammatory bowel disease. , *Nat Genet* 41, 1335-1340.
124. Kotlarz, D., Beier, R., Murugan, D., Diestelhorst, J., Jensen, O., Boztug, K., et al. (2012) Loss of interleukin-10 signaling and infantile inflammatory bowel disease: implications for diagnosis and therapy, *Gastroenterology* 143, 347-355.

125. Mattar, M. C., Lough, D., Pishvaian, M. J., and Charabaty, A. (2011) Current management of inflammatory bowel disease and colorectal cancer, *Gastrointest Cancer Res* 4, 53-61.
126. Neumann, H., Vieth, M., Langner, C., Neurath, M. F., and Mudter, J. (2011) Cancer risk in IBD: how to diagnose and how to manage DALM and ALM, *World J Gastroenterol* 17, 3184-3191.
127. Bernstein, C. N., Shanahan, F., and Weinstein, W. M. (1994) Are we telling patients the truth about surveillance colonoscopy in ulcerative colitis?, *Lancet* 343, 71-74.
128. Mescoli, C., Frego, M., and Rugge, M. (2011) Pathology of dysplasia and cancer in inflammatory bowel disease, *Ann Ital Chir* 82, 11-18.
129. Bressenot, A., Cahn, V., Danese, S., and Peyrin-Biroulet, L. (2014) Microscopic features of colorectal neoplasia in inflammatory bowel diseases, *World J Gastroenterol* 20, 3164-3172.
130. Geboes, K. (2006) Review article: what are the important endoscopic lesions for detection of dysplasia in inflammatory bowel disease?, *Aliment Pharmacol Ther* 24 Suppl 3, 50-55.
131. Neumann, H., Neurath, M. F., and Mudter, J. (2011) New endoscopic approaches in IBD, *World J Gastroenterol* 17, 63-68.
132. Choi, P. M., and Zelig, M. P. (1994) Similarity of colorectal cancer in Crohn's disease and ulcerative colitis: implications for carcinogenesis and prevention, *Gut* 35, 950-954.
133. Gillen, C. D., Walmsley, R. S., Prior, P., Andrews, H. A., and Allan, R. N. (1994) Ulcerative colitis and Crohn's disease: a comparison of the colorectal cancer risk in extensive colitis, *Gut* 35, 1590-1592.
134. Lutgens, M. W., Vleggaar, F. P., Schipper, M. E., Stokkers, P. C., van der Woude, C. J., Hommes, D. W., et al. (2008) High frequency of early colorectal cancer in inflammatory bowel disease, *Gut* 57, 1246-1251.
135. Watanabe, T., Konishi, T., Kishimoto, J., Kotake, K., Muto, T., and Sugihara, K. (2011) Ulcerative colitis-associated colorectal cancer shows a poorer survival than sporadic colorectal cancer: a nationwide Japanese study, *Inflamm Bowel Dis* 17, 802-808.
136. Rutter, M. D., Saunders, B. P., Wilkinson, K. H., Kamm, M. A., Williams, C. B., and Forbes, A. (2004) Most dysplasia in ulcerative colitis is visible at colonoscopy, *Gastrointest Endosc* 60, 334-339.
137. Eaden, J. A., Abrams, K. R., and Mayberry, J. F. (2001) The risk of colorectal cancer in ulcerative colitis: a meta-analysis, *Gut* 48, 526-535.
138. Jess, T., Rungoe, C., and Peyrin-Biroulet, L. (2012) Risk of colorectal cancer in patients with ulcerative colitis: a meta-analysis of population-based cohort studies, *Clin Gastroenterol Hepatol* 10, 639-645.

139. Lakatos, L., Mester, G., Erdelyi, Z., David, G., Pandur, T., Balogh, M., et al. (2006) Risk factors for ulcerative colitis-associated colorectal cancer in a Hungarian cohort of patients with ulcerative colitis: results of a population-based study, *Inflamm Bowel Dis* 12, 205-211.
140. Mills, S., and Stamos, M. J. (2007) Colonic Crohn's disease, *Clin Colon Rectal Surg* 20, 309-313.
141. Ekbom, A., Helmick, C., Zack, M., and Adami, H. O. (1990) Increased risk of large-bowel cancer in Crohn's disease with colonic involvement, *Lancet* 336, 357-359.
142. Ekbom, A., Helmick, C., Zack, M., and Adami, H. O. (1990) Ulcerative colitis and colorectal cancer. A population-based study, *N Engl J Med* 323, 1228-1233.
143. Lutgens, M. W., van Oijen, M. G., van der Heijden, G. J., Vleggaar, F. P., Siersema, P. D., and Oldenburg, B. (2013) Declining risk of colorectal cancer in inflammatory bowel disease: an updated meta-analysis of population-based cohort studies, *Inflamm Bowel Dis* 19, 789-799.
144. Canavan, C., Abrams, K. R., and Mayberry, J. (2006) Meta-analysis: colorectal and small bowel cancer risk in patients with Crohn's disease, *Aliment Pharmacol Ther* 23, 1097-1104.
145. von Roon, A. C., Reese, G., Teare, J., Constantinides, V., Darzi, A. W., and Tekkis, P. P. (2007) The risk of cancer in patients with Crohn's disease, *Dis Colon Rectum* 50, 839-855.
146. Eaden, J. (2003) Review article: the data supporting a role for aminosalicylates in the chemoprevention of colorectal cancer in patients with inflammatory bowel disease, *Aliment Pharmacol Ther* 18 Suppl 2, 15-21.
147. Askling, J., Dickman, P. W., Karlen, P., Brostrom, O., Lapidus, A., Lofberg, R., and Ekbom, A. (2001) Family history as a risk factor for colorectal cancer in inflammatory bowel disease, *Gastroenterology* 120, 1356-1362.
148. Foersch, S., and Neurath, M. F. (2014) Colitis-associated neoplasia: molecular basis and clinical translation, *Cell Mol Life Sci.* 71, 3523-3535.
149. Tara M. Connelly, A. S. B., Leonard R. Harris III, David L. Brinton, John P. Hegarty, Susan M. Deiling, David B. Stewart, Walter A. Koltun, . Ulcerative colitis neoplasia is not associated with common IBD SNPs, *Surgery*, 156, 253-262.
150. Baker, S. J., Preisinger, A. C., Jessup, J. M., Paraskeva, C., Markowitz, S., Willson, J. K., et al. (1990) p53 gene mutations occur in combination with 17p allelic deletions as late events in colorectal tumorigenesis, *Cancer Res* 50, 7717-7722.
151. Goss, K. H., and Groden, J. (2000) Biology of the adenomatous polyposis coli tumor suppressor, *J Clin Oncol* 18, 1967-1979.

152. Melum, E., Franke A, Karlsen TH. (2009) Genome-wide association studies--a summary for the clinical gastroenterologist., *World J Gastroenterol.* 15, 5377-5396.
153. McCarroll, S. A., and Altshuler, D. M. (2007) Copy-number variation and association studies of human disease, *Nat Genet* 39, S37-42.
154. Abecasis, G. R., Auton, A., Brooks, L. D., DePristo, M. A., Durbin, R. M., Handsaker, R. E., et al. (2012) An integrated map of genetic variation from 1,092 human genomes, *Nature* 491, 56-65.
155. National Center for Biotechnology Information. NCBI dB SNP. <http://www.ncbi.nlm.nih.gov/snp>.
156. Bush, W. S., and Moore, J. H. (2012) Chapter 11: Genome-wide association studies, *PLoS Comput Biol* 8, e1002822.
157. Stadler, Z. K., Thom, P., Robson, M. E., Weitzel, J. N., Kauff, N. D., Hurley, K. E., et al. (2010) Genome-wide association studies of cancer, *J Clin Oncol* 28, 4255-4267.
158. Iyengar, S. K., and Elston, R. C. (2007) The genetic basis of complex traits: rare variants or "common gene, common disease"?, *Methods Mol Biol* 376, 71-84.
159. Welter, D., MacArthur, J., Morales, J., Burdett, T., Hall, P., Junkins, H., et al. (2014) The NHGRI GWAS Catalog, a curated resource of SNP-trait associations, *Nucleic Acids Res* 42, D1001-1006.
160. National Human Genome Research Institute. A Catalog of Published Genome-Wide Association Studies. <http://www.genome.gov/gwastudies>.
161. Kraft, P., and Cox, D. G. (2008) Study designs for genome-wide association studies, *Adv Genet* 60, 465-504.
162. Stranger, B. E., Stahl, E. A., and Raj, T. (2011) Progress and promise of genome-wide association studies for human complex trait genetics, *Genetics* 187, 367-383.
163. Panagiotou, O. A., Willer, C. J., Hirschhorn, J. N., and Ioannidis, J. P. (2013) The power of meta-analysis in genome-wide association studies, *Annu Rev Genomics Hum Genet* 14, 441-465.
164. Freedman, M. L., Monteiro, A. N., Gayther, S. A., Coetzee, G. A., Risch, A., Plass, C., et al. (2011) Principles for the post-GWAS functional characterization of cancer risk loci, *Nat Genet* 43, 513-518.
165. Franke, L., and Jansen, R. C. (2009) eQTL analysis in humans, *Methods Mol Biol* 573, 311-328.

166. He, X., Fuller, C. K., Song, Y., Meng, Q., Zhang, B., Yang, X., and Li, H. (2013) Sherlock: detecting gene-disease associations by matching patterns of expression QTL and GWAS, *Am J Hum Genet* 92, 667-680.
167. Fernandez-Rozadilla, C., Cazier, J. B., Tomlinson, I. P., Carvajal-Carmona, L. G., Palles, C., Lamas, M. J., et al. (2013) A colorectal cancer genome-wide association study in a Spanish cohort identifies two variants associated with colorectal cancer risk at 1p33 and 8p12, *BMC Genomics* 14, 55.
168. Houlston, R. S., Cheadle, J., Dobbins, S. E., Tenesa, A., Jones, A. M., Howarth, K., et al. (2010) Meta-analysis of three genome-wide association studies identifies susceptibility loci for colorectal cancer at 1q41, 3q26.2, 12q13.13 and 20q13.33, *Nat Genet* 42, 973-977.
169. Peters, U., Hutter, C. M., Hsu, L., Schumacher, F. R., Conti, D. V., Carlson, C. S., et al. (2012) Meta-analysis of new genome-wide association studies of colorectal cancer risk, *Hum Genet* 131, 217-234.
170. Jia, W. H., Zhang, B., Matsuo, K., Shin, A., Xiang, Y. B., Jee, S. H., et al. (2013) Genome-wide association analyses in East Asians identify new susceptibility loci for colorectal cancer, *Nat Genet* 45, 191-196.
171. Dunlop, M. G., Dobbins, S. E., Farrington, S. M., Jones, A. M., Palles, C., Whiffin, N., et al. (2012) Common variation near CDKN1A, POLD3 and SHROOM2 influences colorectal cancer risk, *Nat Genet* 44, 770-776.
172. Cui, R., Okada, Y., Jang, S. G., Ku, J. L., Park, J. G., Kamatani, Y., et al. (2011) Common variant in 6q26-q27 is associated with distal colon cancer in an Asian population, *Gut* 60, 799-805.
173. Tomlinson, I., Webb, E., Carvajal-Carmona, L., Broderick, P., Howarth, K., Pittman, A.M., Spain, S., et al. (2008) A genome-wide association study identifies colorectal cancer susceptibility loci on chromosomes 10p14 and 8q23.3., *Nat Genet* 40, 623-630.
174. Tomlinson, I., Webb, E., Carvajal-Carmona, L., Broderick, P., Kemp, Z., Spain, S., et al. (2007) A genome-wide association scan of tag SNPs identifies a susceptibility variant for colorectal cancer at 8q24.21., *Nat Genet* 39, 984-988.
175. Zanke, B. W., Greenwood, C.M., Rangrej, J., Kustra, R., Tenesa, A., Farrington, S.M., et al. (2007) Genome-wide association scan identifies a colorectal cancer susceptibility locus on chromosome 8q24., *Nat Genet* 39, 989-994.
176. Poynter, J., Figueiredo, J.C., Conti, D.V., Kennedy, K., Gallinger, S., Siegmund, K.D., et al. (2007) Variants on 9p24 and 8q24 are associated with risk of colorectal cancer: results from the Colon Cancer Family Registry., *Cancer Res* 67, 11128-11132.

177. Whiffin, N., Hosking, F. J., Farrington, S. M., Palles, C., Dobbins, S. E., Zgaga, L., et al. (2014) Identification of susceptibility loci for colorectal cancer in a genome-wide meta-analysis, *Hum Mol Genet*.
178. Fernandez-Rozadilla, C., Cazier, J. B., Tomlinson, I., Brea-Fernandez, A., Lamas, M. J., Baiget, M., et al. (2014) A genome-wide association study on copy-number variation identifies a 11q11 loss as a candidate susceptibility variant for colorectal cancer, *Hum Genet* 133, 525-534.
179. Tenesa, A., Farrington, S.M., Prendergast, J.G., Porteous, M.E., Walker, M., Haq, N., et al. (2008) Genome-wide association scan identifies a colorectal cancer susceptibility locus on 11q23 and replicates risk loci at 8q24 and 18q21., *Nat Genet* 40, 631-637.
180. Houlston, R., Webb, E., Broderick, P., Pittman, A.M., Di Bernardo, M.C., Lubbe, S., et al. (2008) Meta-analysis of genome-wide association data identifies four new susceptibility loci for colorectal cancer., *Nat Genet* 40, 1426-1435.
181. Jaeger, E., Webb, E., Howarth, K., Carvajal-Carmona, L., Rowan, A., Broderick, P., et al. (2008) Common genetic variants at the CRAC1 (HMPS) locus on chromosome 15q13.3 influence colorectal cancer risk, *Nat Genet* 40, 26-28.
182. Broderick, P., Carvajal-Carmona, L., Pittman, A.M., Webb, E., Howarth, K., Rowan, A., et al. (2007) A genome-wide association study shows that common alleles of SMAD7 influence colorectal cancer risk., *Nat Genet* 39, 1315-1317.
183. Haerian, M. S., Baum, L., and Haerian, B. S. (2011) Association of 8q24.21 loci with the risk of colorectal cancer: a systematic review and meta-analysis, *J Gastroenterol Hepatol* 26, 1475-1484.
184. He, J., Wilkens, L. R., Stram, D. O., Kolonel, L. N., Henderson, B. E., Wu, A. H., et al. (2011) Generalizability and epidemiologic characterization of eleven colorectal cancer GWAS hits in multiple populations, *Cancer Epidemiol Biomarkers Prev* 20, 70-81.
185. Brisbin, A. G., Asmann, Y. W., Song, H., Tsai, Y. Y., Aakre, J. A., Yang, P., et al. (2011) Meta-analysis of 8q24 for seven cancers reveals a locus between NOV and ENPP2 associated with cancer development, *BMC Med Genet* 12, 156.
186. Ling, H., Spizzo, R., Atlasi, Y., Nicoloso, M., Shimizu, M., Redis, R. S., et al. (2013) CCAT2, a novel noncoding RNA mapping to 8q24, underlies metastatic progression and chromosomal instability in colon cancer, *Genome Res* 23, 1446-1461.
187. Wijnen, J. T., Brohet, R. M., van Eijk, R., Jagmohan-Changur, S., Middeldorp, A., Tops, C. M., et al. (2009) Chromosome 8q23.3 and 11q23.1 variants modify colorectal cancer risk in Lynch syndrome, *Gastroenterology* 136, 131-137.
188. Giraldez, M. D., Lopez-Doriga, A., Bujanda, L., Abuli, A., Bessa, X., Fernandez-Rozadilla, C., et al. (2012) Susceptibility genetic variants associated with early-onset colorectal cancer, *Carcinogenesis* 33, 613-619.

189. Peltekova, V. D., Lemire, M., Qazi, A. M., Zaidi, S. H., Trinh, Q. M., Bielecki, R., et al. (2014) Identification of genes expressed by immune cells of the colon that are regulated by colorectal cancer-associated variants, *Int J Cancer* 134, 2330-2341.
190. Closa, A., Cordero, D., Sanz-Pamplona, R., Sole, X., Crous-Bou, M., Pare-Brunet, L., et al. (2014) Identification of candidate susceptibility genes for colorectal cancer through eQTL analysis, *Carcinogenesis*.
191. Tomlinson, I. P., Carvajal-Carmona, L. G., Dobbins, S. E., Tenesa, A., Jones, A. M., Howarth, K., et al. (2011) Multiple common susceptibility variants near BMP pathway loci GREM1, BMP4, and BMP2 explain part of the missing heritability of colorectal cancer, *PLoS Genet* 7, e1002105.
192. Bellam, N., and Pasche, B. (2010) Tgf-beta signaling alterations and colon cancer, *Cancer Treat Res* 155, 85-103.
193. Zhang, K., Civan, J., Mukherjee, S., Patel, F., and Yang, H. (2014) Genetic variations in colorectal cancer risk and clinical outcome, *World J Gastroenterol* 20, 4167-4177.
194. Jiao, S., Peters, U., Berndt, S., Brenner, H., Butterbach, K., Caan, B. J., et al. (2014) Estimating the heritability of colorectal cancer, *Hum Mol Genet* 23, 3898-3905.
195. Tomlinson, I. P., Webb, E., Carvajal-Carmona, L., Broderick, P., Howarth, K., Pittman, A. M., et al. (2008) A genome-wide association study identifies colorectal cancer susceptibility loci on chromosomes 10p14 and 8q23.3, *Nat Genet* 40, 623-630.
196. Moen, C. J., Groot, P.C., Hart, A.A., Snoek, M., Demant, P. (1996) Fine mapping of colon tumor susceptibility (Scs) genes in the mouse, different from the genes known to be somatically mutated in colon cancer., *Proc Natl Acad Sci U S A* 93, 1082-1086.
197. van Wezel, T., Ruivenkamp, C.A., Stassen, A.P., Moen, C.J., Demant, P. (1999) Four new colon cancer susceptibility loci, Scs6 to Scs9 in the mouse., *Cancer Res* 59, 4216-4218.
198. van Wezel, T., Stassen, A. P., Moen, C. J., Hart, A. A., van der Valk, M. A., and Demant, P. (1996) Gene interaction and single gene effects in colon tumour susceptibility in mice, *Nat Genet* 14, 468-470.
199. Ruivenkamp, C., Csikós, T., Klous, A.M., van Wezel, T., Demant, P. (2003) Five new mouse susceptibility to colon cancer loci, Scs11-Scs15., *Oncogene*. 22, 7258-7260.
200. Jiao, S., Hsu, L., Berndt, S., Bezieau, S., Brenner, H., Buchanan, D., et al. (2012) Genome-wide search for gene-gene interactions in colorectal cancer, *PLoS One* 7, e52535.
201. Figueiredo, J. C., Hsu, L., Hutter, C. M., Lin, Y., Campbell, P. T., Baron, J. A., et al. (2014) Genome-wide diet-gene interaction analyses for risk of colorectal cancer, *PLoS Genet* 10, e1004228.

202. Yang, S. K., Hong, M., Zhao, W., Jung, Y., Baek, J., Tayebi, N., et al. (2014) Genome-wide association study of Crohn's disease in Koreans revealed three new susceptibility loci and common attributes of genetic susceptibility across ethnic populations, *Gut* 63, 80-87.
203. Yamazaki, K., Umeno, J., Takahashi, A., Hirano, A., Johnson, T. A., Kumasaka, N., et al. (2013) A genome-wide association study identifies 2 susceptibility Loci for Crohn's disease in a Japanese population, *Gastroenterology* 144, 781-788.
204. Cardinale, C. J., Kelsen, J. R., Baldassano, R. N., and Hakonarson, H. (2013) Impact of exome sequencing in inflammatory bowel disease, *World J Gastroenterol* 19, 6721-6729.
205. Naser, S. A., Arce, M., Khaja, A., Fernandez, M., Naser, N., Elwasila, S., and Thanigachalam, S. (2012) Role of ATG16L, NOD2 and IL23R in Crohn's disease pathogenesis, *World J Gastroenterol* 18, 412-424.
206. Rivas, M. A., Beaudoin, M., Gardet, A., Stevens, C., Sharma, Y., Zhang, C. K., et al. (2011) Deep resequencing of GWAS loci identifies independent rare variants associated with inflammatory bowel disease, *Nat Genet* 43, 1066-1073.
207. Beaudoin, M., Goyette, P., Boucher, G., Lo, K. S., Rivas, M. A., Stevens, C., et al. (2013) Deep resequencing of GWAS loci identifies rare variants in CARD9, IL23R and RNF186 that are associated with ulcerative colitis, *PLoS Genet* 9, e1003723.
208. Wang, M. H., Fiocchi, C., Zhu, X., Ripke, S., Kamboh, M. I., Rebert, N., Duerr, R. H., and Achkar, J. P. (2014) Gene-gene and gene-environment interactions in ulcerative colitis, *Hum Genet* 133, 547-558.
209. Khor, B., Gardet, A., and Xavier, R. J. (2011) Genetics and pathogenesis of inflammatory bowel disease, *Nature* 474, 307-317.
210. Mankertz, J., and Schulzke, J. D. (2007) Altered permeability in inflammatory bowel disease: pathophysiology and clinical implications, *Curr Opin Gastroenterol* 23, 379-383.
211. Lees, C. W., and Satsangi, J. (2009) Genetics of inflammatory bowel disease: implications for disease pathogenesis and natural history, *Expert Rev Gastroenterol Hepatol* 3, 513-534.
212. Rogler, G., and Andus, T. (1998) Cytokines in inflammatory bowel disease, *World J Surg* 22, 382-389.
213. Glick, D., Barth, S., and Macleod, K. F. (2010) Autophagy: cellular and molecular mechanisms, *J Pathol* 221, 3-12.
214. Knights, D., Lassen, K. G., and Xavier, R. J. (2013) Advances in inflammatory bowel disease pathogenesis: linking host genetics and the microbiome, *Gut* 62, 1505-1510.
215. Graham, D. B., and Xavier, R. J. (2013) From genetics of inflammatory bowel disease towards mechanistic insights, *Trends Immunol* 34, 371-378.

216. Cho, J. H., and Brant, S. R. (2011) Recent insights into the genetics of inflammatory bowel disease, *Gastroenterology* 140, 1704-1712.
217. Winther, K. V., Jess, T., Langholz, E., Munkholm, P., and Binder, V. (2004) Long-term risk of cancer in ulcerative colitis: a population-based cohort study from Copenhagen County, *Clin Gastroenterol Hepatol* 2, 1088-1095.
218. UK IBD Genetics Consortium, Barrett, J.C., Lee, J.C., Lees, C.W., Prescott, N.J., Anderson, C.A. et al. (2009) Genome-wide association study of ulcerative colitis identifies three new susceptibility loci, including the HNF4A region., *Nat Genet* 41, 1330-1334.
219. McCarthy, M. I., and Hirschhorn, J. N. (2008) Genome-wide association studies: potential next steps on a genetic journey, *Hum Mol Genet* 17, R156-165.
220. Cadwell, K., Liu, J. Y., Brown, S. L., Miyoshi, H., Loh, J., Lennerz, J. K., et al. (2008) A key role for autophagy and the autophagy gene Atg16l1 in mouse and human intestinal Paneth cells, *Nature* 456, 259-263.
221. Hutter, C. M., Chang-Claude, J., Slattery, M. L., Pflugeisen, B. M., Lin, Y., Duggan, D., et al. (2012) Characterization of gene-environment interactions for colorectal cancer susceptibility loci, *Cancer Res* 72, 2036-2044.
222. Tomlinson, I., Dunlop, M., Campbell, H., Zanke, B., Gallinger, S., Hudson, T., et al. (2010) COGENT (COlorectal cancer GENEtics): an international consortium to study the role of polymorphic variation on the risk of colorectal cancer., *Br J Cancer*. 102, 447-454.
223. Rosenberg, D., Giardina C, Tanaka T. (2009) Mouse models for the study of colon carcinogenesis., *Carcinogenesis* 30, 183-196.
224. Ruivenkamp, C., Hermsen M, Postma C, Klous A, Baak J, Meijer G, Demant P. (2003) LOH of PTPRJ occurs early in colorectal cancer and is associated with chromosomal loss of 18q12-21., *Oncogene* 22, 3472-3474.
225. Mita, Y., Yasuda, Y., Sakai, A., Yamamoto, H., Toyooka, S., Gunduz, M., et al. (2010) Missense polymorphisms of PTPRJ and PTPN13 genes affect susceptibility to a variety of human cancers, *J Cancer Res Clin Oncol* 136, 249-259.
226. Mahler, M., Bristol, I. J., Sundberg, J. P., Churchill, G. A., Birkenmeier, E. H., Elson, C. O., and Leiter, E. H. (1999) Genetic analysis of susceptibility to dextran sulfate sodium-induced colitis in mice, *Genomics* 55, 147-156.
227. Pizarro, T. T., Pastorelli, L., Bamias, G., Garg, R. R., Reuter, B. K., Mercado, J. R., et al. (2011) SAMP1/YitFc mouse strain: a spontaneous model of Crohn's disease-like ileitis, *Inflamm Bowel Dis* 17, 2566-2584.
228. Mahler, M., Most, C., Schmidtke, S., Sundberg, J. P., Li, R., Hedrich, H. J., and Churchill, G. A. (2002) Genetics of colitis susceptibility in IL-10-deficient mice: backcross versus F2 results contrasted by principal component analysis, *Genomics* 80, 274-282.

229. Meunier, C., Kwan, T., Turbide, C., Beauchemin, N., and Gros, P. (2011) Genetic control of susceptibility to carcinogen-induced colorectal cancer in mice: the *Ccs3* and *Ccs5* loci regulate different aspects of tumorigenesis, *Cell Cycle* 10, 1739-1749.
230. Guenet, J. L. (2005) The mouse genome, *Genome Res* 15, 1729-1740.
231. Jackson Laboratory. <http://www.jax.org/>.
232. Perse, M., and Cerar, A. (2011) Morphological and molecular alterations in 1,2 dimethylhydrazine and azoxymethane induced colon carcinogenesis in rats, *J Biomed Biotechnol* 2011, 473964.
233. Mizoguchi, A. (2012) Animal models of inflammatory bowel disease, *Prog Mol Biol Transl Sci* 105, 263-320.
234. Kanneganti, M., Mino-Kenudson, M., and Mizoguchi, E. (2011) Animal models of colitis-associated carcinogenesis, *J Biomed Biotechnol* 2011, 342637.
235. Westbrook, A. M., Szakmary, A., and Schiestl, R. H. (2010) Mechanisms of intestinal inflammation and development of associated cancers: lessons learned from mouse models, *Mutat Res* 705, 40-59.
236. Beutler, B., Du, X., and Xia, Y. (2007) Precipitous forward genetics in mice, *Nat Immunol* 8, 659-664.
237. Justice, M. J., Siracusa, L. D., and Stewart, A. F. (2011) Technical approaches for mouse models of human disease, *Dis Model Mech* 4, 305-310.
238. Eisener-Dorman, A. F., Lawrence, D. A., and Bolivar, V. J. (2009) Cautionary insights on knockout mouse studies: the gene or not the gene?, *Brain, behavior, and immunity* 23, 318-324.
239. Beier, D. R., and Herron, B. J. (2004) Genetic mapping and ENU mutagenesis, *Genetica* 122, 65-69.
240. Moser, A. R., Pitot, H. C., and Dove, W. F. (1990) A dominant mutation that predisposes to multiple intestinal neoplasia in the mouse, *Science* 247, 322-324.
241. Demant, P. (2003) Cancer susceptibility in the mouse: genetics, biology and implications for human cancer, *Nat Rev Genet* 4, 721-734.
242. Flint, J., and Eskin, E. (2012) Genome-wide association studies in mice, *Nat Rev Genet* 13, 807-817.
243. Rogner, U. C., and Avner, P. (2003) Congenic mice: cutting tools for complex immune disorders, *Nat Rev Immunol* 3, 243-252.

244. Peters, L. L., Robledo, R. F., Bult, C. J., Churchill, G. A., Paigen, B. J., and Svenson, K. L. (2007) The mouse as a model for human biology: a resource guide for complex trait analysis, *Nat Rev Genet* 8, 58-69.
245. Nandan, M., Yang VW. (2010) Genetic and Chemical Models of Colorectal Cancer in Mice., *Curr Colorectal Cancer Rep.* 10, 51-59.
246. Zeineldin, M., and Neufeld, K. L. (2013) Understanding phenotypic variation in rodent models with germline Apc mutations, *Cancer Res* 73, 2389-2399.
247. Kwong, L. N., and Dove, W. F. (2009) APC and its modifiers in colon cancer, *Adv Exp Med Biol* 656, 85-106.
248. Su, L. K., Kinzler, K. W., Vogelstein, B., Preisinger, A. C., Moser, A. R., Luongo, C., Gould, K. A., and Dove, W. F. (1992) Multiple intestinal neoplasia caused by a mutation in the murine homolog of the APC gene, *Science* 256, 668-670.
249. Oshima, M., Oshima H, Kitagawa K, Kobayashi M, Itakura C, Taketo M. (1995) Loss of Apc heterozygosity and abnormal tissue building in nascent intestinal polyps in mice carrying a truncated Apc gene., *Proc Natl Acad Sci U S A* 92, 4482-4486.
250. Fodde, R., Edelmann W, Yang K, van Leeuwen C, Carlson C, Renault B, Breukel C, Alt E, Lipkin M, Khan PM, et al. (1994) A targeted chain-termination mutation in the mouse Apc gene results in multiple intestinal tumors., *Proc Natl Acad Sci U S A* 91, 8969-8973.
251. Colnot, S., Niwa-Kawakita, M., Hamard, G., Godard, C., Le Plenier, S., Houbron, C., et al. (2004) Colorectal cancers in a new mouse model of familial adenomatous polyposis: influence of genetic and environmental modifiers., *Lab Invest.* 84, 1619-1630.
252. McCart, A. E., Vickaryous, N. K., and Silver, A. (2008) Apc mice: models, modifiers and mutants, *Pathol Res Pract* 204, 479-490.
253. MacPhee, M., Chepenik KP, Liddell RA, Nelson KK, Siracusa LD, Buchberg AM. (1995) The secretory phospholipase A2 gene is a candidate for the Mom1 locus, a major modifier of ApcMin-induced intestinal neoplasia., *Cell* 81, 957-966.
254. Buhmeida, A., Bendardaf R, Hilska M, Laine J, Collan Y, Laato M, Syrjänen K, Pyrhönen S. (2009) PLA2 (group IIA phospholipase A2) as a prognostic determinant in stage II colorectal carcinoma., *Ann Oncol* 20, 1230-1235.
255. Baran, A. A., Silverman, K. A., Zeskand, J., Koratkar, R., Palmer, A., McCullen, K., et al. (2007) The modifier of Min 2 (Mom2) locus: embryonic lethality of a mutation in the Atp5a1 gene suggests a novel mechanism of polyp suppression, *Genome Res* 17, 566-576.
256. Cormier, R. T., Bilger, A., Lillich, A. J., Halberg, R. B., Hong, K. H., Gould, K. A., et al. (2000) The Mom1AKR intestinal tumor resistance region consists of Pla2g2a and a locus distal to D4Mit64, *Oncogene* 19, 3182-3192.

257. Crist, R. C., Roth, J. J., Lisanti, M. P., Siracusa, L. D., and Buchberg, A. M. (2011) Identification of Mom12 and Mom13, two novel modifier loci of Apc (Min) -mediated intestinal tumorigenesis, *Cell Cycle* 10, 1092-1099.
258. Nnadi, S. C., Watson, R., Innocent, J., Gonye, G. E., Buchberg, A. M., and Siracusa, L. D. (2012) Identification of five novel modifier loci of Apc(Min) harbored in the BXH14 recombinant inbred strain, *Carcinogenesis* 33, 1589-1597.
259. Haines, J., Johnson, V., Pack, K., Suraweera, N., Slijepcevic, P., Cabuy, E., et al. (2005) Genetic basis of variation in adenoma multiplicity in ApcMin/+ Mom1S mice, *Proc Natl Acad Sci U S A* 102, 2868-2873.
260. Elahi, E., Suraweera, N., Volikos, E., Haines, J., Brown, N., Davidson, G., et al. (2009) Five quantitative trait loci control radiation-induced adenoma multiplicity in Mom1R Apc Min/+ mice, *PLoS One* 4, e4388.
261. Starr, T. K., Scott, P. M., Marsh, B. M., Zhao, L., Than, B. L., O'Sullivan, M. G., et al. (2011) A Sleeping Beauty transposon-mediated screen identifies murine susceptibility genes for adenomatous polyposis coli (Apc)-dependent intestinal tumorigenesis, *Proc Natl Acad Sci U S A* 108, 5765-5770.
262. Wei, K., Kucherlapati, R., and Edelmann, W. (2002) Mouse models for human DNA mismatch-repair gene defects, *Trends Mol Med* 8, 346-353.
263. Pineda, M., Castellsague, E., Musulen, E., Llort, G., Frebourg, T., Baert-Desurmont, S., et al. (2008) Non-Hodgkin lymphoma related to hereditary nonpolyposis colorectal cancer in a patient with a novel heterozygous complex deletion in the MSH2 gene, *Genes Chromosomes Cancer* 47, 326-332.
264. Hirono, I. (1981) Natural carcinogenic products of plant origin., *Crit Rev Toxicol.* 8, 235-277.
265. Yang, M., Mickelsen O, Campbell ME, Laqueur GL, Keresztesy JC. (1966) Cycad flour used by Guamanians: effects produced in rats by long-term feeding., *J Nutr.* 90, 153-156. .
266. Druckrey, H. (1973) Specific Carcinogenic and Teratogenic Effects of 'Indirect' Alkylating Methyl and Ethyl compounds, and their Dependency on Stages of Ontogenic Developments, *Forschergruppe Praeventivmedizin* 3, 271-303.
267. Alrawi, S. J., Schiff, M., Carroll, R. E., Dayton, M., Gibbs, J. F., Kulavlat, M., Tan, D., Berman, K., Stoler, D. L., and Anderson, G. R. (2006) Aberrant crypt foci, *Anticancer Res* 26, 107-119.
268. Meunier, C., Cai, J., Fortin, A., Kwan, T., Marquis, J.F., Turbide, C., et al. (2010) Characterization of a major colon cancer susceptibility locus (Ccs3) on mouse chromosome 3., *Oncogene* 29, 647-661.

269. Liu, P., Lu, Y., Liu, H., Wen, W., Jia, D., Wang, Y., and You, M. (2012) Genome-wide association and fine mapping of genetic loci predisposing to colon carcinogenesis in mice, *Mol Cancer Res* 10, 66-74.
270. Derry, M. M., Raina, K., Agarwal, R., and Agarwal, C. (2014) Characterization of azoxymethane-induced colon tumor metastasis to lung in a mouse model relevant to human sporadic colorectal cancer and evaluation of grape seed extract efficacy, *Exp Toxicol Pathol* 66, 235-242.
271. Jacoby, R., Hohman C, Marshall DJ, Frick TJ, Schlack S, Broda M, Smutko J, Elliott RW. (1994) Genetic analysis of colon cancer susceptibility in mice., *Genomics* 22, 381-387.
272. Eversley, C. D., Yuying, X., Pearsall, R. S., and Threadgill, D. W. (2012) Mapping six new susceptibility to colon cancer (Scs) loci using a mouse interspecific backcross, *G3 (Bethesda)* 2, 1577-1584.
273. Angel, J., Popova N, Lanko N, Turusov VS, DiGiovanni J. (2000) A locus that influences susceptibility to 1,2-dimethylhydrazine-induced colon tumors maps to the distal end of mouse chromosome 3., *Mol Carcinog* 27, 47-54.
274. Meunier, C., Van Der Kraak, L., Turbide, C., Groulx, N., Labouba, I., Cingolani, P., et al. (2013) Positional mapping and candidate gene analysis of the mouse *Ccs3* locus that regulates differential susceptibility to carcinogen-induced colorectal cancer, *PLoS One* 8, e58733.
275. Paul, G., Khare, V., and Gasche, C. (2012) Inflamed gut mucosa: downstream of interleukin-10, *Eur J Clin Invest* 42, 95-109.
276. Kuhn, R., Lohler, J., Rennick, D., Rajewsky, K., and Muller, W. (1993) Interleukin-10-deficient mice develop chronic enterocolitis, *Cell* 75, 263-274.
277. Davidson, N. J., Leach, M. W., Fort, M. M., Thompson-Snipes, L., Kuhn, R., Muller, W., Berg, D. J., and Rennick, D. M. (1996) T helper cell 1-type CD4+ T cells, but not B cells, mediate colitis in interleukin 10-deficient mice, *J Exp Med* 184, 241-251.
278. Berg, D. J., Davidson, N., Kühn, R., Müller, W., Menon, S., Holland, G., et al. (1996) Enterocolitis and colon cancer in interleukin-10-deficient mice are associated with aberrant cytokine production and CD4(+) TH1-like responses., *J Clin Investig* . 98, 1010-1020.
279. Bristol, I. J., Farmer, M. A., Cong, Y., Zheng, X. X., Strom, T. B., Elson, C. O., et al. (2000) Heritable susceptibility for colitis in mice induced by IL-10 deficiency, *Inflamm Bowel Dis* 6, 290-302.
280. Rajagopalan, G., Kudva, Y. C., Sen, M. M., Marietta, E. V., Murali, N., Nath, K., et al. (2006) IL-10-deficiency unmasks unique immune system defects and reveals differential regulation of organ-specific autoimmunity in non-obese diabetic mice, *Cytokine* 34, 85-95.

281. Morampudi, V., Bhinder, G., Wu, X., Dai, C., Sham, H. P., Vallance, B. A., and Jacobson, K. (2014) DNBS/TNBS colitis models: providing insights into inflammatory bowel disease and effects of dietary fat, *J Vis Exp*, e51297.
282. Wirtz, S., Neufert C, Weigmann B, Neurath MF. (2007) Chemically induced mouse models of intestinal inflammation., *Nat Protocols* 2, 541-546.
283. Santiago, C., Pagan, B., Isidro, A. A., and Appleyard, C. B. (2007) Prolonged chronic inflammation progresses to dysplasia in a novel rat model of colitis-associated colon cancer, *Cancer Res* 67, 10766-10773.
284. Scheiffele, F., and Fuss, I. J. (2002) Induction of TNBS colitis in mice, *Curr Protoc Immunol Chapter 15*, Unit 15 19.
285. te Velde, A. A., Verstege, M. I., and Hommes, D. W. (2006) Critical appraisal of the current practice in murine TNBS-induced colitis, *Inflamm Bowel Dis* 12, 995-999.
286. Wallace, J. L., Le, T., Carter, L., Appleyard, C. B., and Beck, P. L. (1995) Hapten-induced chronic colitis in the rat: alternatives to trinitrobenzene sulfonic acid, *J Pharmacol Toxicol Methods* 33, 237-239.
287. Boirivant, M., Fuss, I. J., Chu, A., and Strober, W. (1998) Oxazolone colitis: A murine model of T helper cell type 2 colitis treatable with antibodies to interleukin 4, *J Exp Med* 188, 1929-1939.
288. Kojima, R., Kuroda, S., Ohkishi, T., Nakamaru, K., and Hatakeyama, S. (2004) Oxazolone-induced colitis in BALB/C mice: a new method to evaluate the efficacy of therapeutic agents for ulcerative colitis, *J Pharmacol Sci* 96, 307-313.
289. Heller, F., Fuss, I. J., Nieuwenhuis, E. E., Blumberg, R. S., and Strober, W. (2002) Oxazolone colitis, a Th2 colitis model resembling ulcerative colitis, is mediated by IL-13-producing NK-T cells, *Immunity* 17, 629-638.
290. Tanaka, T. (2012) Development of an inflammation-associated colorectal cancer model and its application for research on carcinogenesis and chemoprevention, *Int J Inflamm* 2012, 658786.
291. Okayasu, I., Hatakeyama, S., Yamada, M., Ohkusa, T., Inagaki, Y., and Nakaya, R. (1990) A novel method in the induction of reliable experimental acute and chronic ulcerative colitis in mice, *Gastroenterology* 98, 694-702.
292. Dieleman, L. A., Ridwan, B. U., Tennyson, G. S., Beagley, K. W., Bucy, R. P., and Elson, C. O. (1994) Dextran sulfate sodium-induced colitis occurs in severe combined immunodeficient mice, *Gastroenterology* 107, 1643-1652.
293. Hall, L. J., Faivre, E., Quinlan, A., Shanahan, F., Nally, K., and Melgar, S. (2011) Induction and activation of adaptive immune populations during acute and chronic phases of a murine model of experimental colitis, *Dig Dis Sci* 56, 79-89.

294. Kitajima, S., Takuma, S., and Morimoto, M. (2000) Histological analysis of murine colitis induced by dextran sulfate sodium of different molecular weights, *Exp Anim* 49, 9-15.
295. Alex, P., Zachos, N. C., Nguyen, T., Gonzales, L., Chen, T. E., Conklin, L. S., Centola, M., and Li, X. (2009) Distinct cytokine patterns identified from multiplex profiles of murine DSS and TNBS-induced colitis, *Inflamm Bowel Dis* 15, 341-352.
296. Cooper, H. S., Murthy, S. N., Shah, R. S., and Sedergran, D. J. (1993) Clinicopathologic study of dextran sulfate sodium experimental murine colitis, *Lab Invest* 69, 238-249.
297. Kitajima, S., Takuma, S., and Morimoto, M. (1999) Tissue distribution of dextran sulfate sodium (DSS) in the acute phase of murine DSS-induced colitis, *J Vet Med Sci* 61, 67-70.
298. Perse, M., and Cerar, A. (2012) Dextran sodium sulphate colitis mouse model: traps and tricks, *J Biomed Biotechnol* 2012, 718617.
299. Laroui, H., Ingersoll, S. A., Liu, H. C., Baker, M. T., Ayyadurai, S., Charania, M. A., et al. (2012) Dextran sodium sulfate (DSS) induces colitis in mice by forming nano-lipocomplexes with medium-chain-length fatty acids in the colon, *PLoS One* 7, e32084.
300. Hans, W., Scholmerich, J., Gross, V., and Falk, W. (2000) The role of the resident intestinal flora in acute and chronic dextran sulfate sodium-induced colitis in mice, *Eur J Gastroenterol Hepatol* 12, 267-273.
301. Mahler, M., Bristol, I. J., Leiter, E. H., Workman, A. E., Birkenmeier, E. H., Elson, C. O., and Sundberg, J. P. (1998) Differential susceptibility of inbred mouse strains to dextran sulfate sodium-induced colitis, *Am J Physiol* 274, G544-551.
302. Melgar, S., Karlsson, A., and Michaelsson, E. (2005) Acute colitis induced by dextran sulfate sodium progresses to chronicity in C57BL/6 but not in BALB/c mice: correlation between symptoms and inflammation, *Am J Physiol Gastrointest Liver Physiol* 288, G1328-1338.
303. Clapper, M. L., Cooper, H. S., and Chang, W. C. (2007) Dextran sulfate sodium-induced colitis-associated neoplasia: a promising model for the development of chemopreventive interventions, *Acta Pharmacol Sin* 28, 1450-1459.
304. Tanaka, T., Kohno H, Suzuki R, Yamada Y, Sugie S, Mori H. (2003) A novel inflammation-related mouse colon carcinogenesis model induced by azoxymethane and dextran sodium sulfate., *Cancer Sci* 94, 965-973. .
305. Suzuki, R., Kohno H, Sugie S, Nakagama H, Tanaka T. (2006) Strain differences in the susceptibility to azoxymethane and dextran sodium sulfate-induced colon carcinogenesis in mice., *Carcinogenesis* 27, 162-169.
306. Okayasu, I., Ohkusa, T., Kajiura, K., Kanno, J., and Sakamoto, S. (1996) Promotion of colorectal neoplasia in experimental murine ulcerative colitis, *Gut* 39, 87-92.

307. Saud, S. M., Young, M. R., Jones-Hall, Y. L., Ileva, L., Evbuomwan, M. O., Wise, J., et al. (2013) Chemopreventive activity of plant flavonoid isorhamnetin in colorectal cancer is mediated by oncogenic Src and beta-catenin, *Cancer Res* 73, 5473-5484.
308. Liang, X., Li, H., Tian, G., and Li, S. (2014) Dynamic microbe and molecule networks in a mouse model of colitis-associated colorectal cancer, *Sci Rep* 4, 4985.
309. Baxter, N. T., Zackular, J. P., Chen, G. Y., and Schloss, P. D. (2014) Structure of the gut microbiome following colonization with human feces determines colonic tumor burden, *Microbiome* 2, 20.
310. De Robertis, M., Massi, E., Poeta, M. L., Carotti, S., Morini, S., Cecchetelli, L., et al. (2011) The AOM/DSS murine model for the study of colon carcinogenesis: From pathways to diagnosis and therapy studies, *J Carcinog* 10, 9.
311. Boulard, O., Kirchberger, S., Royston, D. J., Maloy, K. J., and Powrie, F. M. (2012) Identification of a genetic locus controlling bacteria-driven colitis and associated cancer through effects on innate inflammation, *J Exp Med* 209, 1309-1324.
312. Bouma, G., Kaushiva, A., and Strober, W. (2002) Experimental murine colitis is regulated by two genetic loci, including one on chromosome 11 that regulates IL-12 responses, *Gastroenterology* 123, 554-565.
313. Borm, M. E., He, J., Kelsall, B., Pena, A. S., Strober, W., and Bouma, G. (2005) A major quantitative trait locus on mouse chromosome 3 is involved in disease susceptibility in different colitis models, *Gastroenterology* 128, 74-85.
314. Hillhouse, A. E., Myles, M. H., Taylor, J. F., Bryda, E. C., and Franklin, C. L. (2011) Quantitative trait loci in a bacterially induced model of inflammatory bowel disease, *Mamm Genome* 22, 544-555.
315. Esworthy, R., Aranda R, Martín MG, Doroshov JH, Binder SW, Chu FF. (2001) Mice with combined disruption of Gpx1 and Gpx2 genes have colitis., *Am J Gastrointest Liver Physiol* 281, G848-855.
316. Esworthy, R. S., Kim, B. W., Larson, G. P., Yip, M. L., Smith, D. D., Li, M., and Chu, F. F. (2011) Colitis locus on chromosome 2 impacting the severity of early-onset disease in mice deficient in GPX1 and GPX2, *Inflamm Bowel Dis* 17, 1373-1386.
317. Van Der Kraak, L., Meunier, C., Turbide, C., Jothy, S., Gaboury, L., Marcus, V., et al. (2010) A Two-Locus System Controls Susceptibility to Colitis-Associated Colon Cancer in Mice, *Oncotarget* 1, 436-446.
318. Tanaka, T., Kohno, H., Suzuki, R., Yamada, Y., Sugie, S., and Mori, H. (2003) A novel inflammation-related mouse colon carcinogenesis model induced by azoxymethane and dextran sodium sulfate, *Cancer Sci* 94, 965-973.
319. Canadian Cancer Society (2009) Cancer Statistics 2009. <http://www.cancer.ca>.

320. Kraus, S., Arber N. (2009) Inflammation and colorectal cancer., *Curr Opin Pharmacol.* 9, 405-410.
321. Demant, P. (2003) Cancer susceptibility in the mouse: genetics, biology and implications for human cancer., *Nat Rev Genet* 49, 721-734.
322. Tenesa, A., and Dunlop, MG. (2009) New insights into the aetiology of colorectal cancer from genome-wide association studies, *Nat Rev Genet.* 10, 353-358.
323. Barrett, J. C., Hansoul, S., Nicolae, D.L., Cho, J.H., Duerr, R.H., Rioux, J.D., et al. (2008) Genome-wide association defines more than 30 distinct susceptibility loci for Crohn's disease., *Nat Genet.* 40, 955-962.
324. Anderson, C. A., Massey, D.C., Barrett, J.C., Prescott, N.J., Tremelling, M., Fisher, S.A., et al. (2009) Investigation of Crohn's disease risk loci in ulcerative colitis further defines their molecular relationship., *Gastroenterology.* 136, 523-529.e523.
325. Garrity-Park, M. M., Loftus EV Jr, Sandborn WJ, Bryant SC, Smyrk TC. (2009) MHC Class II alleles in ulcerative colitis-associated colorectal cancer., *Gut* 58, 1226-1233.
326. Ezaki, T., Watanabe M, Inoue N, Kanai T, Ogata H, Iwao Y, Ishii H, Hibi T. (2003) A specific genetic alteration on chromosome 6 in ulcerative colitis-associated colorectal cancers., *Cancer Res* 63, 3747-3749.
327. Dragani, T. A. (2003) 10 years of mouse cancer modifier loci: human relevance., *Cancer Res* 63, 3011-3018.
328. Simpson, S. J., Mizoguchi E, Allen D, Bhan AK, Terhorst C. (1995) Evidence that CD4+, but not CD8+ T cells are responsible for murine interleukin-2-deficient colitis., *Eur J Immunol* 25, 2618-2625.
329. Greten, F. R., Eckmann L, Greten TF, Park JM, Li, Z, Egan LG, Kagnoff MF, Karin M. (2004) IKKbeta Links Inflammation and Tumorigenesis in a Mouse Model of Colitis-Associated Cancer., *Cell* 118, 285-296.
330. Popivanova, B. K., Kitamura, K., Wu, Y., Kondo, T., Kagaya, T., Kaneko, S., et al. (2008) Blocking TNF-alpha in mice reduces colorectal carcinogenesis associated with chronic colitis., *J Clin Investig* 118, 560-570.
331. Fortin, A., Diez, E., Rochefort, D., Laroche, L., Malo, D., Rouleau, G.A. et al. (2001) Recombinant congenic strains derived from A/J and C57BL/6J: A tool for the genetic dissection of complex traits., *Genomics* 74, 21-35.
332. Broman, K. W., Wu H, Sen S, Churchill GA. (2003) R/qtl: QTL mapping in experimental crosses., *Bioinformatics* 19, 889-890.

333. Sakthianandeswaren, A., Curtis, J.M., Elso, C., Kumar, B., Baldwin, T.M., Lopaticki, S., et al. (2010) Fine mapping of *Leishmania major* susceptibility Locus *Imr2* and evidence of a role for *Fli1* in disease and wound healing., *Infect Immun.* 78, 2734-2744.
334. Krezowski, J., Knudson, D., Ebeling, C., Pitstick, R., Giri, R.K., Schenk, D., et al. (2004) Identification of loci determining susceptibility to the lethal effects of amyloid precursor protein transgene overexpression, *Hum Mol Genet* 13, 1989-1997.
335. Siegmund, B. (2010) Interleukin-18 in intestinal inflammation: friend and foe?, *Immunity* 32, 300-302.
336. Dupaul-Chicoine, J., Yeretssian, G., Doiron, K., Bergstrom, K.S., McIntire, C.R., LeBlanc, P.M., et al. (2010) Control of intestinal homeostasis, colitis, and colitis-associated colorectal cancer by the inflammatory caspases., *Immunity* 32, 367-378.
337. Lai, P. S., Cheah, P.Y., Kadam, P., Chua, C.L., Lie, D.K., Li, H.H., et al. (2006) Overexpression of *RBI* transcript is significantly correlated with 13q14 allelic imbalance in colorectal carcinomas., *Int J Cancer* 119, 1061-1066.
338. Pittman, A. M., Webb, E., Carvajal-Carmona, L., Howarth, K., Di Bernardo, M.C., Broderick, P., et al. (2008) Refinement of the basis and impact of common 11q23.1 variation to the risk of developing colorectal cancer., *Hum Mol Genet* 17, 3720-3727.
339. Bernstein, C. N., Wajda, A., Svenson, L. W., MacKenzie, A., Koehoorn, M., Jackson, M., et al. (2006) The epidemiology of inflammatory bowel disease in Canada: a population-based study, *Am J Gastroenterol* 101, 1559-1568.
340. Rocchi, A., Benchimol, E. I., Bernstein, C. N., Bitton, A., Feagan, B., Panaccione, R., et al. (2012) Inflammatory bowel disease: a Canadian burden of illness review, *Can J Gastroenterol* 26, 811-817.
341. Kulaylat, M., Dayton, MT. (2010) Ulcerative Colitis and Cancer, *J Surg Oncol* 101, 706-712.
342. Min-Oo, G., Willemetz, A., Tam, M., Canonne-Hergaux, F., Stevenson, M. M., and Gros, P. (2010) Mapping of *Char10*, a novel malaria susceptibility locus on mouse chromosome 9, *Genes Immun* 11, 113-123.
343. Roy, M., Riendeau N, Loredó-Ostí JC, Malo D. (2006) Complexity in the host response to *Salmonella Typhimurium* infection in AcB and BcA recombinant congenic strains, *Genes and Immunity* 7, 655-666.
344. Wiltshire, S. A., Diez, E., Miao, Q., Dube, M. P., Gagne, M., Paquette, O., et al. (2012) Genetic control of high density lipoprotein-cholesterol in AcB/BcA recombinant congenic strains of mice, *Physiol Genomics* 44, 843-852.
345. Min-Oo, G., Fortin, A., Tam, M. F., Nantel, A., Stevenson, M. M., and Gros, P. (2003) Pyruvate kinase deficiency in mice protects against malaria, *Nat Genet* 35, 357-362.

346. Min-Oo, G., Fortin, A, Tam, MF, Nantel, A, Stevenson, MM and Gros, P. (2003) Pyruvate kinase deficiency in mice protects against malaria, *Nat Genet* 35, 357-362.
347. Lemay, A. M., and Haston, C. K. (2005) Bleomycin-induced pulmonary fibrosis susceptibility genes in AcB/BcA recombinant congenic mice, *Physiol Genomics* 23, 54-61.
348. Tuite, A., Elias, M., Picard, S., Mullick, A., and Gros, P. (2005) Genetic control of susceptibility to *Candida albicans* in susceptible A/J and resistant C57BL/6J mice, *Genes Immun* 6, 672-682.
349. Ramirez-Aquino, R., Radovanovic, I., Fortin, A., Sciutto-Conde, E., Fragoso-Gonzalez, G., Gros, P., and Aguilar-Delfin, I. (2011) Identification of loci controlling restriction of parasite growth in experimental *Taenia crassiceps* cysticercosis, *PLoS Negl Trop Dis* 5, e1435.
350. Beatty, S., Roy, M, LoredO-Osti, JC and Malo, D. (2011) The AcB61 and AcB60 recombinant congenic strains of inbred mice: susceptibility and resistance to a murine model of human Typhoid fever., In *ICHG*, Montreal, Canada.
351. Caron, J., LoredO-Osti, J. C., Morgan, K., and Malo, D. (2005) Mapping of interactions and mouse congenic strains identified novel epistatic QTLs controlling the persistence of *Salmonella Enteritidis* in mice, *Genes Immun* 6, 500-508.
352. Zaki, M. H., Boyd, K. L., Vogel, P., Kastan, M. B., Lamkanfi, M., and Kanneganti, T. D. (2010) The NLRP3 inflammasome protects against loss of epithelial integrity and mortality during experimental colitis, *Immunity* 32, 379-391.
353. Allen, I. C., TeKippe, E. M., Woodford, R. M., Uronis, J. M., Holl, E. K., Rogers, A. B., Herfarth, H. H., Jobin, C., and Ting, J. P. (2010) The NLRP3 inflammasome functions as a negative regulator of tumorigenesis during colitis-associated cancer, *J Exp Med* 207, 1045-1056.
354. Chen, G. Y., Shaw, M. H., Redondo, G., and Nunez, G. (2008) The innate immune receptor Nod1 protects the intestine from inflammation-induced tumorigenesis, *Cancer Res* 68, 10060-10067.
355. World Health Organization. (2010) <http://who.int>.
356. Fijneman, R. J., Jansen, R. C., van der Valk, M. A., and Demant, P. (1998) High frequency of interactions between lung cancer susceptibility genes in the mouse: mapping of Sluc5 to Sluc14, *Cancer Res* 58, 4794-4798.
357. Manenti, G., Gariboldi, M., Fiorino, A., Zanesi, N., Pierotti, M. A., and Dragani, T. A. (1997) Genetic mapping of lung cancer modifier loci specifically affecting tumor initiation and progression, *Cancer Res* 57, 4164-4166.

358. Quan, L., Stassen, A. P., Ruivenkamp, C. A., van Wezel, T., Fijneman, R. J., Hutson, A., et al. (2011) Most lung and colon cancer susceptibility genes are pair-wise linked in mice, humans and rats, *PLoS One* 6, e14727.
359. Fenske, T. S., McMahon, C., Edwin, D., Jarvis, J. C., Cheverud, J. M., Minn, M., et al. (2006) Identification of candidate alkylator-induced cancer susceptibility genes by whole genome scanning in mice, *Cancer Res* 66, 5029-5038.
360. Higashi, S., Murai, T., Mori, S., Kamoto, T., Yoshitomi, M., Arakawa, Y., Makino, S., Fukushima, S., Yoshida, O., and Hiai, H. (1998) Host genes affecting survival period of chemically induced bladder cancer in mice, *J Cancer Res Clin Oncol* 124, 670-676.
361. McIlwain, D. R., Berger, T., and Mak, T. W. (2013) Caspase functions in cell death and disease, *Cold Spring Harb Perspect Biol* 5, a008656.
362. Hu, B., Elinav, E., Huber, S., Booth, C. J., Strowig, T., Jin, C., Eisenbarth, S. C., and Flavell, R. A. (2010) Inflammation-induced tumorigenesis in the colon is regulated by caspase-1 and NLRC4, *Proc Natl Acad Sci U S A* 107, 21635-21640.
363. Young, R. P., Hopkins, R. J., Hay, B. A., Whittington, C. F., Epton, M. J., and Gamble, G. D. (2011) FAM13A locus in COPD is independently associated with lung cancer - evidence of a molecular genetic link between COPD and lung cancer, *Appl Clin Genet* 4, 1-10.
364. Poole, E. M., Curtin, K., Hsu, L., Duggan, D. J., Makar, K. W., Xiao, L., Carlson, C. S., Caan, B. J., Potter, J. D., Slattery, M. L., and Ulrich, C. M. (2012) Genetic variability in IL23R and risk of colorectal adenoma and colorectal cancer, *Cancer Epidemiol* 36, e104-110.
365. Kanai, M., Hamada, J., Takada, M., Asano, T., Murakawa, K., Takahashi, Y., et al. (2010) Aberrant expressions of HOX genes in colorectal and hepatocellular carcinomas, *Oncol Rep* 23, 843-851.
366. Bi, X., Hameed, M., Mirani, N., Pimenta, E. M., Anari, J., and Barnes, B. J. (2011) Loss of interferon regulatory factor 5 (IRF5) expression in human ductal carcinoma correlates with disease stage and contributes to metastasis, *Breast Cancer Res* 13, R111.
367. Tahara, H., Zeh, H. J., 3rd, Storkus, W. J., Pappo, I., Watkins, S. C., Gubler, U., et al. (1994) Fibroblasts genetically engineered to secrete interleukin 12 can suppress tumor growth and induce antitumor immunity to a murine melanoma in vivo, *Cancer Res* 54, 182-189.
368. Wong, K., Bumpstead, S., Van Der Weyden, L., Reinholdt, L. G., Wilming, L. G., Adams, D. J., and Keane, T. M. (2012) Sequencing and characterization of the FVB/NJ mouse genome, *Genome Biol* 13, R72.

369. Zurita, E., Chagoyen, M., Cantero, M., Alonso, R., Gonzalez-Neira, A., Lopez-Jimenez, A., et al. (2011) Genetic polymorphisms among C57BL/6 mouse inbred strains, *Transgenic Res* 20, 481-489.
370. Kang, H. M., Zaitlen, N. A., Wade, C. M., Kirby, A., Heckerman, D., Daly, M. J., and Eskin, E. (2008) Efficient control of population structure in model organism association mapping, *Genetics* 178, 1709-1723.
371. Radovanovic, I., Mullick, A., and Gros, P. (2011) Genetic control of susceptibility to infection with *Candida albicans* in mice, *PLoS One* 6, e18957.
372. Courtney, S. M., and Massett, M. P. (2012) Identification of exercise capacity QTL using association mapping in inbred mice, *Physiol Genomics* 44, 948-955.
373. Rogner, U., Avner P. (2003) Congenic mice: cutting tools for complex immune disorders., *Nat Rev Immunol* 3, 243-252.
374. Arthur, J. C., Perez-Chanona, E., Muhlbauer, M., Tomkovich, S., Uronis, J. M., Fan, T. J., et al. (2012) Intestinal inflammation targets cancer-inducing activity of the microbiota, *Science* 338, 120-123.
375. Becker, C., Fantini, M. C., and Neurath, M. F. (2006) High resolution colonoscopy in live mice, *Nat Protoc* 1, 2900-2904.
376. Peddareddigari, V. G., Wang, D., and Dubois, R. N. (2010) The tumor microenvironment in colorectal carcinogenesis, *Cancer Microenviron* 3, 149-166.
377. Wijnen, J., Brohet, R.M., van Eijk, R., Jagmohan-Changur, S., Middeldorp, A., Tops, C.M., et al. (2009) Chromosome 8q23.3 and 11q23.1 variants modify colorectal cancer risk in Lynch syndrome., *Gastroenterology* 136, 131-137. .
378. Biancolella, M., Fortini, B. K., Tring, S., Plummer, S. J., Mendoza-Fandino, G. A., Hartiala, J., et al. (2014) Identification and characterization of functional risk variants for colorectal cancer mapping to chromosome 11q23.1, *Hum Mol Genet* 23, 2198-2209.
379. Matkowskyj, K., Marrero, J.A., Carroll, R.E., Danilkovich, A.V., Green, R.M., Benya, R.V. (1999) Azoxymethane-induced fulminant hepatic failure in C57BL/6J mice: characterization of a new animal model., *Am J Physiol.* 277, G455-462.

Appendix 1:
Inbred Strain Survey to AOM-Induced CRC

Manuscript in Preparation:

Van Der Kraak, L, Turbide, C, Beauchemin, N, and Gros, P. Susceptibility to AOM-Induced Colorectal Cancer in Inbred Mice.

A.1.1 Connecting Text

Approximately 25-30% of all CRCs arise due to genetic predisposition in a class of genes known as tumor susceptibility genes³⁵. The identification of these genes, by genome-wide association studies (GWAS) in humans, can be complicated due to the complex interplay of genetic, dietary, environmental and lifestyle factors. Inbred mice provide an alternate means to study this class of genes independent to confounding dietary, environmental and lifestyle factors. CRC can be modeled in mice using repeated injections of the carcinogens 1,2-dimethylhydrazine (DMH) or azoxymethane (AOM) and like humans mice vary with respect to CRC susceptibility²²³. DMH and AOM are pro-carcinogens that are metabolically activated generating a free methyl cation, which in turn can react with deoxyguanosine in DNA leading to the formation of deoxymethylguanosine and subsequent G to A transitions, due to mismatch binding. AOM is generated from the spontaneous dehydrogenation and subsequent oxidation of DMH. AOM has since replaced the DMH as the pro-carcinogen of choice in CRC studies due to its increased potency, increased stability and its colon specific mechanism of tumor induction. Prior to commencing this study in 2008, little was known with respect to AOM-induced CRC susceptibility in inbred mice, as the literature was commonly inconsistent or relatively uninformative²²³. This was due to a lack of a common chemically induced CRC protocol and therefore studies varied markedly with respect to choice of carcinogen, dose and time to sacrifice, all which can greatly influence total tumor numbers. Also, researchers used different strains of mice, which limited inter-experiment comparisons. *Therefore, our objective was to conduct a large-scale survey of AOM-induced CRC in inbred mice to identify novel susceptible and resistant mouse strains for gene mapping.*

Before we could submit our results for publication, a 33-strain survey of AOM-induced CRC susceptibility in male mice was published in Molecular Cancer Research²⁶⁹. While this study is more comprehensive than ours with respect to number of strains tested, ours presents some unique findings including two previously unpublished strains in addition to susceptibility in both male and female mice. Therefore, this appendix highlights some novel findings and compares differences between the two studies suggesting an important role for protocol variations with respect to AOM-induced CRC susceptibility.

A.1.2 Contribution of the Authors

The experiments included in this chapter were planned as part of a collaborative effort between LVDK, CM, NB and PG. CT performed the carcinogen injections and LVDK and CT monitored the mice for the duration of the experiments. LVDK, CM and CT sacrificed the mice. LVDK analyzed the colons for tumors and hyperplastic lesions in addition to writing the paper and preparing the figures with feedback from NB and PG.

A.1.3 Abstract

Inbred mice vary markedly with respect to azoxymethane (AOM)-induced colorectal cancer (CRC) susceptibility due to inherited genetic factors. To identify novel susceptible and resistant mouse strains for future gene mapping experiments, we tested 161 mice (male and female) from 16 commonly available inbred mouse strains for AOM-induced CRC susceptibility. Tumor incidence in surviving mice was 89.3%, with A/J mice developing significantly more tumors than all other strains. CAST/EiJ, B6, C3H/HeJ were the most resistant averaging less than 3 tumors per mouse. This is the first recorded screening of the relatively resistant MRL/J and intermediately susceptible NOD/ShiLtJ mice.

A.1.4 Introduction

Colorectal cancer (CRC) affects approximately 9.5% of the world population, with 694,000 deaths in 2012 ¹⁸. CRC arises due to a combination of dietary, lifestyle and genetic factors ^{30, 35}. Twin studies estimate that 35% of CRC risk is heritable, with approximately 5% being attributable to highly penetrant hereditary germline mutations ^{31, 32}. The most common of these hereditary CRCs are Familial Adenomatous Polyposis and Lynch Syndrome associated with mutations in *Adenomatous Polyposis Coli (APC)* and the mismatch repair genes, respectively. The remaining CRCs arising in genetically predisposed individuals are linked to common allelic variants in a class of genes referred to as tumor susceptibility genes ²²². Individually, these genes have little effect on disease outcome, but in combination confer high disease risk. Human genome-wide association studies (GWAS) have detected more than 30 of these low-penetrance genetic variants to date ¹⁶⁷⁻¹⁸².

Together these human GWAS loci account for less than 5.4% of CRC heritability ^{180, 194, 195}. This suggests that much of the genetic risk, most likely in the form of gene x gene/diet/environment interactions or rare variants, has yet to be uncovered. These types of interactions are difficult to uncover in human GWAS, but can be dissected in genetically well

defined inbred, and recombinant congenic mouse strains, in which gene effects fixed by inbreeding can be mapped by linkage analysis and identified by positional cloning²²³. In these studies, CRC is typically induced in permissive mice using repeated injections of the colon-specific carcinogen azoxymethane. In the largest inbred strain survey for AOM-induced CRC susceptibility involving 33 strains, Liu et al. estimated that inter-strain variance accounts for 68.8% and 71.3% of variation with respect to tumor multiplicity and volume, respectively, suggesting that most CRC variation in inbred mice is heritable²⁶⁹. This study however, only assessed susceptibility in male inbred mice.

In this current study, we investigate susceptibility to AOM-induced CRC in male and female mice from 16 different inbred strains confirming many of the results published in Liu et al. Susceptibility in MRL/J and NOD/ShiLtJ, two previously uncharacterized strains is also assessed. In addition, we uncover variations with respect to tumor multiplicity within mice that differ from Liu et al. suggesting an important role of environment and/or procedure on CRC susceptibility in mice.

A.1.5 Materials and Methods:

A.1.5.1 Ethics Statement

All experiments were done in accordance with the national and international guidelines set forth by the Declaration of Helsinki and the McGill University Institutional Review Board.

A.1.5.2 Inbred Mice

Male and female 129S1/SvImJ, AKR/J, BALB/cByJ, BTBRT<+>tf/J, C3H/HeJ, CAST/EiJ, CBA/J, DBA/2J, FVB/NJ, LP/J, MRL/PJ, NOD/ShiLtJ, SM/J, SWR/J (male only) mice, were purchased from Jackson Laboratory (Bar Harbor, ME, USA). A/J and C57BL/6J (B6) control mice had previously been purchased from Jackson Laboratory, but were bred in house. All mice were housed within the McGill Comparative Animal Resource Centre on beta-chip bedding and a 12-hour light/dark schedule. The mice were fed regular chow (Charles River 5075) and water ad libitum. All experiments were conducted on mice 8 weeks of age or older in accordance with the guidelines set out by the Canadian Council on Animal Care. Mice were weighed and visually monitored a minimum of twice a week for clinical symptoms. Animals showing signs of discomfort were humanely sacrificed immediately.

A.1.5.3 Azoxymethane-Induced CRC

All protocols have been previously described in Meunier et al.²⁶⁸. Briefly, animals were divided into two experimental groups with A/J and B6 mice in each. We have previously shown that A/J and B6 mice are highly susceptible and resistant, respectively to AOM-induced CRC and therefore these mice were included in each experiment to serve as controls thus enabling comparison between the two experiments^{229, 268, 274, 317}. Mice in Experiment #1 (129S1/SvImJ, A/J, BALB/cByJ, C57BL/6J (B6), C3H/HeJ, CAST/EiJ, DBA/2J, FVB/NJ, MRL/PJ, SM/J, SWR/J) received 8 weekly intraperitoneal (i.p) injections of 10 mg/kg azoxymethane (AOM, Sigma, St Louis, MO, USA), whereas Experiment # 2 mice (remaining 5 strains, A/J and B6) were treated weekly with graded amounts of AOM (5 mg/kg, 5 mg/kg, 7.5 mg/kg followed by 5 treatments at 10 mg/kg). High concentrations of AOM can induce lethal hepatic failure in mice³⁷⁹. We had previously noted increased weight loss, decreased survival and liver damage upon necropsy [data not shown] in mice given 10 mg/kg from the lot of carcinogen used in the second experiment. Therefore, the staggered AOM treatment in Experiment # 2 was designed to minimize toxic AOM-induced liver damage.

The experimental endpoint, 17 and 19 weeks in Experiment # 1 and # 2, respectively, corresponded to the development of symptoms consistent with CRC in the A/J mice (rectal bleeding, prolapse, weight loss, ruffling and hunching). At sacrifice, the colon was removed and fixed in 10% phosphate-buffered formalin and subsequently enumerated with respect to tumor multiplicity using a 10x-dissecting microscope. Only tumors 0.5 mm² or larger were included in the analysis.

A1.5.4 Statistical Analysis

Data is expressed as the mean +/- the standard deviation. Results were considered significant if $p \leq 0.05$ as calculated using a student's t-test.

A.1.6 Results

A total of 161 inbred mice comprising 16 different inbred strains were subjected to the AOM-induced CRC protocol (8 weekly injections) in two independent experiments. Survival in both experiments was 93%. Of the 11 mice that died, 8 deaths were due to complications of the injections (ascites, abdominal masses or found dead following an injection). The remaining 4 mice (one CAST/EiJ, 2 FVB/NJ and an LP/J) were found dead within the last 6 weeks of the

experiment. Cause of death in these mice was unclear, as mice did not show signs of discomfort (ruffling, hunching) prior to death. Overall, tumor incidence among the 150 surviving mice was 89.3%.

As denoted in Figure A.1.1 A, A/J mice developed significantly more tumors (Experiment # 1: $n = 43$ tumors, Experiment # 2 $n = 67$ tumors) than the resistant B6 mice (Experiment # 1: $n < 1$, $p \leq 5.0 \times 10^{-7}$, Experiment # 2: $n = 2$, $p \leq 5.0 \times 10^{-8}$). A/J mice were statistically more susceptible than all other strains. CAST/EiJ ($n < 1$), C3H/HeJ ($n = 2$) and DBA/2J ($n = 2$) mice were resistant and not statistically different than the B6 controls with respect to tumor multiplicity. Several strains (129S1/SvImJ, AKR/J, BALB/cByJ, CBA/J, LP/J and MRL/MpJ) exhibited a modest but significant increase in tumor numbers ($n = 4-7$) relative to the B6 mice and were considered to be relatively resistant to AOM-induced CRC. The NOD/ShiLtJ ($n = 9$) and BTBRT $\langle + \rangle$ tf/J ($n = 14$) in Experiment # 2 had more intermediate phenotypes, while SM/J ($n = 13$), FVB/NJ ($n = 17$) and SWR/J ($n = 18$) in Experiment # 1 were classified as susceptible. No gender effects were noted between any of the strains tested.

Since the presence of hyperplastic lesions usually precedes the development of tumors, the colons were also examined for the presence of these lesions (Figure A.1.1 B). A/J mice had approximately 2.1 and 2.8 times the numbers of hyperplastic lesions relative to B6 in experiments # 1 and #2, respectively. CAST/EiJ, SWR/J, LP/J, FVB/NJ and 129S1/SvImJ had comparable numbers of hyperplastic lesions to the B6 controls, whereas the remaining strains had distribution patterns more similar to A/J with one exception, NOD/ShiLtJ which had an intermediate response. Figure A.1.1 C shows total overall lesions for each of the 16 strains.

A.1.7 Discussion

Human CRC is a complex trait and is influenced by genetics, diet, environmental and lifestyle factors. Inbred mice vary with respect to AOM-induced CRC susceptibility due to inherited genetic factors and thus provide an excellent model to map the underlying genetic components of CRC diseases in the absence of competing dietary or lifestyle variables^{223, 269}. In this study, we examined the susceptibility of 16 inbred mouse strains (both male and female) to AOM-induced CRC. This is the first large strain study of male and female mice to chemically induced CRC and these results will help facilitate future gene mapping experiments.

In this experiment, the internal control strains, A/J and B6, were highly susceptible and resistant, respectively, to AOM-induced CRC, consistent with past experiments^{229, 268, 274, 317}. Interestingly, A/J mice were statistically more susceptible than all other strains tested, a phenotypic trait ideal for mapping studies. Our lab has since mapped this differential susceptibility between A/J and B6 mice to a novel two-locus system involving chromosomes 3 (*Ccs3*) and 9 (*Ccs5*)^{229, 268, 274}.

This study also confirms the general susceptibility status of several strains including the resistant 129S1/SvImJ, AKR/J, BALB/cByJ, C3H/HeJ, CBA/J, DBA/2J and the susceptible FVB/NJ and A/J strains^{223, 269}. This is first recorded response of the relatively resistant MRL/MpJ and intermediate susceptible NOD/ShiLtJ mice to chemically-induced CRC. NOD/ShiLtJ mice are closely related to NON/ShiLtJ mice, which were previously characterized as intermediately susceptible²⁶⁹. NON/ShiLtJ and NOD/ShiLtJ mice were derived from a common progenitor stock over 120 generations ago (www.jax.org). While additional testing is necessary to confirm susceptibility using a common protocol, this similarity suggests that a retained ancestral allele may be important with respect to AOM-induced CRC susceptibility in these mice.

In Chapters 3 and 4 of this thesis, we demonstrate the impact of differences with respect to carcinogen/stimulant dose and latency period on tumor development in an inflammation-associated model of CRC. Consistent with the observation, there are several differences with respect to strain susceptibility noted between our study and the previous published 33 inbred strain survey by Liu et al²⁶⁹. Our model of AOM-induced CRC differs from the methodology in the Liu study with respect to age at injection (8⁺ vs 5 weeks), number of injections (8 vs 6), tumor latency period (17/19 vs 24 weeks) and diet (Charles River # 5075 vs Purina Rodent Lab Chow #5001). The most striking difference noted between the studies was with respect to A/J mice. In our model, A/J mice are outliers developing significantly more tumors than all other strains, whereas in the Liu study, A/J mice had similar tumor multiplicity to FVB/NJ mice. While we did not calculate surface area within this study, FVB/NJ mice developed larger tumors than A/J mice (Figure A.1.2), consistent with observations by Liu et al. This difference with respect to overall tumor burden may therefore be associated with many of the A/J tumors being too small to detect at time of sacrifice in the Liu model. Other notable differences include SWR/J mice, which behaved similar to susceptible FVB/NJ mice in our model (FVB/NJ tumors = 17,

hyperplastic lesions = 4 and SWR/J: tumors = 18, hyperplastic lesions = 3) and were relatively resistant in Liu et al's study. Similarity between FVB/NJ and SWR/J is not unexpected as these mice are closely related with respect to phylogeny and therefore may have similar genetic susceptibility to CRC. Similar to the Liu study, 129S1/SvImJ, AKR/J, B6, BALB/cByJ, C3H/HeJ, CAST/EiJ CBA/J and DBA/2J were resistant to AOM-induced CRC, although there were slight variations with respect to degree of resistance. The discrepancy between these studies highlights the importance of testing strains within the same experimental protocol prior to determining novel strains for mapping.

Finally, we plan to utilize the information from this study to generate informative crosses between resistant and susceptible mice to map novel genetic factors contributing to CRC susceptibility. As mentioned, our laboratory has already mapped one such locus in two of the most diverse strains, A/J and B6^{229, 268, 274}. Currently, the most interesting strains for future mapping studies are FVB/NJ and SWR/J as they are susceptible to chemically induced CRC and have no phenotypic overlap with several of the resistant strains. Identifying and characterizing susceptibility genes to CRC first in mice with subsequent validation in humans may help to identify those at risk of developing this debilitating disease who could benefit most from treatment to prevent the development of CRC.

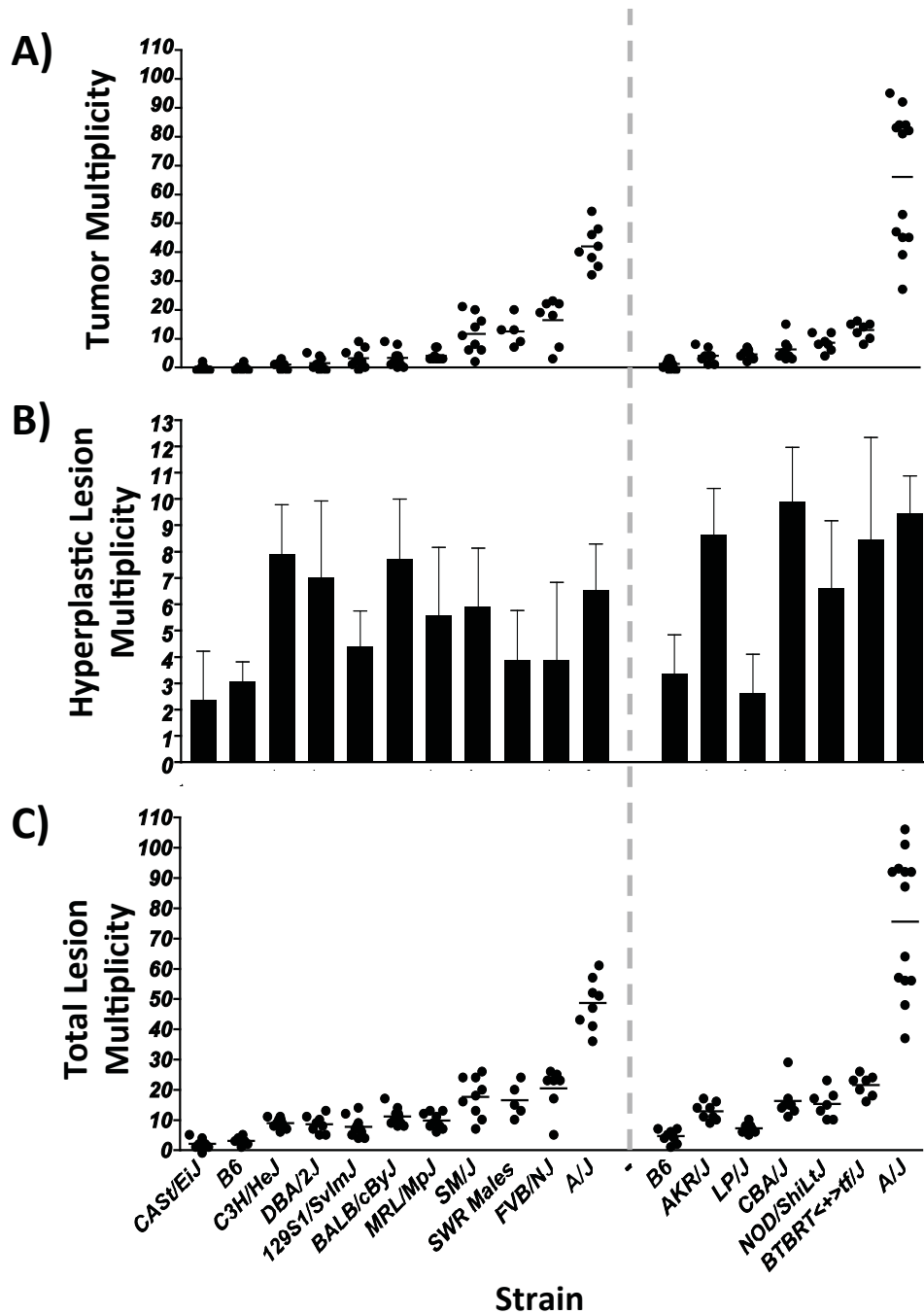


Figure A.1.1: Heterogeneity of response of inbred mice to AOM-induced CRC. Distribution of tumor multiplicity (A), hyperplastic lesion multiplicity (B, mean +/- standard deviation) and total lesion multiplicity (C) in 16 inbred mouse strains. The dotted line indicates the division between two separate experiments with A/J and B6 mice included in each for intra-experimental comparison. A/J mice have significantly more tumors ($p \leq 0.05$) than all other strains tested.

A/J Colons



FVB/NJ Colons

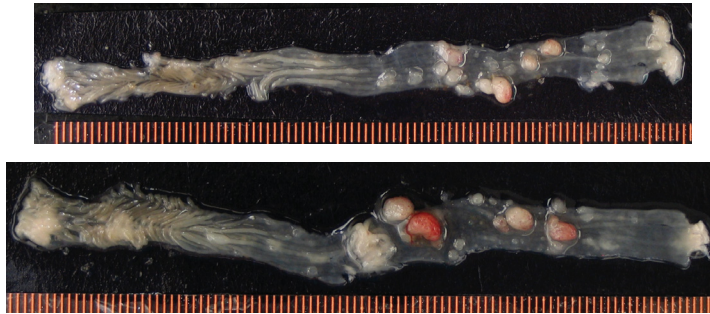


Figure A.1.2: A/J and FVB/NJ colons. Representative images of A/J and FVB/NJ AOM treated colons highlighting differences with respect to tumor size between the two mouse strains.

Appendix 2:

Table A.2.1: Map Location and Plausible Candidate Genes for Inflammatory Bowel Disease Loci identified using Genome-Wide Association Studies. Adapted with permission from Jostins et al. 2012 ⁹⁸.

Chr	Position (Mbps)	SNP	Key Genes (number of additional genes in locus)
Crohn's Disease			
1	78.62	rs17391694	(5)
1	114.3	rs6679677§	<i>PTPN22, DCLRE1B</i> , (7)
1	120.45	rs3897478	<i>ADAM30</i> , (5)
1	172.85	rs9286879	<i>FASLG, TNFSF18</i> , (0)
2	27.63	rs1728918	<i>UCN</i> , (23)
2	62.55	rs10865331	(3)
2	231.09	rs6716753	<i>SPI40</i> , (5)
2	234.145	rs12994997	<i>ATG16L1, INPP5D</i> , (7)
4	48.36	rs6837335	<i>TXK, TEC, SLC10A4</i> , (3)
4	102.86	rs13126505	(1)
5	55.43	rs10065637	<i>IL6ST, IL31RA</i> , (1)
5	72.54	rs7702331	(4)
5	173.34	rs17695092	<i>CPEB4</i> , (2)
6	21.42	rs12663356	(3)
6	31.27	rs9264942	<i>HLA-C, PSORS1C1, NFKB1L1, MICB</i> , (18)
6	127.45	rs9491697	(3)
6	128.24	rs13204742	(2)
6	159.49	rs212388	<i>TAGAP</i> , (5)
7	26.88‡	rs10486483	(2)
7	28.17	rs864745	<i>CREB5, JAZF1</i> , (1)
8	90.87	rs7015630	<i>RIPK2</i> , (4)
8	129.56	rs6651252	(0)
13	44.45	rs3764147	<i>LAC1</i> , (3)
15	38.89	rs16967103	<i>RASGRP1, SPRED1</i> , (2)
16	50.66**	rs2066847§	<i>NOD2, ADCY7</i> , (5)
17	25.84	rs2945412	<i>LGALS9, NOS2</i> , (3)
19	1.12	rs2024092	<i>GPX4, HMHA1</i> , (20)
19	46.85‡	rs4802307	(9)
19	49.2	rs516246	<i>DBP, SPHK2, IZUMO1, FUT2</i> , (22)
21	34.77	rs2284553	<i>IFNGR2, IFNAR1, IFNAR2, IL10RB, GART, TMEM50B</i> , (6)
Ulcerative Colitis			
1	2.5	rs10797432	<i>TNFRSF14, MMEL1, PLCH2</i> , (8)

1	20.15**	rs6426833	(9)
1	200.09	rs2816958	(3)
2	198.65	rs1016883	<i>RFTN2,PLCL1,(7)</i>
2	199.70*	rs17229285	(0)
3	53.05	rs9847710	<i>PRKCD,ITIH4,(8)</i>
4	103.51	rs3774959	<i>NFKB1,MANBA,(2)</i>
5	0.59	rs11739663	<i>SLC9A3,(8)</i>
5	134.44	rs254560	(6)
6	32.595	rs6927022	<i>HLA-DQB1,HLA-DRB1,HLA-DQA1,HLA-DRA,(12)</i>
7	2.78	rs798502	<i>CARD11,GNAI2,TTYH3,(4)</i>
7	27.22‡	rs4722672	(14)
7	107.45*	rs4380874	<i>DLD,(9)</i>
7	128.57	rs4728142	<i>IRF5,TNPO3,TSPAN33,(11)</i>
11	96.02	rs483905	<i>JRKL,MAML2,(2)</i>
11	114.38	rs561722	<i>FAM55A,FAM55D,(5)</i>
15	41.55	rs28374715	<i>ITPKA,NDUFAF1,NUSAP1,(8)</i>
16	30.47	rs11150589	<i>ITGAL,(20)</i>
16	68.58	rs1728785	<i>ZFP90,(6)</i>
17	70.64	rs7210086	(3)
19	47.12‡	rs1126510	<i>CALM3,(14)</i>
20	33.8	rs6088765	<i>PROCR,UQCC,CEP250,(8)</i>
20	43.06	rs6017342	<i>ADA,HNF4A,(9)</i>
Inflammatory Bowel Disease			
1	1.24	rs12103	<i>TNFRSF18,TNFRSF4,(30)</i>
1	8.02	rs35675666	<i>TNFRSF9,(6)</i>
1	22.7	rs12568930†	(3)
1	67.68**	rs11209026†	<i>IL23R,IL12RB2,(4)</i>
1	70.99	rs2651244†	(3)
1	151.79	rs4845604†	<i>RORC,(14)</i>
1	155.67	rs670523†	<i>UBQLN4,RIT1,MSTO1,(28)</i>
1	160.85	rs4656958†	<i>CD48,SLAMF1,ITLN1,CD244,F11R,USF1,SLAMF7,ARHGAP30,(8)</i>
1	161.47	rs1801274†	<i>FCGR2A,FCGR2B,FCGR3A,HSPA6,FCGR3B,FCRLA,(9)</i>
1	197.6	rs2488389	<i>C1orf53,(2)</i>
1	200.87	rs7554511	<i>KIF21B,(6)</i>
1	206.93	rs3024505†	<i>IL10,IL20,IL19,IL24,PIGR,MAPKAPK2,FAIM3,RASSF5,(3)</i>
2	25.12	rs6545800†	<i>ADCY3,(6)</i>
2	28.61	rs925255†	<i>FOSL2,BRE,(1)</i>

2	43.81	rs10495903†	(5)
2	61.2	rs7608910	<i>REL,C2orf74,KIAA1841,AHSA2,(6)</i>
2	65.67	rs6740462	<i>SPRED2,(1)</i>
2	102.86*	rs917997†	<i>IL1R2,IL18RAP,IL18R1,IL1R1,IL1RL1,IL1RL2,(3)</i>)
2	163.1	rs2111485	<i>IFIH1,(5)</i>
2	191.92	rs1517352	<i>STAT1,STAT4,(2)</i>
2	219.14	rs2382817	<i>SLC11A1,CXCR2,CXCR1,PNKD,ARPC2,TMBIM1,CTDSP1,(8)</i>
2	241.57*	rs3749171†	<i>GPR35,(12)</i>
3	18.76	rs4256159†	(0)
3	48.96**	rs3197999	<i>MST1,PFKFB4,MST1R,UCN2,GPX1,IP6K2,BSN,IP6K1,USP4,(56)</i>
4	74.85	rs2472649†	<i>CXCL5,CXCL1,CXCL3,IL8,CXCL6,PF4,CXCL2,PF4V1,(3)</i>
4	123.22	rs7657746	<i>IL2,IL21,(2)</i>
5	10.69	rs2930047	<i>DAP,(2)</i>
5	40.38**	rs11742570†	<i>PTGER4,(1)</i>
5	96.24	rs1363907	<i>ERAP2,ERAP1,LNPEP,(2)</i>
5	130.005	rs4836519†	(1)
5	131.19*	rs2188962†	<i>IRF1,IL13,CSF2,SLC22A4,IL4,IL3,IL5,PDLIM4,SLC22A5,ACSL6,(8)</i>
5	141.51	rs6863411†	<i>SPRY4,NDFIP1,(5)</i>
5	150.27	rs11741861†	<i>TNIP1,IRGM,ZNF300P1,(8)</i>
5	158.8**	rs6871626†	<i>IL12B,(3)</i>
5	176.79	rs12654812	<i>DOK3,(17)</i>
6	14.71	rs17119	(0)
6	20.77*	rs9358372†	(2)
6	90.96	rs1847472	(1)
6	106.43	rs6568421†	(2)
6	111.82	rs3851228	<i>TRAF3IP2,FYN,REV3L,(2)</i>
6	138	rs6920220†	<i>TNFAIP3,(1)</i>
6	143.9	rs12199775	<i>PHACTR2,(5)</i>
6	167.37	rs1819333†	<i>CCR6,RPS6KA2,RNASET2,(3)</i>
7	50.245*	rs1456896	<i>ZPBP,IKZF1,(4)</i>
7	98.75	rs9297145	<i>SMURF1,(6)</i>
7	100.335	rs1734907†	<i>EPO,(21)</i>
7	116.89	rs38904†	(6)
8	126.53	rs921720†	<i>TRIB1,(1)</i>
8	130.62	rs1991866	(2)
9	4.98	rs10758669	<i>JAK2,(4)</i>
9	93.92	rs4743820†	<i>NFIL3,(2)</i>

9	117.60**	rs4246905	<i>TNFSF8,TNFSF15,TNC,(2)</i>
9	139.32*	rs10781499†	<i>CARD9,PMPCA,SDCCAG3,INPP5E,(19)</i>
10	6.08	rs12722515†	<i>IL2RA,IL15RA,(6)</i>
10	30.72	rs1042058†	<i>MAP3K8,(3)</i>
10	35.295	rs11010067†	<i>CREM,(3)</i>
10	59.99	rs2790216	<i>CISD1,IPMK,(2)</i>
10	64.51**	rs10761659†	<i>(3)</i>
10	75.67	rs2227564†	<i>(13)</i>
10	81.03	rs1250546†	<i>(5)</i>
10	82.25	rs6586030†	<i>TSPAN14,C10orf58,(4)</i>
10	94.43	rs7911264	<i>(4)</i>
10	101.28	rs4409764	<i>NKX2-3,(6)</i>
11	1.87	rs907611	<i>TNNI2,LSP1,(17)</i>
11	58.33	rs10896794	<i>CNTF,LPXN,(8)</i>
11	60.77	rs11230563	<i>CD6,CD5,PTGDR2,(12)</i>
11	61.56	rs4246215†	<i>C11orf9,FADS1,FADS2,(12)</i>
11	64.12	rs559928	<i>CCDC88B,RPS6KA4,TRPT1,FLRT1,(20)</i>
11	65.65	rs2231884†	<i>RELA,FOSL1,CTSW,SNX32,(22)</i>
11	76.29	rs2155219†	<i>(5)</i>
11	87.12	rs6592362	<i>(1)</i>
11	118.74	rs630923†	<i>CXCR5,(17)</i>
12	12.65	rs11612508†	<i>LOH12CR1,(8)</i>
12	40.77*	rs11564258†	<i>LRRK2,MUC19</i>
12	48.2	rs11168249†	<i>VDR,(8)</i>
12	68.49	rs7134599†	<i>IFNG,IL26,IL22,(1)</i>
13	27.52	rs17085007†	<i>(2)</i>
13	40.86**	rs941823†	<i>(3)</i>
13	99.95	rs9557195	<i>GPR183,GPR18,(6)</i>
14	69.27	rs194749†	<i>ZFP36L1,(4)</i>
14	75.7	rs4899554†	<i>FOS,MLH3,(6)</i>
14	88.47	rs8005161	<i>GPR65,GALC,(1)</i>
15	67.43	rs17293632†	<i>SMAD3,(2)</i>
15	91.17	rs7495132	<i>CRTC3,(3)</i>
16	11.54*	rs529866†	<i>SOCS1,LITAF,RMI2,(10)</i>
16	23.86	rs7404095	<i>PRKCB,(5)</i>
16	28.595	rs26528†	<i>RABEP2,IL27,EIF3C,SULT1A1,SULT1A2,NUPR1,(9)</i>
16	86	rs10521318†	<i>IRF8,(4)</i>
17	32.59	rs3091316†	<i>CCL13,CCL2,CCL11,(4)</i>
17	37.91	rs12946510	<i>IKZF3,ZBP2,GSDMB,ORMDL3,GSDMA,(12)</i>
17	40.53	rs12942547†	<i>STAT3,STAT5B,STAT5A,(13)</i>

17	57.96	rs1292053 †	<i>TUBD1,RPS6KB1,(9)</i>
18	12.8	rs1893217 †	(6)
18	46.39	rs7240004†	<i>SMAD7,(2)</i>
18	67.53	rs727088	CD226,(2)
19	10.49*	rs11879191	<i>TYK2,PPAN-P2RY11,ICAM1,(25)</i>
19	33.73	rs17694108	<i>CEBPG,(8)</i>
19	55.38	rs11672983	<i>NLRP7,NLRP2,KIR2DL1,LILRB4,(15)</i>
20	30.75	rs6142618†	<i>HCK,(10)</i>
20	31.37	rs4911259	<i>DNMT3B,(8)</i>
20	44.74	rs1569723 †	<i>CD40,MMP9,PLTP,(11)</i>
20	48.95	rs913678	<i>CEBPB,(5)</i>
20	57.82	rs259964	<i>ZNF831,CTSZ,(5)</i>
20	62.34	rs6062504	<i>TNFRSF6B,LIME1,SLC2A4RG,ZGPAT,(23)</i>
21	16.81	rs2823286 †	(0)
21	40.46	rs2836878 †	(3)
21	45.62	rs7282490	<i>ICOSLG,(9)</i>
22	21.92	rs2266959	<i>MAPK1,YDJC,UBE2L3,RIMBP3,CCDC116,(8)</i>
22	30.425	rs2412970	<i>LIF,OSM,MTMR3,(8)</i>
22	39.69*	rs2413583 †	<i>ATF4,TAB1,APOBEC3G,(16)</i>

The position given is the middle of the locus window

* = additional genome-wide significant associated SNP in the region

** = two or more additional genome-wide significant SNPs in the region

‡ = These regions have overlapping but distinct UC and CD signals

Bolded rs numbers indicate SNPs with p-values less than 10^{-13}

† = heterogeneity of odds ratios

§ = CD risk allele is significantly protective in UC

Listed are genes implicated by one or more candidate genes approaches.

Bolded genes have been implicated by two or more candidate gene approaches.

For each locus, the top two candidate genes are listed.